Interplay between the exocyst complex and TOR signal transduction in the fission yeast *Schizosaccharomyces pombe*

Submitted by Connor George Horton to the University of Exeter
as a thesis for the degree of
Doctor of Philosophy in Biological Sciences
In September 2019

I certify that all material in this thesis which is not my own work has been identified and that no material has previously been submitted and approved for the award of a degree by this or any other University.

Signature: ……..

Abstract

Adaptation to environmental changes is required for organism survival. Single celled organisms need to maintain a good surface area to volume ratio in order to take up enough nutrients without reaching an unsustainable size. Bending and shaping the plasma membrane through interplay between lipid domains and the actin cytoskeleton is required to localise permeases and sensors that detect environmental nutrients. This relies on a fine balance of exo- and endocytosis of plasma membrane components. The molecular mechanisms controlling nutrient sensing and uptake are not completely understood. The conserved exocyst complex has been implicated in both secretion and endocytosis making it a good candidate for regulating these membrane processes.

Here, I use a combination of yeast genetics, biochemistry, and imaging to investigate how the exocyst member Sec3 influences nutrient sensing and uptake in the fission yeast *Schizosaccharomyces pombe*. I find that growth of temperature sensitive (ts) *sec3* mutants is compromised in a leucine-rich environment via a mechanism independent of amino acid import. Because leucine regulates the target of rapamycin (TOR) growth signalling pathway, I examined the relationship between Sec3 and the TOR signalling axis. I found that inhibition of TOR by the macrolide rapamycin rescues the ts phenotype of *sec3* mutants. Surprisingly, this was via the plasma membrane-associated TORC2 complex, which has been regarded as rapamycin insensitive. I asked if Sec3 cooperates with TORC2 to regulate membrane tension, and found that both *sec3* and *tor1* mutants had depolarised membrane sterols. Proteomic analyses of Sec3 binding partners indicated that a direct interaction between TOR and Sec3 is unlikely. Instead, Sec3 interacted with small GTPases that regulate TORC2 signalling and endocytic actin patch components. As both TORC2 and actin patches influence membrane tension, I hypothesised that Sec3 and TORC2 may intersect at the actin patch. I found that deletion of the endocytic myosin MyoI rescues the temperature sensitivity of *sec3* mutants. I propose that Sec3 and TORC2 differentially regulate MyoI to control sterol polarisation and membrane tension. In conclusion, this thesis provides new insight into how fission yeast regulates membrane content and tension through a novel interaction between the exocyst complex and TORC2 signalling.

Acknowledgements

This work would not have been possible without the continual support from my supervisors; Isabelle Jourdain for turning me into an enthusiastic fission yeast biologist, John Chilton for his expert cloning skills and for teaching me how take beautiful confocal images, and Helen Dawe for stepping in and nodding and smiling when it came to questions about yeast biology and for enlightening me about the align tool in Illustrator. I would like to thank them for their continuous support and guidance (and drinks) throughout the last four years and ensuring I submitted on time.

Next, I would also like to thank Lauren Adams and Beth Dean for making the Jourdain/Dawe supergroup one of the best lab environments I've worked in. I would like to thank them for their immense amount of support over the last four years, for being great company in San Diego at the ASCB 2018 conference and listening to my rants about the TOR signalling axis in the pub. Solidarity!

To everyone else on the BBSRC SWBio DTP and in Lab 211 of the Geoffrey Pope building, I am grateful for their guidance, support, and company over the last four years. It's been a pleasure!

I would also like to thank Kate Heesom at the Bristol proteomics facility for performing the mass spectrometry analysis that was integral to the success of this thesis.

It has been a privilege to have been part of the Pombe community and I would like to thank them for their advice and sending the strains I have needed throughout my PhD.

This work was funded by the BBSRC and without it would not have been possible to achieve this work.

Finally, thank you to my incredible family who have provided emotional support, helped me move house numerous times, and have always been there for me over the last four years. I really could not have done this without you!

Table of Contents

List of Figures and Tables

Chapter 1: **Introduction**

1.1 Overview

Regulation to ensure the correct growth and development of organisms is paramount for the survival of every organism. Single celled organisms such as yeasts require the correct surface area to volume ratio in order to maximise nutrient uptake without reaching an unsustainable size. This is more complicated in multicellular fungi, plants or animals where multiple cell types grow in tissues that comprise organs within an organism. Defects in growth and development of these organs can lead to severe consequences. One example is seen in cancer where mutations in cells lead to uncontrolled cell cycle progression and growth leading to tumorigenesis. This results in consequences such tumour metastasis where cancerous cells break off and no longer require cell contact for growth. This causes the spread of cancerous cells around the organism.

For cellular homeostasis to be maintained, cells have evolved with ever more complex processes that regulate growth and division. All these processes involve the sensing of the environment for nutrients or stressors. Nutrients and stressors affect specific proteins in the plasma membrane and cytosol which act as molecular switches to regulate stress and growth signalling pathways. These pathways act to either reduce growth of the organism in cases of starvation and stress, but also promote growth and division in nutrient rich environments. Thus regulation of nutrient sensing, uptake, and metabolism is important for homeostasis.

Once activated these signalling networks control cellular processes involved in modulating cell growth and size. One of these includes intracellular trafficking. Both exocytosis and endocytosis play key roles in the delivery of materials needed to protrude the cell periphery, but also the removal of nutrient transporters, receptors and lipid domains in the plasma membrane so that growth occurs in the correct cellular location and at a regulated rate. One trafficking complex that has been implicated in both exo- and endocytosis is the exocyst complex (Finger and Novick, 1997; Gachet and Hyams, 2005; Jourdain et al., 2012). The exocyst is a conserved hetero-octameric complex that is thought to tether cargoes to the plasma membrane. While most of these exocyst related cargoes are still awaiting identification, proteins involved in nutrient uptake have

been shown to be dependent on exocyst mediated exocytosis (Inoue et al., 2003). Mutation of exocyst members also results in defects in endocytosis revealing a role for this complex in the retrograde transport of these components too. Furthermore members of the exocyst have been implicated in the activation of stress signalling pathways. This places the exocyst as a potential master regulator of stress and nutrient sensing via its modulation of the level of stress and nutrient sensors at the cell surface and possible bridging of this to signalling networks.

1.2 Growth and nutrient sensing

Cellular growth requires the synthesis of materials such as lipids and proteins to the plasma membrane which accounts for the increase in cell size. Nucleotides must also be generated so that DNA replication and subsequent cell division can occur. The generation of these materials requires a lot of energy, which is provided to the cell by the mitochondria in the form of adenosine triphosphate (ATP). All of these materials are generated from complex metabolic pathways that metabolise nutrients into these final products. These processes are conserved across all eukaryotes showing that they are fundamental for their growth and survival. The most common nutrients required are carbohydrates and amino acids.

1.3 Carbohydrates fuel cellular energy production

Carbohydrates are the main source of energy for most organisms. The most common of these is the sugar glucose. Glucose transport across the plasma membrane can be either an active or passive process and is performed by transmembrane hexose transporters. Once in the cytoplasm glucose is phosphorylated to glucose-6-phosphate where it is then converted to pyruvate via a series of enzymatic reactions in the glycolysis pathway (Akram, 2013). Pyruvate can enter the mitochondria where it is converted to Acetyl-CoA which then enters the tricarboxylic acid (TCA) cycle (Akram, 2014). The TCA cycle functions to generate intermediates that enter the electron transport chain situated on the mitochondrial inner membrane which results in a large net production of ATP via a process called oxidative phosphorylation (OXPHOS). Some of the intermediates produced by the TCA cycle can also be used to generate non-essential amino acids (Newsholme et al., 2011).

While respiration is the main source of ATP production in mammals, some yeasts prefer ATP production through fermentation. The fission yeast *Schizosaccharomyces pombe* produces energy primarily through fermentation in the presence of glucose (Rolland et al., 2002). However switching the carbohydrate source to a more complex, non-fermentable sugar such as galactose promotes respiration through OXPHOS (Chiron et al., 2007). Galactose requires additional ATP to convert it to glucose meaning there is no net gain of ATP from glycolysis, therefore the mitochondria are needed to generate energy.

While glucose is primarily used for production of ATP, it can also be considered as a signalling molecule. The budding yeast *Saccharomyces cerevisiae* has been used extensively as a model of glucose signalling (Kim et al., 2013). Studies have shown that glucose can act like a hormone by binding to the sensors Snf3 and Rgt2 (Özcan et al., 1996). Activation of these proteins by glucose binding causes downstream transcription changes that cause an increase in expression of glucose transporter proteins (Özcan, 2002). Glucose has also been shown to cause the activation of two prominent signalling pathways; cAMP/PKA and TOR, which both regulate cellular growth, division, metabolism, morphology, stress resistance and autophagy (Byrne and Hoffman, 1993; Carrillo et al., 1994; Cohen et al., 2014; Hatano et al., 2015; Thevelein, 1984). These signalling axes link environmental glucose availability to cell growth and division.

1.4 Amino acids play a vital role in cellular growth and metabolism in yeast.

Amino acids are a vital source of nitrogen for cellular growth and can either be produced through cellular metabolism (non-essential) or obtained via uptake from the environment only (essential). Mammalian cells require 10 essential amino acids, including arginine, histidine, leucine, isoleucine, lysine, methionine, phenylalanine, threonine, tryptophan, and valine. Conversely fungi possess the biosynthetic pathways needed to make these essential amino acids.

Amino acids directly feed into the citrate cycle through conversion into different intermediates found in the cycle (Newsholme et al., 2011). Most amino acids are commonly converted to glutamate in order to enter the TCA cycle, however a subset are metabolised to acetyl-CoA before entering. This connection between amino acids and the TCA cycle allows proteins to be broken down into amino

acids and used to generate NADPH for production of ATP in oxidative phosphorylation in a process called gluconeogenesis. Metabolism of leucine into acetyl-CoA is also the initial step of the mevalonate pathway. Acetyl-CoA is converted to HMG-CoA and then to mevalonate by HMG-CoA reductase (Goldstein and Brown, 1990). Mevalonate is then a precursor for the synthesis of cholesterols, cofactors, vitamins, and steroid hormones.

As mentioned previously amino acids can be synthesised de novo through metabolic pathways, but cells also possess the means to take up amino acids from the environment. Amino acids are actively imported across the plasma membrane via importers that belong to a family called the amino acid permeases. There are a variety of importers that are specific to specific amino acids, for example ones that receive amino acids with a basic charge, or ones that are branched (Regenberg et al., 1999). The dynamics how these importers are trafficked, respond to nutrients, or even their specificity towards amino acids remains unclear. Work in fission yeast has begun to address these questions The most studied amino acid permeases in fission yeast are the arginine/lysine transporters Cat1 and Aat1. In a nitrogen deprived environment Cat1 is expressed on the plasma membrane (Nakashima et al., 2014), and the opposite is seen in Aat1 (Nakase et al., 2012). However in the presence of ammonium chloride (NH_4Cl) and/or amino acids Cat1 is trafficked in a retrograde manner to the vacuole (Nakashima et al., 2014). Endocytosis of Cat1 is regulated by the E3 ubiquitin ligase Pub1 and its arrestin adapter Arn1 (Nakashima et al., 2014), and retrograde transport appears to be performed by the ESCRT family of proteins (Nakase et al., 2012). Deletion of Pub1 or Arn1 resulted in Cat1-GFP signal remaining on the plasma membrane, indicating a defect in retrograde transport (Nakashima et al., 2014). The retrograde transport of amino acid permeases is beginning to be defined, however the mechanism of how they are secreted remains unclear.

Both carbohydrates and amino acids provide the building blocks for cellular growth, but the link between nutrient availability and growth must be tightly regulated. In the absence of nutrients growth cannot be sustained and process that promote growth need to be turned off, while ones that are involved in stress and starvation responses must be switched on. Loss of regulation between nutrient availability and growth signalling can also lead to disease. A key example

of this is seen in cancer where growth and division is not regulated and leads to tumour formation. To ensure regulation occurs, nutrients feed into several signalling pathways, and this ultimately links nutrient availability to cell growth.

1.5 Nutrient sensing and growth are connected by the TOR signalling axis

The cellular nutrient sensing machinery relies on the target of rapamycin (TOR) signalling axis. TOR receives signals from the plasma membrane and converts them into downstream signals that alter cellular metabolism in response to nutrient availability. In a nutrient rich environment TOR signalling is promoted and maintained, causing the upregulation of genes involved in anabolic processes such as protein, lipid, ribosome synthesis, DNA replication, mitochondrial biogenesis, whilst downregulating autophagy signalling (Barbet et al., 1996; Fingar et al., 2002; Hosokawa et al., 2009; Noda and Ohsumi, 1998). This leads to an overall push towards cellular growth and replication. In response to starvation TOR signalling is not maintained, driving the cell towards catabolic metabolism, mainly through the autophagy pathway. This leads to a decrease in cellular size and replication, leading the cell to enter the G0 phase of the cell cycle (Fingar et al., 2002; Matsuo et al., 2007).

TOR signalling consists of two sensory complexes, TORC1 and TORC2 (Loewith et al., 2002). While mammals only possess one mTOR kinase, yeasts have 2 kinases, Tor1 and Tor2 (Heitman et al., 1991; Kunz et al., 1993) (Figure 1.1).

	S. cerevisiae	*S. pombe*	*H. sapiens*
Kinases	Tor1p	Tor2	mTOR
	Tor2p	Tor1	mTOR
Interactors	Lst8p	Wat1/Pop3	mLST8
	Avo1p	Sin1	SIN1
	Avo3p	Ste20	Rictor
	Kog1p	Mip1	Raptor

Table 1.1: Table of TOR proteins and their homologues in yeasts and *H. sapiens*

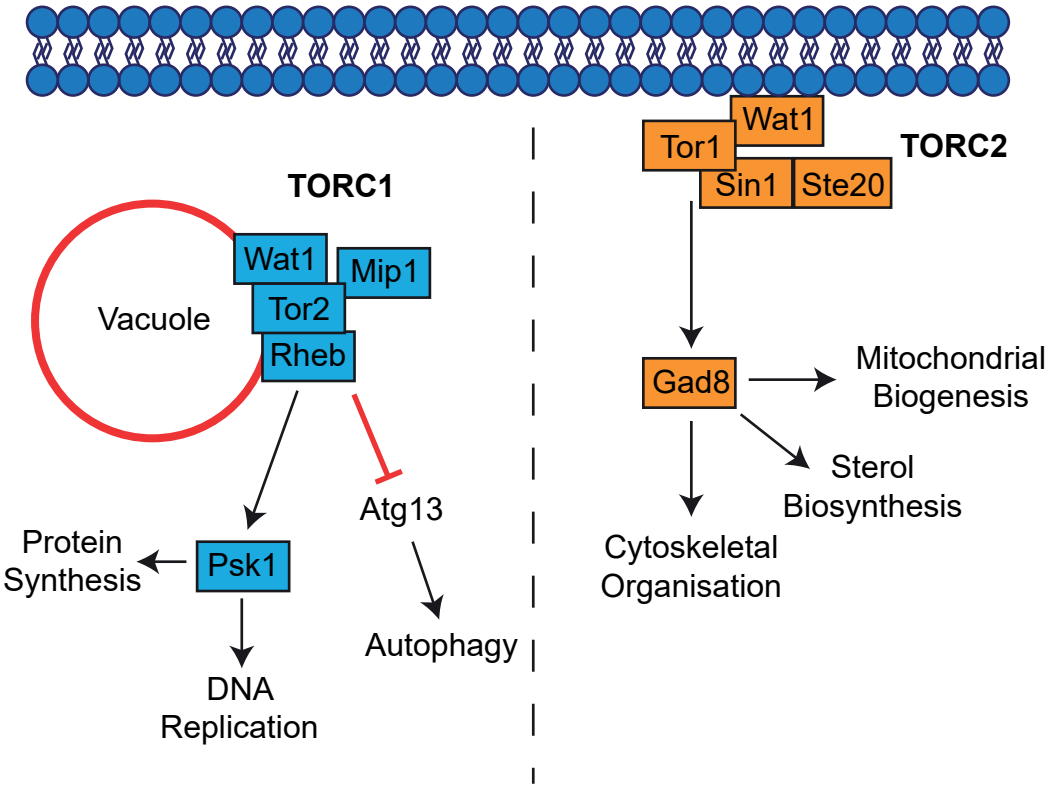

Figure 1.1: The TORC1 and TORC2 signalling complexes in the fission yeast *Schizosaccharomyces pombe*.

1.5.1 TORC1

The TORC1 complex consists of multiple proteins including Tor2 kinase, the mLST8 homologue Wat1, and the Raptor homologue Mip1 (see Table 1.1) (Hara et al., 2002; Kim et al., 2002; Loewith et al., 2002). Interestingly it is possible for Tor1 kinase to also form a TORC1 complex (Hartmuth and Petersen, 2009). When amino acids are present, predominantly leucine in yeast (Binda et al., 2009), the TORC1 complex translocates from the cytoplasm to the membrane of the yeast vacuole. This occurs through recruitment of the complex by the Rag GTPase family members Gtr1 and Gtr2 which are present on the vacuolar membrane (Sancak et al., 2008). Under starvation conditions, Gtr1/2 is sequestered by a vacuolar ATPase. When Leucine is stored in the vacuole or lysosome, it activates the v-ATPase proton pump causing a conformational change which releases Gtr1/2 allowing it to recruit the TORC1 complex to membrane (Saliba et al., 2018; Takayama et al., 2018). The vacuolar membrane also contains the Ras GTPase Rheb which activates TORC1 when the complex is in close proximity (Bai et al., 2007; Long et al., 2005; Sancak et al., 2010). This mechanism is slightly different in mammals. Instead of leucine, arginine is the main activating amino acid of TORC1 in the lysosome (Hara et al., 1998; Wang et al., 2018). Leucine still feeds into TORC1 signalling but via a family of proteins called the sestrins (Chantranupong et al., 2014; Kimball et al., 2016; Xu et al., 2019).

Once TORC1 is activated, it controls anabolic metabolism through activating a protein called P70-S6 kinase, or Psk1 in *S. pombe* (Chung et al., 1992; Hara et al., 1998; Nakashima et al., 2012). P70-S6 kinase transduces signals via many downstream targets to control cell growth and size, and even survival (Magnuson et al., 2012). One of the more characterised examples of this is its role in phosphorylating the fission yeast ribosomal S6 proteins Rps601 and Rps602, which are part of the translation machinery of the target genes involved in ribosome biogenesis (Nakashima et al., 2010). Simultaneously TORC1 signalling also stops the phosphorylation of the eukaryotic initiation factor protein eIF2α (Valbuena et al., 2012). The phosphorylation of eIF2α leads to a downstream repression of protein synthesis, therefore TORC1 signalling acts to maintain protein synthesis through eIF2α (Valbuena et al., 2012). Nutrient dependent inhibition of autophagy has also been shown to be due to TORC1

directly phosphorylating the autophagy protein Atg13 (Hosokawa et al., 2009). This event ensures that Atg13 cannot interact with the key autophagy protein Atg1, preventing the process from occurring (Hosokawa et al., 2009). When nutrients are depleted, TORC1 is switched off and rapid dephosphorylation of Atg13 occurs, leading to autophagic events (Ganley et al., 2009).

Inhibition of TORC1 is performed by the Tsc1/2 complex, named as such because both these genes are mutated in the disease tuberous sclerosis (Consortium, 1993; Kandt et al., 1992; Van Slegtenhorst et al., 1997). Tsc1/2 promotes the exchange of GTP to GDP on Rheb GTPase therefore deactivating TORC1 signalling (Inoki et al., 2003). It is not clear whether there are other mechanisms of TORC1 inhibition, and the knowledge of negative regulators of the signalling complex is also lacking. Pharmacological inhibition of the complex is also possible. The macrolide compound rapamycin is produced by the bacterium *Streptomyces hygroscopicus*, and forms a complex with the cytosolic-FK-binding protein FKBP12 (Vilella-Bach et al., 1999). This complex binds to the ATP binding pocket of Tor2 kinase preventing its activation and thus reducing growth signalling (Vilella-Bach et al., 1999). Because of this there already several approved drugs including Everolimus and Sirolimus which are used for the pharmacological inhibtion of TOR signalling (Li et al., 2014). Furthermore rapamycin has been used extensively as a tool to dissect the TORC1 signalling pathway.

1.5.2 TORC2

Fission yeast TORC2 contains the catalytic subunit Tor1 kinase which interacts with the RICTOR homologue Ste20, SAPK interacting protein Sin1, and Lst8 (see Table 1.1) (Loewith et al., 2002). Activation of TORC2 causes downstream activation of the AGC kinase Gad8 (Ikeda et al., 2008). TORC2 is situated mainly at the plasma membrane but there is growing evidence in mammalian systems of TORC2 being present on both the vacuole membrane and on the mitochondria at specific regions called the mitochondrial associated membranes (Betz et al., 2013; Ebner et al., 2017). MAMs are regions in which the ER and mitochondria make contact and is important for lipid import and for mitophagy (Achleitner et al., 1999; Gelmetti et al., 2017). TORC2 has been found to improve MAM integrity and also affect ATP production, calcium uptake, and membrane potential in the mitochondria (Betz et al., 2013). TORC2 is also found at the division plane where

it plays a role in the cytokinetic actin ring dynamics through modulating myosins (Baker et al., 2016). TORC2 is an important complex in regulating cytokinesis, but is also important for regulating the tension of the plasma membrane.

Unlike TORC1, TORC2 does not appear to be activated by amino acids, although one recent study has provided a link between catabolites of glutamine and TORC2 activation potentially linking the complex to amino acids (Moloughney et al., 2016). Glucose has been shown to activate TORC2 via the cAMP/PKA pathway and through the Rab GTPase Ryh1 in fission yeast (Cohen, Kupiec, & Weisman, 2014; Hatano, Morigasaki, Tatebe, Ikeda, & Shiozaki, 2015). Membrane tension has also been implicated in the activation of TORC2 in budding yeast where an increase in tension was shown to increase Ypk1/Gad8 phosphorylation (Riggi et al., 2018). The Gad8 homologue Ypk1 in *S. cerevisiae* was found to directly phosphorylate the enzyme ceramide synthase which is a key step in driving lipid biosynthesis (Muir et al., 2014). This means tension driven activation of TORC2 stimulates the production of sterols which are trafficked to the plasma membrane in order to improve fluidity and reduce tension.

1.6 Phenotypes of TORC signalling mutants

1.6.1 Tor2 kinase

Microarray analysis of fission yeast Tor2 kinase revealed that it functions to control the expression of many genes involved in nitrogen starvation (Matsuo et al., 2007). The nitrogen starvation response in fission yeast is characterised by two rounds of cell cycle progression followed by arrest in G0 of the cell cycle and cell size is decreased from the normal 15 μm down to around 5 μm (Fantes and Nurse, 1977; Young and Fantes, 1987). Mutation of *tor2* kinase causes cells to decrease in size, mimicking nitrogen starvation (Matsuo et al., 2007). Mating and sporulation of fission yeast requires a low nitrogen environment (Forsburg and Rhind, 2006). Because *tor2* mutants mimic nitrogen starvation, they also exhibited a higher mating efficiency (Matsuo et al., 2007). Further evidence for this role of TORC1 in nitrogen sensing was seen in strains lacking the TORC1 activating Rab GTPase, Rheb (Rhb1), which also mimicked nitrogen starvation in a similar manner to *tor2* mutants (Mach et al., 2000).

1.6.2 Tor1 kinase

Growth of strains lacking Tor1 in media without nitrogen was not logarithmic and instead plateaued immediately indicating that cell division does not occur in this strain during nitrogen starvation (Kawai et al., 2001). Furthermore cell size of *tor1D* was unaltered compared to the wild type which reduced in size as expected (Kawai et al., 2001). This shows that the TORC2 plays a role in nitrogen starvation sensing. Deletion of *tor1* also leads to sterility (Kawai et al., 2001). This is the opposite phenotype to that of *tor2* mutants, showing that TORC1 and 2 might perform opposite roles in during nitrogen starvation. Other phenotypes of this mutant include sensitivity of growth to environmental stressors such as heat, pH, and osmolarity. This is in keeping with TORC2's signalling into the stress related SAPK signalling pathway (Hartmuth and Petersen, 2009; Petersen and Nurse, 2007).

1.7 Cross talk between TOR and MAPK signalling pathways

Both the MAPK and TOR signalling networks play prominent roles in controlling the growth and division of eukaryotic cells, but also their responses to environmental stressors. Because of this it is unsurprising that both signalling networks are entwined with multiple levels of crosstalk having been identified (Figure 1.2). One important process that both signalling pathways. The MAPK pathway triggers mitotic entry via Sty1 (Petersen and Nurse, 2007). Sty1 activates the polo-kinase Plo1 where it is then recruited to the spindle pole body (SPB) to initiate mitosis (Petersen and Hagan, 2005).

Deletion of the TORC2 specific kinase Tor1 in fission yeast causes a delay in mitotic entry in response to nutrient stress with cells maintaining a long cell length (Hartmuth & Petersen, 2009). Surprisingly Tor1 was found to regulate mitotic entry via an interaction with the TORC1 specific Raptor homologue Mip1, meaning that a second TORC1 complex containing Tor1 rather than Tor2 may be the key signalling complex in regulating mitosis (Hartmuth & Petersen, 2009). Both MAPK and TOR signalling appear to crosstalk via Sty1 as inhibition of TOR increases Sty1 activity thus promoting mitotic commitment (Hartmuth & Petersen, 2009). Nutrient import and how they are sensed through growth signalling pathways relies on sensors and importers in the plasma membrane. Therefore the fine tuning of these sensors to environmental nutrients depends on both the

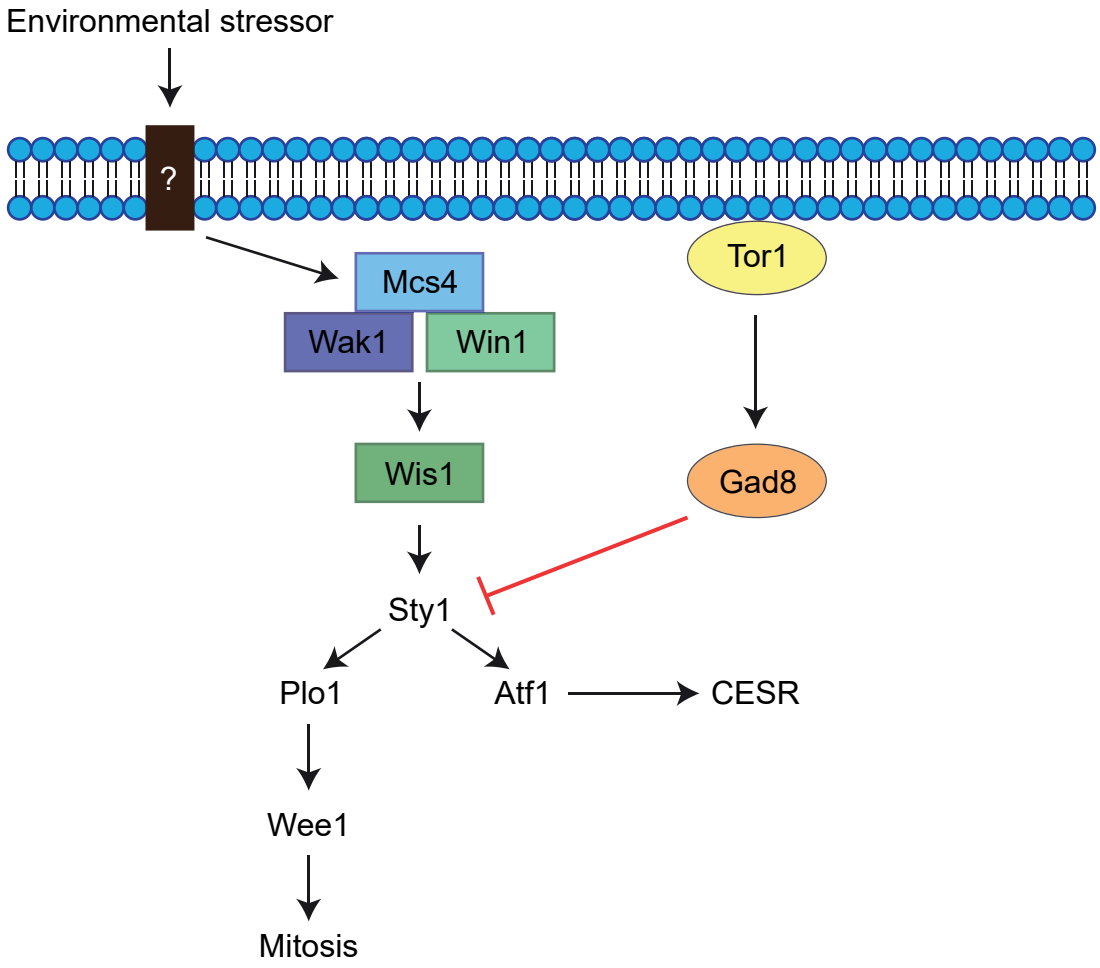

Figure 1.2: Crosstalk between the MAPK and TOR signalling pathways.

retrograde transport, but also secretion. Exocytosis involves the trafficking of post-Golgi vesicles containing cargoes to the plasma membrane, where they are tethered and subsequently secreted. The trafficking and tethering of these cargoes has been proposed to be regulated by the exocyst complex.

1.8 The exocyst is a conserved complex

The exocyst complex (Figure 1.3) is a conserved hetero-octameric complex that is involved in the trafficking and tethering of post-Golgi secretory vesicles at the plasma membrane (Guo et al., 1999; Hsu et al., 1996; TerBush et al., 1996; Yeaman et al., 2001). The complex contains the proteins Sec3, Sec5, Sec6, Sec8, Sec10, Sec15 which are named Sec after the landmark genetic screen in budding yeast where 23 temperature sensitive mutants defective in acid phosphatase secretion were identified (Novick et al., 1980). Exo70 and Exo84 were found to bind with the exocyst complex in *S. cerevisiae* and were named Exo for exocyst (Guo et al., 1999; TerBush et al., 1996). These exocyst components have also been identified in fission yeast, plants, trypanosomes, and mammals (Boehm et al., 2017; Elias et al., 2003; Hsu et al., 1996; Wang et al., 2002). While these proteins exhibit similar functionality between species, their amino acid sequence identity are very different showing that they are functional homologues of each other rather than sequential (Jourdain et al., 2012). The trypanosome exocyst was originally found to contain 6 of the 8 components found in mammals and fungi (Koumandou et al., 2007), however a recent study showed that they do contain all 8 classical subunits plus a novel ninth member called Exo99 (Boehm et al., 2017).

Further complexity of the exocyst complex is seen in mammals and plants. The exocyst of *Arabidopsis thaliana* has isoforms of most components with SEC3, SEC5, SEC10, and SEC15 having 2 isoforms, 3 for Exo84, and over 20 for Exo70 (Elias et al., 2003; Hála et al., 2008; Synek et al., 2006). Similarly to plants, mammals also possess splice variants for members of the exocyst (Lu et al., 2013). However they also have Exocyst-like proteins. One example is exocyst complex 3-like (Exoc3l) protein which has 31% identity and 53% similarity to Sec6 (Saito et al., 2008). Interestingly this is an apparent isoform of Sec6 but is encoded on a separate allele to Sec6 rather than being a splice isoform (Saito et al., 2008).

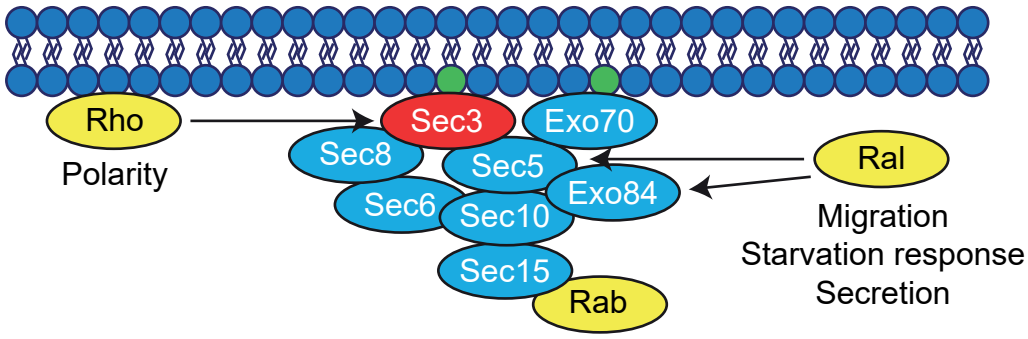

Sec3:

Figure 1.3: Sec3 is a member of the octameric exocyst complex. (Top panel) Illustration of the exocyst complex at the plasma membrane, showing key small GTPase regulators of the complex in yellow. Sec3 is highlighted in red. (Bottom panel) Domain architecture of Sec3. Amino acid positions are shown, with annotated structural domains shown in red. Arrows indicate the positions of mutations in the *sec3-913* mutant.

The exocyst complex is mainly found at regions of cell growth where it secretes materials needed to expand cell size, but also at sites of cell division (Boyd et al., 2004; Finger et al., 1998; Wang et al., 2002). This appears to be conserved throughout eukaryotes. In yeasts the exocyst is positioned at the site of the tips of new buds and the mother-bud neck in *S. cerevisiae* (TerBush et al., 1996), and the growing tips and division plane of fission yeast (Finger et al., 1998). Similar localisation to fission yeast is seen in the growing tips of root hair cells and pollen tubes of plants (Hála et al., 2008; Synek et al., 2006). In mammalian cells the exocyst is found at the leading edge where it helps with cell migration (Zuo et al., 2006), but also exhibits localisation to the synapses of neurons (Hazuka et al., 1999; Vik-Mo et al., 2003). Furthermore the exocyst localises to the site of mammalian cell division called the mid body (Chen et al., 2006; Gromley et al., 2005). This shows that the exocyst has conserved roles at sites of cell growth and division.

1.9 The exocyst is a tethering complex involved in exocytosis, endocytosis, and cell division

1.9.1 Exocytosis

The exocyst complex member Sec3 possesses a pleckstrin-homology (PH) domain in its N-terminus (Figure 1.3) which has been shown to be important for its recruitment to the plasma membrane (Baek et al., 2010; Yamashita et al., 2010). Exo70 is proposed to perform a similar interaction but via specific region in its N-terminus that contains lots of basic residues (He et al., 2007). Here they have been proposed to act as landmarks for the rest of complex that is thought to arrive on post-Golgi secretory vesicles in a myosin V dependent manner (Boyd et al., 2004). Further evidence for this model in budding yeast was shown when fusion of a transmembrane domain to either Sec3 or Exo70 resulted in exocyst assembly at the membrane (Liu et al., 2018). The localisation of Sec3 has been shown to be independent of other secretory components and the actin cytoskeleton, with the actin mutant act1-3 and the actin sequestering drug latrunculin-A not altering the position of Sec3 in fission yeast (Finger et al., 1998).

Instead the positioning of the exocyst to the correct site on the plasma membrane is performed by PIP_2 and the Rho GTPases. Sites requiring membrane expansion such as the growing tip in fission yeast and the leading edge of migrating mammalian cells are marked by the Rho family of GTPases, and this family is

important for the recruitment of the exocyst (Guo et al., 2001; Zhang et al., 2001). The N terminal PH domain of Sec3 is imperative for its binding to the polarity factor Cdc42, and the GTPase Rho1 (Zhang et al., 2001). Mutation of both Cdc42 and the PIP_2 kinase Its3 resulted in a loss of Sec3 localisation, showing that both Cdc42 and PIP_2 recruit Sec3 to the plasma membrane (Bendezú and Martin, 2011).

Once assembled, the exocyst is thought to tether secretory vesicles and complete secretion through an interaction with the SNARE complex. The budding yeast SNARES Sso1 and Sec9 assemble into a complex to exocytose secretory vesicles (Rossi et al., 1997). Mutation of the exocyst member Sec6 resulted in a block in SNARE complex assembly (Grote et al., 2000). This appears to be through an interaction between Sec6 and Sec9 where it was proposed that Sec6 releases Sec9 thus to interact with Sso1 stimulating SNARE complex assembly (Dubuke et al., 2015; Morgera et al., 2012). The model for how Sec9 is released from the exocyst is thought to be through an interaction between Sec6 and the SNARE regulator Sec1/Munc18 (Dubuke et al., 2015). The current model suggests that the binding of Sec1 to Sec6 causes the release of Sec9 (Morgera et al., 2012). This means that Sec6 may govern when and where SNARE complexes form at the plasma membrane (Morgera et al., 2012), meaning the exocyst may correctly position exocytic events to polarised regions of the plasma membrane. A caveat to this model is seen in neurons where secretion of synaptic vesicles can occur independently of the exocyst (Murthy et al., 2003). This suggests that SNAREs in mammalian neurons can form complexes independently of the exocyst.

1.9.2 Endocytosis

While it was thought the exocyst was solely involved in secretion it is now apparent that it also functions in the internalisation of cargo via endocytosis. To date, over 50 proteins have been found to play a role clathrin mediated endocytosis including components of the actin cytoskeleton (Goode et al., 2014). Endocytosis relies on the actin cytoskeleton to form a branched mesh work around clathrin coated pits that form on cargoes destined for internalisation (Ayscough, 2000; Gachet and Hyams, 2005). The branching of actin is dependent on the Arp2/3 complex which nucleates new filaments at 70^{o} angle off of existing mother filaments ultimately generating an actin mesh (Svitkina and Borisy, 1999;

Volkmann et al., 2001). Rapid polymerisation of this mesh stimulated by the myosin I family pulls the clathrin coated pit into the cytoplasm (Lee et al., 2000), which then pinches off in a dynamin dependent manner forming an endosome (Smaczynska-de Rooij et al., 2010). The actin meshwork surrounding the endosome is then depolymerised by cofilin (Lappalainen and Drubin, 1997).

Exo70 has been found to interact with the Arp2/3 complex by co-immunoprecipitation in mammalian cells (Zuo et al., 2006). Furthermore Sec3 is required for the polarisation of fission yeast endocytic patches which are generated by Arp2/3 showing that an interaction between the exocyst and Arp2/3 appears to be conserved from yeast to humans (Jourdain et al., 2012). The Arp2/3 complex is regulated by myosin-1 (Lee et al., 2000; Sirotkin et al., 2005), and by the Wiskott-Aldrich syndrome protein and Scar homologue (WASH) and WAVE complexes which regulate Arp2/3 nucleation of actin at different cellular locations (Duleh and Welch, 2010; Suetsugu et al., 1999). Using GST purified mammalian Exo70 and Sec6 bound directly to members of the WAVE complex (Biondini et al., 2016). Furthermore Sec8 and Exo84 co-immunoprecipitated with the WASH complex in HeLa cells (Monteiro et al., 2013). These studies show that the exocyst may interact with endocytic machinery via interacting with regulators of the Arp2/3 complex therefore controlling the spatial and temporal nucleation of actin patches.

Further conservation of the exocyst's role in endocytosis has been seen in many other organisms. The plant Exo70 isoform EXO70B1 co-localised with markers of clathrin-mediated endocytosis in tobacco pollen tubes (Sekereš et al., 2017), Exo70 and Exo84 mutants in *C. elegans* caused the accumulation of endocytic markers suggesting a role for them in endocytic recycling of endocytic cargoes (Jiu et al., 2012), and in *D. melanogaster* where Sec5 co-localised to with the endocytic vacuoles of oocytes and is needed to endocytose proteins involved in yolk uptake (Sommer et al., 2005). Furthermore knockdown of *Trypanosoma brucei* Sec15 and the 9th exocyst component Exo99 by RNAi slowed down the uptake of the lectin binding Concanavalin A, showing that endocytosis is also affected by the exocyst in trypanosomes (Boehm et al., 2017).

1.9.3 Cell division

The exocyst is also found at sites of cell division. Exocyst mutants in yeast display cell division defects, with phenotypes including multi-septation in fission yeast

(Bendezú et al., 2012; Jourdain et al., 2012). Work in fission yeast has identified that the exocyst is recruited to the division plane where it co-localises with endosomes, hinting towards a possible endocytic role of the exocyst during cytokinesis (Gachet and Hyams, 2005). The localisation of the exocyst the division plane is dependent on Rho GTPases. While being the markers of sites of polarised secretion, the Rho GTPases Rho3, and Rho4 are also indispensable for polarising the sites of cell division (Pérez et al., 2015; Wang et al., 2003). The regulation of the exocyst by Rho4 brings the exocyst into contact with the septin family of proteins where they are thought to secrete lytic enzymes that break down the septum causing cell separation (Martín-Cuadrado et al., 2005; Pérez et al., 2015). The *sec8-1* mutant strain is synthetic lethal when Rho3 is deleted, highlighting the importance of their interaction for cell survival.

While the exocyst appears to function in endocytosis and secretion of enzymes during division, it may also dictate the inheritance of organelles. Deletion of Sec3 in budding yeast leads perturbed inheritance of the cortical endoplasmic reticulum across the mother-bud neck (Wiederkehr et al., 2003). Interestingly this action of the exocyst is ER specific as both the Golgi and mitochondria were inherited correctly in the absence of Sec3 (Wiederkehr et al., 2003). All in all it still remains unclear what role the exocyst plays during cytokinesis.

Due to the roles the exocyst plays in growth and division, it is unsurprising that a non-functional exocyst can lead to severe cellular defects and disease.

1.10 The exocyst complex in disease

Both Exo70 and Sec3 are conditionally essential in budding and fission yeast (Bendezú and Martin, 2011; Kim et al., 2010), highlighting their importance for growth, division and survival. Mutation of Sec3 in fission yeast leads to multiseptation and issues with cell division, plus an increase in width which is associated with changes in cortical actin (Jourdain et al., 2012). These changes reveal a role for the exocyst in morphology. It was proposed that the morphology of fission yeast is established via the exocyst and actin cytoskeleton which are both polarised by Cdc42 but act independently of each other (Bendezú and Martin, 2011). However evidence against is that mutation of *sec3* causes the abolishment of formin mediated actin cables which are required for transport, and also depolarisation of actin patches which are required for endocytosis (Jourdain

et al., 2012). This revealed that rather than actin and the exocyst controlling morphology independently of each other, Sec3 might bridge the two pathways together, positioning Sec3 as a key regulator of morphology. Therefore the exocyst is important for the establishment of cellular morphology.

In higher eukaryotes cell polarity and morphology is paramount for cells to perform tissue specific functions correctly. Neurons are highly polar cells that function to create complex circuits within the central and peripheral nervous systems. They possess a region of arborized dendrites which receive signals, a soma which houses the cell body and nucleus, and an axon that sends signals to neighbouring neurons or target organs (Hall and Sanes, 1993; Li and Sheng, 2003). Kidney cells must be able to polarise to form apical and basolateral membranes which are specialised for different functions. Fibroblasts and immune cells must be able to rapidly repolarise their growth to allow for directional migration which is important for wound closure and also immunity. The exocyst has been found to play a role in all of these (Wu and Guo, 2015).

1.11 The exocyst is important for polarisation and morphology of neurons

Transmission of signals from neurons occurs via the exocytosis of neurotransmitters from specialised structures called the synapse which are located at the end of the axon. These are received by receptors positioned on the dendrites, which relay the signal by producing an action potential throughout the neuron. The exocyst appears to mark the site of future synapse formation (Hazuka et al., 1999), but plasma membrane localisation of Sec6 has also been seen in the mature synapse (Vik-Mo et al., 2003). This polarisation appears to be the result of an interaction between the exocyst and the Par3-aPKC-Par6 (Partitioning-defective and atypical protein kinase C) where the exocyst has been shown to traffic this complex to polarised zones where Par-aPKC operates in feedback loop to promote further exocyst delivery (Ahmed and MacAra, 2017; Lalli, 2009).

Positioning of the exocyst is important for synaptic plasticity where Sec8 and the GTPase RalA bind to the scaffold protein post-synaptic density 95 (PSD-95) and regulate the trafficking of the N-methyl-D-aspartic acid (NMDA) and a-amino-3-hydroxy-5-methyl-4-isoxazolepropionic acid (AMPA) neurotransmitter receptors (Gerges et al., 2006; Sans et al., 2003). Synaptic plasticity is thought to underlie

learning and memory (Bliss and Collingridge, 1993), making the exocyst-RalA interaction an integral part of this process. Contrary to this, mutation of Sec5 in *Drosophila melanogaster* did not affect secretion of neurotransmitters which rely on SNAREs for exocytosis (Murthy et al., 2003). It is not clear as to whether this type of exocytosis is specific to neurons, but it raises questions about the functional relationship between the exocyst and the SNAREs complex in higher eukaryotes.

While Sec5 did not affect neurotransmitter secretion, mutation of the exocyst member resulted in a loss of neurite outgrowth showing the exocyst affects neuronal morphology (Murthy et al., 2003). Neurite outgrowth depends on a specialised structure at the leading membrane of the axon called growth cones (O'Donnell et al., 2009). These structures are rich in protrusions called filopodia which sense the environment for chemoattractants released by neighbouring neurons in order to form synapses with neighbouring dendrites (O'Donnell et al., 2009). The exocyst localises to filopodia where it is thought to secrete materials needed for the growth of the axon, however it may also modulate the actin cytoskeleton within the filopodia (Sugihara et al., 2002). While the exocyst appears to be important for neurite outgrowth, research also suggests it plays a role in morphology of dendritic region at the other pole. The worm *Caenorhabditis elegans* contains a highly branched sensory neuron called the PVD which is an excellent model for studying neuronal morphology and development (Albeg et al., 2011). Interaction between *C. elegans* Rab10 and the exocyst is important for dendritic morphology of the PVD (Taylor et al., 2015; Zou et al., 2015). In disagreement with these studies deletion of the exocyst member Sec15 in *D. melanogaster* does not affect morphology of photoreceptor neurons but they fail to connect to the correct circuit (Mehta et al., 2005). Taken together these studies show that exocyst is present at the polar regions of the neuron where it regulates morphology and the fine-tuning synaptic membranes.

1.12 The exocyst complex is required for apical and basolateral determination

The epithelial cells of multicellular organisms organise in an adjacent manner and connect through cell-cell junctions that include desmosomes and adherens junctions. Adhesion is regulated via the cadherin family of adherens molecules (Hill et al., 2001; Nollet et al., 2000). When these adhesion molecules mediate

cell-cell contact, the exocyst is recruited from cytoplasmic pools to the adherens junctions in a Rab dependent manner (Andersen and Yeaman, 2010; Jafar-Nejad et al., 2005). This relationship was found to be cadherin dependent as the exocyst no longer localises to cell-cell junctions in cell lines lacking cadherin molecules (Yeaman et al., 2004). In Madin-Darby canine kidney (MDCK) cells, knockdown of Exo70 and Sec3 affects E-cadherin and desmosome localisation respectively (Andersen and Yeaman, 2010; Xiong et al., 2012).

The relationship between the exocyst and cell-cell contacts is important for the role of the epithelium as a protective barrier, especially against infection. The bacterium *Vibrio cholerae* secretes Cholera toxin which has been shown to weaken the cell-cell junctions of the intestinal epithelium through inhibiting Rab11/exocyst E-cadherin trafficking to adherens junctions (Guichard et al., 2013). This results in disruption of the endothelial barrier leading to an efflux of water over the barrier which causes the characteristic watery diarrhoea seen in *V. cholera* infections. Similarly *Bacillus anthracis* also targets the exocyst E-cadherin pathway in the endothelial barrier leading to vascular leakage (Guichard et al., 2010).

The role of the exocyst in determining apical and basolateral polarity is not just important for the trafficking and localisation of junctions, but also cargoes. Insulin signalling in adipocytes results in the activation of the G protein TC10 which has been found to recruit the exocyst and along with it GLUT4 containing vesicles to the plasma membrane for secretion (Inoue et al., 2003). Lipid raft domains in adipocytes contain the insulin receptor, TC10, and the exocyst making the polarisation of lipid domains an integral part of insulin signalling (Inoue et al., 2006; Watson et al., 2001). Failure to traffic GLUT4 to the apical membrane results in the high blood glucose seen in diabetes.

Another important factor for establishing cell polarity is the trafficking of intracellular cargoes in a retrograde fashion. Endocytosis can occur at apical and basolateral regions and rely on different Rab GTPases to direct them (Zhang et al., 2016). The exocyst members Sec8 and Exo70 were found to co-localise with basal and ectopic recycling endosomes positive for the transferrin receptor (Tf) (Oztan et al., 2007). The same exocyst members were also found to be situated on apical recycling endosomes (ARE) which are marked by the GTPase Rab11

(Oztan et al., 2007). The C-terminus of Sec15 was also found to be important in the recruitment of Rab11a to the medial region of MDCK cells (Oztan et al., 2007).

1.13 The exocyst is involved in cell migration

Another important process in higher eukaryotes is cell migration. Examples of this include immune cells which need to migrate in order to move after pathogens and subsequently endocytose and break them down. Fibroblasts also need to be motile so that wound closure can be completed after an assault to the skin.

Mutation of the exocyst member Sec3 in fission yeast resulted in loss of polarisation of endocytic actin patches and slower endocytosis (Jourdain et al., 2012). While Arp2/3 has a sole role in endocytic actin patches in fission yeast, it is important for many processes in mammalian cells, one being cell migration. RalB and the exocyst has been shown be important in this function (Rosse et al., 2006). Knockdown of either the exocyst or RalB reduced motility of fibroblasts in a scratch assay (Rosse et al., 2006). RalB was found to bind to Sec5 of the exocyst where it appears to recruit exocyst members to the leading edge of migrating cells (Rosse et al., 2006). This could presumably be due to the exocyst being required for secretion of components needed to grow the leading edge, however RalB recruitment could also stimulate the interaction between the exocyst and the cortical actin meshwork via the Arp2/3 complex (Zuo et al., 2006).

Cell migration is also a key part of tumour metastasis where projections called invadipodia secrete matrix metalloproteinases (MMPs) to break down the extracellular matrix and invade surrounding tissue. The exocyst is positioned at the tip of these projections where it delivers material, but also interacts with the actin in these protrusions through the Arp2/3 complex (Liu et al., 2009). The exocyst Arp2/3 interaction in invadipodia formation is due to a splice isoform of Exo70 generated by the pre-mRNA splicing factor ESRP1 (Lu et al., 2013). This isoform interacts with Arp2/3 to branch actin and generate projections during the epithelial-mesenchymal transition (EMT) where cells lose contact with the matrix and can become motile and invasive (Lu et al., 2013).

1.14 Autophagy requires the exocyst

Autophagy is a process in which the cell breaks down components that are faulty or are recycled into metabolites in response to starvation. Nutrients activate TORC1 signalling which subsequently causes the phosphorylation of the

autophagy protein Atg13 (Kamada et al., 2010). This event ensures that Atg13 cannot interact with the key autophagy protein Atg1, preventing the process from occurring. When nutrients are depleted, TORC1 is switched off and rapid dephosphorylation of Atg13 occurs, leading to autophagic events (Kamada et al., 2010). Mutation of budding yeast *sec3*, *sec5*, *sec6*, *sec8*, *sec10*, and *exo84* blocked the selective breakdown of peroxisomes (pexophagy) (Singh et al., 2019). This was found to be due to exocyst dependent trafficking of Atg9 which is required for membrane addition and maturation of the autophagosome (Singh et al., 2019). Furthermore it was found that RalB and Exo84 interact with Beclin-1 in response to nutrient starvation to activate autophagosome biogenesis thus activating autophagy (Bodemann et al., 2011). These findings reveal a role for the exocyst in autophagosome formation and maturation.

In plants an exocyst subcomplex containing the Exo70 isoform EXO70B1 colocalised with ATG8 and is involved in the internalisation of autophagic bodies into the vacuole (Kulich et al., 2013). Interestingly Exo70 is was found not to be involved in autophagy in budding yeast (Singh et al., 2019). The conclusion that can be drawn from these studies is that the exocyst has a conserved function in autophagy but different exocyst members may have taken on these roles in different species.

1.15 The exocyst is involved in primary ciliogenesis

Most mammalian cells contain a signalling organelle called the primary cilium, which is situated on the cell surface and protrudes in a microtubule dependent manner. Developmental disease such as Meckel-Gruber, Bardet-Biedl, and Joubert syndrome arise when the cilia are non-functional. Knockdown of the exocyst component Sec10 by short hairpin RNA and overexpression by stable transfection showed that Sec10 regulates primary ciliogenesis in MDCK cells (Zuo et al., 2009). Furthermore the exocyst members Sec6 and Sec8 have been shown to localise to the primary cilium by fluorescence microscopy (Babbey et al., 2010; Rogers et al., 2004), adding weight to the argument that the exocyst is involved in ciliogenesis.

1.16 What accounts for the diverse functions of the exocyst?

Evidence for differential roles of exocyst complex subunits is becoming more abundant. This is mainly seen in the exocyst's role in autophagy. In budding yeast

only certain members of the complex were found to affect pexophagy, while both Sec15 and Exo70 had no effect (Singh et al., 2019). This proposes the model of a 6 member exocyst complex without Sec15 and Exo70 that is involved in autophagy. In higher eukaryotes evidence of different functions and possible subcomplexes containing Sec6 also adds weight to this argument. Sec6 was shown to localise to multiple cellular compartments depending on what epitope was stained for by immunofluorescence (Inamdar et al., 2016). Antibodies towards the N-terminus of Sec6 revealed cytoplasmic and nuclear localisation, while epitopes on the C-terminus showed localisation to desmosomes, the endoplasmic reticulum, and intermediate filaments (Inamdar et al., 2016).

However a landmark study dissecting the assembly of the exocyst complex provides evidence against the idea of subcomplexes. Through the tagging of every exocyst member with an auxin inducible degradation (AID) tag, it was possible to see how the complex precipitated in the absence of each member (Heider et al., 2016). This studied showed that the complex forms as two 4 subunit holocomplexes, one consisting of Sec3, Sec5, Sec6, and Sec8, and the other consisting of Exo70, Exo84, Sec10, and Sec15 (Heider et al., 2016). Furthermore all members pulled down each other at a 1:1 stoichiometry meaning that they are likely to all be assembled as an 8 protein complex at all times (Heider et al., 2016). However the authors do mention that if there are sub-complexes they are likely to occur at low levels which are not sensitive to biochemistry (Heider et al., 2016).

Another consideration is the presence of isoforms in mammalian cells and plants. In plants the Exo70 isoform EXO70A1a was found to localise to PIP_2 rich regions at the tip of pollen tubes similarly to the classical localisation of the component in other organisms (Sekereš et al., 2017). This localisation is important for the secretory role of the exocyst (Zhang et al., 2001). Conversely the Exo70 isoform EXO70B1 was found to colocalise more with phosphatidic acid (PA) than PIP_2 (Sekereš et al., 2017). The binding of EXO70B1 with PA is associated with an endocytic role of the exocyst. EXO70B1 is also involved in autophagy where as EXO70A1 does not (Kulich et al., 2013). Evidence in mammalian cells also agrees with this. Certain splice isoforms of Exo70 cannot interact with the Arp2/3 complex (Lu et al., 2013), showing that these variants are needed for separate processes.

1.17 Structure of Sec3

The amino acid sequence of Sec3 in fission yeast shares a 13.2% sequence identity with that of the human EXOC1 (Jourdain et al., 2012). However it was shown that growth of *sec3* mutants in fission yeast can rescued by transformation with a plasmid containing the gene for human Sec3, *EXOC1* (Jourdain et al., 2012). This shows that the Sec3 protein between species is functionally homologous.

To analyse the structure of Sec3, crystallography has been performed to determine which domains the protein possesses. The N terminal residues (71-241) of Sec3 was successfully crystallised in budding yeast (Baek et al., 2010). It was found that this region folded in to a pleckstrin homology domain (PH) and three variable loops that form a phosphoinositide-binding pocket (Baek et al., 2010). The C-terminal region between residues 320 and 470 of Sec3 is annotated as a coiled-coil domain and between residues 610 and 727 is predicted to form helical bundles which is characteristic of the other members of the exocyst (Munson and Novick, 2006). It remains unclear what roles these domains play.

The N terminus of Sec3 is not only important for targeting the exocyst and its function (Zhang et al., 2001), but recent work has identified that Sec3 is also the target for phosphorylation and activation of the exocyst (Tay et al., 2019). Recently fission yeast Sec3 was identified as a target of Orb6 kinase where it phosphorylates the exocyst member at serine 201 (Tay et al., 2019). Mutation of *sec3* with S201A revealed that the phosphorylation of Sec3 is not important for localisation to the plasma membrane (PM) but is imperative for its function in exocytosis (Tay et al., 2019). Taken together these studies propose two distinct functions of the N terminus of Sec3 in which the PH domain and phosphoinositide-binding pocket target to the protein to Cdc42 and PIP_2 rich domains, where it is then activated in a Cdc42-Orb6-Sec3 fashion to promote exocytosis. The exocyst member Sec5 was also found to be phosphorylated by Orb6 (Tay et al., 2019). Sec5 was also identified as a strong pairwise interactor with Sec3, in fact Sec3 was found to only bind to Sec5 (Heider et al., 2016). This means the Sec3-Sec5 region of the exocyst is where it is activated for secretion.

1.17.1 Sec3/EXOC1 in mammalian cells

In mouse mammary cells it was shown that Sec3/EXOC1 departs from the complex before fusion of the secretory vesicle with PM occurs (Ahmed et al., 2018). The authors suggest that the departure of Sec3 allows the SNARE complex to trigger exocytosis (Ahmed et al., 2018). Further evidence for a role for Sec3 in SNARE complex formation has been seen in yeast. Sec3 was found to interact with the SNARE Sso2 by yeast 2-hybrid and co-immunoprecipitation and this promotes the formation of a complex between Sso2 and Sec9 (Yue et al., 2017). Furthermore Sec9 displaces Sec3 (Yue et al., 2017), which could mean that Sec9 causes Sec3 to be displaced from the exocyst complex explaining why it is seen to fall off during mammalian cell exocytosis.

Sec3 is also integral to cellular adhesion. Work in mammalian epithelial cells has revealed that Sec3 is recruited to sites of cell-cell contact in an E-cadherin dependent manner where it helps to assemble desmosomes (Andersen and Yeaman, 2010). Knockdown of Sec3 reduced the stability of desmosomes and showed weaker cell adhesion after cell trituration showing that Sec3 is important for cell-cell adhesion (Andersen and Yeaman, 2010).

Studies in animals have also revealed that Sec3 plays a key role in development. Of nine genes that are deleted mice exhibiting ventral depigmentation, Exoc1 was found to be the causative allele that contributed to this phenotype (Mizuno et al., 2015). Interestingly *Exoc1*$^{-/-}$ mutant embryos exhibited a peri-implantation lethality phenotype, highlighting that Sec3 is important for embryonic development (Mizuno et al., 2015). Development of the egg chamber in *Drosophila melanogaster* was also found to be perturbed by loss of Sec3 (Wan et al., 2019). Knockdown of Sec3 caused accumulation of Notch signalling molecules that are required for growth and development leading to fusion of the egg chamber (Wan et al., 2019). This was presumably due to a loss of exocytosis, showing that Sec3 is important for development through Notch signalling (Wan et al., 2019).

1.17.2 Degradation and turnover of Sec3

Surprisingly little is known about the turnover or regulation of exocyst expression. Recent work in fission yeast has shown that Sec3 is degraded via the proteasome pathway. The temperature sensitive phenotype of *sec3-913* is rescued in the presence of proteasome inhibitors and also when protein members of the

proteasome are not functional revealing (Kampmeyer et al., 2017). Furthermore wild-type Sec3 protein was found to have a half-life of around 8 hours, whereas Sec3-913 degraded at a half-life of around 2 hours showing that the mutant protein is more readily degraded than the wild type (Kampmeyer et al., 2017). Blocking the proteasome with bortezimib stopped degradation of both proteins showing that Sec3 is degraded via the proteasome (Kampmeyer et al., 2017). This mechanism involves the E3 ubiquitin-protein ligase Pib1 and the deubiquitylating enzyme Ubp3 (Kampmeyer et al., 2017). The rescue via the deletion of the UPS components is probably due to raising intracellular levels of the Sec3-913 protein as it has previously been shown that over-expression of Sec3-913 via ectopic expression also rescues the temperature sensitive phenotype (Jourdain et al., 2012).

The exocyst is gradually becoming characterised in many systems, however the fundamentals of how it performs its function and trafficking and in other roles remains elusive. Further complexity is seen in higher eukaryotes with the presence of isoforms. In order to study how the exocyst is involved in nutritional sensing and signalling a simpler organism may provide a clearer picture. Nutritional sensing and metabolism in the fission yeast *S. pombe* has been well characterised and is very similar to metabolism in higher eukaryotes. The yeast also lacks isoforms of the exocyst making it easier elucidate the function of each exocyst component. Therefore fission yeast are a useful tool to investigate the relationship between the exocyst and nutrient metabolism.

1.18 The fission yeast *S. pombe* as a model organism

The fission yeast *S. pombe* is a unicellular eukaryote that is a powerful tool for the study of molecular and cellular biology for many reasons. Due to it being a single celled organism, it is possible to analyse large numbers of cells allowing for easy analysis of genetic interactors, and robust statistical power of data generated from experiments. Fission yeast can be grown in various conditions. Suspended growth in liquid culture can produce a large amount of cells that can be processed to produce concentrated protein lysates allowing for consistent biochemical analysis. Fission yeast can also grow a large variety of different solid media. This allows for analysis of how mutants grow in different nutrient conditions by changing the carbon and nitrogen sources, how they respond to drugs that target specific pathways and also allows for easy selection of mutants.

Genetic manipulation is easy to perform due to strains being haploid and possessing only one copy of each chromosome making gene edits easier than in higher eukaryotes which require both copies to be modified. Fission yeast can perform homologous recombination of genetic material which can be utilised to introduce modified alleles producing strains possessing genes which are mutated, tagged, or even deleted. Furthermore crossing and selection of new strains is easily performed allowing for the generation of strains possessing multiple modified alleles, which are a great tool for studying protein and genetic interactions.

The biology of *S. pombe* is highly conserved and is more common with higher eukaryotes than the budding yeast *S. cerevisiae*. Fission yeast contain conserved components of the actin cytoskeleton which are involved in cell morphology in both yeast and higher eukaryotes (Takaine and Mabuchi, 2007). Due to the highly polar, uniform, cylindrical shape of *S. pombe*, it is a great model for dissecting the mechanisms behind the establishment of polarity, cell morphology, and polarised trafficking of secretory and endocytic cargoes. The growth and stress signalling pathways including TOR and cAMP/PKA are also highly conserved between fission yeast and higher eukaryotes (Hatanaka and Shimoda, 2001; Nakashima and Tamanoi, 2010), making it a great model for the assessment of cellular responses to stress and nutrient availability.

1.19 Cell growth and division is well defined in *S. pombe*

Fission yeast proved to be a powerful tool in the dissection of the mechanisms behind cell growth and division. The elegant work of Sir Paul Nurse that led to the discovery of cyclins utilised the simplicity of cell length phenotypes to understand which genes were involved promoting mitotic commitment (Russell and Nurse, 1986). Furthermore fission yeast divides through the formation of a division plane in the middle of the cell which constricts via tension generated by the highly conserved contractile actinomyosin ring (CAR). Extensive work has been performed in *S. pombe* to understand the components of the division plane, how it forms, and how it is resolved. These studies have provided the foundation of the fundamental processes behind cell growth and division which have been translated into mammalian systems where they have informed our understanding of mammalian cell growth and division, which has been particularly useful in the generation of treatments towards cancer.

The fission yeast *S. pombe* is a highly polar organism that grows outwards from bipolar tips, and divides through a septum located in the middle (Figure 1.4). After division the mother tip continues to grow exclusively until a phase called New End Take Off (NETO) begins at the opposite end resulting in bipolar growth (Mitchison and Nurse, 1985). The site of growth is dependent on a complex of proteins called the polarisome which is positioned at the tip of growing ends (Martin et al., 2005;

Miller and Johnson, 1994). This complex contains many proteins important for determining polarity, such as the Rho family of GTPases (Miller and Johnson, 1994). The trafficking of cargo needed to expand the growing tip is actin dependent in fission yeast (Boyd et al., 2004; Govindan et al., 1995). The formin For3 is present in the polarisome and is important for the formation of actin filaments that emanate from the tip and provide tracks for secretory trafficking (Feierbach and Chang, 2001). The anterograde trafficking of post-Golgi secretory vesicles destined for the growing tip occurs in a myosin V dependent manner (Govindan et al., 1995). Another actin structure present at the growing tip is the endocytic actin patch (Gachet and Hyams, 2005). This structure is dependent on nucleation by the Arp2/3 complex (Sirotkin et al., 2005). The role of endocytosis at the growing tip is unclear, but it is possibly involved in the remodelling of the cell wall which displays dynamic changes in thickness during growth (Davì et al., 2018; Lesage et al., 2005).

Plasma membrane lipid content has also been shown to affect polarisation of fission yeast. Unlike mammalian cells which utilise cholesterol as the main sterol in the plasma membrane, *S. pombe* mainly uses ergosterol. Sterol domains have been proposed to be important in establishing the polarity of fission yeast, where it aids the recruitment and localisation Cdc42 (Makushok et al., 2016). Endocytosis functions to remove ectopic sterols so that they are focussed at the growing tip (Makushok et al., 2016).

Fission yeast can grow up to 15 μm length and at this point mitosis can be initiated. Mitosis is promoted by the cyclin dependent kinase Cdk1 (Wood and Nurse, 2015). Cdk1 itself is inhibited via phosphorylation from the kinase Wee1 (Wood and Nurse, 2015). Deletion of Wee1 promotes early entry into mitosis due to the loss of inhibition of Cdk1, causing cells to exhibit shorter length than normal (Wood and Nurse, 2015). Cell length is linked to mitosis via the kinase Pom1 (Moseley et al., 2009). Pom1 is localised to the growing tips and creates a

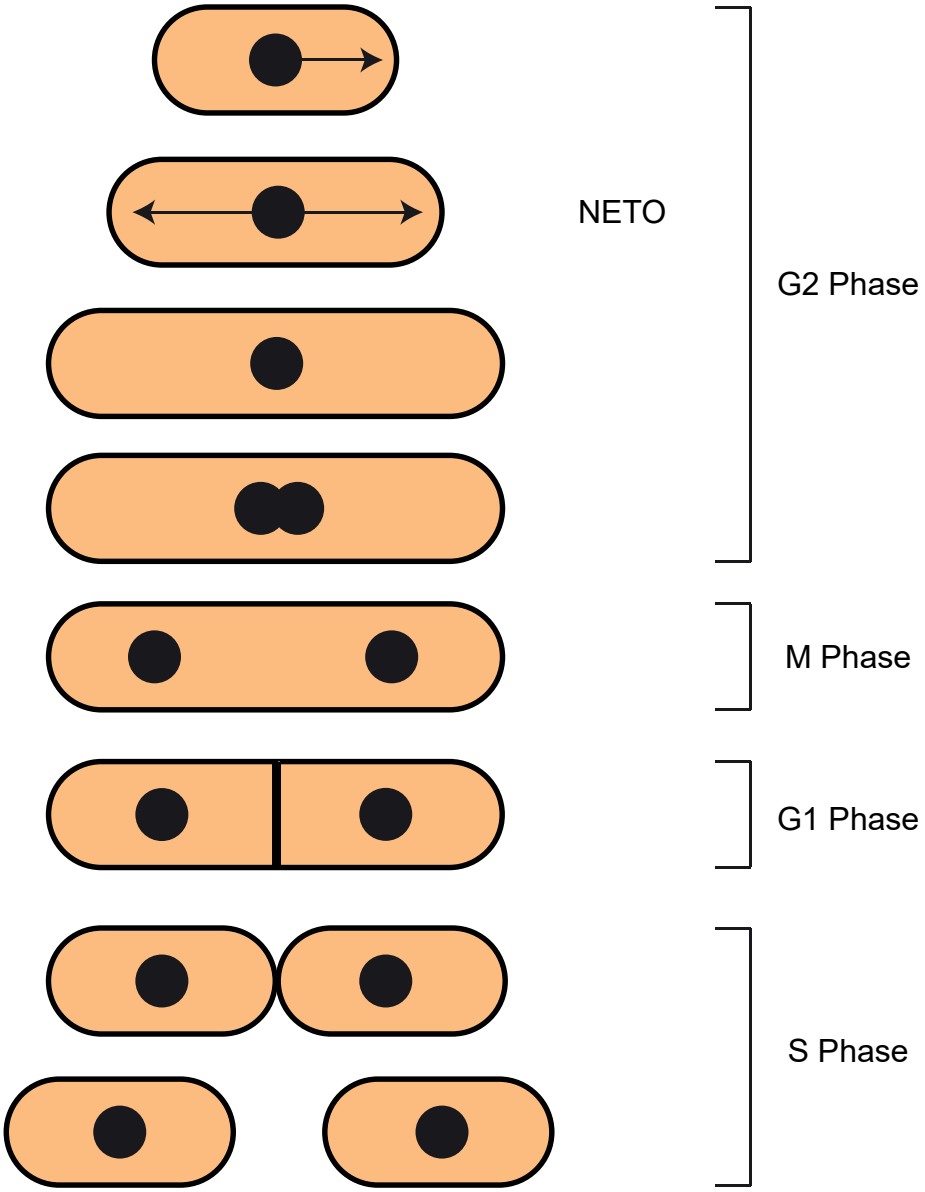

Figure 1.4: The cell cycle of fission yeast *Schizosaccharomyces pombe*.

gradient which keeps Wee1 active, inhibiting mitosis (Moseley et al., 2009). As the tips grow, the gradient of Pom1 in the middle of the cell gets weaker and Wee1 activity becomes reduced allowing Cdk1 to promote mitosis (Moseley et al., 2009).

Cytokinesis requires the positioning of the CAR to site of division (Hachet and Simanis, 2008; Pu et al., 2015). Once in place the CAR determines the site of septum formation which creates the cell wall for the ends of the mother and daughter cell (Martín-García et al., 2014). For cytokinesis to be completed the CAR needs to constrict in a myosin type II dependent manner and closes the cleavage furrow resulting in the separation of the cells (Kitayama et al., 1997).

1.20 Nutrient sensing in *S. pombe*

1.20.1 Glucose

As mentioned previously fission yeast utilise glucose for the production of ATP, but unlike higher eukaryotes which respire, *S. pombe* prefers fermentation (Malecki et al., 2016). Fission yeast contains 6 hexose transporters (Heiland et al., 2000). Glucose entry into the cell and subsequent sensing causes a rise in intracellular cyclic-AMP (cAMP) through activation of the G-protein Gpa2 which activates the enzyme adenylate cyclase (Thevelein, 1984; Welton and Hoffman, 2000). The rise in cAMP causes activation of the protein kinase A (PKA) pathway (Byrne and Hoffman, 1993). PKA signalling functions to regulate growth and cell cycle progression (Yu et al., 2005). This signalling pathway also causes changes in the expression of genes related to glucose signalling (Cherry et al., 1989).

Glucose also activates the TORC2 complex through two mechanisms. Firstly the activation of PKA signalling was found to have a positive on TORC2 signalling (Cohen et al., 2014). Deletion of various G proteins which activate Pka1 inhibited the phosphorylation of the downstream target of TORC2, Gad8 kinase (Cohen et al., 2014). A second PKA independent mechanism has also been described. Glucose signalling activates the Rab-like GTPase Ryh1 which interacts with TORC2 via the complex member Bit61 causing activation of TORC2 signalling (Hatano et al., 2015). TORC2 signalling signals to inhibit stress signalling through negative interactions with kinases in the SAPK signalling pathway and promotes of amino acids (Hartmuth and Petersen, 2009; Weisman et al., 2005).

1.20.2 Amino acids

Amino acids in fission yeast can be synthesised de novo through biosynthetic pathways, or taken up from the environment. While it has not been shown in *S. pombe*, the budding yeast vacuole is the site of storage for amino acids meaning that this is likely to occur in fission yeast (Wiemken and Dürr, 1974). The presence of amino acids in the vacuole, particularly leucine, promotes the recruitment of TORC1 to the vacuole via activation of the Rag family of GTPases (Binda et al., 2009). When inactive the Rags display a nucleotide pattern where Gtr1/2 are bound to GDP, and Gtr3/4 to GTP (Kira et al., 2016). Activation by amino acids switches this conformation (Kira et al., 2016; Sancak et al., 2008). Recruitment of TORC1 to the Rags brings the complex in contact with the Ras GTPase Rheb which activates Tor2 kinase, promoting signalling for growth and division (Bai et al., 2007). Conversely fission yeast TORC2 signalling does not appear to be activated by amino acids, but instead regulates the uptake of leucine (Weisman et al., 2005). This could represent a positive feedback loop where TORC2 acts to promote TORC1 signalling by refilling the cell with amino acids.

Amino acid starvation also triggers a cellular stress response that is not transduced through the Tor signalling axis. The general amino acid control (GAAC) pathway budding in yeast and the mammalian amino acid response (AAR) are examples of these (Hinnebusch, 2005; Kilberg et al., 2012). These processes are regulated by the conserved Gcn2 protein kinase family which senses cellular amino acid levels via tRNAs and functions to repress mRNA translation through the phosphorylation of eIF2 in response to amino acid starvation (Dever et al., 1992). Gcn2 controls translation of stress response genes through transcription factors, with Gcn4p and ATF4 being the transcription factors in budding yeast and mammals respectively (Dever et al., 1992; Kilberg et al., 2009). Recently the fission yeast Gcn4 homologue, Fil1, was identified (Duncan et al., 2018). Despite the low sequence homology between Fil1 and Gcn4/ATF4, transcriptomics of cells treated with 3-amino-1,2,4-triazol (3-AT) to stimulate amino acid starvation revealed Fil1 regulates the expression of similar genes to its homologues (Duncan et al., 2018). Fil1 is also regulated in a similar manner to its homologues, via the kinase Gcn2 (Duncan et al., 2018).

1.20.3 Vacuoles and autophagy

As mentioned above, it is presumed that amino acids are stored in the yeast vacuole (Wiemken and Dürr, 1974). The vacuole shares many similarities to the mammalian lysosome as it is the site of protein recycling and degradation. The vacuole is also involved in the process of autophagy (Tucker et al., 2003). Autophagy is stimulated by rapid changes in the environment, including starvation (Shang et al., 2011). It is a non-specific process required for the breakdown of bulk protein from faulty organelles and proteins destined for turnover (Marshall and Vierstra, 2018). The formation of a vesicle deemed the autophagosome is required for the isolation of these proteins and organelles, which then fuses with the lytic vacuole to break them down (Liu and Klionsky, 2016). Autophagy is inhibited by TOR where active TORC1 signalling phosphorylates the autophagy (Atg) protein Atg13 (Kamada et al., 2010). Phosphorylation of Atg13 inhibits it's binding to the key autophagy serine/threonine kinase Atg1 (Kamada et al., 2010). Loss of TORC1 signalling allows Atg13 to bind to Atg1 stimulating autophagy (Kamada et al., 2010).

While most autophagy is non-specific, selective pathways for specific organelles exist (peroxisomes = pexophagy, mitochondria = mitophagy etc.). Budding yeast possess 30 proteins involved in autophagy (Mukaiyama et al., 2010). However it was found that fission yeast lack 9 of these proteins (Mukaiyama et al., 2010). It is unclear whether these have not been characterised in *S. pombe* yet, or whether they do not exist in this organism. Of these 9 genes many of them are involved in selective autophagy, including the pexophagy specific Atg28-30 and the mitophagy specific Atg32 and Atg33 (Mukaiyama et al., 2010). This highlights that selective autophagy of organelles remains to be discovered in fission yeast.

Fusion of vacuoles is required for autophagy and this is regulated by the Rab family of GTPases. Deletion of the Rab7 homologue Ypt7 in fission yeast resulted in the formation of vacuoles with a small diameter indicating that Ypt7 is crucial for fusion of vacuoles (Kashiwazaki et al., 2009). Conversely deletion of another Rab7 homologue Ypt71 resulted in large, oversized vacuoles (Kashiwazaki et al., 2009). This has led to the model that Ypt7 and Ypt71 play opposing roles in vacuole fusion (Kashiwazaki et al., 2009).

1.21 The fission yeast exocyst

As mentioned earlier fission yeast possesses all 8 exocyst subunits that appear to be homologous in terms of function rather than sequence identity (Jourdain et al., 2012). However the characterisation of the function of the exocyst is not as extensive in fission yeast as it is in budding yeast and higher eukaryotes. The positioning of the complex and the regulatory GTPases in these processes have been defined (Figure 1.5). The fission yeast exocyst components Sec3 and Exo70 localised to the growing tip independently of actin and instead through Cdc42 and PIP_2 at the growing tip (Bendezú and Martin, 2011). Recruitment of the exocyst to the division plane is performed via Rho3 where it is proposed to be involved in both endocytosis and secretion lytic enzymes at the septum via an interaction with the septin family of proteins (Pérez et al., 2015; Wang et al., 2003). These show the fission yeast exocyst is involved in both growth and division in fission yeast.

One of the best characterised exocyst proteins in fission yeast is Sec3 which is an essential gene in this organism (Kim et al., 2010). The temperature sensitive mutants *sec3-913* and *sec3-916* were generated by mutagenic polymerase chain reaction (PCR) and have defects in septation, secretion, morphology, and both the formation of actin cables and polarisation of endocytic patches (Jourdain et al., 2012). Furthermore Sec3 interacts with the formin For3 at the growing tip, and components of endocytic actin patches revealing a role for Sec3 in regulation of the actin cytoskeleton (Jourdain et al., 2012). The osmotic stressor sorbitol rescues the growth of *sec3* mutants which was proposed to be through altering the membrane tension in this strain by altering osmotic gradients (Bendezú et al., 2012). It is possible that Sec3 may remodel the cell wall and therefore alter membrane tension, however no cell wall defects were seen in *sec3-913* and *sec3-916* (Jourdain et al., 2012). Ultimately it is still unclear if Sec3 regulates membrane tension.

1.22 Aims and strategy

The aim of this thesis is to further the understanding of the role the exocyst plays in nutrient and stress sensing and the bridge between this and growth signalling. To achieve this I have used *Schizosaccharomyces pombe* a model organism due to its ease of genetic manipulation. To answer various questions I have used a combination of growth assays, live cell fluorescence microscopy, and

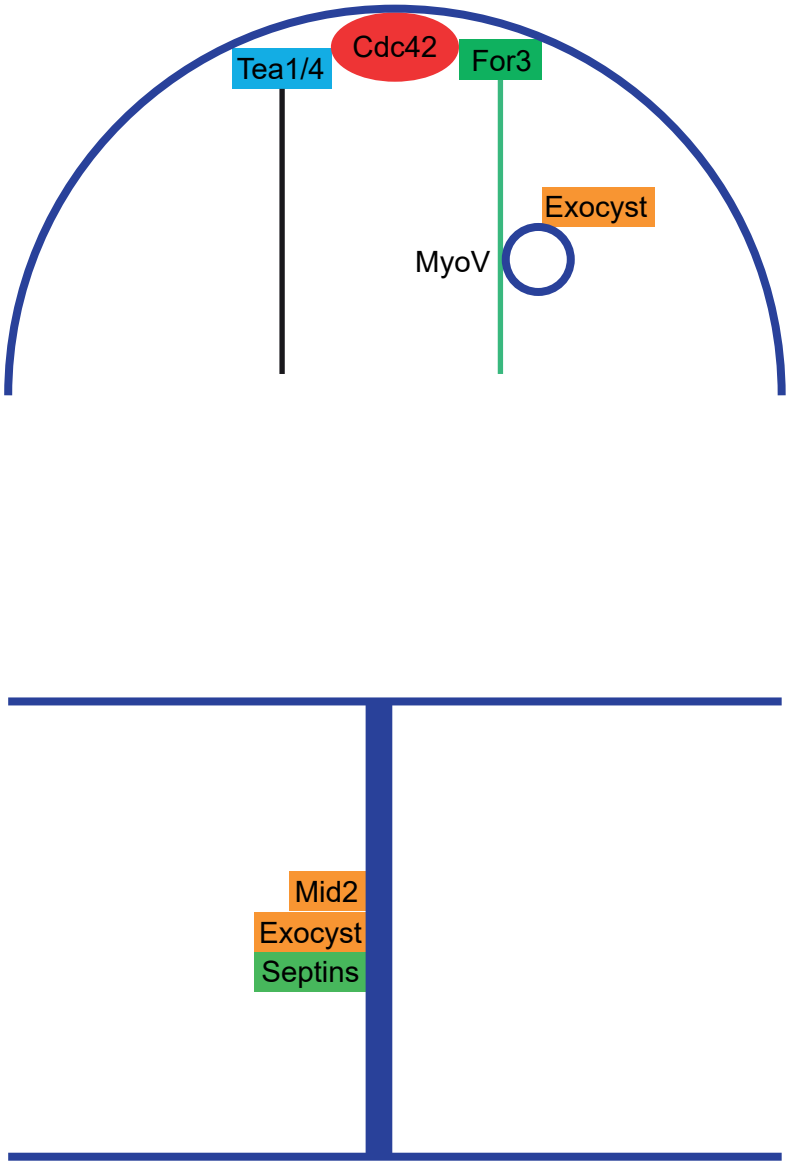

Figure 1.5: Exocyst localisation in polarised fission yeast structures. Diagram to show the localisation of the exocyst complex at the cell tip (top panel) and the septum (bottom panel).

biochemistry techniques to understand how mutation of Sec3 affects growth on specific mediums and interactions with various signalling pathways and biological processes.

In Chapter 3 I assess why exocyst mutants grow better on minimal medium as opposed to rich medium. I answer this question utilising growth assays on a variety of different media and timelapse imaging in starvation media to test the sensing and metabolism of carbon and nitrogen sources in mutants of *sec3* (*sec3-913* and *sec3-916*). I define specific components of media which alter the temperature sensitive phenotype and either improve or hinder growth. In Chapter 4 I assess the growth signalling pathways that the identified nutrients from Chapter 3 are sensed by to see if the exocyst interacts with these. To examine this I use yeast genetics to create *sec3* mutant strains with labelled or mutated/deleted components of specific signalling axis to see if Sec3 shares a genetic interaction with these pathways. These strains were analysed by growth assays and fluorescence imaging to dissect these pathways and localisation of components.

After identifying genetic interactors of Sec3 that are involved in growth signalling, it was important to ask whether these interactions were also physical. In Chapter 5, the question of what does Sec3 physically interact with is addressed. This is answered by using a GFP Trap technique where both Sec3 and Sec3-913 with a GFP label were pulled down on beads and analysed by mass spectrometry. Bioinformatic techniques are utilised to sort positive interactors of Sec3 into specific processes to gain a better understanding of the role of Sec3 in known or novel processes in fission yeast. The data from this indicate a role for Sec3 in the regulation of membrane tension and this is possibly through the endocytic myosin Myo1.

Chapter 2: **Methods**

2.1 Yeast strains and maintenance

Strains used in this study are listed in Table 2.1. Unless otherwise stated, prototrophic strains were used. Cells were cultured, maintained and stored as described in Moreno et al, 1991 (Moreno et al., 1991). Briefly, cells were woken up on from frozen on agar plates made of YE5S agar plates and kept for no longer than a week. Cells were grown to mid-log phase in 100 mL conical flasks containing 50 mL of rich (YE) or minimum (EMM) media plus appropriate supplements, alternative carbon or nitrogen source or drugs (see below for details). For most of the strains used here, the permissive temperature was 27 ^{o}C, and the restrictive temperature was 34-36 ^{o}C.

Cell concentration was measured by optical density at 600 nm (OD_{600}). OD units were converted into a cell number per mL using the following equation previously established in the laboratory: Cell number ($x10^6$)/mL = 5.8 X OD_{600} + 0.007. When grown in poor EMM medium, cells were considered in their exponential phase of growth when at a concentration of up to ~ $6x10^6$ cells/mL, whereas in rich YE5S, cells were still exponentially growing at ~ $1x10^8$ cells/mL

Verified new strains were scraped off YE5S plates, mixed in Yellow Freezing Mix (YFM) medium in cryogenic tubes and frozen at -80 ^{o}C.

2.2 Yeast genetics

To delete or tag genes, primers were designed to flank the gene of interest using the Pombe PCR Primer Program (Penkett et al., 2006). PCR fragments were generated essentially as described (Bähler et al., 1998).

For *S. pombe*, transformations were performed using the lithium acetate method (Morita and Takegawa, 2004). Strains were cultured overnight in 50 ml YE5S at 27 ^{o}C. $2x10^8$ cells were pelleted in a 50 ml conical tube, washed with 1 volume of H_2O, and transferred to a microfuge tube. Cells were washed once more in 1 ml of H_2O and then once in 1x lithium acetate. Cells were resuspended in 100 μl of 1x Lithium Acetate. Prior to this salmon sperm DNA (Sigma) was boiled for 5 minutes at 95 ^{o}C before adding 20 μg of this to the cells along with 7 μl of PCR product. This suspension was then incubated for 10 minutes at room temperature. After incubation 260 μl of PEG solution was added and this was

Strain #	Genotype	Source
IJ8	*myo1D::his3 ura4.d18 leu1.32 ade6.M216 his3.D1 h-*	Lab strain
IJ392	*tor2-287*	Lab strain
IJ426	*leu1.32::nmt1::coxIVDsRFP:leu1 ade6-M216 ura4-D18 h-*	Lab strain
IJ688	*sec3-913:hphMX h+*	Lab strain
IJ692	*sec3-916:hphMX h+*	Lab strain
IJ862	*sec3-913:hphMX myo1::his3*	Lab strain
IJ1205	*972h-*	P. Nurse
IJ1546	*sec3-913:hphMX leu1.32::nmt1::coxIVDsRFP:leu1*	This thesis
IJ1587	*sec3-916:hphMX leu1.32::nmt1::coxIVDsRFP:leu1*	This thesis
IJ1657	*sst4::kanMX6 h-*	This thesis
IJ1658	*hse1::kanMX6*	This thesis
IJ1664	*hse1::kanMX6 sec3-913::hphMX*	This thesis
IJ1666	*leu1.32 h-*	This thesis
IJ1670	*sec3-913:hphMX leu1.32 h-*	This thesis
IJ1676	*tor2-287 sec3-913:hphMX*	This thesis
IJ1678	*cat1-gfp-hphMX h-*	This thesis
IJ1680	*psk1-13myc-hphMX h-*	This thesis
IJ1690	*atg1::kanMX6 h+*	This thesis
IJ1691	*aat1-gfp-kanMX6 h+*	This thesis
IJ1692	*sst4::kanMX6 sec3-913::hphMX*	This thesis
IJ1698	*cat1-gfp-hphMX sec3-916:hphMX*	This thesis
IJ1700	*psk1-13myc-hphMX sec3-913:hphMX*	This thesis
IJ1716	*atg1::kanMX6 sec3-913:hphMX*	This thesis
IJ1720	*sec3-913:hphMX aat1-gfp-kanMX6*	This thesis
IJ1732	*pop3-gfp-kanMX6 h-*	S. Moreno
IJ1733	*gtr1-gfp-kanMX6 h-*	S. Moreno
IJ1734	*gtr1::kanMX6 h-*	S. Moreno
IJ1735	*sec8.1*	This thesis
IJ1736	*exo70::kanMX6*	This thesis
IJ1740	*sec3-916:hphMX pop3-gfp-kanMX6*	This thesis
IJ1742	*sec3-916:hphMX gtr1-gfp-kanMX6*	This thesis
IJ1744	*fkh1::natR h-*	YGRC/NBRP Japan FY25848 (NI1145)
IJ1747	*tor1-L2045D:hphMX h-*	YGRC/NBRP Japan FY25826 (NI1082)
IJ1750	*sec3-916:hphMX leu1.32 h-*	This thesis
IJ1752	*sec3-913:hphMX gtr1::kanMX6h-*	This thesis
IJ1766	*sec3-913:hphMX fkh1::natR*	This thesis
IJ1770	*sec3-913:hphMX tor1-L2045D:HphMX*	This thesis
IJ1772	*sec3-GFP:kanMX6 tor1-L2045D:hphMX*	This thesis
IJ1774	*sec3-GFP:kanMX6*	This thesis
IJ1776	*sec3-916:hphMX tor1-L2045D:hphMX*	This thesis
IJ1778	*ste20-3gfp:kanMX6 h-*	D. Mulvihill
IJ1783	*sec3-916:hphMX ste20-3gfp:kanMX6*	This thesis
IJ1789	*gad8-HA-kanMX6*	This thesis
IJ1793	*sec3-913-gfp-kanMX6*	This thesis
IJ1795	*sec3-913:hphMX gad8-HA-kanMX6*	This thesis
IJ1797	*sec3-916:hphMX gad8-HA-kanMX6*	This thesis
IJ1799	*tor1-L2045D:hphMX gad8-HA-kanMX6*	This thesis
IJ1801	*tor1-L2045D:hphMX sec3-913-gfp:kanMX6*	This thesis

Table 2.1: Strains used in this thesis

incubated for a further 45 minutes at 30 °C, shaking at 180 rpm. DMSO was added to a final concentration of 10% and tubes were heat shocked for 10 minutes at 42 °C. The tubes were then pelleted at 2000 rpm for 2 minutes, washed once in 1 ml of YE5S, and re-suspended in 500 μl of YE5S. Tubes were then incubated for 1.5 hours at 27 °C shaking, pelleted and re-suspended in 150 μl of YE5S before being spread on YE5S plates using glass beads and shaking. Plates were incubated for 24 hours at 27 °C.

For selection of positive transformants, the YE5S plates were replica plated on to YE5S plates containing the drug complementary to the resistance cassette present in the PCR fragment and incubated at 27 °C until colonies were seen. Colonies were picked and re-streaked on the same selection medium. Verification of these colonies was performed by colony PCR. A small amount of yeast was scraped using a toothpick and placed in the bottom of a PCR tube. To this 20 μl of a master mix containing 10x buffer (1.2x final), dNTPs (0.2 mM final) and primers flanking the correct genomic insertion site (0.5 μM final) was added to the yeast pellets. Tubes then underwent polymerase chain reaction and bands were separated by gel electrophoresis so that fragments of the expected size could be identified (Figure 2.1).

To cross strains, each cell type was scraped with a pipette tip from plate and mixed together in 15 μl sterile water. The mixture was spread on to malt extract agar plates (ME4S) and incubated for 24 to 48 hours until tetrads could be seen by light microscopy. Tetrads were dissected on YE5S plates, using an MSM 400 dissecting microscope (Singer instruments). Plates were incubated at 27 °C until colonies formed (approximately 4 days).

Alternatively, random spore analysis was occasionally used. To digest the asci and release the spores, tetrads were mixed with 0.5% snail helix pomatia (SHP, a kind gift from Takashi Toda) in a total volume of 100 μl and incubated at 30 °C for 2 hours. Absolute ethanol was added at a final concentration of 40% and incubated at room temperature for 20 minutes. Spores were then pelleted and re-suspended in ~200 μl water or until clear. Serial dilutions were made and spread on to YE5S to get single colonies.

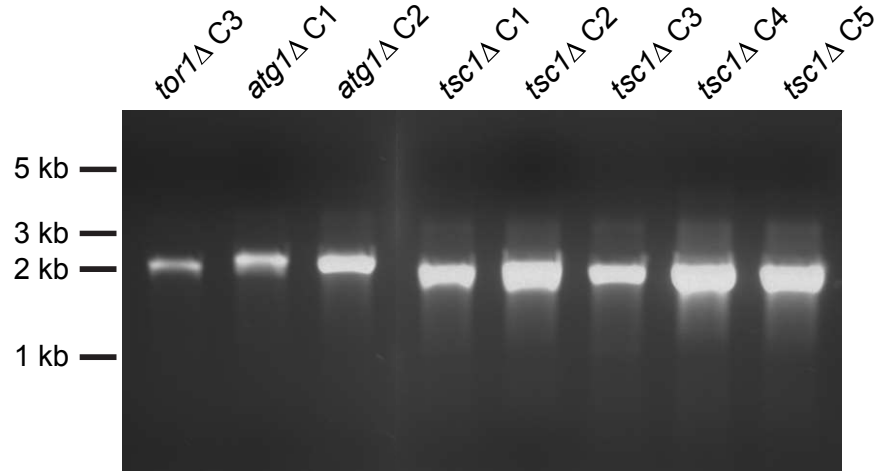

Primer name	Sequence	Expected size
*tor1*Δ-check-F	ATTTAATCAAACTGGAAGGCCA	1972 bp
*tor1*Δ-check-R	ACGCTAAAGAAATTTGCTCCAA	
*atg1*Δ-check-F	TCCCATAAAACTTGTTATCCCG	2097 bp
*atg1*Δ-check-R	GGGTCGTTTGAACAAAAACATT	
*tsc1*Δ-check-F	ATGTGGCAGACTACGCTATCCT	1961 bp
*tsc1*Δ-check-R	AGCAACCTACGAGAGGAAGATG	

Figure 2.1: Example verification of transformed fission yeast strains. To examine whether the deletion cassettes of the above strains had integrated correctly, checking primers that flank the predicted site of integration were used to amplify the regions of gDNA from antibiotic-resistant clones (C). Gel electrophoresis showed bands of the expected size were present in all clones, indicating that the deletion cassettes had integrated correctly into the genome.

After colonies reached an appropriate size, plates replica-duplicated onto medium containing a selection relevant to the markers present in the strains that were crossed.

For identifying antibiotic resistance cassettes stocks of Geneticin (G418, Merck), Hygromycin B (Hph, Invitrogen), or Nourseothricin-dihydrogen sulfate (clonNAT, Werner) were prepared and added to YE5S at specific concentrations (see Table 2.2) For selection based on auxotrophy, minimal media with a combination of adenine, uracil, and leucine complementing the strains genotype was used (Table 2.2). To select for prototrophs, EMM with no amino acids was used. Colonies that survived the selection pressures were selected and kept for further analysis. On the contrary some temperature-sensitive mutants were selected for an absence of growth at their respective restrictive temperature (usually 36 ^{o}C). Two positive clones were re-streaked onto YE5S and frozen until further analysis.

Antibiotic	Supplier	Catalogue Number	Diluent	Stock (mg/ml)	Final concentration (μg/ml)
G418	Sigma	A1720	H_20	50	200
Hph	Invitrogen	10687-010	PBS	50	300
clonNAT	Werner Bioagents	503000	H_20	200	100

Table 2.2: Table of antibiotics used for selecting strains

2.3 Spot test

The OD_{600} of cultures were measured by spectrophotometry and x10^8 cells were pelleted by centrifugation (3000 rpm, 5 minutes) and resuspended in 5 ml of sterile H_2O, to approx. 2x10^7 cells/ml. The density of all strains were then adjusted to each other with sterile water. Ten-fold dilutions of each strain were prepared in a flat bottom, 96-well plate (corning) and spotted on indicated agar plates using a replica plater for 96 well plate (Sigma). For each condition, duplicates or

triplicates were made. Plates derived from YE5S were incubated for 2 days at 34 ºC and 36 ºC, 3 days at 27 ºC as growth speed differs due to temperature. On minimal medium plates were incubated at 34 ºC and 36 ºC for 3 days, and 27 ºC for 4 days. Plates were then imaged on a black background using a Canon EOS 1200D camera.

Spot tests were used to assess cell growth on the following variations of YE or EMM media: YE5S + glycerol plates contained. YE5S + N contained 5 g/l NH_4Cl. NH_4Cl was added to EMM to 5 g/L (1x; (Moreno et al., 1991)) and 10 g/l (2x). Stocks of Proline were made at 1M and added to EMM or EMM-N at a final concentration of 20 mM. The standard concentration of amino acids in EMM is 225 mg/l (1x; Moreno et al); 450 mg/l (2x) and 900 mg/l (4x) were also used.

To assess the effect of TOR inhibition, cell growth was assessed on YE5S and EMM medium containing Rapamycin. Rapamycin (Merck, UK) stocks were made at 2 mg/ml in DMSO and used at a final concentration of 25 ng/ml (unless otherwise stated, see below for concentrations used in liquid cultures).

For assessment of lipids on growth YE5S medium containing either myriocin (Merck, UK), or Amphotericin B (Merck, UK) was used. Myriocin stocks were made up to 2 mg/ml in methanol and used at a final concentration of 0.8 to 0.9 μM. Amphotericin B powder was re-suspended at 10 mg/ml in DMSO and used at a final concentration of 0.1 μg/ml.

Amino acid uptake was assessed through growth of strains on EMM media containing canavanine at a final concentration of 5 μg/ml.

2.4 Cell imaging

For live cell imaging, cells were cultured exponentially in EMM and observed on an agarose pad made of EMM, to reduce the background. Strains were spread on an agarose pad (2 % agarose in EMM) in a CoverWell Imaging Chamber Gasket (ThermoFisher), sealed with a 22x22 mm glass coverslip, and imaged using a Zeiss axio-observer Z1 equipped with 100x 1.4 NA oil objective and a cool-snap HQ2 camera controlled by Axiovision software.

For media changes and temperature sensitive studies, cultures were incubated at the indicated temperature for 1 generation (~4 hours at 27 ºC) before imaging.

For the analysis of sterols in liquid culture, strains were incubated in 50 ml of EMM overnight at 27 ^{o}C. On the morning either 1.25 μM myriocin or the equivalent volume of methanol was added to the flasks and incubated for a further two hours at 27 ^{o}C. Strains were then pelleted and labelled for sterols (see methods 2.5) and imaged immediately.

2.5 Cell staining

Vacuolar membranes were stained with FM4-64 dye. FM4-64 (Thermo Fisher) was re-suspended at 1.64 mM in DMSO. For imaging, 1 ml of cells were incubated with FM4-64 at a final concentration of 8.2 μM for 1 hour, in the dark, at the indicated temperature.

A stock solution of calcofluor white (fluorescent brightener 28 Sigma) was prepared at 5 mg/mL in H2O vortexed for up to 24 h and centrifuged to eliminate the undissolved powder. To stain the cell wall, 0.7 ul of calcofluor of this stock was pipetted onto cells on the agarose pad and spread by application of the sealing coverslip. Cells were observed immediately.

To visualise 2 strains simultaneously, for example to compare fluorescent intensities, identification of one of the strains was achieved by staining it with fluorescent lectin. Stocks of lectin-594 were prepared at 2 mg/ml in H_2O. Lectin staining of cells was performed by incubating 500 μl of cells with 4 ng/ml lectin for 30 minutes at room temperature. Cells were then washed 3 times in EMM and mixed with non-stained cells at a 1:1 ratio before imaging.

Staining of sterols was performed by adding Filipin (Merck, UK) to 1 ml of cells at a final concentration of 5 μg/ml and then imaging immediately. Filipin stocks were made at 2.5 mg/ml in DMSO.

To visualise actin, YE5S cultures were fixed with 3% formaldehyde for 1 hour rotating at room temperature. Cells were pelleted and washed 3 times in PEM buffer (100mM Pipes, 1mM EGTA, 1mM $MgSO_4$). Digestion of the cell wall was performed by incubation with 0.6 mg/ml Zymolyase 100T (Amsbio) in PEM with 1.2M Sorbitol (PEMS) for 20 minutes at 37 ^{o}C shaking regularly. Cells were pelleted and treated with PEMS plus 1% Triton X-100 for 30 seconds. After 3 washes in PEM, the final pellets were treated with 0.13 μM of BODIPY-FL-

Phallacidin (Invitrogen) in PEM. Stocks of BODIPY-FL-Phallacidin were prepared in methanol at a concentration of 6.6 μM.

2.6 Image analysis

Counts, measurements, and image presentations were made using Fiji open source software and downloaded to Microsoft Excel or GraphPad for analyses. Measurements of vacuoles were performed by drawing lines across the diameter of each vacuole in FM4-64 labelled cells.

In the nitrogen starvation experiment, cell length was measured the same way, on calcofluor-labelled cells. The septation index was determined as the percentage of septate cells compared to the total number of cells.

Fluorescent intensity measurements were generated by drawing equal sized region of interests (ROIs) over parts of the cell and recording the mean intensity and integrated density. The mean grey value of the background was recorded for each image and used for background subtraction. For Cat1 and Aat1, ROIs were drawn over the cell tip. For cells in which both tips exhibited fluorescence, the tip with more intense signal was measured.

For mitochondrial fission/fusion events, a gain of contact between separate mitochondria was called a fusion event, and a fission event was counted when one mitochondrion became two.

Statistical analyses of data was performed using Prism (GraphPad). For all data, the Shapiro-Wilkes test was used to assess normality. All datasets had a non-parametric distribution. For the mitochondrial and vacuole analysis, the Kruskal-Wallis test was used followed by Dunn's multiple comparisons as a post-hoc test to visualise the significance of the difference in means between all groups. For fluorescence intensity of Cat1 and Aat1, the Mann-Whitney test was used.

2.7 Protein extraction

50 ml of mid-log YE5S cultures were pelleted (3000 rpm, 5 minutes) and re-suspended in 100 μl of cold extraction buffer (EB). The cell suspension was transferred to cylindrical, 2 mL microfuge tubes with screw caps and mixed with ~300 μl of acid-washed glass beads (Merck, UK). Cells were then lysed using the Qiagen TissueLyser II at a frequency of 30/s for 40 seconds, and then placed on ice for 1 minute. This was repeated 3-4 times. The bottoms of the tubes were

punctured with a needle (Microlance, 21G 1 ½), placed into 1.5 ml microfuge tubes, and then centrifuged (13000 rpm, 1 minute, 4 °C). The lysate was then placed into fresh microfuge tubes and centrifuged again (13000 rpm, 5 minutes, 4 °C). The final lysate was aliquoted into fresh 1.5 ml microfuge tubes.

For analysis of TORC1 signalling, cultures were treated with either 200 nM of rapamycin or the equivalent volume DMSO for 2 hours at either 27 °C or 36 °C prior to protein extraction.

To measure protein concentration, 999 µl of 1x BioRad Protein Assay solution was aliquoted into cuvettes (Greiner Bio-One) and 1 µl of either EB buffer (blank) or lysate was added. Cuvettes were vortexed and resuspended before placing in a spectrophotometer (Jenway) and the OD_{600} was taken. Measurements were plotted alongside a curve of BSA standards to obtain the protein concentration.

2.8 GFP Trap

Strains possessing a GFP tagged protein of interest were lysed following the protein extraction method above. It is possible to create a GFP control strain by inserting the *gfp* gene into the *leu1* locus and titrating its expression to match the gene of interest (Matsuyama et al., 2008). However the control used was just a wild-type strain that went through the same process. After protein extraction, all lysates were adjusted to the same protein concentration and volumes, with lysis buffer. 20-30 mg/ml of each lysate was kept (Whole Cell Extract, WCE) and made up in Laemmli sample buffer for SDS-PAGE. The remaining of the lysate was subjected to GFP Trap. Two independent replicates were performed per condition.

GFP-Trap A (Chromotek) beads were washed in lysis buffer, and 50 µl of beads were added to 5 mg of protein lysate per sample. Tubes were incubated overnight rotating at 4 °C. On the morning beads were pelleted at 4 °C and washed with cold lysis buffer. Pellets were re-suspended in 50 µl of cold lysis buffer and 5 µl was made up in Laemmli for SDS-PAGE. Western blotting was performed with an α-GFP antibody (Table 2.3) to show the pull-down was successful. After confirmation, samples were sent to the University of Bristol for mass spectrometry.

The lists of proteins generated from the mass spectrometry were sorted using a stringent cut-off to remove false positives. Proteins with a peptide score of 0 were deleted, and then any hits that were not in the negative control or had a score 2.5-fold higher score than the negative control were considered true hits. This was the optimal threshold that kept most known biological interactors of Sec3 in the lists. Duplicate lists of Sec3 and Sec3-913 were merged to give a list of double positives and a list of all the true hits in both lists. The total number of double positives was 34 proteins for Sec3 and 18 for Sec3-913. In order to avoid the loss of transient interactors, biological relevance and literature was also used to define the cut off.

Functional clustering was performed using String-DB (Szklarczyk et al., 2017). The lists of positive interactors for each protein were clustered according to data from databases and experiments only to ensure only confirmed interactions were shown. The significance Gene Ontology (GO) terms calculated by String-DB were highlighted on the maps. In cases where large GO:Terms were refined, the list of proteins annotated in these GO:Terms were clustered through String-DB again to identify specific protein complexes and biological processes.

2.9 Western blotting

Polyacrylamide gels were made at 10% using ProtoGel (30%) acrylamide solution and stacking buffer (National Diagnostics).

Samples were reduced by boiling in Laemmli reducing sample buffer at 95°C for 5 minutes, then loaded alongside PageRuler Plus prestained protein ladder (Thermo Scientific). Protein was run through the stacking gel at 60 volts and the separated by electrophoresis at 160 volts for 1-2 hours, and transferred to a nitrocellulose membrane using either a wet transfer system (Mini-Protean 3, BioRad) at 30 volts overnight at 4 ^{o}C.

Membranes were blocked with continuous rotation at room temperature for 1 hour in PBS with 0.1% Tween-20 (Fisher Scientific) and 5% Marvel milk powder (Premier Foods Group, UK). To probe membranes, antibodies were diluted 5% milk PBS-T, and membranes were incubated in primary antibody with continuous rotation at room temperature for 1 hour or at 4°C overnight, washed for 3 x 5 minutes in PBS-T, incubated in secondary antibody (Table 2.3) with rotation at room temperature for 30 minutes to 1 hour. Antibodies used in this study are

listed Table 2.3. The membrane was washed for 3 x 5 minutes in PBS-T. To visualise protein, the membrane was treated with ECL reagent and exposed to X-ray film (Super RX, FujiFilm).

Membranes were stripped for re-probing by incubation in stripping buffer (100 mM glycine, 2% SDS, pH 2.0) for 2 x 10 minutes at room temperature, washed with PBS for 3 x 10 minutes, then re-blocked, treated with ECL, and exposed to check for residual signal before re-probing.

Antigen	**Host Species**	**Supplier**	**Cat no.**	**WB dilution**
GFP	Mouse	Roche	11814460001	1:1000
Flag	Mouse	Sigma	F3165-1MG	1:1000
Myc (1A5A2)	Mouse	ProteinTech	60003-2-Ig	1:1000
HA (C29F4)	Rabbit	ProteinTech	3724	1:1000
Alpha tubulin	Mouse	(Woods et al., 1989)	N/A	1:200
Mouse Ig	Rabbit	Sigma	A9044	1:40000
Rabbit Ig	Goat	Sigma	A0545	1:40000

Table 2.3: Table of antibodies used in this thesis

Chapter 3: **Sec3 is involved in the cellular sensing of the amino acid leucine**

3.1 Introduction

Cellular uptake and sensing of nutrients, and how this is translated into growth and survival has been a subject of research for quite some time. This is an important mechanism as cellular survival depends upon the ability to adapt conditions of starvation. To do this, biological processes that generate nutrients from other routes, such as autophagy, become active in the absence of nutrients (Hosokawa et al., 2009). If these pathways do not work or are not regulated efficiently, glucose and amino acid metabolites are not generated to meet demand. This leads problems in the generation of ATP, but also synthesis of nucleotides, proteins, and lipids which can ultimately lead to disease. Glucose is metabolised by glycolysis to produce pyruvate which enters the TCA cycle to ultimately produce ATP. Most amino acids are metabolised to glutamate and also enter the TCA cycle. However leucine is converted to acetyl-CoA before enters this biochemical process. Leucine can also be metabolised through the mevalonate pathway which is important for producing sterols. Transport of nutrients over the plasma membrane relies on various families of importers that are transported dynamically to and from the cell membrane depending on nutrient demands and availability.

In mammalian cells glucose is transported by the GLUT family of active transporters which are expressed on the plasma membrane in response to a hypoglycemic environment, but also in response to insulin hormone signalling (Ewart et al., 2005). Orthologues of GLUT transporters exist in fission yeast and comprise the glucose hexose transporters Ght family of proteins which contains 6 importers (Heiland et al., 2000). Glucose metabolism is different between fission yeast and mammals. Glucose acts to inhibit respiration as fission yeast grow mainly by fermentation (Malecki et al., 2016). Glucose is sensed by cAMP/Pka1 signalling (Welton and Hoffman, 2000), but also through the Rab GTPase Ryh1 which both activate TORC2 signalling which plays a role in stress response and morphology (Cohen et al., 2014; Hatano et al., 2015; Tatebe and Shiozaki, 2010).

Amino acids travel across the plasma membrane in an active manner by utilising a family of transporters called amino acid permeases. Interestingly most aspects of the amino acid importer family of proteins remain poorly characterised. Structural analyses of the uracil permease in both budding and fission yeast has revealed that it contains 10 transmembrane helix domains (De Montigny et al., 1998), however it remains unclear if all amino acid permeases share this structure. Out of the 38 annotated amino acid transporters in *S. pombe*, two of the best characterised are the permeases Aat1 and Cat1. Deregulation of Cat1 was shown to affect the uptake of arginine, lysine, and histidine (Aspuria and Tamanoi, 2008; Ryuko et al., 2012), while deletion of Aat1 altered the uptake of arginine (Nakase et al., 2012). A question that still remains to be answered is how specific these importers are to specific amino acids. In nutrient rich conditions Aat1 is localised at the Golgi apparatus, and in nutrient deplete conditions it is trafficked to the plasma membrane and later sorted to the vacuolar lumen (Nakase et al., 2012). Conversely Cat1 is located on the plasma membrane in nutrient rich conditions and undergoes retrograde transport from the PM to the vacuole when starved (Nakashima et al., 2014). The dynamics of these permeases is still largely unclear. Retrograde transport has been found to require the poly-ubiquitinase Pub1 and members of the ESCRT family of protein (Nakase et al., 2012; Nakashima et al., 2014). However what traffics these proteins to the plasma membrane is still unknown.

Import of amino acids is dependent on several mechanisms. The environmental pH and active H+ ion transporters in the plasma membrane create an electrochemical gradient which has shown to be necessary for the uptake of amino acids (Horák, 1986; Horák and Ŕíhová, 1982; Thwaites et al., 1995). Secondly the availability for free nitrogen in the form of NH_4^+, which in *S. pombe* media is commonly donated from ammonium chloride (NH_4Cl), affects the internalisation of NH_4^+ sensitive permeases (Karagiannis et al., 1999). Increasing the concentration of NH_4Cl was shown to drastically reduce the level of cytoplasmic leucine in *S. pombe* (Karagiannis et al., 1999). Environmental NH_4^+ appears to regulate the activity of the polyubiquitinase Pub1 (Karagiannis et al., 1999). Polyubiquitinases are required to add ubiquitin to membrane cargoes that are destined for endocytosis, and there are three in fission yeast, Pub1, 2, and 3 (Nakase et al., 2012). Deletion of *pub1* causes sensitivity to the toxic arginine analogue canavanine indicating an increase in amino acid uptake (Nakase et al.,

2012). This increase in uptake was attributed to the fact that *pub1Δ* strains exhibit a loss in retrograde transport the permeases Cat1 and Aat1 (Nakashima et al., 2014). In the case of Cat1, Pub1 interacts with and ubiquitinates the arrestin-related adaptor Arn1, which then causes the internalisation of Cat1 (Nakashima et al., 2014). It is not clear whether this mechanism is the same for all amino acid permeases, or whether specific subsets require specific poly-ubiquitnases and/or adaptors, however these studies have shown that levels Environmental NH_4^+ can regulate amino acid uptake through affecting proteins involved in tagging amino acid permeases for internalisation.

The process of secretion through exocytosis is needed to place these importers in the plasma membrane, whilst endocytosis controls the retrograde transport of these channels from the plasma membrane into the vacuolar system for sequestering or destruction. The exocyst complex of proteins were found to be important in exocytosis where they are proposed to tether secretory cargoes to the plasma membrane (Grote et al., 2000). This complex is anchored to the plasma membrane by both Exo70 and Sec3 through their Pleckstrin homology domains which bind to PIP_2 (Baek et al., 2010; Bendezú and Martin, 2011; He et al., 2007). In *S. pombe* Sec3 is an essential gene but Exo70 is not (Kim et al., 2010). So far the cargoes of the exocyst remain relatively unknown, however work in mammalian adipocytes showed that the exocyst member Sec3 is responsible for the trafficking of the GLUT4 hexose importer in response to insulin hormone signalling (Ewart et al., 2005; Inoue et al., 2003). This shows that the exocyst is required for glucose uptake in mammals, however it is not known if this is conserved between species, or whether the exocyst is required for uptake of other nutrients.

The plasma membrane binding member Sec3 was also showed to be involved with Arp2/3-mediated endocytic actin patches in *S. pombe* (Jourdain et al., 2012). Furthermore the deletion of *pub1* in mutants of *sec3* partially rescued the temperature sensitivity of these strains (Kampmeyer et al., 2017), possibly highlighting that the trafficking of amino acids transporters is perturbed in exocyst mutants. Due to this dual role in both anterograde and retrograde transport of cargo, it is possible that the exocyst may affect nutrient sensing and uptake by controlling the dynamics of nutrient importers.

Two temperature sensitive (*ts*) mutants of Sec3, *sec3-913* and *sec3-916*, were previously generated (Jourdain et al., 2012). The *sec3-913* mutant contains single point mutations near the PH domain and in the C-terminus, which appears to stop the exocyst from functioning correctly (Jourdain et al., 2012). The mutant *sec3-916* contains point mutations at different bases and exhibits a more aggressive *ts* phenotype than *sec3-913*. Using these strains, this chapter will investigate whether the *S. pombe* exocyst complex plays a role in the uptake and sensing of nutrients within the environment.

3.2 Results

3.2.1 The ts *phenotype of the sec3 mutants is more severe in rich medium than in poor medium.*

Previous observations from the laboratory suggested that the two *sec3* temperature sensitive mutants *sec3-913* and *sec3-916* showed different temperature sensitivity phenotypes when grown in different media. To confirm these preliminary observations, WT and *sec3* mutants were plated on rich medium (YE5S) and minimal medium (EMM with no amino acids) and incubated at permissive and restrictive temperatures. Growth of *sec3-913* and the more aggressive *sec3-916* mutants was very temperature sensitive on YE5S at restrictive temperatures than compared to EMM where both strains grew even at 36 ^{o}C (Figure 3.1). These data show that mutation of *sec3* causes a reduction in growth when in a nutrient-rich environment.

3.2.2 Glucose is not responsible the growth deficit in sec3 mutants.

To examine what component of the YE5S medium is causing the deficit in growth, each component was examined for its effect on the growth of *sec3* mutants. Carbon sources such as glucose are needed for cellular growth. Glucose concentrations in YE5S are higher than in EMM at 3% and 2% volume, respectively. Therefore higher glucose concentrations may cause the higher sensitivity on YE5S. To examine whether glucose played a role in the growth deficit of *sec3* mutants, prototrophic strains were plated on EMM medium containing normal levels of glucose (2%) and medium containing twice the amount (4%). All strains grew similarly on both normal and high glucose medium (Figure 3.2). To further verify this, strains were also spotted YE5S containing

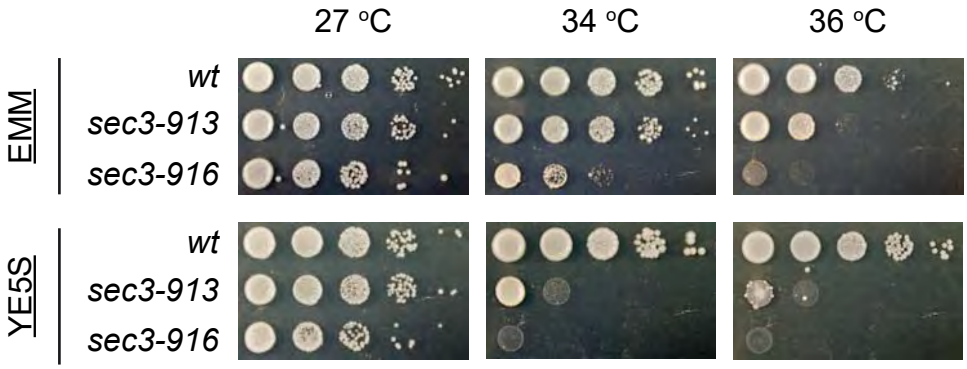

Figure 3.1: *sec3* mutants are more temperature sensitive in rich medium than in poor medium. Serial dilutions of wild-type (*wt*), *sec3-913* and *sec3-916* cells were spotted on minimal (EMM) or rich (YE5S) agar medium and incubated at the permissive (27 °C), semi-restrictive (34 °C) and restrictive (36 °C) temperatures. The temperature sensitivity phenotype of both mutants is exacerbated in rich medium.

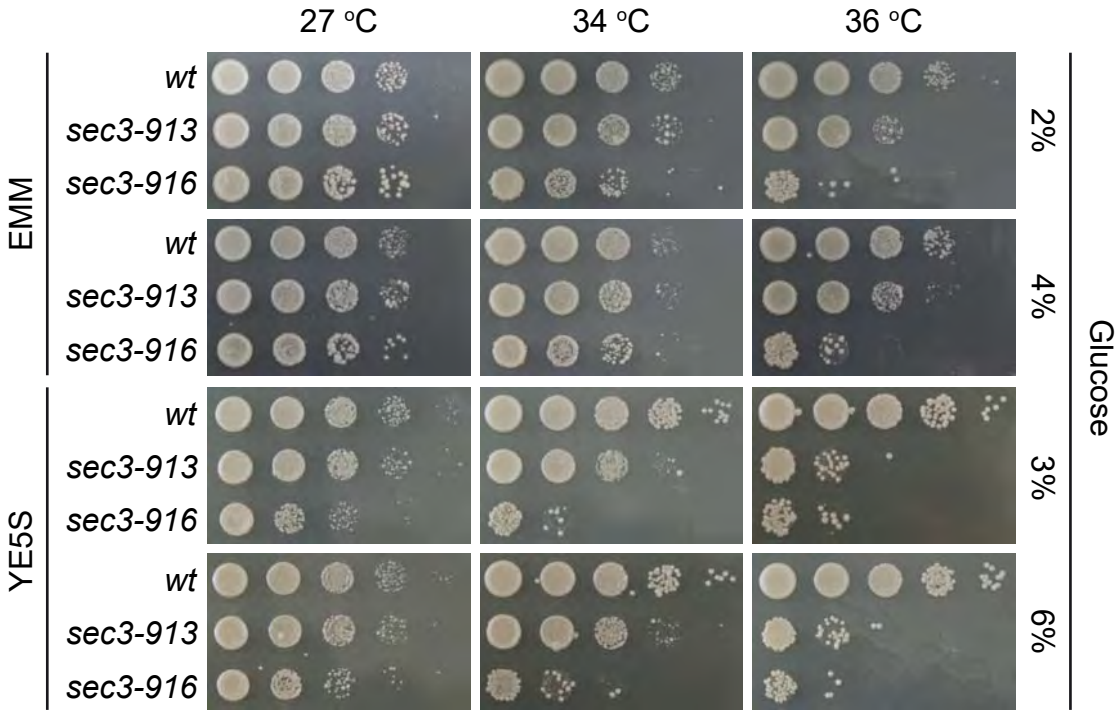

Figure 3.2: High amounts of glucose do not affect the growth of *sec3* mutants. Wild-type (*wt*), *sec3-913* and *sec3-916* cells were spotted in 10-fold serial dilutions on EMM or YE5S plates containing the standard amount of glucose (2 % or 3 %, respectively), or twice the amount of glucose (4 % or 6 %, respectively). Plates were then incubated at the indicated temperatures. None of the mutants are sensitive to high concentrations of glucose in any condition.

normal (3%) and double (6%) glucose. Similarly to EMM both the wild type and *sec3* mutant strains were not sensitive to an increase in glucose (Figure 3.2), showing that the temperature sensitivity of *sec3* mutants is not due to an increase in environmental glucose.

Conversely the reduction in glucose between YE5S and EMM could be the reason exocyst mutants grow better on EMM. To verify this hypothesis, I performed a growth assay of wild type and *sec3* mutants on EMM and YE5S medium containing a gradient of lower glucose concentrations. Growth of the wild type was unaffected by the glucose concentrations (Figure 3.3). Furthermore the growth of the *sec3* mutants were also found to be unaffected at both the permissive and restrictive temperature in response to changes in glucose availability (Figure 3.3). These data show that the exocyst is not involved in glucose sensing or metabolism.

3.2.3 Nitrogen partially rescues the growth of the sec3 mutants.

Another key component of the media is nitrogen. This is present as free ammonium chloride (NH_4Cl) in EMM and also from amino acids in the medium. It is unclear how much nitrogen is present in YE5S medium, however yeast extract contains both nitrogen and amino acids. This medium is further supplemented with 5 amino acids meaning it is reasonable to suggest that nitrogen is present in excess compared to EMM where it is tightly regulated. To assess whether nitrogen is sensed and processed correctly in the *sec3* mutants, prototrophic strains were spotted on media containing increasing amounts of NH_4Cl, and no amino acid.

In the standard recipe for YE, no NH_4Cl is added, presumably because it naturally contains this essential supplement. However the concentration of NH_4Cl in YE is unknown. I therefore wondered if excess amounts of NH_4Cl may rescue the growth of *sec3* mutants in a YE-based medium. Strains were spotted on medium containing YE5S with no amino acids (YE), YE with 5 g/l NH4Cl (YE + N), YE5S, and YE5S with 5 g/l NH_4Cl (YE5S + N). NH_4Cl has no effect on the growth of the wild type, at any temperature. Interestingly, the addition NH_4Cl appeared to partially rescue the growth of *sec3-913* cells regardless of the presence of amino acids (Figure 3.4). These data show that the presence of more nitrogen in rich media enhances the growth of *sec3* mutants. Similarly, the *ts* phenotype of both

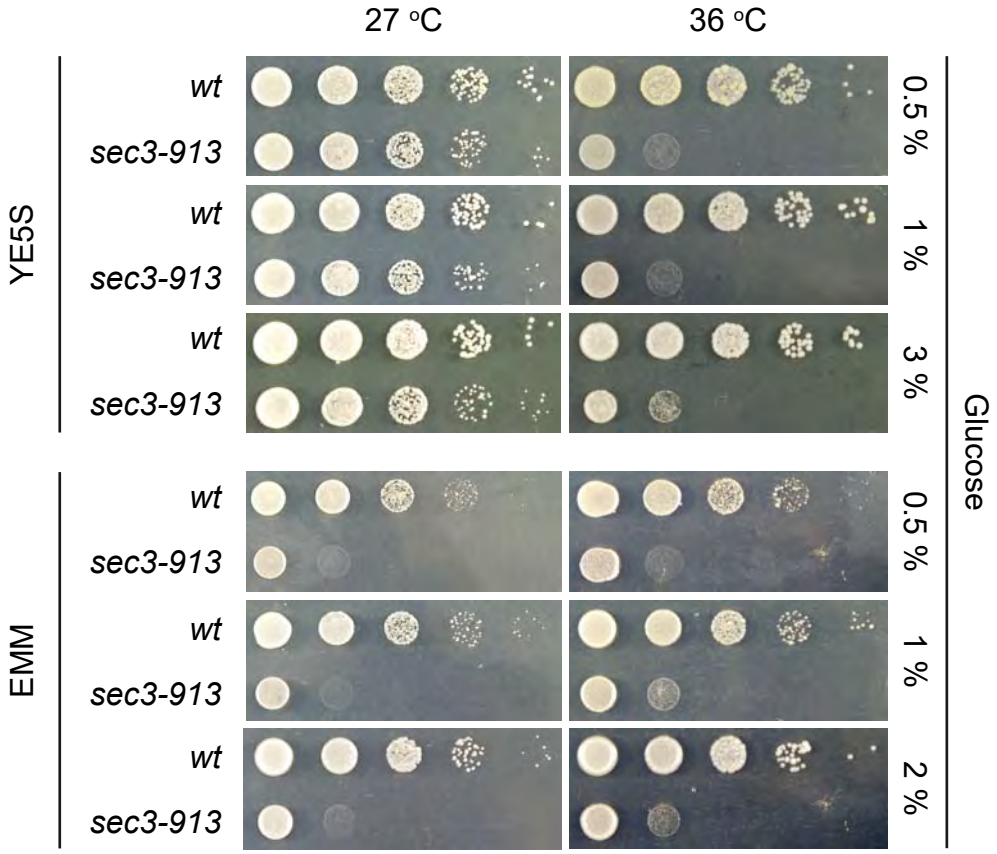

Figure 3.3: Low amounts of glucose do not affect the growth of *sec3* mutants. Wild-type (*wt*), *sec3-913* and *sec3-916* cells were spotted in 10-fold serial dilutions on EMM or YE5S plates containing low amounts of glucose, compared to standard levels (3 % for YE5S and 2 % for EMM). Plates were then incubated at the indicated temperatures. None of the mutants are sensitive to low concentrations of glucose in any condition.

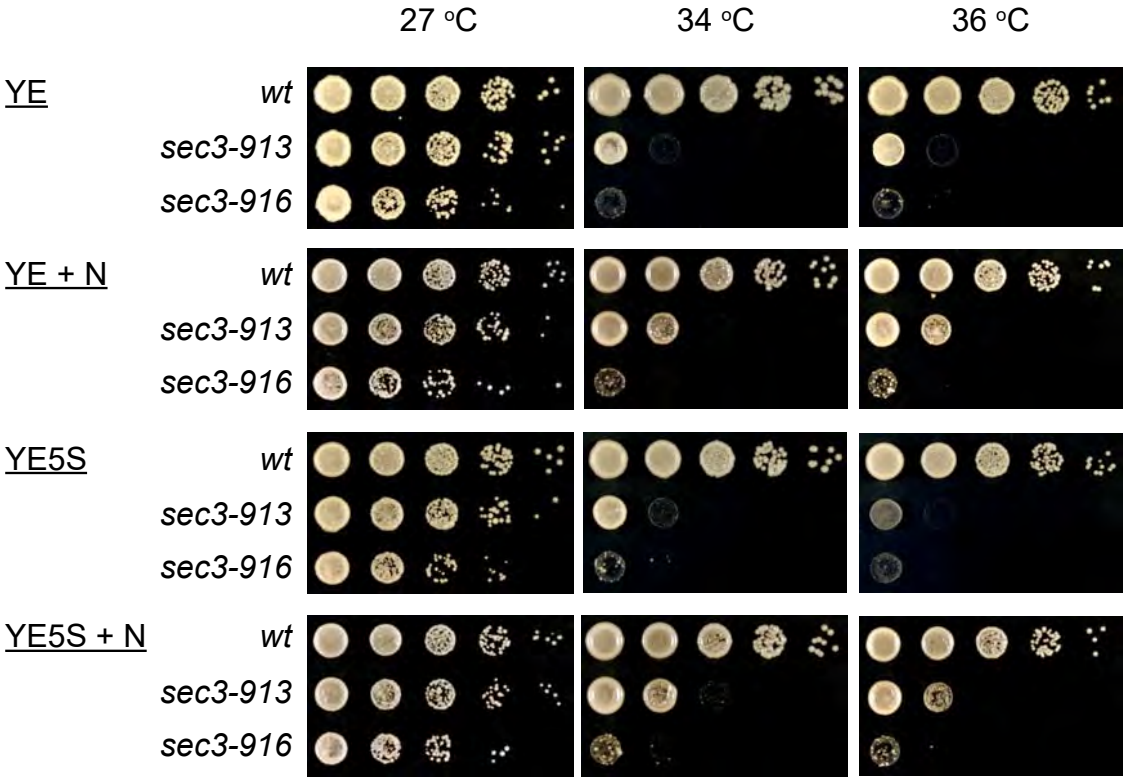

Figure 3.4: The growth of a *sec3* mutant is partially rescued by high amounts of NH_4Cl. Wild-type (*wt*), *sec3-913* and *sec3-916* cells were spotted in 10-fold serial dilutions on yeast extract with no amino acids (YE), yeast extract with no amino acids but with 5 g/l NH_4Cl (YE + N), yeast extract with 5 supplements (adenine, uracil, leucine, histidine and lysine; YE5S), and YE5S with 5 g/l NH_4Cl (YE5S + N).

sec3 mutants is rescued by high amounts of NH_4Cl in minimum medium (Figure 3.10, “No Leu”, 5 g/l NH_4Cl” vs 10g/l NH_4Cl).

By contrast, low levels of NH_4Cl did not appear to worsen the growth of *sec3* mutants on EMM-agar. To further assess if *sec3* mutants are sensitive to low amounts of NH_4Cl, I asked if they could enter G0. In low NH_4Cl, *S. pombe* cells leave the mitotic cell cycle and enter a latent G0 state (Young and Fantes, 1987). In wild type cells, this is characterised by a loss of cell polarity and a decrease in cell length (cells round up), a reduction of the septation index and an arrest of cell growth after 2 generations following the switch to starvation conditions. To check what happens when Sec3 in not fully functional, prototroph *wt*, *sec3-913* and *sec3-916* strains were grown overnight in EMM and then switched to nitrogen free (EMM-N) medium and incubated at 27 ^oC. Cell number, shape and septation index were measured every 2 hours for 8 hours, and then again at 12 and 24 hours. Staining with calcofluor showed that the septation index of both strains decreased to 5% after 8 hours of starvation showing a reduction in cell division (Figure 3.5, panel A). Both wild type and *sec3-913* strains reduced in size from ~ 10 μm to ~ 5 μm (Figure 3.5, panels B and C). This is further reflected by the cell density counts which increased logarithmically for 2 generations (from ~ 2.10^6 cells/ml to ~ 8.10^6 cells/ml) after which they plateaued (Figure 3.5, panel D). These data show that mutation of the exocyst does not affect the nitrogen starvation response.

These data show that reducing nitrogen availability does not affect growth of *sec3* mutants, whereas high levels of environmental $NH4^+$ appears alleviate the temperature sensitivity of *sec3* mutants on both rich and minimal medium.

3.2.4 sec3 mutants are sensitive to leucine

Amino acids are another nitrogen source that could cause the growth deficit in *sec3* mutants. To examine this, prototroph strains were spotted on EMM without amino acids, or EMM containing uracil, leucine and arginine at standard working concentrations (1x = 225 mg/l) or twice the concentration (2x = 450 mg/l). Growth of the strains on both arginine and uracil were not affected by the addition of these amino acids at both normal and double the concentrations (Figure 3.6; see below for leucine result).

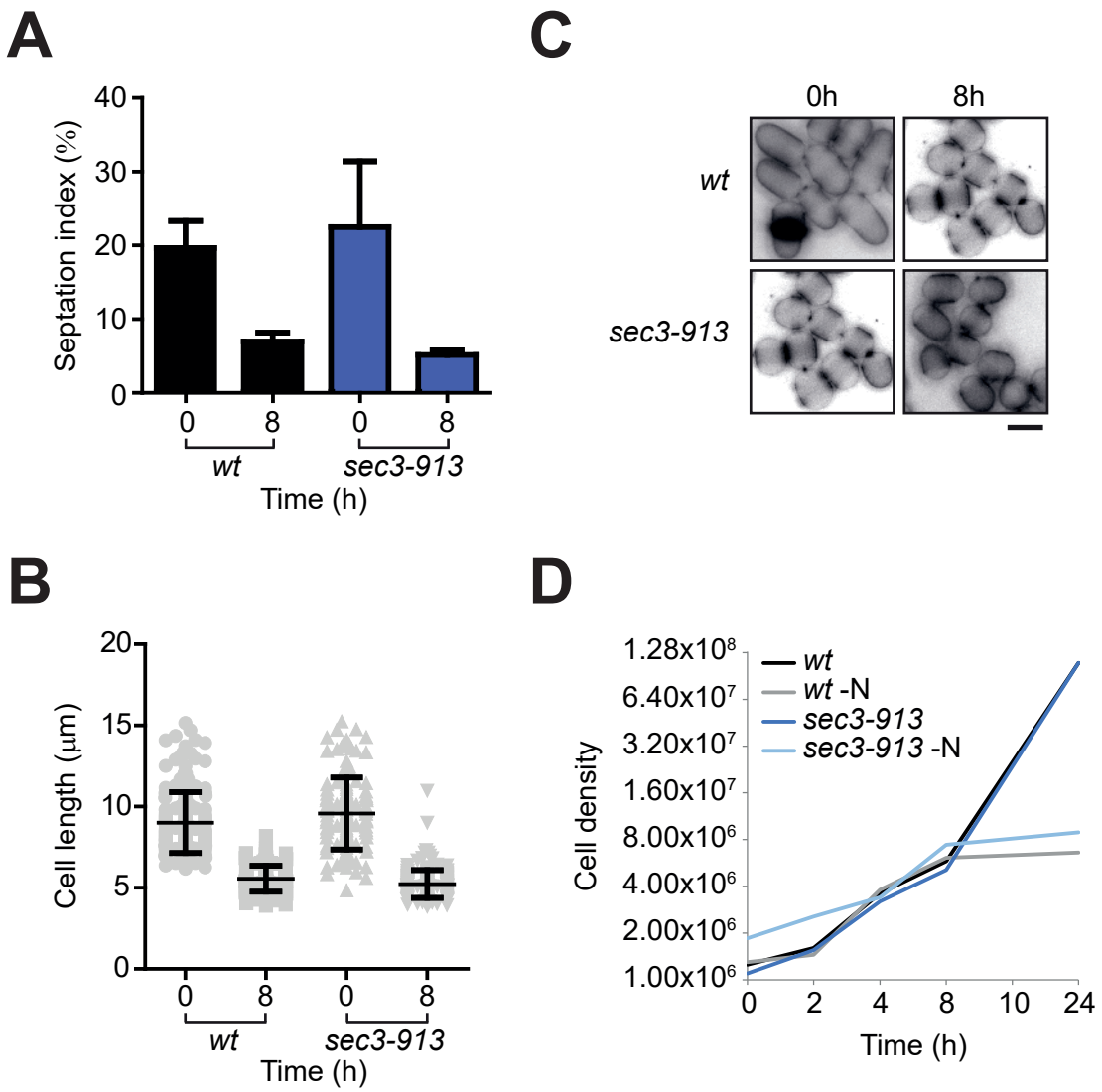

Figure 3.5: *sec3* mutants respond to nitrogen starvation. Wild-type (*wt*) and *sec3-913* cells were cultured to early mid-log phase in standard EMM, then switched to EMM without nitrogen (EMM-N) at time t=0. Cells were subsequently stained, measured and counted at various time points. For clarity, selected time points are shown. The proportion of septated cells **[A]**, and cell length **[B]** were determined from calcofluor-labelled cells **[C]**. **[D]** Cell density was measured by haemocytometer. Dark lines show constant growth of both strains in standard EMM; lighter lines show that both strains stop growing after two rounds of division. Scale bar = 5 μm. N = 2 experiments, >124 cells per condition.

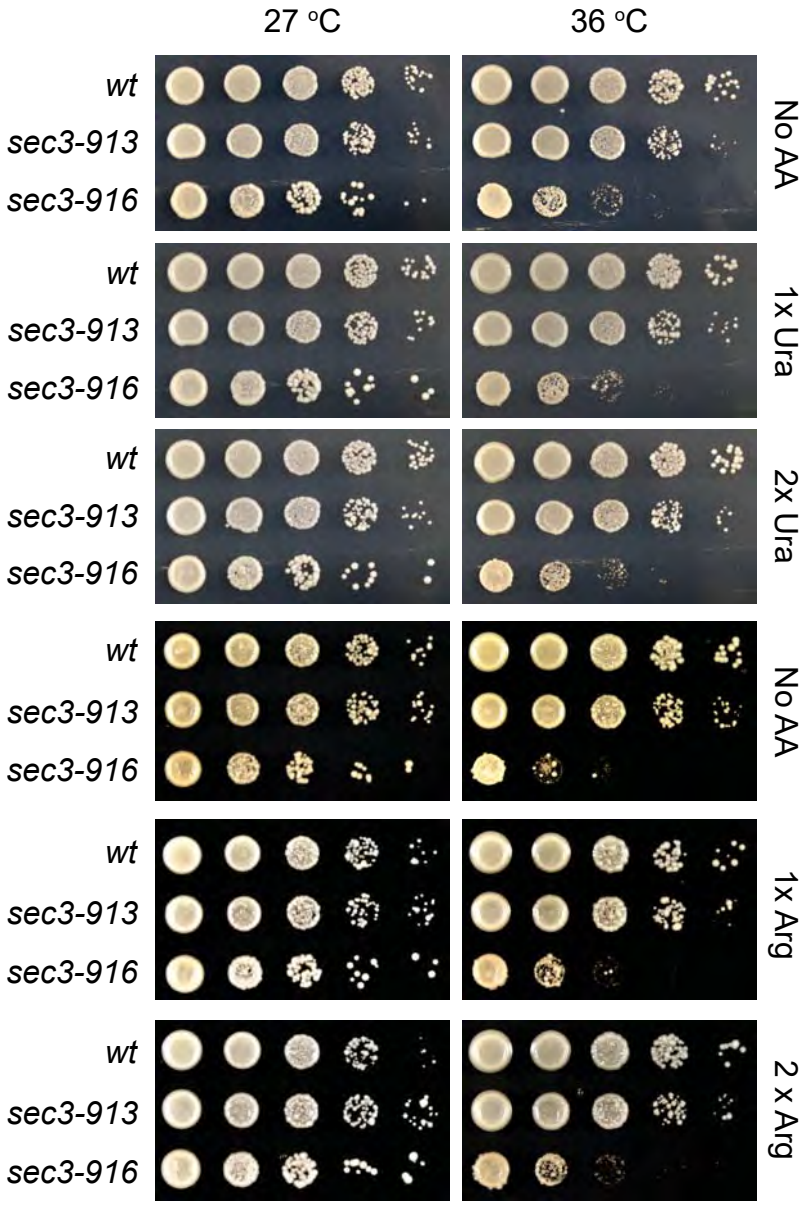

Figure 3.6: The amino acids uracil and arginine do not affect the growth of *sec3* mutants. Wild-type (*wt*), *sec3-913* and *sec3-916* cells were spotted in 10-fold serial dilutions on EMM plates containing standard (1x = 225 mg/l) or twice (2x= 450 mg/l) the amount of uracil (Ura) or arginine (Arg). Plates were then incubated at the indicated temperatures. None of the mutants are sensitive to high concentrations of these amino acids.

Canavanine is a toxic analogue of arginine which enters the cell via arginine/lysine transporters, and can be used to assess uptake of amino acids (Rosenthal, 1977). To check if arginine/lysine import was functional in the *sec3* mutants, strains were spotted on EMM with or without 5 μg/ml canavanine (Figure 3.7). As expected in cells where import is functional, canavanine impaired the growth of WT control cells at all temperatures. At 36 ºC, compared to their level of growth without treatment, *sec3.913* cells were sensitive to canavanine, albeit slightly less than the WT. By contrast, *sec3-196* cells were neither sensitive, nor resistant to the compound, but appeared rescued by it. In view of this puzzling result, I observed strains at the semi-permissive temperature. At 34 ºC, all strains were equally affected by the compound. All in all, canavanine seems toxic to all strains observed, suggesting that arginine/lysine uptake may be generally functional in these cells.

In contrast to arginine and uracil which had no effect on *sec3* mutants, the addition of leucine to EMM exhibited a dose-dependent reduction in growth. Although this is true for both mutants, this is particular obvious for the *sec3-916* strain, which was very sensitive to 1x and 2x leucine at the restrictive temperature (Figure 3.8; see also Figures 3.9 and 3.10). These data show that mutation of *sec3* causes cellular sensitive to leucine specifically.

As mutating *sec3* leads to sensitivity to leucine, I asked whether this was specific to *sec3* or whether it also was seen in the other mutants of the exocyst complex. To examine this, *sec3-913* and *sec3-916* were spotted alongside the *ts sec8.1* mutant and a strain where *exo70* had been deleted. Prototrophic strains were grown on EMM with a gradient from no to high leucine (Figure 3.9). Both the *sec3* and *sec8* mutants exhibited a reduction in growth when leucine concentrations were increased at the restrictive temperature. Interestingly, deleting the *exo70* member of the exocyst showed no sensitivity to increasing levels of leucine. These data show that mutating *sec3* or *sec8* leads to leucine sensitivity in *S. pombe*, but deletion of *exo70* has no effect.

The addition of NH_4Cl to media has been shown to reduce the uptake of amino acids (Karagiannis et al., 1999). To assess whether reducing the uptake of amino acids rescues the leucine sensitivity phenotype of *sec3* mutants, strains were spotted on EMM containing increasing concentrations of both leucine and NH_4Cl. As expected, growth deficit of strains was more aggressive when NH_4Cl was

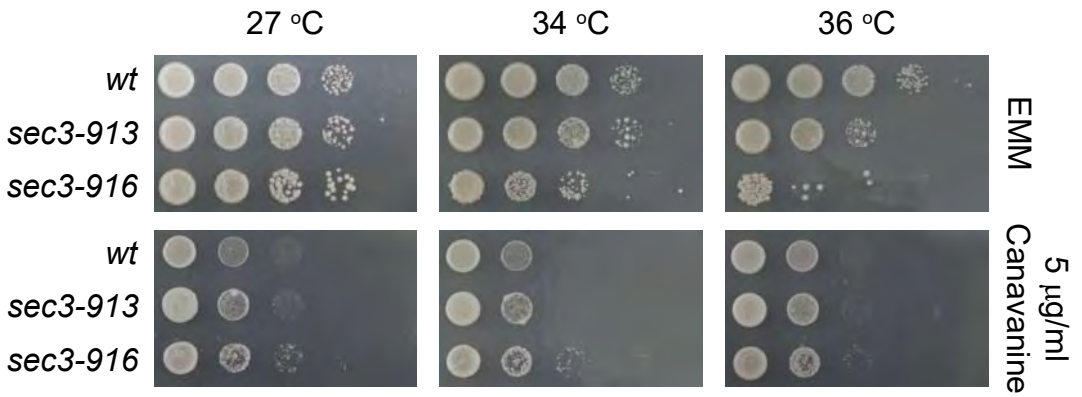

Figure 3.7: *sec3* mutants are not resistant to the toxic arginine analogue canavanine. Serial dilutions of wild-type (*wt*), *sec3-913* and *sec3-916* cells were spotted on EMM medium with or without 5 µg/ml canavanine and incubated at the indicated temperatures. Canavanine impairs the growth of cells where amino acid import is functional.

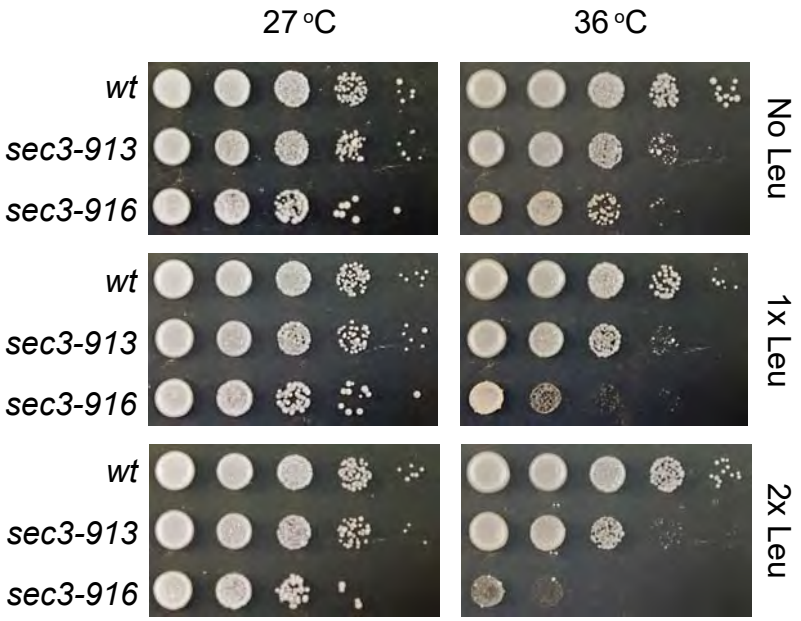

Figure 3.8: The amino acid leucine is toxic to the *sec3* mutants. Wild-type (*wt*), *sec3-913* and *sec3-916* cells were spotted in 10-fold serial dilutions on EMM plates containing standard (1x = 225 mg/l) or twice (2x = 450 mg/l) the amount of leucine (Leu), and incubated at the indicated temperatures. The growth of both sec3 mutants, but not wild-type cells, is impaired by increased amounts of leucine.

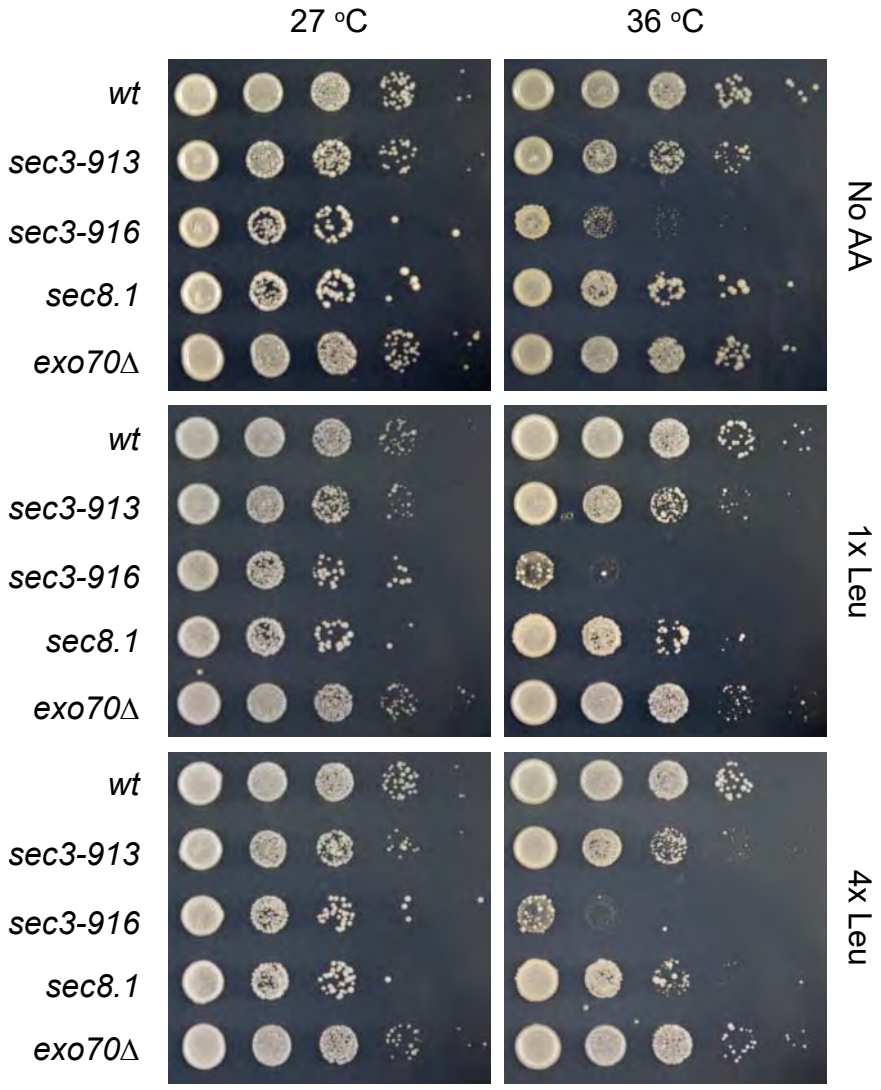

Figure 3.9: *sec8.1*, but not *exo70Δ*, is also sensitive to leucine. Wild-type (*wt*), *sec3-913* and *sec3-916*, *sec8.1* and *exo70Δ* cells were spotted as in Figure 3.8.

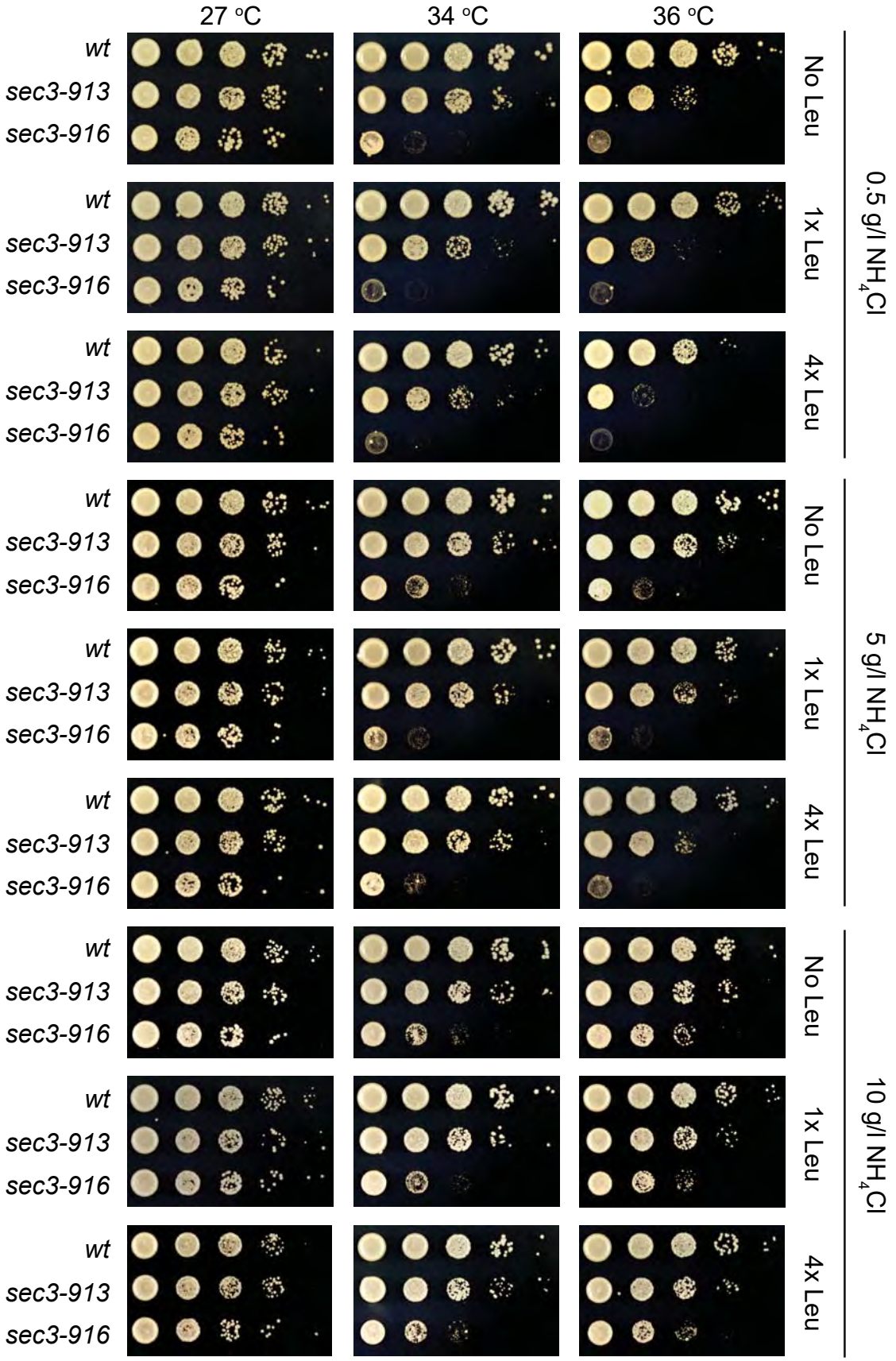

Figure 3.10: NH_4Cl reduces the leucine sensitivity of the *sec3* mutants. Serial dilutions of wild-type (*wt*), *sec3-913* and *sec3-916* cells were spotted on EMM containing the indicated concentrations of both leucine and NH_4Cl. *sec3* mutants become less sensitive to leucine as the concentration of NH_4Cl increases.

reduced to 0.5 g/l and leucine was present at 4 times the normal concentration (Figure 3.10). As the NH_4Cl concentration was increased to normal concentration (5 g/l), growth of the *sec3* mutants was restored but they were still sensitive to increasing leucine concentrations. Intriguingly, when the NH_4Cl concentration was present at double the normal concentration (10 g/l), both the *sec3-913* and *sec3-916* strains were less sensitive to increasing levels of leucine, with no deficit in growth seen at 4x Leucine. These data show that reducing the uptake of the amino acid leucine rescues the leucine sensitive phenotype in the *sec3* mutants.

The data presented above show that the growth of strains possessing a mutation in *sec3* is rescued by the presence of NH_4Cl (see Figures 3.4 and 3.10). It is established that the presence of ammonium causes the repression of genes involved in the nitrogen catabolite repression (NCR) system (Georis et al., 2009). The expression of these genes is promoted in response to a low nitrogen environment or the presence of non-repressible amino acids including proline and L-glutamic acid (Georis et al., 2009). To investigate whether the NCR affects the growth of sec3 mutants, I spotted serial dilutions of the wild type, *sec3-913*, and *sec3-916* strains on EMM containing 20 mM proline, and EMM without nitrogen (EMM-N) containing 20 mM proline or 3.75 g/l L-glutamic acid. EMM media was used as a control as growth of strains is not possible on EMM without a nitrogen source. Growth of all strains did not appear to be affected by the presence of L-glutamic acid (Figure 3.11). Strains grown on EMM and EMM with 20 mM proline showed a similar growth pattern, however a reduction of growth in all strains was observed on EMM-N with 20 mM proline (Figure 3.11). This shows that non-repressible amino acids do not affect the growth of *sec3* mutants.

3.2.5 Sec3 regulates the localisation of some amino acid transporters at the PM

The experiments presented above indicate that the growth of the *sec3* mutants is sensitive to the amount of some nutrients in the medium. The mis-localisation of cell surface transporters may account for these phenotypes. Although a number of amino acid transporters seem to have orthologues in *S. pombe*, our knowledge of their specificity to amino acids, dynamics and regulation, is very patchy. I therefore chose to study the influence of Sec3 on the 2 best characterised amino acid transporters, Aat1 and Cat1. Wild type and *sec3-916* strains expressing either transporter tagged with GFP at their endogenous levels, were grown overnight in EMM at permissive temperature, and then imaged. Due

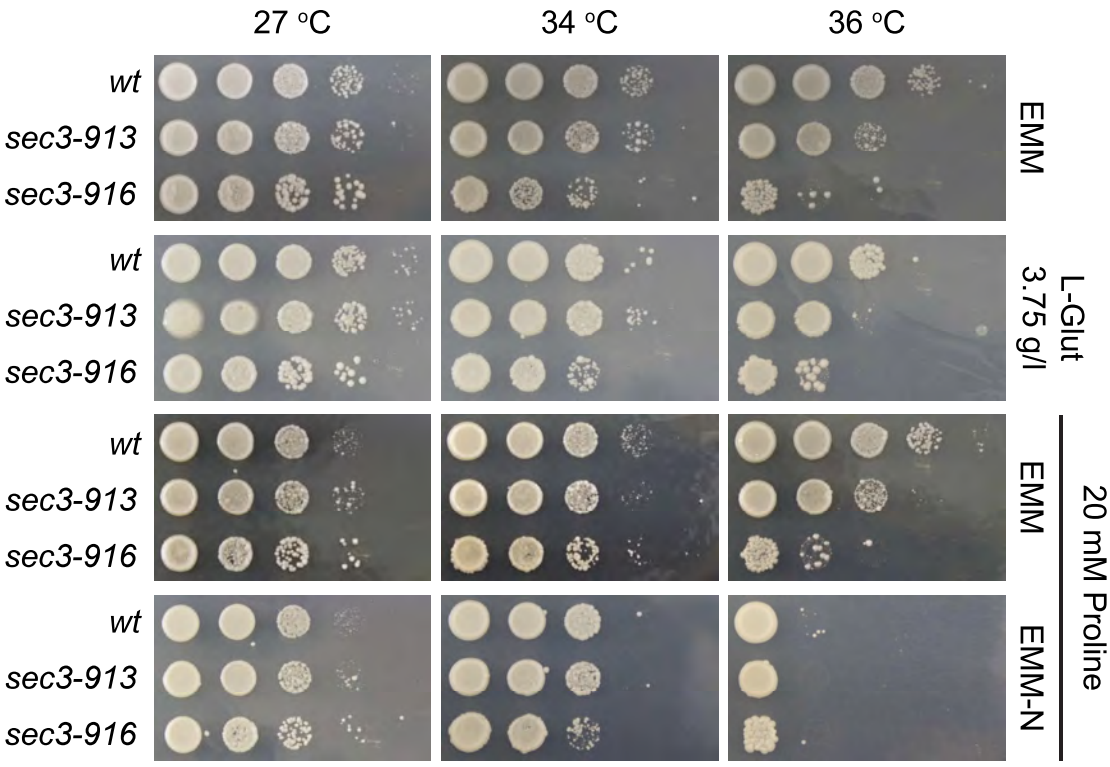

Figure 3.11: Non-repressible nitrogen sources do not affect the growth of *sec3* mutants. Serial dilutions of wild-type (*wt*), *sec3-913* and *sec3-916* cells were spotted on EMM with or without 20 mM proline, or on EMM without nitrogen (EMM-N) containing the indicated concentrations of L-glutamic acid (L-Glut) and proline. Plates were then incubated at the indicated temperatures. Growth of both *sec3-913* and *sec3-916* was not affected by L-glutamic acid or proline.

to the stability of the GFP tag being low at 36 ^{o}C, the *sec3-916* strain was chosen for this experiment as it exhibits a stronger phenotype than *sec3-913* at 27 ^{o}C. Wild type cells were stained with lectin before mixing with *sec3-916* cells to allow differentiation between strains and more accurate intensity observations (see Chapter 2).

In my hands, Aat1 showed a strong localisation at the plasma membrane of the growing tip of vegetative wild type cells but was also associated with cytoplasmic structures (Figure 3.12, panel A). These structures are presumably Golgi-related as this has previously been characterised (Nakase et al., 2012). The *sec3-913* mutant also had positivity with internal structures but exhibited weaker GFP signal at the growing tip than the wild type (Figure 3.12, panel A), indicating that the abundance of Aat1 at the membrane in nutrient rich conditions could be slightly reduced.

The localisation of some amino acid transporters depends on nutrient availability and Aat1 in particular is known to be trafficked to the plasma membrane and then degraded in the vacuolar lumen, in conditions of nitrogen starvation (Nakase et al., 2012). To see if Sec3 played a role in this specific process, *sec3-913* and control WT cells were starved, and the localisation of Aat1-GFP was observed at 1.5 and 6 h by fluorescent microscopy. After 24 hours of starvation, cells were replenished with nitrogen and observed at times 1 and 4 hour. Figure 3.12B, shows no noticeable in difference in the localisation of Aat1-GFP, between WT and *sec3-916* cells during starvation and replenishment indicating that Aat1 appears to be trafficked correctly when Sec3 is not functional.

As described by others (Nakashima et al., 2014), Cat1 was trafficked to the cell tips in vegetative WT cells. This localisation was also observed in the *sec3-916* mutant (Figure 3.13, panel A), however the intensity of the Cat1-GFP signal was higher in *sec3-916* cells when compared to the wild type. When starved, Cat1-GFP was recycled from the tip back to the cytoplasm into structures that are presumably vacuoles in both strains, and during starvation recovery, it was trafficked back to the cell tips again (Figure 3.13, panel B). These data show that Cat1-GFP may be present at higher levels on the plasma membrane in *sec3-916*, but the trafficking dynamics of the amino acid permease function correctly.

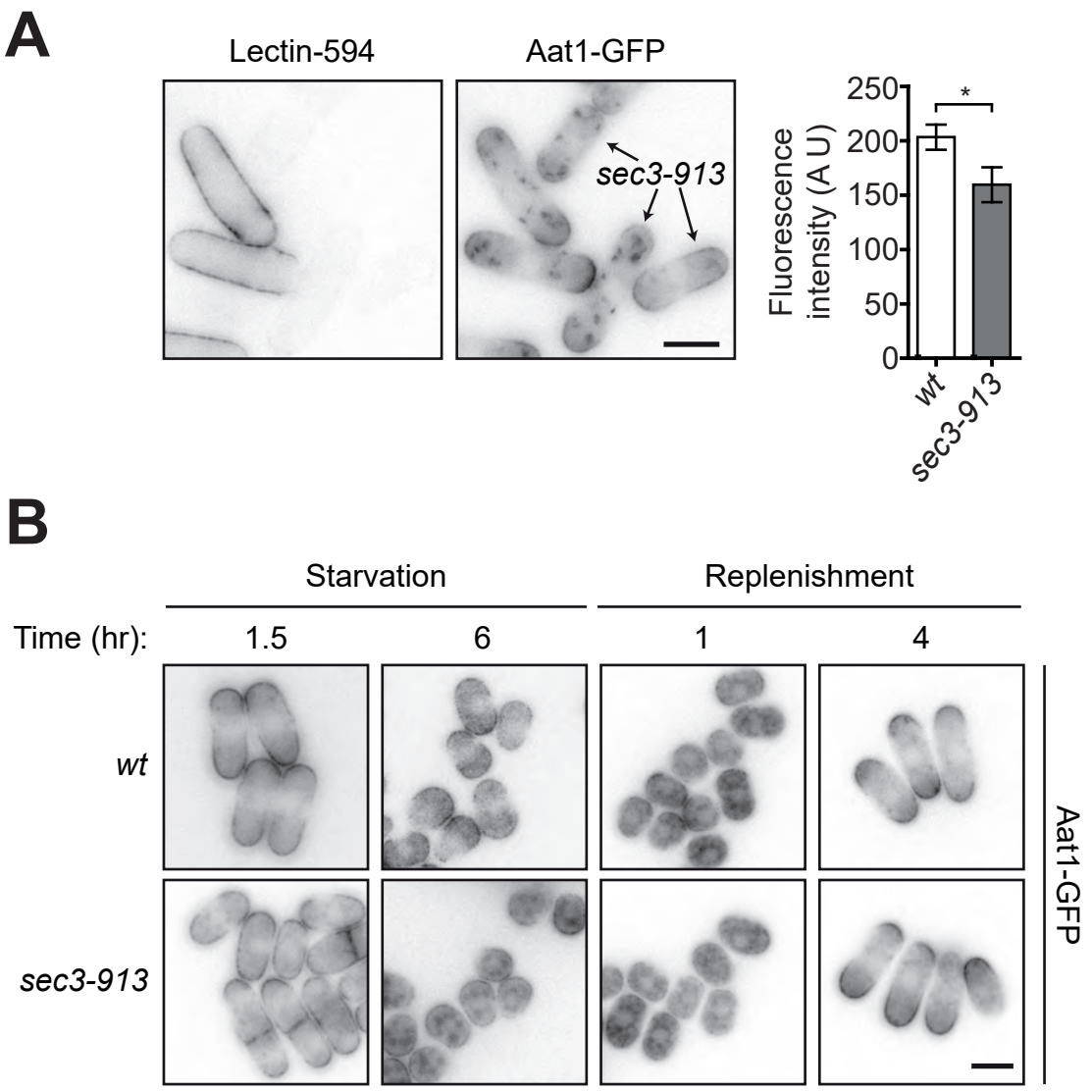

Figure 3.12: Sec3 regulates the localisation of the amino acid transporter Aat1 in vegetative cells. The localisation of Aat1-GFP was observed by wide-field microscopy at 27 °C in wild-type (*wt*) and *sec3-913* cells. **[A]** Both cell types were grown in EMM and observed simultaneously during the mitotic cell cycle. To differentiate the wild type from the mutant, wild-type cells were pre-stained with lectin-red (lectin-594). Arrows point at *sec3-913* cells. The *sec3-913* strain exhibited significantly weaker signal intensity than the *wt* at the cell tips (Mann-Whitney, * p = <0.05, N = >44 cells per condition). **[B]** Each strain was switched from EMM to EMM minus nitrogen (starvation) and observed at 1.5 and 6 hours following this first switch. In both strains Aat1-GFP relocates from the plasma membrane to the lumen of vacuoles. After 24 hours of starvation, cells were replenished with fresh EMM (replenishment) and observed at the indicated time points following this second switch. In both strains, Aat1-GFP relocates from the vacuoles to the plasma membrane. Scale bars = 5 µm.

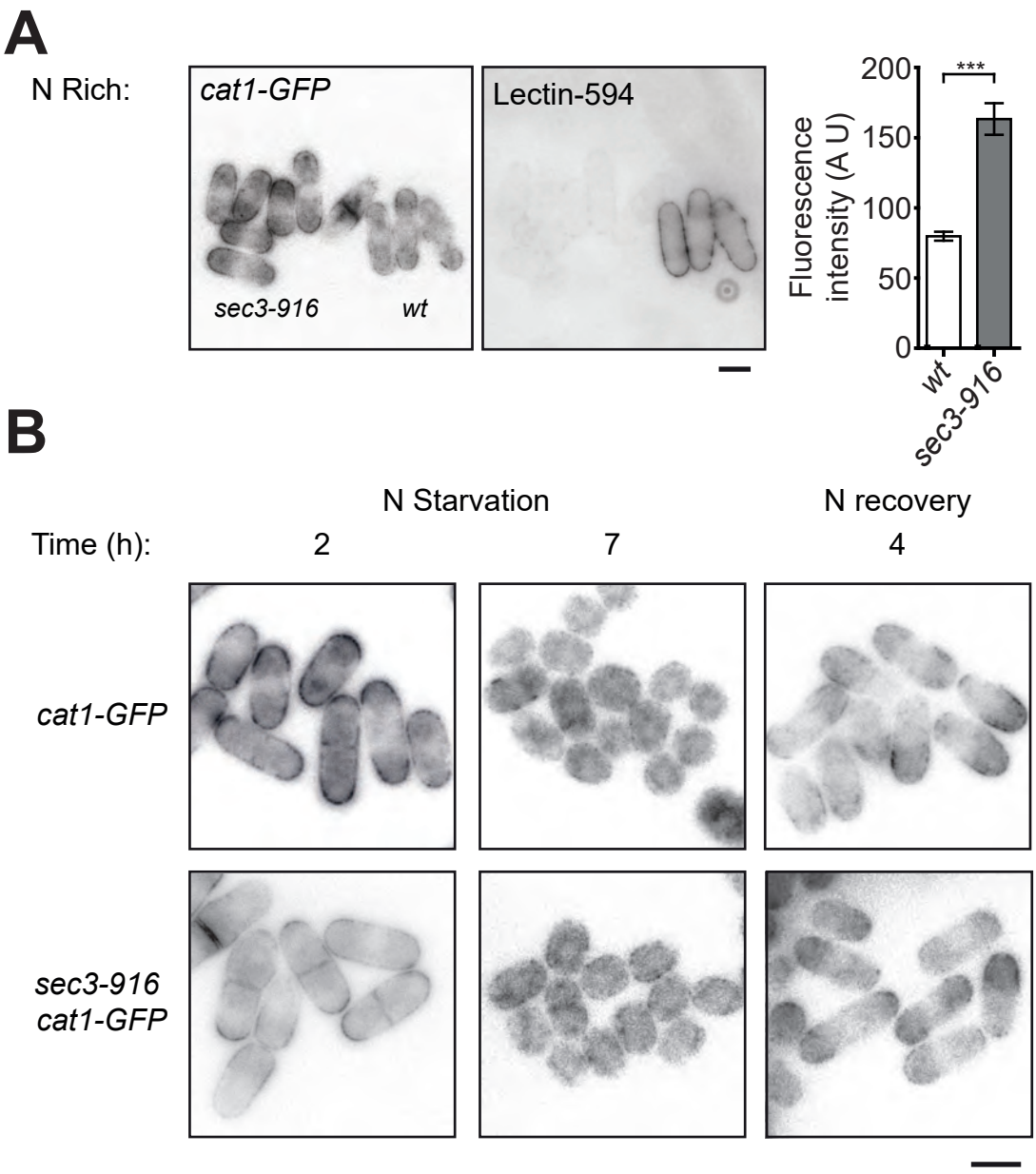

Figure 3.13: Sec3 regulates the localisation of the amino acid transporter Cat1 in vegetative cells. The localisation of Cat1-GFP was observed by wide-field microscopy at 27 ºC in wild-type (*wt*) and *sec3-916* cells. **[A]** Both cell types were grown in EMM and observed simultaneously during the mitotic cell cycle. To differentiate the *wt* from the mutant, *wt* cells were pre-stained with lectin-red (lectin-594). The signal intensity at the tips of *sec3-916* cells is significantly stronger than the wild type (Mann-Whitney, *** p = <0.0001, N = >34 cells per condition). **[B]** Each strain was switched from EMM to EMM minus nitrogen (starvation) and observed at 2 and 7 hours following this first switch. In both strains the Cat1-GFP signal at the cell surface decreased, and possibly relocated to vacuoles. After 24 hours of starvation, cells were replenished with fresh EMM (recovery) and observed at the indicated time points following this second switch. In both strains Cat1-GFP relocates from the vacuoles to the plasma membrane. Scale bars = 5 µm.

Due to the role of the ESCRT complex in the retrograde trafficking of amino acid permeases (Nakase et al., 2012), I investigated whether Sec3 and ESCRT genetically interact. The *sec3-913* mutant was crossed with strains where the ESCRT0 components Sst4 and Hse1 were deleted. A growth assay of these strains with the wild type was then performed on YE5S. All strains grew like the wild type at the permissive temperature of 27 ^{o}C (Figure 3.14). However at the restrictive temperature of 36 ^{o}C the *hse1D* and *sst4D* grew like the wild type, but were temperature sensitive when they possessed the *sec3-913* mutation (Figure 3.14). This shows that Sec3 and ESCRT0 do not interact and therefore the amino acid permease phenotype is not through ESCRT.

3.3 Discussion

Cellular growth and division requires the ability to be able to sense environmental nutrient concentrations, and also the uptake of nutrients that drive the production of energy, proteins, lipids, and nucleotides needed for growth. All of this requires the correct trafficking and positioning of nutrient importers in the plasma membrane. Due to the exocyst's vital role in both the exocytosis and endocytosis of cargoes (Grote et al., 2000; Jourdain et al., 2012; Morgera et al., 2012; Sommer et al., 2005), I asked the question of whether the exocyst may play a role in the sensing and/or uptake of nutrients. In this chapter I found that environmental levels of glucose do not affect the growth of *sec3* mutants, however high levels of ammonium and the amino acid leucine do, highlighting that exocyst may be involved in nitrogen and leucine uptake and metabolism. Further analysis showed that the arginine/lysine transporter Cat1 and Aat1 levels at the plasma membrane may be altered by Sec3, but treatment with canavanine shows that uptake of arginine does not appear to be increased. This chapter shows that the exocyst complex appears to function in cellular growth in response to environmental nitrogen and leucine.

3.3.1 Leucine is toxic to sec3 mutant cells.

Interestingly the data presented here show a novel interaction between Sec3 and the cells' ability to sense or metabolise the amino acid leucine. High levels of environmental leucine reduced the growth of exocyst mutants, but did not affect the wild type. This shows that a non-functional exocyst makes leucine toxic to

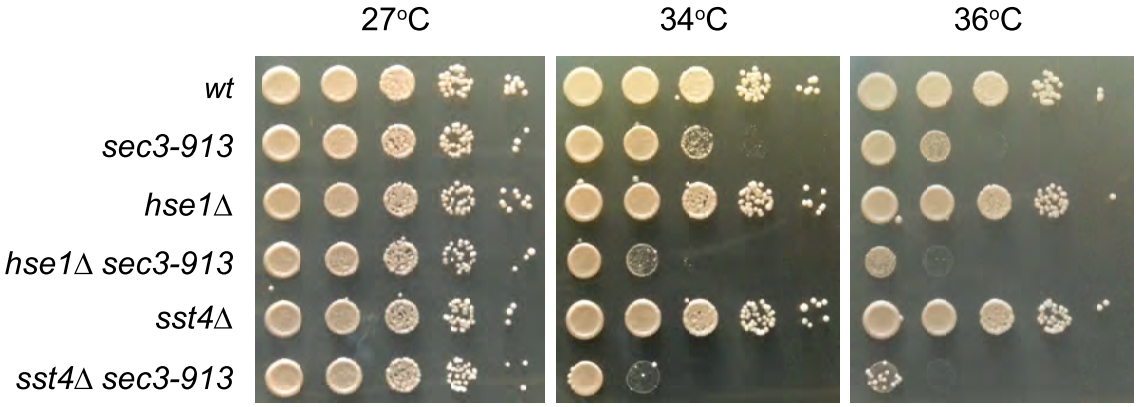

Figure 3.14: *sec3* and the ESCRT0 complex sit in two different pathways. Serial dilutions of wild-type (*wt*), *sec3-913*, *hse1*Δ, *sst4*Δ, *hse1*Δ *sec3-913* and *sst4*Δ *sec3-913* cells were spotted on YE5S agar medium, and incubated at the permissive (27 °C), semi-restrictive (34 °C) or restrictive (36 °C) temperatures.

fission yeast. Leucine is one of three branched chained amino acids and is metabolised to acetyl-CoA where it enters the TCA cycle to produce ATP. However leucine has additional intracellular roles compared to other amino acids. It can be metabolised to HMG-CoA in the mevalonate pathway which is responsible for the production sterols. Also leucine can be stored in fission yeast vacuoles where it activates the TORC1 complex through the Rag GTPases Gtr1/2 on the vacuolar membrane (Sancak et al., 2008; Wiemken and Dürr, 1974). TORC1 signalling leads to activation of anabolic pathways and cellular growth (see Introduction) (Düvel et al., 2010; Mayer et al., 2004; Nakashima et al., 2010; Porstmann et al., 2008), linking leucine sensing to cell growth and division. In mammalian cells leucine is a potent activator or mTORC1 via the sestrin family of proteins (Chantranupong et al., 2014; Kimball et al., 2016; Xu et al., 2019). It remains unclear why leucine specifically is a potent activator of TOR. One hypothesis is that leucine is poorly metabolised in the liver so therefore activation of TOR would promote anabolic pathways that help to metabolise leucine reducing cellular concentrations (Ichihara and Koyama, 1966; Lynch et al., 2003).

3.3.2 How does Sec3 control the amount of importers at the cell surface?

When examining the dynamics of the amino acid transporter Cat1, I found that the GFP signal was more intense at the plasma membrane when Sec3 is not functional. Several reasons may account for this observation.

The mutation of *sec3* leads to an accumulation of secretory vesicles, indicating that there is a defect in exocytosis (Jourdain et al., 2012). Because of this it was expected that less of the cargoes involved in transporting nutrients into the cell should be delivered to the plasma membrane in exocyst mutants. This is interesting as the intensity should be dimmer in exocyst mutants due to the defect in secretion. A possible explanation for this is due to Sec3's role in endocytosis. Mutation of Sec3 leads to a loss of polarity in endocytic actin patches, and slower patch internalisation (Jourdain et al., 2012). This means that it is possible that the mutation of *sec3* is affecting the endocytosis of Cat1 instead, which could therefore account for the sensitivity to amino acids. However upon starvation Cat1 leaves the membrane in *sec3-916* indicating that retrograde trafficking via endocytosis still appears to be functional. It is possible that exocytosis of amino acid transporters can still occur as Exo70 also localises the exocyst to sites of

secretion and plays a redundant role in the absence of functional Sec3 (Bendezú et al., 2012). Another possibility is secretion of amino acid permeases via an interaction with the SNARES and bypassing the exocyst. In neurons it was shown that the secretion of synaptic vesicles can occur regardless of whether the exocyst is present or not (Murthy et al., 2003). Therefore Cat1 could still be secreted by the SNARES, but the exocyst may fine tune this process to ensure correct number of permeases reach the membrane.

As mentioned earlier, Sec3 was found to possibly play a role in the trafficking of Cat1. Characterisation of Cat1 has identified that it is involved in the uptake of arginine, lysine, and histidine (Aspuria and Tamanoi, 2008). Whilst this is a novel phenotype of the exocyst mutant, it cannot explain the leucine sensitivity as this amino acid appears to be taken up through a separate permease. The SAGA histone modification complex modulates leucine uptake through promoting transcription of the amino acid permease Agp3 (Takahashi et al., 2012). Agp3 is trafficked to the plasma membrane in response to nitrogen starvation, and this is modulated by the TORC1 signalling as deletion of the TORC1 inhibitor Tsc1 resulted in a delay of Agp3 trafficking from endosomes to the PM (Liu et al., 2015). However it's homologue in *S. cerevisiae* was shown to not be specific just to leucine (Schreve and Garrett, 2004). Because of this it was a better strategy to examine Aat1 and Cat1 as much more is known about their trafficking, response to nutrients, and amino acids they regulate.

3.3.3 Is amino acid uptake perturbed in sec3 mutants?

Addition of $NH4^+$ has previously been shown to reduce the uptake of leucine in *S. pombe* through the polyubiquitinase Pub1 (Karagiannis et al., 1999). Deletion of Pub1 completely blocked the effect of $NH4^+$ on reducing leucine uptake, showing that Pub1 regulates uptake of the nutrients in conjunction with ammonium (Karagiannis et al., 1999). Pub1 regulates the level of amino acid permeases on the membrane through ubiquitinating adaptors such as Arn1 which then promote retrograde transport of the cargo (Aspuria and Tamanoi, 2008; Nakase et al., 2012; Nakashima et al., 2014). Putting these together it appears that $NH4^+$ promotes amino acid permease endocytosis via Pub1, which reduces cellular uptake of amino acids. The data presented in this chapter shows that Sec3 is hypersensitive to leucine concentrations in the environment, and this is rescued when ammonium chloride is supplemented at twice the level of normal

media. This means that the rescue by $NH4^+$ could be through the removal of amino acid permeases by Pub1, meaning that amino acid uptake may be increased in *sec3* mutants. Further evidence for this is the increase of Cat1 signal on the plasma membrane seen in *sec3-916*, as Cat1 is also regulated by Pub1 (Nakashima et al., 2014).

Evidence against this argument is that the *sec3* mutants do not appear to be much more sensitive to the toxic arginine analogue canavanine than the wild type, indicating no major difference in amino acid uptake. This notion is further reinforced by the data showing that arginine concentrations do not affect growth of *sec3* mutants. Unfortunately no know toxic leucine analogue exists so therefore leucine uptake could not be examined. Previous studies have shown this relationship between ammonium chloride and radiolabelled leucine (Karagiannis et al., 1999). It was not possible to possible to perform a similar experiment in my PhD due to time constraints on radioactive training and sourcing a scintillator. All in all it appears that Sec3 may localise permeases but has no effect on amino acid uptake, and furthermore the leucine phenotype appears to be due to metabolism or functions in the side the cell and independent of uptake.

3.3.4 The whole exocyst complex may not be necessary to sense nutrients

When examining other exocyst members for leucine sensitivity I found that *sec3* and *sec8* mutants were both sensitive in a similar manner to leucine. Interestingly deletion of *exo70* did not show the same thing. This is interesting as both *sec3* and *exo70* are members of the exocyst that bind to the plasma membrane and are thought to help localise the complex to the right place (Boyd et al., 2004). So therefore one would expect both *sec3* and *exo70* to share a similar phenotype. This could be due to the fact that *sec3* is essential and *exo70* is not (Kim et al., 2010). This phenotype is more likely due to *sec3-913* possessing both Exo70 and a semi functional Sec3, whereas *exo70Δ* only possesses Sec3 as a targeting member.

Alternatively it could be possible that the exocyst forms sub complexes and *sec3* and *sec8* belong to one that helps sense leucine. The notion of exocyst sub-complexes is still unclear in the field. One study revealed that in *S. cerevisae*, all the exocyst members co-immunoprecipitate with each other providing evidence against the notion of subcomplexes (Heider et al., 2016). However the study also showed that the exocyst may assemble as 2 holocomplexes before assembling

into the final hetero-octameric structure (Heider et al., 2016). This shows that exocyst subunits do have the ability to assemble in different groups. Furthermore, the staining of different epitopes of mammalian Sec6 revealed that it co-localises with many intracellular structures such as the endoplasmic reticulum, intermediate filaments, and desmosomes depending on the epitope stained for (Inamdar et al., 2016). This shows that depending on how exocyst members fold and mask epitopes could reveal which function they undertake, and that this differential folding could be due different members in the complex.

3.3.5 Sensing or metabolism?

Mutations in the exocyst result in strains growing poorly on rich media, suggesting that they may exhibit a nutrient toxicity phenotype. I expected that the strains may not respond to starvation as they are hyper-sensitive to nutrients. The *sec3-913* mutant was found to respond nitrogen starvation as expected (Young and Fantes, 1987). Starvation also triggers autophagy (Hosokawa et al., 2009). The exocyst has been found to be required for the initiation of autophagy by acting as a scaffold for atg-related components (Bodemann et al., 2011; Singh et al., 2019). This evidence made it more likely that *sec3* mutants may have a starvation defect due to problems with autophagy, but this did not appear to be true. The relationship between Sec3 and autophagy will be presented in Chapter 4.

Leucine promotes cellular growth by activating the target of rapamycin (TORC1) complex. Leucine activates a vacuolar ATPase, stimulating a conformational change (Takayama et al., 2018). This change in shape releases the Rag GTPases Gtr1 and Gtr2 which recruit the TORC1 complex to the vacuole and place it next to its activator Rheb (Binda et al., 2009; Sancak et al., 2008). Once activated Tor2 kinase phosphorylates its downstream target S6 kinase. S6 kinase then promotes expression of genes needed for growth which are involved in processes such as ribosomal biogenesis, DNA replication, protein expression (Nakashima et al., 2012). When leucine is not available, the tuberous sclerosis complex (TSC1/2) deactivates TORC1 by acting as guanine activating protein (GAP) for Rheb and releases it from the vacuole (Inoki et al., 2003). This causes S6 kinase to become dephosphorylated which causes the cell to stop growing. TORC1 also directly inhibits autophagy, and so when it is inactivated, autophagy becomes activated (Kamada et al., 2010). One hypothesis for the leucine sensitivity in *sec3* mutants is that the exocyst may negatively regulate TORC1,

and therefore loss of Sec3 allows TORC1 to be overactive which is exacerbated by excess leucine. I have tested this hypothesis and results will be presented in Chapter 4.

Chapter 4: Sec3 genetically interacts with the TORC2 signalling complex

4.1 Introduction

Cellular growth is regulated by the highly conserved target of rapamycin (Tor) signalling network. Tor consists of two complexes TORC1 and TORC2 (Loewith et al., 2002). These complexes sense the nutrient availability in the environment: in nutrient rich conditions they promote growth by stimulating anabolic processes such as nucleotide, protein, lipid synthesis, and ribosome biogenesis whilst inhibiting catabolic processes such as autophagy and proteolysis. When deactivated in environments of poor nutrient availability, growth signalling is stopped allowing the cell to proceed down a catabolic route to recycle components and generate a free pool of monomers of amino acids and fats *etc*. (Settembre et al., 2013).

Both budding yeast and fission yeast possess two conserved Tor kinases. ScTor1p is the homologue of SpTor2 which is the kinase that associates with TORC1 (see Table 1.1) (Loewith et al., 2002). Similarly ScTor2p and SpTor1 are the yeast homologues that are central to TORC2 signalling (see Table 1.1) (Loewith et al., 2002). For clarity the *S. pombe* nomenclature for Tor will be used throughout. While these kinases are considered specific to each complex, work in fission yeast has shown that Tor1 can also associate with a TORC1 like complex which plays a role in mitotic entry in response to nutrient stress (Hartmuth and Petersen, 2009). In contrast to yeast, mammals only contain one Tor kinase called mTOR (Brown et al., 1994; Sabatini et al., 1995; Sabers et al., 1995).

4.1.1 The TORC1 complex

A surplus of lipids, proteins and nucleotides is required for cellular growth and division, and TORC1 is responsible for the production of these components by controlling the balance between anabolic and catabolic pathways in response to environmental nutrients. The TORC1 complex consists of multiple proteins including Tor2 kinase, the mLST8 homologue Pop3/Wat1, and the Raptor homologue Mip1 (Loewith et al., 2002). This complex is recruited to the vacuole when nutrients, especially leucine, are available (Binda et al., 2009; Chia et al., 2017; Noda and Ohsumi, 1998). Leucine is stored in the vacuoles or lysosomes

whose membranes house a vATPase protein that functions to sequester the Rag GTPase family members Gtr1 and Gtr2 (Binda et al., 2009; Saliba et al., 2018; Takayama et al., 2018; Wiemken and Dürr, 1974). In the presence of leucine, the vATPase undergoes a conformational change which releases Gtr1 and Gtr2 thus changing their nucleotide loading from GDP to GTP (Binda et al., 2009). The Rag GTPases recruit the TORC1 complex to the vacuolar membrane where its activator, the Ras GTPase Rheb, is situated (Bai et al., 2007). The close proximity allows Rheb-GTP to activate TORC1 by removing its inhibitor FKBP38 leading to growth signalling (Bai et al., 2007). This process is different in mammalian cells where arginine is a potent Tor activating amino acid in the vacuole. Leucine still activates mTOR but through proteins called sestrins in the cytoplasm, rather than in the vacuole (Chantranupong et al., 2014; Xu et al., 2019). So far no sestrin homologues have been found in *S. pombe*, at the amino acid level. The closest functional sestrin homologues in yeast are the *S. cerevisiae* SEACAT/SEACIT complexes and *S. pombe* GATOR1/2 complexes which have been shown to affect TORC1 activity in response to amino acids through the Rag GTPases (Chia et al., 2017; Dokudovskaya and Rout, 2011).

Once activated TORC1 phosphorylates its specific downstream targets including the AGC kinases Psk1 S6 kinase, Sck1 and Sck2 (Nakashima et al., 2012). These kinases then activate downstream targets including ribosomal protein S6 which stimulates ribosomal biogenesis, and the greatwall/endosulfine pathway proteins Ppk18 and Igo1 which control cell size and division in response to nutrient availability (Chica et al., 2016). TORC1 also phosphorylates targets in order to inhibit them. One such target includes the autophagy protein Atg13 which is phosphorylated to inhibit autophagy when nutrients are available (Hosokawa et al., 2009; Kamada et al., 2010). Targets involved in translation of genes in response to stress and nitrogen starvation are also negatively regulated by phosphorylation (Matsuo et al., 2007). Ultimately TORC1 activation drives the cell towards cell growth and division and away from stress and starvation responses.

Deactivation of TORC1 mainly occurs through the tuberous sclerosis complex of proteins Tsc1/2. This protein complex possess a GTPase activating protein (GAP) which deactivates TORC1 by converting Rheb-GTP into Rheb-GDP (Inoki et al., 2003). Rheb-GDP can no longer sequester FKBP38 and therefore TORC1 becomes inhibited, and released back in to the cytoplasm from the vacuole. The

TORC1 complex is also rapidly inhibited by the drug rapamycin. Rapamycin binds to a protein called FKBP12, which then binds to the FKBP38 site situated on Tor2 kinase (Vilella-Bach et al., 1999). This makes it a good tool for the study of the Tor signalling.

4.1.2 The TORC2 complex

The Tor signalling axis contains a second complex called TORC2. Rather than growth and division, TORC2 is strongly linked to stress signalling, regulation of membrane tension through sterol biosynthesis, reorganisation of actin cytoskeleton, uptake of leucine, and mitochondrial biogenesis (Muir et al., 2014; Niles and Powers, 2014; Weisman et al., 2005; Wu et al., 2006). This complex is situated at the plasma membrane and consists of Tor1 kinase, Sin1, Rictor homologue Ste20, and similarly to TORC1, Pop3/Wat1 (Loewith et al., 2002). The targeting of TORC2 to the PM is still not understood, however TORC2 interacting proteins Slm1 and Slm2 possess PH domains which are thought to target the complex to PIP_2 domains (Fadri et al., 2005). Rictor stands for Rapamycin Insensitive Component of Tor, and this is due to TORC2 widely being regarded as rapamycin insensitive and therefore not inhibited by the drug (Gaubitz et al., 2015; Loewith et al., 2002). However prolonged exposure to rapamycin has been seen to inhibit TORC2 (Sarbassov et al., 2006).

It is still unclear how TORC2 is regulated but recent studies have started to figure out how it is activated and deactivated. TORC2 may possibly be regulated by amino acids like its counterpart (Moloughney et al., 2016). Instead TORC2 is sensitive to levels of environmental glucose, in which glucose signals through the GTPase Ryh1 to activate the complex (Hatano et al., 2015). TORC2 is also regulated by plasma membrane tension (Riggi et al., 2018). The presence of sterols in the plasma membrane reduces membrane tension and increases fluidity (Riggi et al., 2018). *S. cerevisiae* TORC2 is activated by the eisosome protein Slm1 which is released from eisosomes when membrane tension is high (Berchtold et al., 2012). Activation of TORC2 causes the phosphorylation of its downstream effector SpGad8/ScYpk1 (Ikeda et al., 2008). Phosphorylation of Gad8 causes the upregulation of genes involved in sphingolipid biosynthesis, generating sterols which are then delivered to the plasma membrane reducing membrane tension. If the membrane is fluid enough, it starts to fold in on itself

generating zones rich in PIP_2 lipids. TORC2 is then translocated to these zones and deactivated by PIP_2 (Riggi et al., 2018).

TORC2 activation also plays a role in the polarisation of endocytic actin patches and contraction of the cytokinetic actomyosin ring (CAR). The TORC2 component Ste20 localises to the CAR where it plays a role in CAR contraction through interactions with myosins (Baker et al., 2016). In a similar fashion, Ste20 has been shown to activate the endocytosis specific myosin, myosin I, via the TORC2-Gad8 signalling axis, revealing a mechanism of how TORC2 modulates endocytosis at the plasma membrane (Baker et al., 2019).

In the previous chapter, mutants of *sec3* were found to be sensitive to the amino acid leucine only. This sensitivity did not appear to be due to an increase in amino acid import as canavanine uptake showed no difference in cell death between the *sec3* strains and the wild type, indicating amino acid uptake is at a homeostatic level. This instead indicates that it is something that leucine is doing inside the cell that is causing the sensitivity seen in both *sec3-913* and *sec3-916*. As leucine activates TORC1 and its uptake is regulated by TORC2 (Binda et al., 2009; Weisman et al., 2005), it is reasonable to suggest that Tor signalling might be affected by the mutation in *sec3*. This chapter examines the possibility of a novel interaction between the exocyst member Sec3 and the Tor signalling network.

It is also possible that the exocyst interacts with the TORC2 complex. Added weight to this comes from the fact the *sec3* mutants phenocopy *ste20* deletion strains. Deletion of *ste20* in budding yeast alters the polarisation of the actin cytoskeleton (Eby et al., 1998) and mutation of *sec3* in fission yeast causes the depolarisation of actin patches, and also decreases the speed of endocytic patch internalisation (Jourdain et al., 2012). Furthermore the temperature sensitive phenotype of *sec3* mutants can be rescued by the presence of the osmotic stressor sorbitol (Bendezú et al., 2012). This compound alters the osmotic gradient of the cell, which is an important regulatory process in the maintenance of membrane tension which also regulates TORC2 (Riggi et al., 2018).

4.2 Results

4.2.1 Turning off Tor rescues mutants of the exocyst complex.

To examine whether the nutrient toxicity in *sec3* mutants is due to an effect of the Tor signalling axis, wild-type and *sec3* mutant strains were spotted on YE5S containing rapamycin. Rapamycin is a compound that selective inhibits the Tor complex, which results in a loss of Tor signalling and therefore stunted growth. Initially, I used working concentrations of rapamycin that are described in the literature (~ 25 ng/ml; examples in (Weisman et al., 2001)). Intriguingly rapamycin showed complete rescue of *sec3-913* and partial rescue of *sec3-916* at the restrictive temperature (Figure 4.1). To see in what extend rapamycin rescues the growth of the *sec3* mutants, I conducted a dose- response experiment (1 to 25 ng/ml). Figure 4.1 shows that amounts of rapamycin 25 x times lower than what are usually used in the field, still rescued the growth of *sec3-913* and *sec3-916* at the restrictive temperature.

To show that the rapamycin rescue of the *sec3* mutants is Tor specific I examined the growth of *sec3-913* in which the FKBP12 homologue Fkh1 is deleted. Rapamycin forms a complex with Fkh1 to inhibit Tor kinase, so therefore deletion of this gene confers resistance to rapamycin (Vilella-Bach et al., 1999). All strains grew at a similar rate on YE5S at the permissive temperature with both rapamycin and DMSO (Figure 4.2). At the restrictive temperature the *fkh1Δ* strain grew to the same extent as the wild type in both DMSO and with the addition of 25 ng/ml rapamycin. On YE5S with DMSO *sec3-913* and *sec3-913 fkh1Δ* were both temperature sensitive to the same degree, however addition of rapamycin only rescued *sec3-913* and not *sec3-913 fkh1Δ*. This result shows that Fkh1 is needed for the rapamycin rescue of *sec3-913* cells and that this rescue is specific to Tor.

To see if this response to rapamycin is Sec3 specific or related to the exocyst complex as a whole, *exo70Δ* was spotted alongside *sec3* and *sec8* mutants on YE5S containing DMSO or rapamycin (25 ng/ml). At the restrictive temperature all exocyst mutants exhibited temperature sensitivity, and all were rescued by the addition of rapamycin to the medium (Figure 4.3). These data show that the link between Tor signalling and exocyst is not specific to Sec3.

Nutrients affect Tor signalling and as I have shown in Chapter 3, also affect the growth of *sec3 ts* mutants. I therefore wondered whether the response to

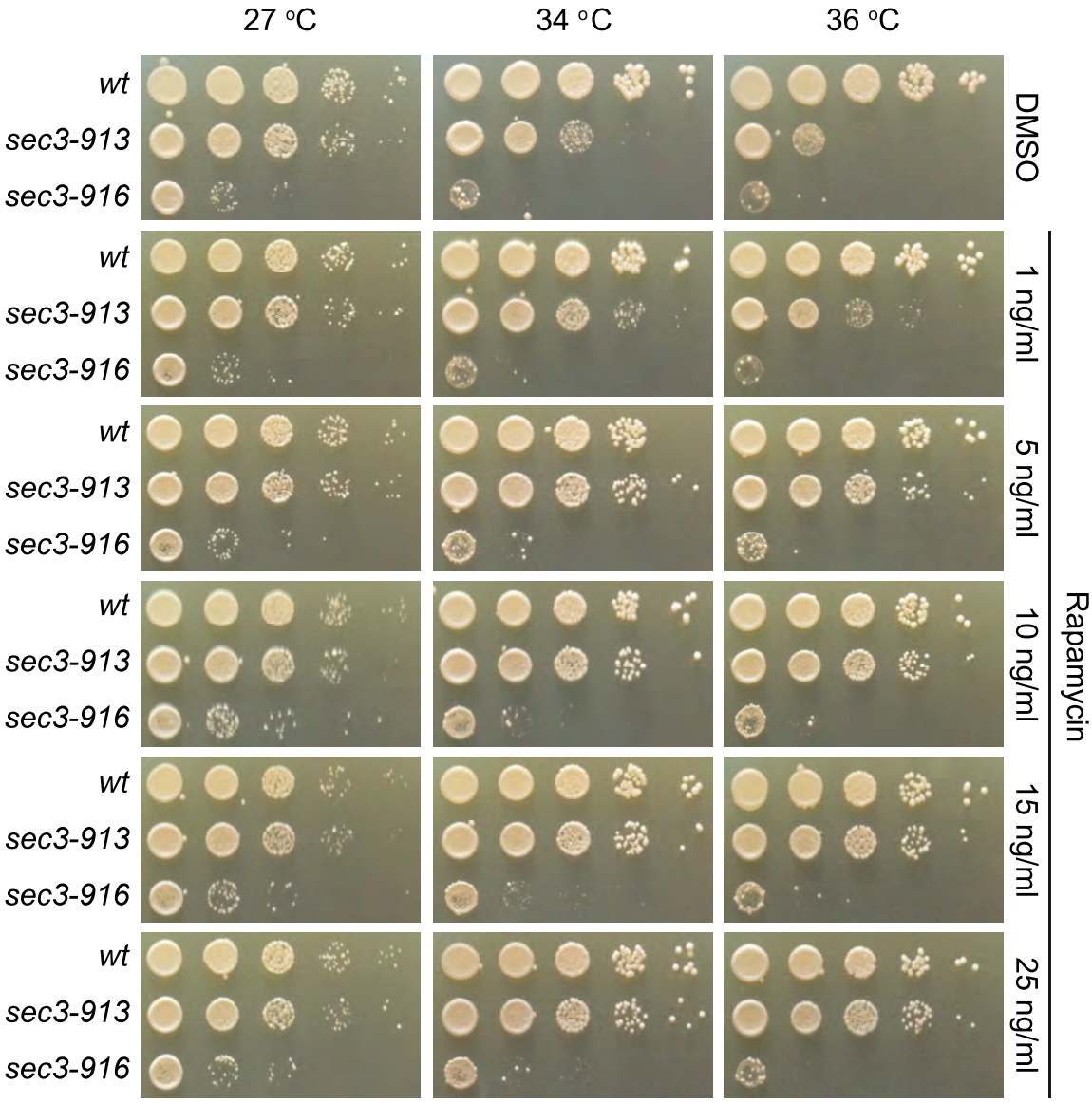

Figure 4.1: The growth of *sec3-913* is completely rescued by rapamycin. Serial dilutions of wild-type (*wt*), *sec3-913* and *sec3-916* cells were spotted on YE5S agar medium containing no rapamycin (DMSO), or increasing concentrations of rapamycin, up to 25 ng/ml. For this type of growth assay on solid medium, the fission yeast community typically uses rapamycin at 25-100 ng/ml. Plates were incubated at the permissive (27 °C), semi-restrictive (34 °C), and restrictive (36 °C) temperatures. The temperature sensitivity phenotype of both mutants is completely rescued by very low amounts of rapamycin.

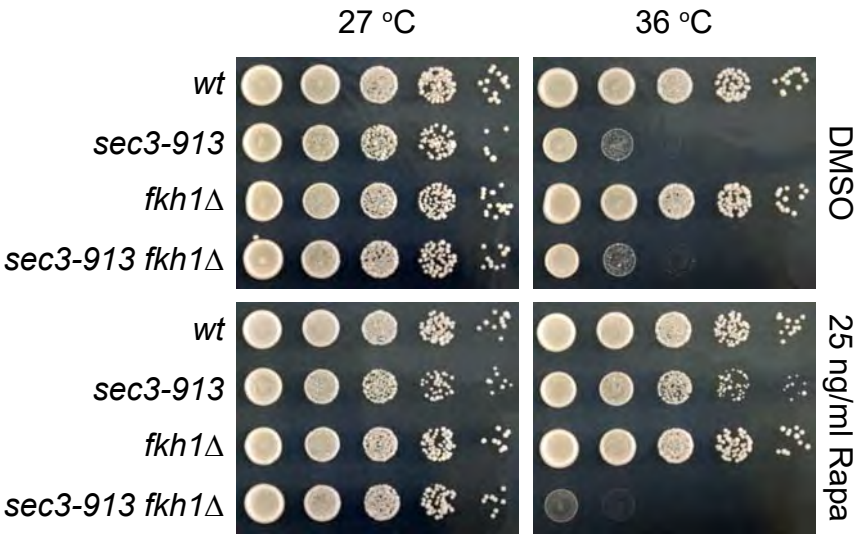

Figure 4.2: The rapamycin rescue of *sec3-913* cells is via *fkh1*. Spot test showing the growth of wild-type (*wt*), *sec3-913*, *fkh1*Δ and *sec3-913 fkh1*Δ strains on YE5S –agar containing no (DMSO) or 25 ng/ml rapamycin (Rapa) at the indicated temperatures. Rapamycin no longer rescues the growth of *sec3-913* cells when *fkh1* is also deleted.

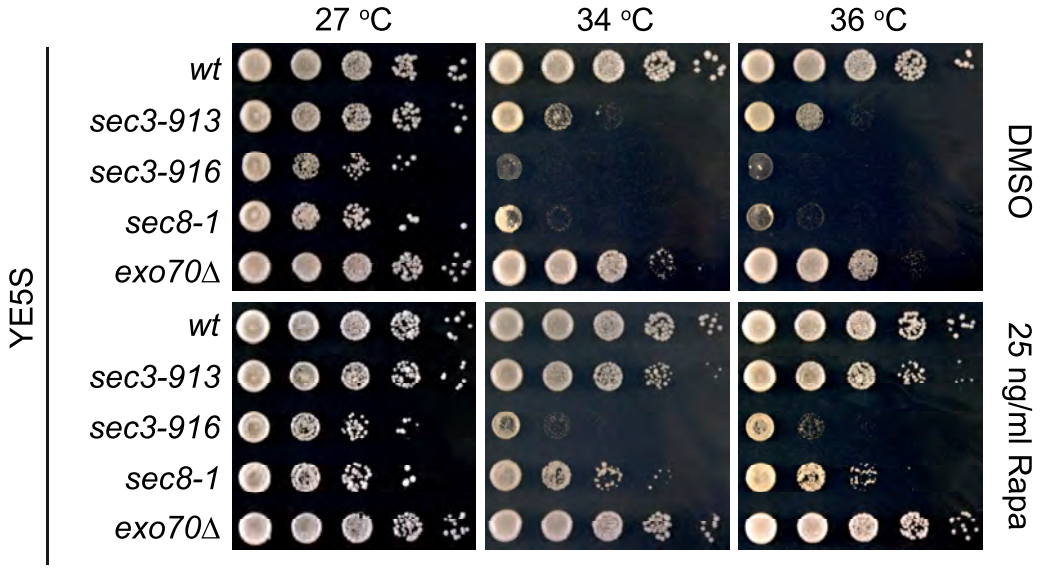

Figure 4.3: The growth of *sec8* and *exo70* mutants is also rescued by rapamycin. The growth of *sec8-1* and *exo70*Δ cells on rapamycin was assessed by spot test assay, on YE5S plates containing no (DMSO) or 25 ng/ml rapamycin (Rapa). The wild type (*wt*) was used as a negative control, and *sec3-913* and *sec3-916* were used as positive controls

rapamycin observed in rich media translates on to minimal media. Wild-type and *sec3* mutant strains were grown on EMM without amino acids and containing either DMSO or rapamycin. Rescue of growth was still seen with rapamycin, although it was less pronounced than in YE5S (Figure 4.4). These data show that rapamycin rescues the temperature sensitive phenotype of both strains on minimal medium.

To see whether rapamycin rescued the leucine sensitivity phenotype seen in *sec3* mutants, wild-type and *sec3* mutant strains were spotted on EMM with no amino acids or containing increasing concentrations of leucine with DMSO or rapamycin. Reduction in growth was seen with increasing concentrations of leucine at the restrictive temperature (Figure 4.5). Addition of rapamycin completely rescued both mutants when on media containing 1x (225 mg/l) and 4x (900 mg/l) leucine. Interestingly leucine sensitivity appeared again at 4x leucine when grown on media containing rapamycin. These data show that rapamycin can rescue the leucine sensitivity of *sec3* mutants when leucine concentrations are up to double, but high levels of leucine appear to override the rapamycin rescue. All in all these results show that inhibiting Tor signalling rescues the growth of the *sec3* mutants.

4.2.2 Sec3 does not interact genetically with TORC1

As TORC1 appears to be the more sensitive to leucine levels of the two complexes, the leucine sensitivity of the *sec3* mutants makes TORC1 the likely candidate for this phenotype. In other organisms, the exocyst also plays a fundamental role in the initiation and regulation of autophagy, which is a process that is also governed by TORC1 signalling and not TORC2 (Hosokawa et al., 2009; Kamada et al., 2010). Because of this it could be possible that TORC1 regulates the exocyst as part of its control over autophagy.

4.2.2.1 sec3 mutants do not genetically interact with atg *genes but have abnormal vacuoles.*

Due to the exocyst's prominent role in the scaffolding of autophagy proteins, it was possible that rescue by rapamycin could be due to modulation of autophagy. To examine this I performed a growth assay to examine the rapamycin rescue of *sec3-913* in a strain that also had the autophagy protein Atg1 deleted. Atg1 is the key kinase involved in initiating autophagy, so therefore rapamycin treatment of *atg1Δ* should not initiate autophagy (Kamada et al., 2010). At 27 ^{o}C all strains

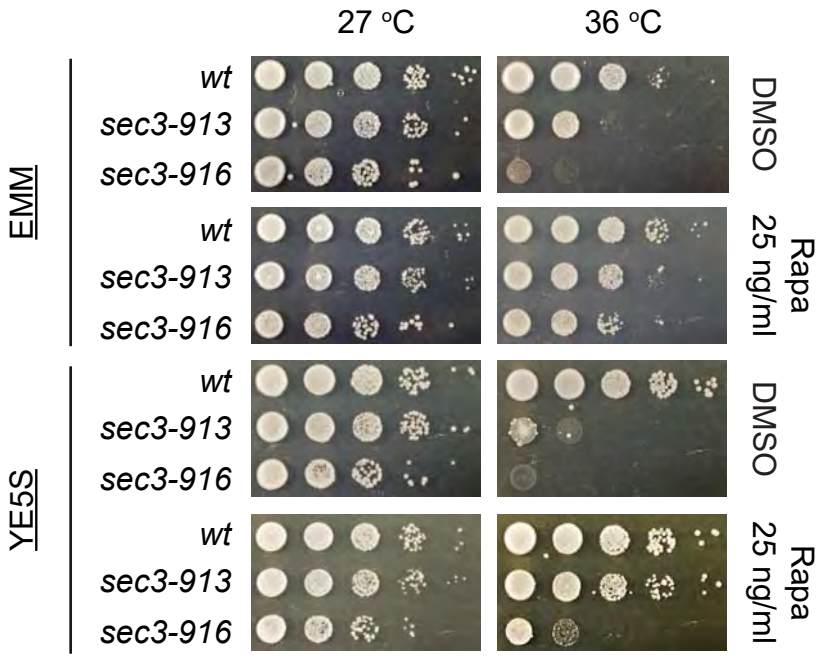

Figure 4.4: Rapamycin rescues the growth of *sec3-913* cells in both rich and minimal media. Wild-type (*wt*), *sec3-913*, and *sec3-916* cells were spotted in 10-fold serial dilutions on EMM or YE5S containing either no (DMSO) or 25 ng/ml rapamycin (Rapa) and observed at the indicated temperatures. The growth rescue of *sec3* mutants is less pronounced in EMM than in YE5S.

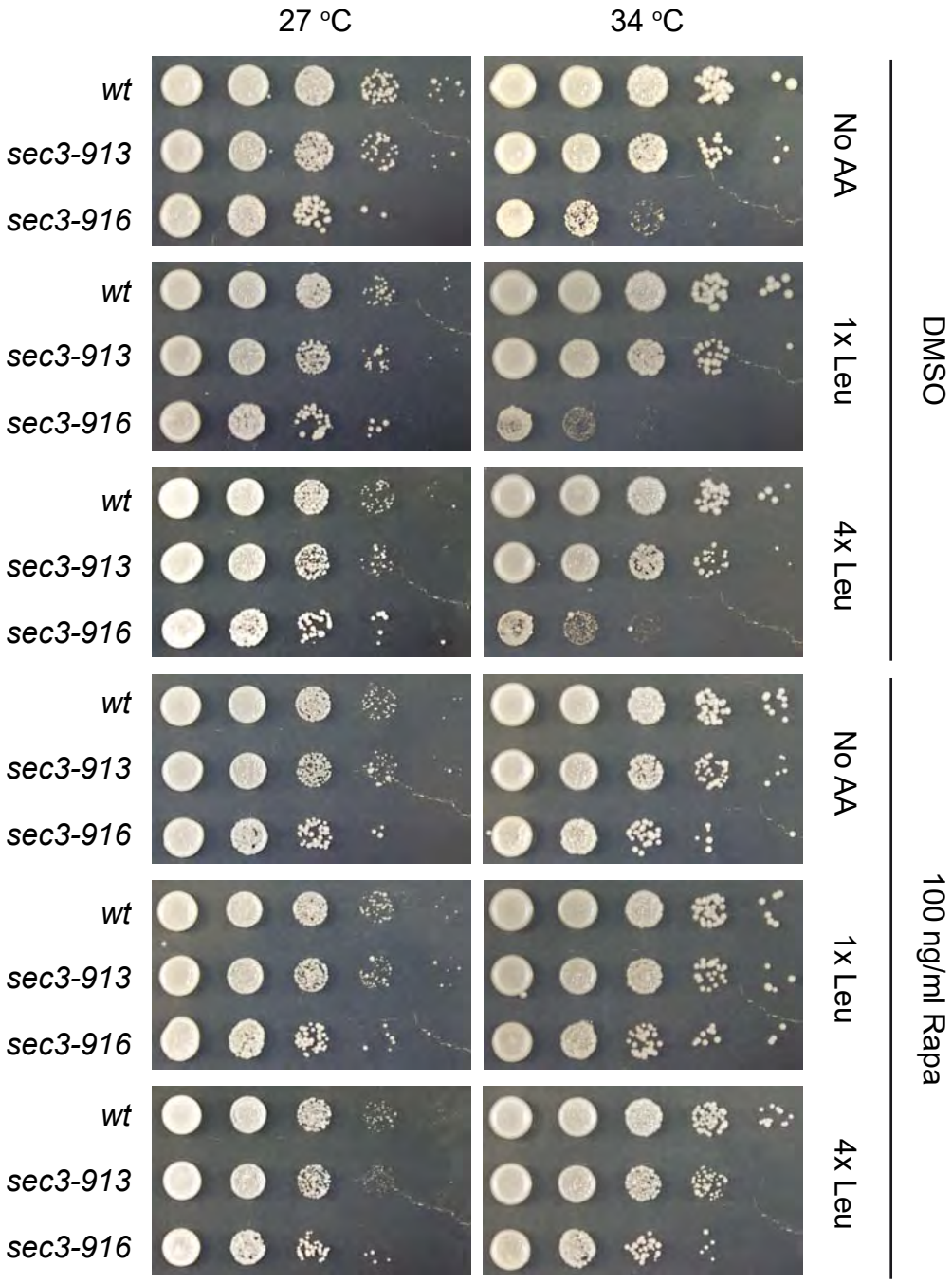

Figure 4.5: Rapamycin abolishes the leucine sensitivity of *sec3* mutants. Serial dilutions of wild-type (*wt*), *sec3-913* and *sec3-916* cells were spotted on EMM containing various concentrations of leucine in combination with either 100 ng/ml rapamycin (Rapa) or the equivalent volume of DMSO. 1x leucine is the standard concentration of 225 mg/ml used in EMM. Plates were incubated at the indicated temperatures.

grew in line with the wild type and exhibited no sensitivity to 25 ng/ml rapamycin (Figure 4.6). At the restrictive temperature *atg1Δ* grew similarly to the wild type, and *sec3-913* and *sec3-913 atg1Δ* were both temperature sensitive with treatment of DMSO. Treatment with rapamycin rescued the temperature sensitivity of both *sec3-913* and *sec3-913 atg1Δ*, highlighting that the rapamycin rescue of *sec3* is independent of autophagy.

To further verify this I examined the morphology of the yeast vacuole which is involved in amino acid storage (Wiemken and Dürr, 1974), and is also widely regarded as an autophagy organelle. To examine this, I used the lipophilic dye FM4-64 to visualise the vacuoles of wild-type, *sec3-913* and *sec3-916* cells by fluorescence microscopy. The vacuole diameter in *sec3-913* cells was significantly smaller than the wild type (Figure 4.7, Panel B, At least 500 vacuoles were measured, N = 2 independent replicates, Kruskal-Wallis test, $P<0.001$). The vacuoles in *sec3-916* cells were so small that their diameter could not be determined (Figure 4.7, panel A). These data reveal *sec3* plays a role in establishing the correct morphology of vacuoles in fission yeast.

4.2.2.2 Sec3 does not control the localisation of the TORC1 machinery at vacuoles.

As the exocyst is proposed to be involved in tethering (Grote et al., 2000), it could be possible that Sec3 helps to tether TORC1 to the vacuole. Given the vacuole phenotype described above, I hypothesised that the import of vesicles that shape vacuoles may be altered in *sec3* mutants, and that cargoes such as TORC1 are not properly delivered to vacuoles from where they act. To examine this wild type and *sec3-916* strains possessing GFP tagged Gtr1 or the Tor complex protein Pop3 were stained with the dye FM4-64 to enable visualisation of the vacuoles, and imaged. All strains showed colocalisation of both the Rag GTPases and TORC1 components to the vacuole membrane (Figure 4.8). This shows that Sec3 does not play a role in correctly localising both TORC1 and its recruiting machinery to the vacuolar membrane.

To confirm this examined a strain in which the Rag GTPase Gtr1 deleted (a kind gift from Sergio Moreno). This strain was crossed with *sec3-913* and the single

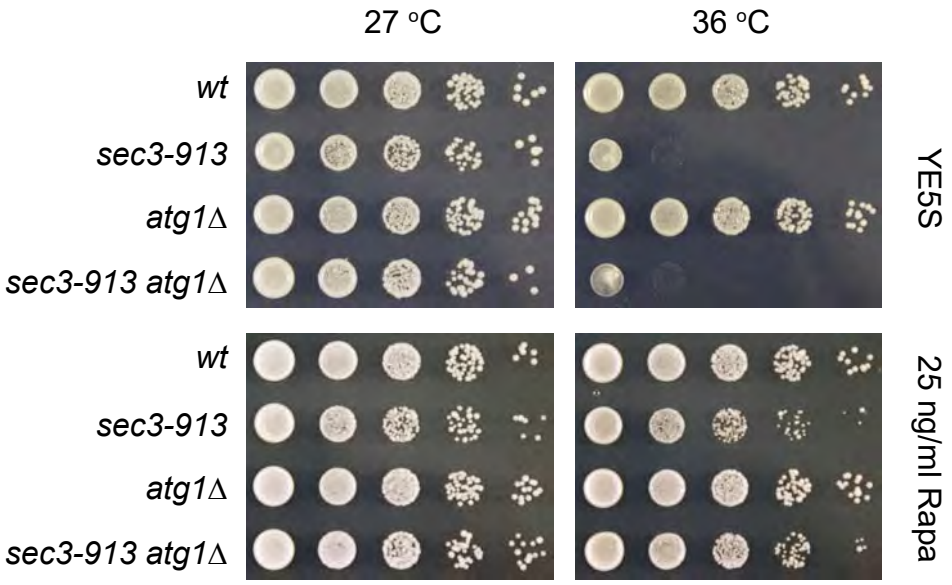

Figure 4.6: The rapamycin rescue of *sec3-913* is independent of autophagy. Wild-type (*wt*), *sec3-913*, *atg1*Δ and *sec3-913 atg1*Δ cells were spotted in 10-fold serial dilutions on rich medium containing no or 25 ng/ml rapamycin (Rapa), and were incubated at the indicated temperatures. The double mutant behaved like the *sec3-913* strain, indicating that *sec3* does not genetically interact with the autophagy machinery.

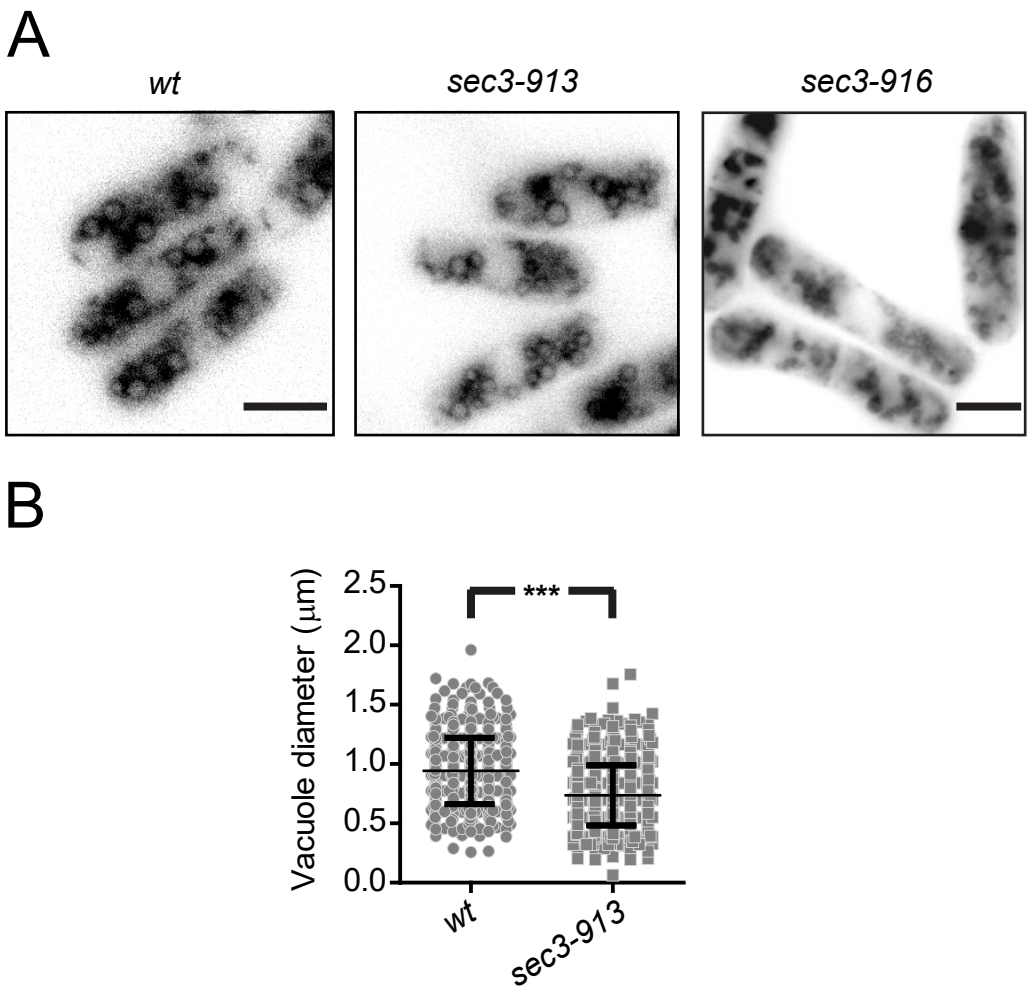

Figure 4.7: *sec3* mutants have small vacuoles. Wild-type (*wt*), *sec3-913*, and *sec3-916* cells were cultured to mid-log in EMM at 27 °C and stained with the lipophilic dye FM4-64. Cells were imaged **[A]** and vacuole diameter was measured **[B]**. The vacuole diameter was significantly smaller in *sec3-913* than in the wild type. The *sec3-916* strain also exhibited small vacuoles, and appeared to contain many more vacuoles than both *sec3-913* and the wild type, but these were too numerous to quantify. Scale bar = 5 μm. *** $p < 0.001$, Kruskal-Wallis test, N = >448 vacuoles per condition.

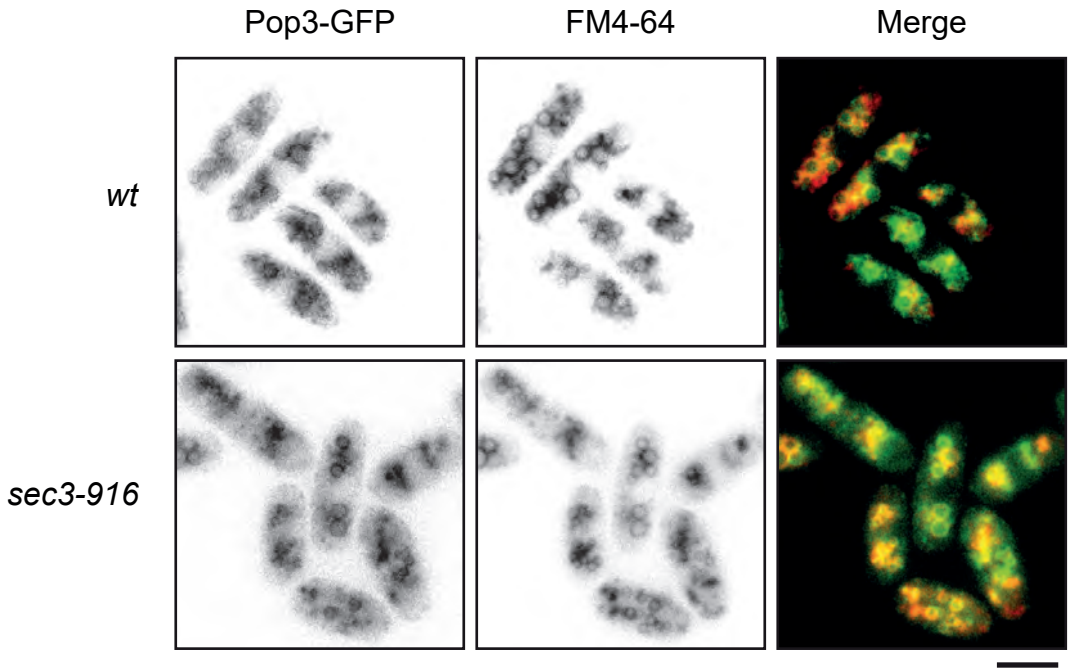

Figure 4.8: Sec3 does not control the localisation of the TORC1 machinery at vacuoles. The localisation of Pop3-GFP (green) in wild-type (*wt*) and *sec3-916* cells was observed in EMM at 27 ºC. To confirm the localisation at vacuoles, cells were also stained with FM4-64 (red). *sec3-916* vacuoles are very small, but the vacuolar localisation of Pop3-GFP is un-affected. Scale bar = 5 µm

and dual strains were spotted on rich and minimal medium (Figure 4.9). The *gtr1Δ* strain was not temperature sensitive, however the dual strain was synthetic sick, showing that Sec3 and Gtr1 operate in separate pathways that might operate towards a similar objective.

4.2.2.3 *Sec3 does not affect the activation of S6 kinase.*

Another possibility is that Sec3 plays a role in regulating TORC1 signalling. To verify this result, I looked at the phosphorylation status of TORC1's target S6 kinase. Wild type and *sec3-913* strains expressing Psk1, the *S. pombe* homologue of S6 kinase, tagged with a Myc tag were cultured at 27 ^{o}C or 36 ^{o}C for 3 hours. Cultures were treated with 200 nM rapamycin, or the equivalent volume of DMSO for 1 hour, as phosphorylation of S6 kinase has been shown to completely disappear at this concentration for this amount of time in budding yeast (González et al., 2015). Proteins were extracted and separated by SDS-PAGE, and then stained with an anti-Myc antibody. DMSO treated strains exhibited the double band of Psk1-Myc, with the top band being the phosphorylated version of Psk1 (Figure 4.10). Rapamycin treatment successfully eliminated the phospho-Psk1-Myc band in all strains. There was no difference in levels of phospho-Psk1-Myc between *sec3-913* and the wild type at both the restrictive and permissive temperature, showing that TORC1 signalling is functioning at the same level in both strains.

4.2.2.4 sec3 does not genetically interact with tor2 *kinase.*

I confirmed this finding using the *tor2-287* strain (a kind gift from Mitushiro Yanagida). This strain possesses an L2048S substitution in the ATP catalytic domain of Tor2 that makes it exhibit a nutrient deficient phenotype and hypersensitivity to rapamycin (Hayashi et al., 2007). This strain was then crossed with *sec3-913* and these strains were spotted on to rich and minimal media at permissive and restrictive temperatures. As this strain possesses a variant of Tor2 in which the TORC1 complex is switched off, the expected result was that it should mimic the rapamycin rescue. Both the *sec3-913* and *tor2-287* strains showed temperature sensitivity on YE5S at 34^{o}C (Figure 4.11). The dual strain did not show any rescue showing and in fact grew less than the single strains. These data show that there does not appear to be any genetic interaction between *sec3* and the TORC1 complex.

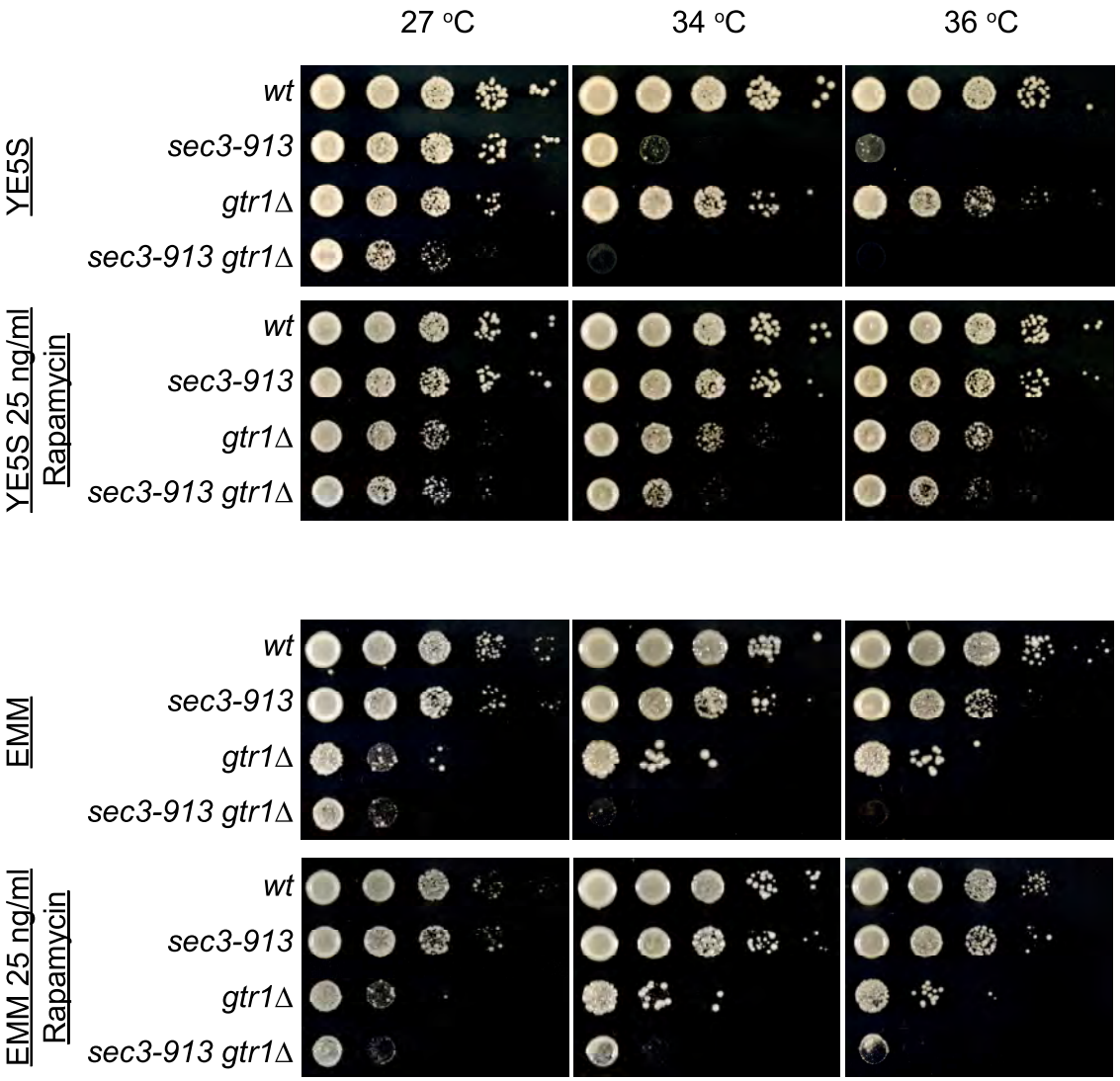

Figure 4.9: *sec3* and *gtr1* sit in two different pathways. Serial dilutions of wild-type (*wt*), *sec3-913*, *gtr1*Δ and *sec3-913 gtr1*Δ cells were spotted on either EMM or YE5S with (Rapa) or without (DMSO) 25 ng/ml rapamycin. In the absence of rapamycin, the double mutant is synthetic sick; this additive phenotype indicates that the two genes lie in two different pathways. *gtr1*Δ is not sensitive to rapamycin and the double mutant behaves like *sec3-913*.

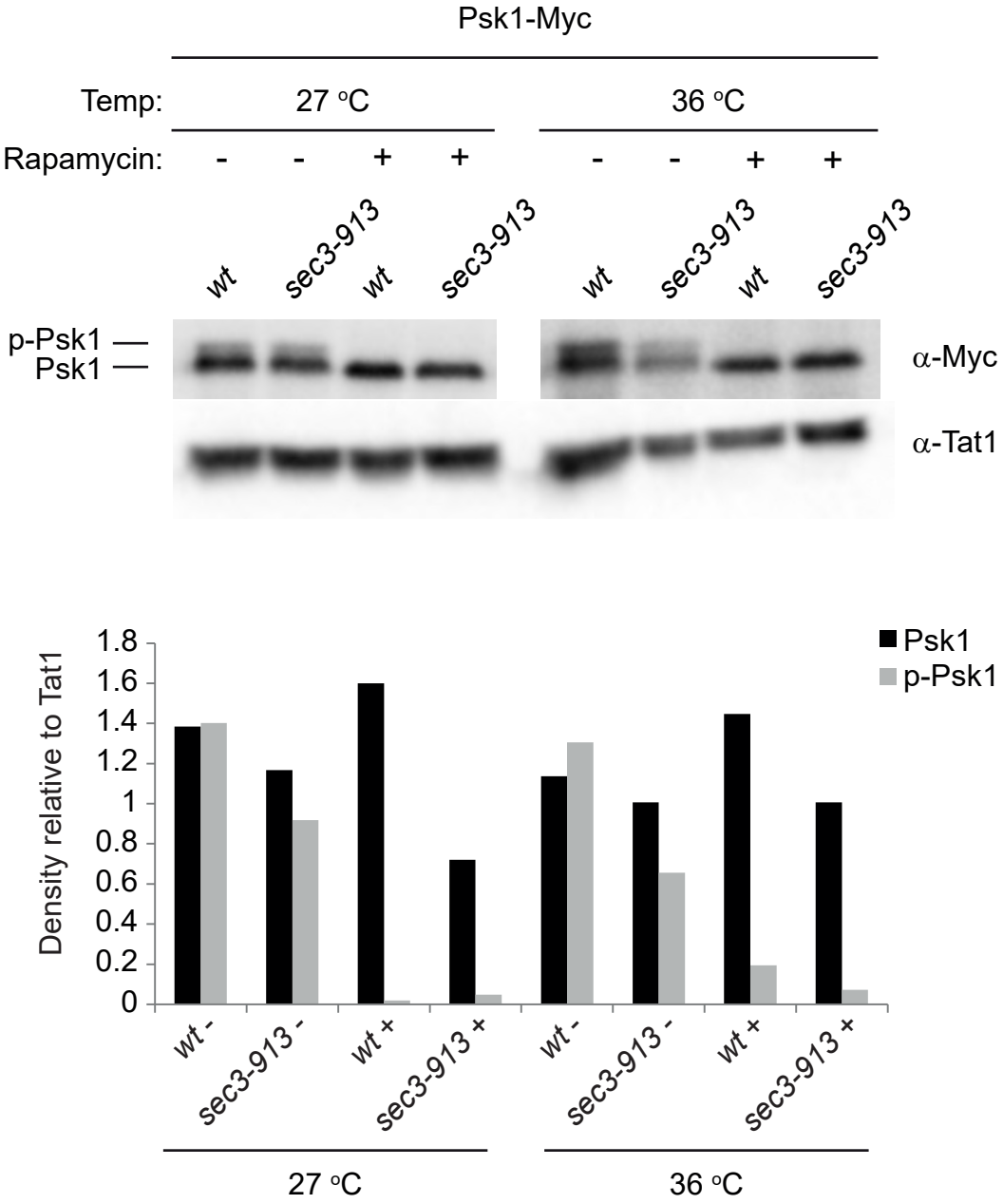

Figure 4.10: TORC1 signalling is functional in *sec3* mutants. Western-blot showing the migration pattern of the fission yeast S6 kinase Psk1 tagged with cMyc, in wild-type (*wt*) and *sec3-913* cells. Cells were cultured at the permissive (27 °C) or restrictive (36 °C) temperature for 1 generation, and were treated (+) or not (-) for 2 hour with 200 nM rapamycin. The upper band represents a phospho-form (p-Psk1), which disappears upon treatment with rapamycin. Tubulin was used as a loading control (TAT-1). The phosphorylation status of Psk1, is unaffected by mutations in *sec3*. Densitometry is representative of blot shown.

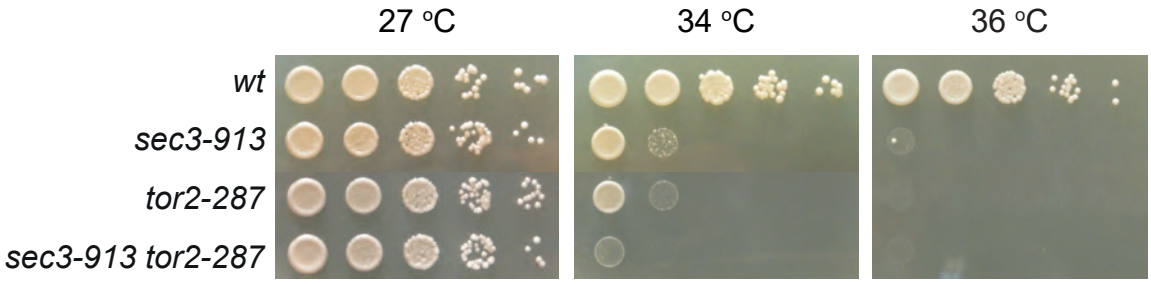

Figure 4.11: *sec3* and *tor2* sit in two different pathways. Serial dilutions of wild-type (*wt*), *sec3-913*, *tor2-287* and *sec3-913 tor2-287* cells were spotted on YE5S, and incubated at the permissive (27 °C), semi-restrictive (34 °C), or restrictive (36 °C) temperatures. The additive growth phenotype in the double mutant indicates that the two genes lie in two different pathways.

4.2.3 The rescue by rapamycin is via TORC2.

Since Sec3 and the TORC1 related proteins do not appear to function in the same pathway, the only other target that rapamycin could rescue *sec3* mutants through was the TORC2 complex.

4.2.3.1 sec3 interacts genetically with tor1.

To see whether TORC2 signalling was perturbed in *sec3* mutant strains, the phosphorylation status of the TORC2 specific Gad8 kinase was examined. Wild type and *sec3* mutant strains possessing Gad8 tagged with HA were grown overnight at the permissive temperature. For a negative control a *tor1-L2045D* strain also possessing Gad8-HA was used as Gad8 should not be phosphorylated in this strain. The Tor1-L2045D variant possess a substitution at the ATP binding pocket of the kinase, which means it cannot be active, thus turning off TORC2 signalling (Ikai et al., 2011). Strains were incubated for a further 4 hours at 27 ^{o}C or at 36 ^{o}C before proteins were extracted and separated by SDS-PAGE. Probing for the HA tag revealed two distinct bands (Figure 4.12). However both bands were also present in the *tor1-L2045D* strain revealing that it was unlikely that these bands corresponded to phospho-bound activated Gad8. Further reading of studies that also performed this experiment in fission yeast showed that a specific antibody towards the phospho-bound N terminus of Gad8 is needed to verify its activation status (Du et al., 2016), however the antibody is not commercially available and could not be obtained before submission of this thesis.

Wild-type, *sec3-913* and *sec3-916* strains possessing the *tor1-L2045D* mutation, were spotted on rich and minimal media at permissive and restrictive temperatures (Figure 4.13). The *tor1-L2045D* mutant strain showed slight temperature sensitivity at 36 ^{o}C. The temperature sensitive phenotype of both *sec3* mutants was found to be rescued by the presence of the inactive Tor1 kinase. This shows that TORC2 signalling genetically interacts with the exocyst member Sec3.

The recruitment of TORC2 to the plasma membrane is imperative for it to function correctly. To see if TORC2 is correctly localised in the Sec3 mutant, wild-type and *sec3-916* strains possessing Ste20 tagged with 3 x GFP (a kind gift from Dan Mulvihill) were imaged. The *sec3-916* strain was used as it exhibits a more aggressive phenotype than *sec3-913* at the permissive temperature. Ste20

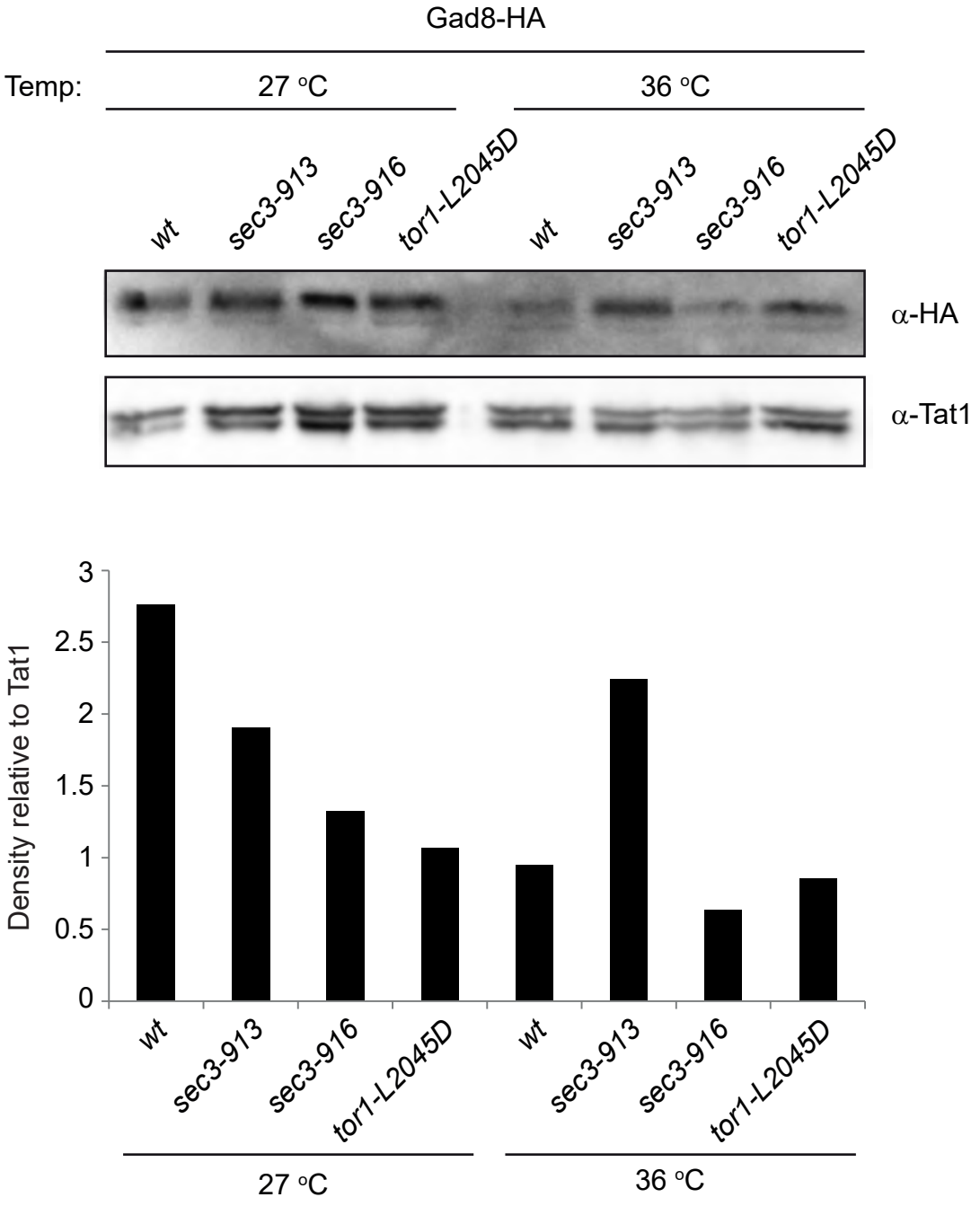

Figure 4.12: Analysis of Gad8 levels in *sec3* and *tor1* mutants. Western-blot showing the migration pattern of the fission yeast Gad8 tagged with HA, in wild-type (*wt*) and mutant strains indicated. Cells were cultured at the permissive (27 °C) or restrictive (36 °C) temperature for 1 generation. The levels of Gad8 remain consistent in all mutants, however the bands representing phosphorylated Gad8 can not be seen. The Tat1 antibody (tubulin) was used as a loading control. Densitometry is representative of blot shown.

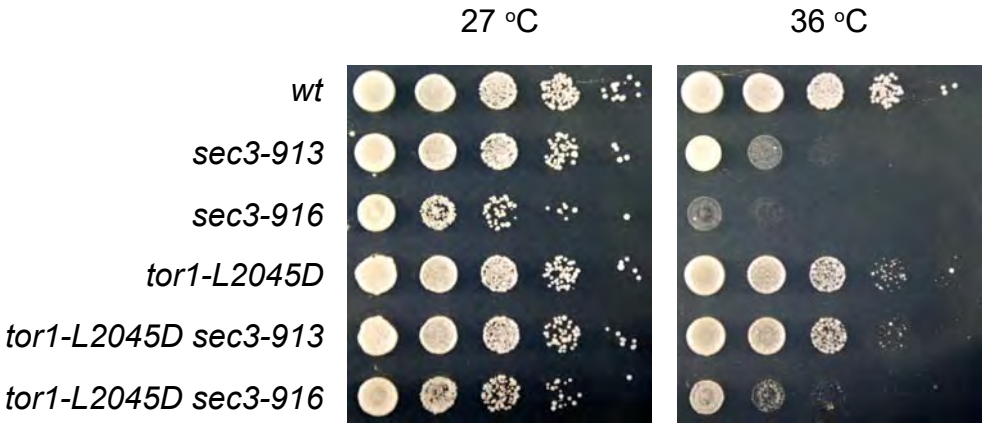

Figure 4.13: Deactivating TORC2 rescues the growth of *sec3* mutants. Serial dilutions of wild-type (*wt*), *sec3-913, sec3-916*, *tor1-L2045D, tor1-L2045D sec3-913* and *tor1-L2045D sec3-916* cells were spotted on YE5S agar medium. Plates were incubated at the permissive (27 °C) or restrictive (36 °C) temperatures. The temperature sensitivity phenotype of both *sec3* mutants is rescued when *tor1* is inactive.

localised to speckled domains on the plasma membrane (Figure 4.14), and also to the division plane in the wild type as previously cited (Baker et al., 2016). Similar localisation was seen in the *sec3-916* strain. As Ste20 localised correctly in both strains, it shows that the exocyst does not control the localisation of components of TORC2.

4.2.4 Sec3 is involved osmotic stress signalling.

Due to TORC2 playing a prominent role in stress signalling (Hartmuth and Petersen, 2009; Raitt, 2000), I assessed *sec3-913* to see if it responded to osmotic stress correctly. Wild-type and *sec3-913* strains were spotted onto YE5S medium supplemented with either 1 M KCl or 0.1 M NaCl and incubated at the permissive and restrictive temperatures. Both strains were not sensitive to either KCl or NaCl at the permissive temperature (Figure 4.15). Growth of *sec3-913* remained temperature sensitive on both YE5S and media supplemented with NaCl, however growth of *sec3-913* was rescued on media containing 1 M KCl. These results show that stimulation of the osmotic stress response by KCl, but not NaCl, rescues the growth of *sec3-913*. Therefore the exocyst may be involved in osmotic stress signalling.

4.2.5 TORC2 does not regulate the expression of Sec3

Increasing the level of Sec3-913 protein, either by overexpression or blocking its degradation, has also been found to rescue the temperature sensitivity of *sec3-913* (Kampmeyer et al., 2017). Because of this it was necessary to see whether the protein level of Sec3 was affected by TORC2 signalling. To test this, I crossed the *tor1-L2045D* strain with wild-type strains possessing either GFP tagged Sec3 or Sec3-913. The strains were grown to mid-log phase in YE5S overnight and grown for a further 4 hours in the morning at either 27 ^{o}C or 36 ^{o}C. Protein lysates were prepared, separated by SDS-PAGE, and then probed for GFP and the loading control Tat1. Expression of both Sec3-GFP and Sec3-913-GFP were similar in the wild type at 27 ^{o}C however levels of Sec3-913-GFP but not Sec3-GFP appeared to be reduced in the *tor1-L2045D* strain at 27 ^{o}C (Figure 4.16). At the restrictive temperature levels of Sec3-913-GFP were reduced compared to Sec3-GFP in the wild type. The same pattern was observed in the tor-L2045D strain, however it appears that the levels of both Sec3 and Sec3-913 are reduced compared to the wild type. These data show that TORC2 rescue of *sec3* mutants

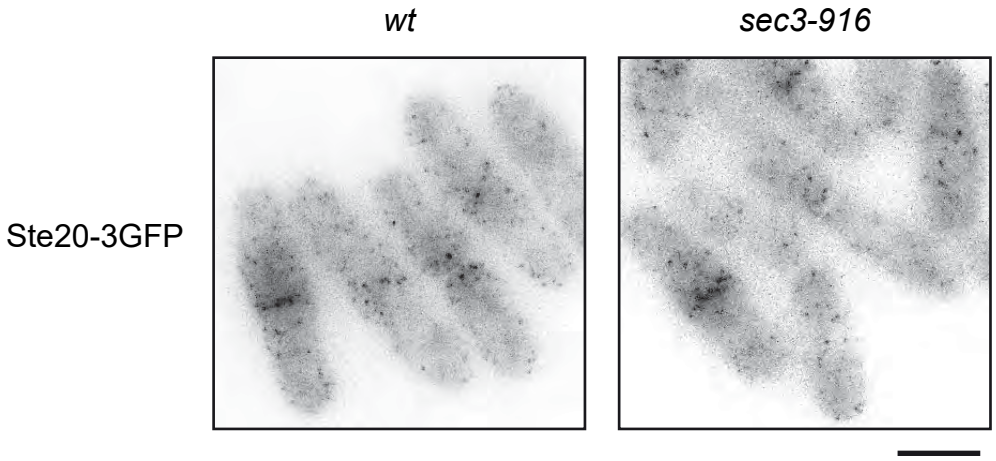

Figure 4.14: Sec3 does not control the localisation of the TORC2 component Ste20. The localisation of Ste20-3GFP in wild-type (*wt*) and *sec3-916* cells was observed in EMM at 27°C. In *sec3-916*, localisation of Ste20-3GFP is un-affected. Scale bar = 5 µm

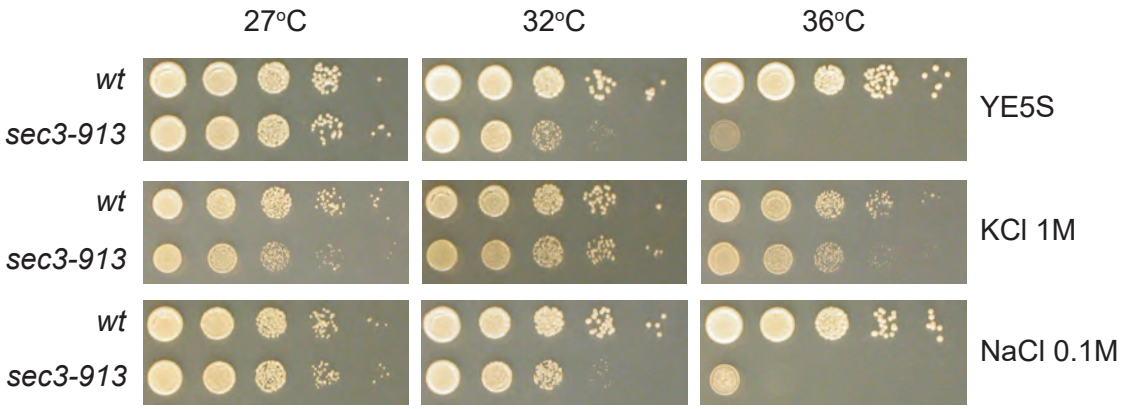

Figure 4.15: *sec3-913* is sensitive to osmotic gradients. Wild-type (*wt*) and *sec3-913* cells were spotted on YE5S with or without either KCl or NaCl (concentrations based on Eaton et al., 2008), and incubated at the permissive (27 °C), semi-restrictive (32 °C) and restrictive (36 °C) temperatures. No effect on growth was seen with NaCl, but KCl appeared to rescue the growth of *sec3-913*. Data provided by Isabelle Jourdain.

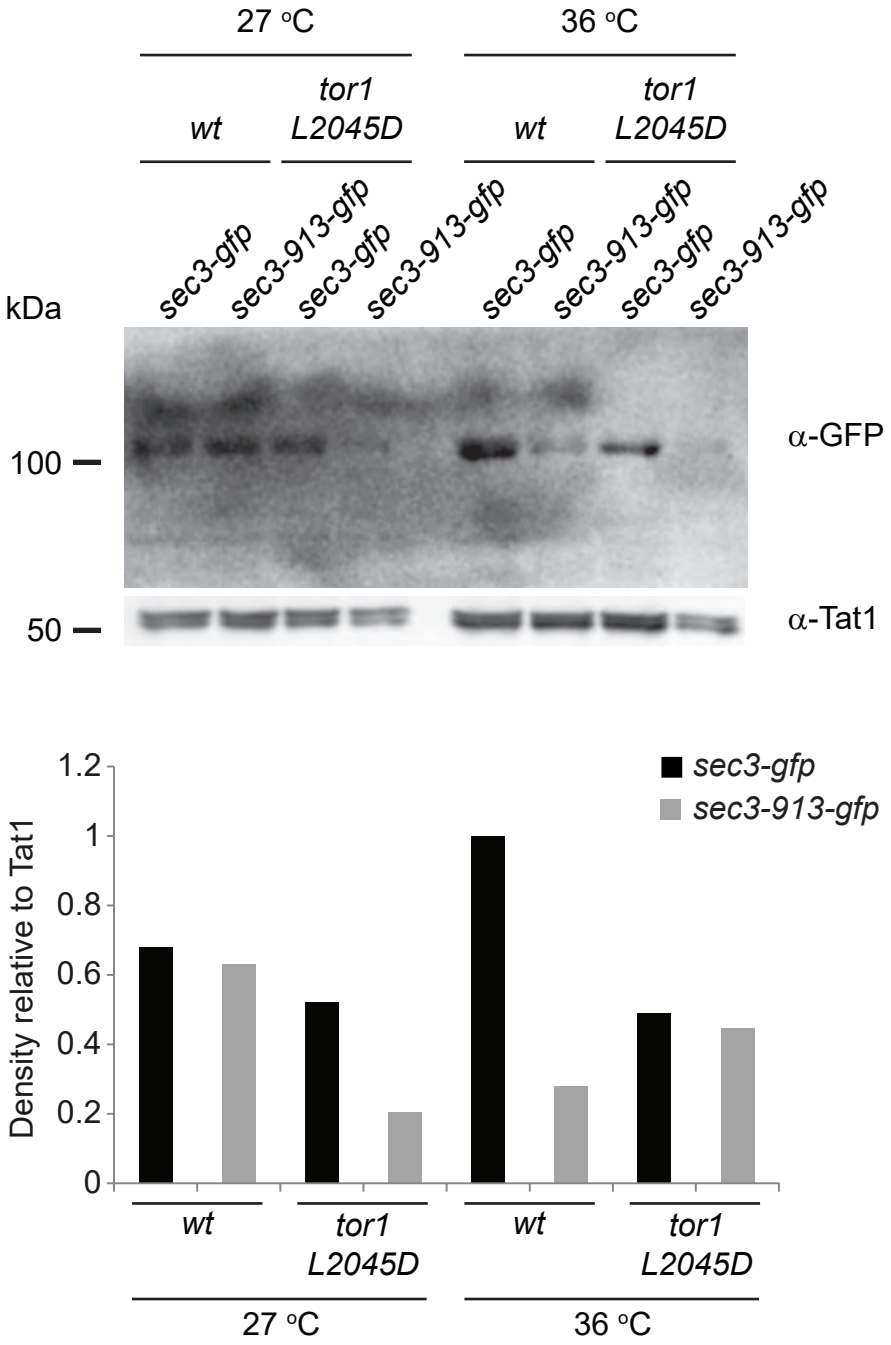

Figure 4.16: TORC2 does not influence the expression of Sec3. Western-blot showing the migration pattern of the fission yeast Sec3 tagged with GFP, in the strains indicated. Cells were cultured at the permissive (27 °C) or restrictive (36 °C) temperature for 1 generation. The levels of Sec3-GFP are not affected by the inactivation of *tor1*. The Tat1 antibody (tubulin) was used as a loading control. Densitometry is representative of blot shown.

is not due to an increase in the level of Sec3 protein, and in fact levels of Sec3 are reduced when TORC2 signalling is off.

4.2.6 Sec3 and TORC2 regulate the polarisation of sterols in the plasma membrane.

TORC2 signals downstream to regulate the biosynthesis of sphingolipids in order to regulate the fluidity and tension of the plasma membrane (Riggi et al., 2018). In order for these lipids to be incorporated into the PM, they must be trafficked and secreted by exocytosis. The trafficking and secretion could be performed by the exocyst, whose role is to traffic and tether secretory cargoes at the plasma membrane (Grote et al., 2000). Ergosterol is the main sterol lipid component of the plasma membrane in *S. pombe* (Iwaki et al., 2008). To examine the location of ergosterol in various strain, filipin conjugated to a dye that fluoresces under ultraviolet light was used. Filipin is a macrolide antibiotic that binds to the cholesterol family of lipids (Castanho et al., 1999). Staining of the *sec3* and *tor1* single and dual strains with filipin showed that the sterols in both the *sec3* and *tor1* mutants are mislocalised, and are present all over the membrane rather than being polarised at the cell tips (Figure 4.17). Contrastingly, sterols in the dual strain appear to repolarise to the cell tips although the fluorescence intensity appears lower. This figure shows that Sec3 and Tor1 both regulate the localisation sterols in the plasma membrane, and thus may work together to regulate cellular sterol homeostasis.

To verify whether the sterol depolarisation was due to secretion or endocytosis of sterols I treated the wild type, *sec3-916*, *tor1-L2045D*, and dual mutant strains with 1.25 μM myriocin to reduce the total sterol content of the cell. I then labelled the strains with filipin-594 to visualise the sterols (Figure 4.18). The wild type and dual mutant exhibited the same phenotype with complete loss of sterols at both the growing tip and septum (Figure 4.18). However *sec3-916* and *tor1-L2045D* lost sterols at the growing tip, but retained signal at the septum (Figure 4.18). This shows that Sec3 and Tor1 may control retrograde trafficking of sterols at the septum but not the tips.

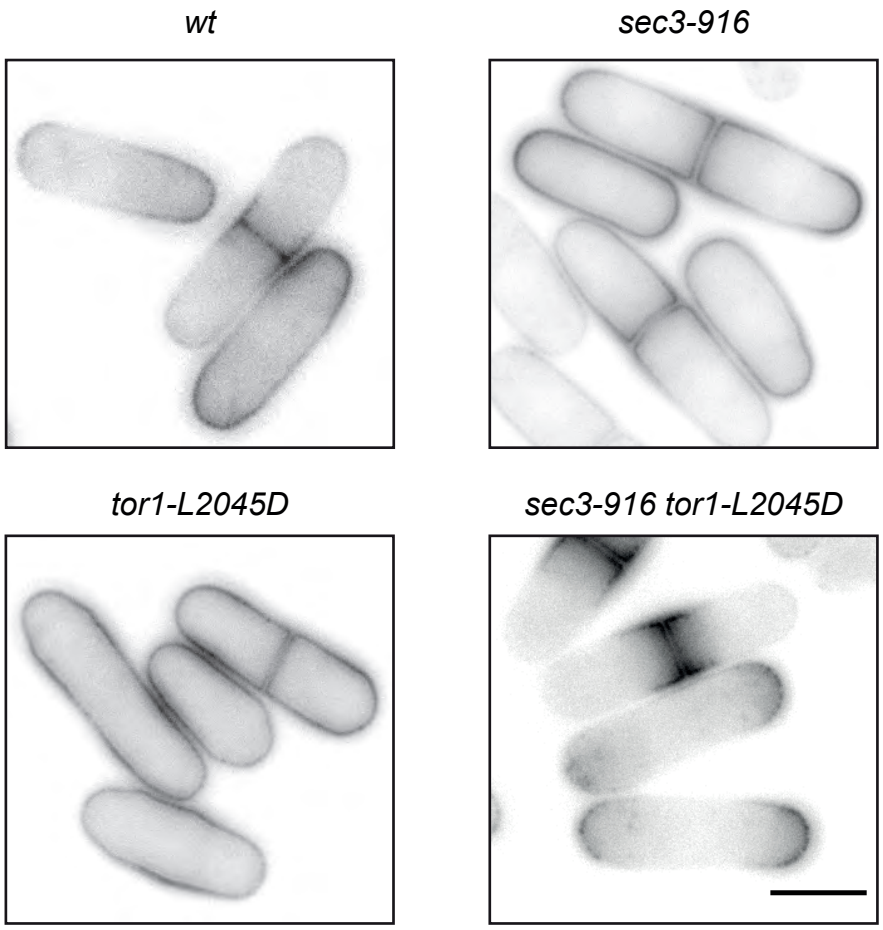

Figure 4.17: Both Sec3 and TORC2 control localisation of sterols at the plasma membrane. Wild-type (*wt*), *sec3-916, tor1-L2045D and sec3-916 tor1-L2045D* cells were grown overnight at 27 °C in EMM containing no amino acids. Cells were stained with 5 µg/ml filipin to label sterols, and imaged. The wild-type and double mutant showed accumulation at the tip and septum, whereas both *sec3-916* and *tor1-L2045D* mutants showed sterol signal all over the plasma membrane. Scale bar = 5 µm.

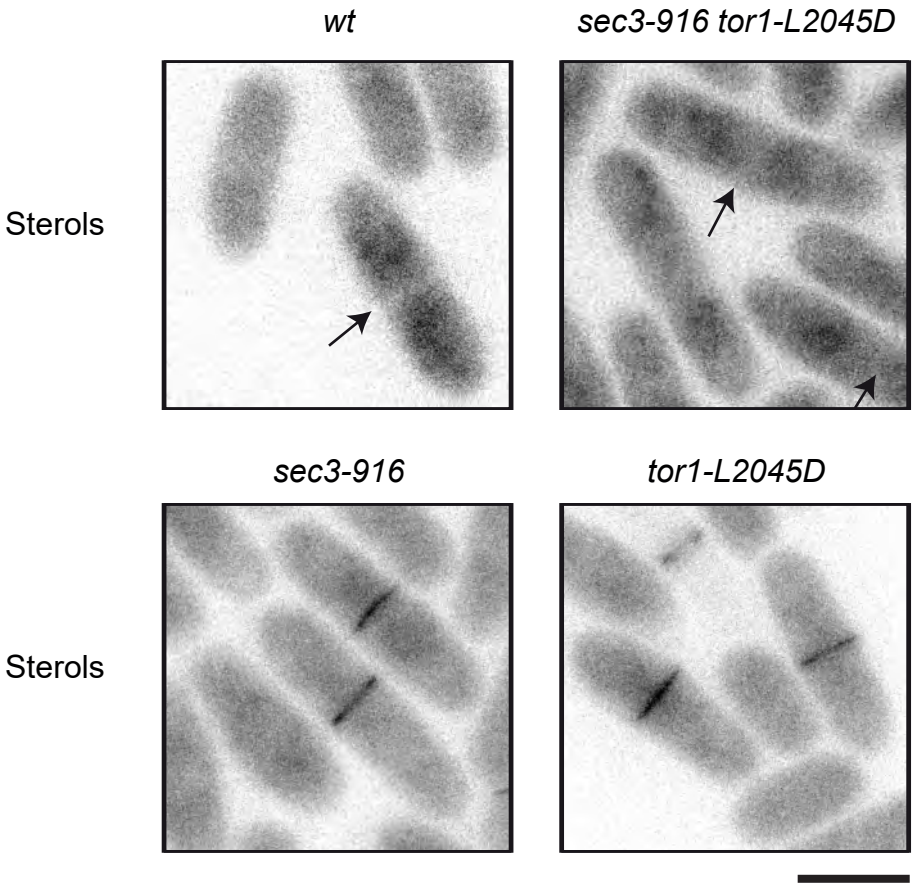

Figure 4.18: The interplay between Sec3 and TORC2 regulates sterol retention at the septum. Wild-type (*wt*), *sec3-916, tor1-L2045D and sec3-916 tor1-L2045D* cells were grown overnight at 27 °C in EMM containing no amino acids. Cells were incubated with 1.25 µM Myriocin for 2 hours to block sterol biosynthesis, before being stained with 5 µg/ml filipin to label sterols, and imaged. The wild-type and double mutant showed no sterol content at the septum (arrows) or plasma membrane. However, both *sec3-916* and *tor1-L2045D* showed sterol positivity at the septum only. Scale bar = 5 µm.

4.3 Discussion

In the previous chapter I identified that Sec3 appears to play a role in the metabolism of leucine (Chapter 3). Further verification of this leucine sensitivity suggested that amino acid uptake was not affected by Sec3, so therefore an intracellular role of leucine must be the cause of the sensitivity in mutants of *sec3*. Leucine has previously been described as a potent activator of TOR signalling in both budding yeast and *H. sapiens* (Binda et al., 2009; Hara et al., 1998; Xu et al., 2019), so it was reasonable to suggest that leucine performs a similar function in fission yeast. The TORC1 signalling axis is also conserved in fission yeast making it an ideal model organism for examining this (Nakashima and Tamanoi, 2010).

4.3.1 The exocyst complex is involved in TORC2 signalling.

Leucine directly affects TORC1 which is sensitive to the drug rapamycin (Binda et al., 2009; Loewith et al., 2002), and treatment of *sec3* mutants with rapamycin rescued the temperature sensitive phenotype of these strains. Therefore it seemed likely that inhibition of TORC1 signalling was the source of the rescue. In *H. sapiens* leucine activates TORC1 via a family of regulatory proteins called sestrins (Chantranupong et al., 2014). The model in yeast remains unclear. While yeast do not possess proteins that share sequence identity with the sestrins, the budding yeast SEACAT and fission yeast GATOR complexes have been identified as potential homologues (Chia et al., 2017; Dokudovskaya and Rout, 2011). Both complexes recruit the TORC1 complex to the yeast vacuole via the Rag GTPases (Binda et al., 2009; Chia et al., 2017). Due to the role of the exocyst in tethering proteins to membranes (Grote et al., 2000), it was possible that Sec3 may interact with the Rag GTPases Gtr1 and 2 in order to tether TORC1 to the vacuole. However imaging and assessment of genetic interaction of *sec3* with *gtr1* revealed that the exocyst and Rag GTPase do not function together in the same pathway.

Crossing *sec3* mutants with a strain possessing an inactive Tor2 kinase also did not phenocopy the rapamycin result revealing that the exocyst is not involved in TORC1 signalling. Further to this deletion of Tor2 kinase exhibits a nitrogen starvation phenotype (Matsuo et al., 2007). Starvation of *sec3-913* revealed that they exit into G0 similarly to the wild type (see Chapter 3). This reinforces the

notion that Sec3 and TORC1 are not related genetically as *sec3* mutants should exhibit a nitrogen starvation phenotype.

As rapamycin is cited to only affect TOR signalling, the only other possibility for the rescue of the temperature sensitivity was through TORC2 signalling. This seemed unlikely as rapamycin is not predicted to affect TORC2 as the complex contains the component Ste20/Rictor which stands for rapamycin insensitive component of TOR (Gaubitz et al., 2015; Loewith et al., 2002). Contrastingly crossing *sec3* mutants with a strain possessing an inactive form of the TORC2 kinase Tor1 rescued the temperature sensitive phenotype in a similar manner to rapamycin. These results not only provide evidence of a novel interaction between the exocyst and TORC2, but also add further evidence that TORC2 could be inhibited by rapamycin, raising questions about how rapamycin can affect the TORC2 complex.

How TORC2 is localised to specific cellular regions still remains a question for the field. TORC2 is thought be localised by Slm1 and Slm2 which contain Pleckstrin Homology (PH) domains which may possibly explain how the complex is anchored to the plasma membrane (Fadri et al., 2005). As the exocyst complex is involved in trafficking components to the PM, it was plausible that the exocyst could be responsible for TORC2 localisation. Fluorescence microscopy revealed that Ste20 is aberrantly localised at the PM making it hard to see if its position changes in the *sec3-916* strain. However Ste20 localises to the division plane in both the wild type and *sec3-916* making it unlikely that the exocyst traffics TORC2. However the exocyst complex is needed for endocytic events at the division plane (Gachet and Hyams, 2005), so it could be possible that while the 2 complexes may not localise each other, they could function together in the completion of cytokinesis.

The mechanism of the link between Sec3 and TORC2 remains elusive. As turning off TORC2 rescued *sec3* mutants, it was reasonable to hypothesise that TORC2 signalling might be more active when Sec3 is non-functional. This positioned Sec3 as a potential negative regulator of TORC2. TORC2 signals through the AGC kinase Gad8 (Ikeda et al., 2008), so therefore examining the level of Gad8 phosphorylation can inform about TORC2 signalling activity. Unfortunately Gad8 phosphorylation status could not be determined by band shift. However activated Gad8 has also been shown to regulate the phosphorylation of Psk1 in *S. pombe*

(Du et al., 2012), and due to the fact that *sec3-913* did not exhibit any change in Psk1 phosphorylation compared to the wild type, it is reasonable to suggest that Gad8 phosphorylation is also unchanged in *sec3* mutants.

The finding that *sec3* mutants are also not sensitive to changes in environmental glucose provides further evidence for that Sec3 may not activate TORC2 (see Chapter 3). Previous work has shown that glucose regulates the activation of the TORC2 complex (Hatano et al., 2015). Glucose performs this role through two different mechanisms in fission yeast. Activation of the Rab GTPase Ryh1 is glucose dependent and GTP bound Ryh1 activates TORC2 via the component Bit61 (Hatano et al., 2015; Tatebe et al., 2010), Glucose also stimulates the cyclic AMP (cAMP) dependent activation of protein kinase A (Pka1) which subsequently activates TORC2 (Cohen et al., 2014). Therefore if mutation of *sec3* affected the activation of TORC2, one would expect to see a phenotype associated with environmental glucose. This evidence coupled with the idea that Gad8 phosphorylation is unlikely to be affected makes it reasonable to suggest that Sec3 is more likely to be a downstream effector of the TORC2-Gad8 signalling axis rather than an upstream activator.

4.3.2 TORC2 and Sec3 appear to regulate similar pathways.

Mutation of *sec3* leads to profound effects on multiple biological processes including secretion, but also endocytosis, cell division and organisation of the actin cytoskeleton (Bendezú et al., 2012; Jourdain et al., 2012; Novick et al., 1980). Similarly ablation of the TORC2 component Ste20/Rictor also leads to defects in cell division and endocytosis (Eby et al., 1998). These phenotypes were found to be caused by a loss of interaction between Ste20 and components of the actin cytoskeleton. The Ste20 dependent phosphorylation site on MyoI is important for its localisation to endocytic sites where it activates Arp2/3 nucleation (Attanapola et al., 2009). The cytokinetic actomyosin ring (CAR) is needed to generate the contractile forces for efficient cell division, and Ste20 affects CAR stability by modulating the heterodimer formation of actin capping proteins (Baker et al., 2016). As Ste20 appears to phenocopy *sec3* mutants, this adds weight to the argument that Sec3 and TORC2 may operate in a similar pathway.

4.3.3 The roles of TORC2 and Sec3 in sterol localisation

Sterol domains are required for the localisation and promotion of many of the processes affected by Sec3 and Ste20. Sterols provide membrane fluidity which

allows for the movement of proteins in the PM are also important signalling molecules for events that occur at the cell membrane (Helms and Zurzolo, 2004; Mukherjee and Maxfield, 2000). TORC2 signalling has been implicated not only in the production of sphingolipids, but also the distribution of sterol domains in budding yeast (Muir et al., 2014; Roelants et al., 2018). TORC2 also promotes the uptake of leucine (Weisman et al., 2005), an amino acid that is metabolised through the mevalonate pathway to generate cholesterol (Miettinen and Penttilä, 1968). As leucine and TORC2 affect *sec3* mutants it was possible that the exocyst may function in sterol metabolism or trafficking. A novel function of Sec3 in the polarisation of sterols was observed. The same phenotype was seen in the *tor1-L2045D* strain. However when both the exocyst and TORC2 are both non-functional, the sterols appear to repolarise. This showed that the exocyst plays a novel role in sterol distribution, and possibly in conjunction with TORC2.

In *S. cerevisiae* TORC2 signalling regulates sterol localisation by inhibiting retrograde transport of sterols from the PM (Roelants et al., 2018). As the exocyst interacts with both the secretory and endocytic pathways at the PM, it is unclear whether the phenotype observed in *sec3* mutants is due to issues with anterograde or retrograde transport. Intriguingly deletion of the endocytic myosin Myo1 also results in a similar depolarisation of sterols (Takeda and Chang, 2005). Ste20/Rictor also interacts with Myo1 to activate the Arp2/3 complex (Baker et al., 2019). In fission yeast, Sec3 polarises the Arp2/3 complex and in higher eukaryotes there is now evidence of an exocyst Arp2/3 interaction (Biondini et al., 2016; Jourdain et al., 2012; Monteiro et al., 2013; Zuo et al., 2006). A possible model for this sterol trafficking could be that both Sec3 and TORC2 intersect at the actin patch through Myo1 and Arp2/3 in order to regulate endocytosis of sterol domains. However a caveat to this is that mutation of both components results in an apparent repolarisation of sterols. Ultimately this process is complex and still not understood, but I believe this work presents a new role for the exocyst complex in sterol homeostasis.

4.3.4 Could SAPK signalling link Sec3 and TORC2?

Sterol homeostasis is not only important for signalling and polarity, but membrane fluidity also regulates the tension of the plasma membrane. As Sec3 may be involved in sterol homeostasis, it potentially means the exocyst might regulate membrane tension. Previous work on *sec3* mutants in fission yeast showed that

growth can be rescued by the presence of the sugar alcohol sorbitol (Bendezú et al., 2012). This was proposed to be via a potential defect in membrane tension in exocyst mutants due to their role in secretion (Bendezú et al., 2012). Sorbitol alters the osmolarity of medium modulating the intracellular pressure exerted on the inside of the plasma membrane thus regulating tension. TORC2 in budding yeast has been shown to be activated by an increase in tension (Riggi et al., 2018). It is then proposed to counteract this stimulating sterol biosynthesis, which in turn increases membrane fluidity to maintain homeostatic tension (Muir et al., 2014). It is therefore possible that the exocyst and TORC2 may function together to modulate cellular membrane tension.

Contrary to this, sorbitol also activates osmotic stress signalling through the SAPK signalling pathway (Madrid et al., 2006). Both SAPK and TORC2 signalling interact apparently to oppose each other. SAPK signalling is transduced through the kinase Sty1 which causes the transcription factor Atf1 to express genes involved in stress responses (Hartmuth and Petersen, 2009; Wilkinson et al., 1996). However TORC2 signalling through Gad8 enacts to inhibit Sty1 activation (Ikeda et al., 2008). Another kinase involved in SAPK signalling is Pmk1 which was shown to respond more to KCl than other stressors (Madrid et al., 2006). As NaCl did not rescue *sec3-913*, it is possible that KCl activation of Pmk1 might rescue this strain, indicating that exocyst mutants might be defective in SAPK signalling. Furthermore inhibition of TORC2 would also serve to activate SAPK as Sty1/Pmk1 would no longer be inhibited by Gad8 (Ikeda et al., 2008). Therefore Sec3 and TORC2 may oppose each other by functioning on opposite sides of the SAPK signalling pathway.

Chapter 5: **GFP Trap of the exocyst member Sec3**

5.1 Introduction

The Tor signalling axis is central to cellular growth and survival and as such, regulation of both TORC1 and TORC2 is imperative for maintaining cellular homeostasis. The macrolide inhibitor of Tor, rapamycin, was found to be effective in restoring the growth of temperature sensitive mutants of both Sec3 and Sec8 (Figure 4.3). This suggested that the exocyst may be a negative regulator of the Tor signalling axis, and that mutation of the exocyst causes a loss of negative regulation. Inactivation of the TORC2 complex through the use of the *tor1-L2045D* strain was found to mimic the rapamycin rescue in *sec3-913* and *sec3-916*, confirming a genetic interaction between Tor1 kinase and Sec3. As both the exocyst and TORC2 complex reside at the plasma membrane (Berchtold and Walther, 2009; Boyd et al., 2004), it is not unreasonable to suggest that their interaction could also be physical.

As well as identifying components of the Tor machinery, evaluation of other binding partners of the exocyst such as the cargoes that it traffics is also important for understanding its possible role in nutrient sensing. Little is known about the cargo of the exocyst in *S. pombe*. In mammalian adipocytes, the carbohydrate transporter Glut4 was identified as a cargo for the exocyst (Ewart et al., 2005; Inoue et al., 2003). Fission yeast contain 6 known hexose transporters Ght1 to 6 of which Ght1, 2, and 5 displayed specificity to glucose (Heiland et al., 2000). Assessing the physical interactions between the exocyst and glucose transporters in fission yeast would show whether this interaction is conserved from yeast to humans. A novel link between the exocyst, and the expression of the arginine/lysine transporter Cat1 at the PM was also observed, highlighting that the exocyst may also be responsible for the trafficking of amino acid importers.

The raised expression of Cat1 at the plasma membrane in *sec3-916* could also be due to the defective endocytosis seen in *sec3* mutants (Jourdain et al., 2012). Endocytosis is the main pathway regulating the turnover of transporters at the plasma membrane (Nakase et al., 2012; Nakashima et al., 2014). Previous work has shown that the exocyst member Exo70 interacts with the Arp2/3 complex in

mammalian cells (Zuo et al., 2006), and Arp2/3 is the endocytic actin nucleator in fission yeast (Naqvi et al., 1998). However; the mechanism by which Sec3 regulates endocytosis remains elusive, and analysis of Sec3 binding partners may help to answer this question.

This chapter will focus on the direct interactors of the exocyst identified using the GFP trap technique. It will try to establish the links between Tor signalling and the exocyst to help generate a testable model, and also find novel cargoes and actin binding proteins that may help understand the phenotypes seen in Sec3 mutants.

5.2 Results

5.2.1 GFP-Trap identifies multiple putative Sec3 interacting proteins

To assess binding partners of Sec3 the GFP trap method was employed (Figure 5.1). Strains expressing Sec3-GFP, Sec8-GFP and Sec3-913-GFP were lysed and the proteins were collected. Due to it not being possible to have a strain expressing endogenous GFP only, the control for this was a wild-type strain. Protein extracts were mixed with Chromogen GFP-Trap A beads and incubated. After washing, 10% of the beads were analysed by Western blotting (data not shown) to confirm successful pull-down of GFP-exocyst components, and the rest was sent for mass spectrometry.

After receiving the mass spectrometry data (Appendix 1.1 to 1.4), it was necessary to use stringent sorting and thresholding methods in order to reduce background hits and identify true positives for each of the exocyst members. To achieve this, proteins were sorted on different criteria (Figure 5.2a). Proteins that were pulled down in the exocyst strains but not in the wild type control were deemed positive hits (Figure 5.2a). Proteins that were pulled down by the control and the exocyst strains were only accepted if their score was 2.5 fold higher than the control score as this was the point where known Sec3 interactors could be identified (Figure 5.2a). The score in mass spectrometry data outputs reflects the confidence of that protein as a true hit by factoring in all the data such as number of unique peptides detected, and peptide masses. The greater the score the more confidence.

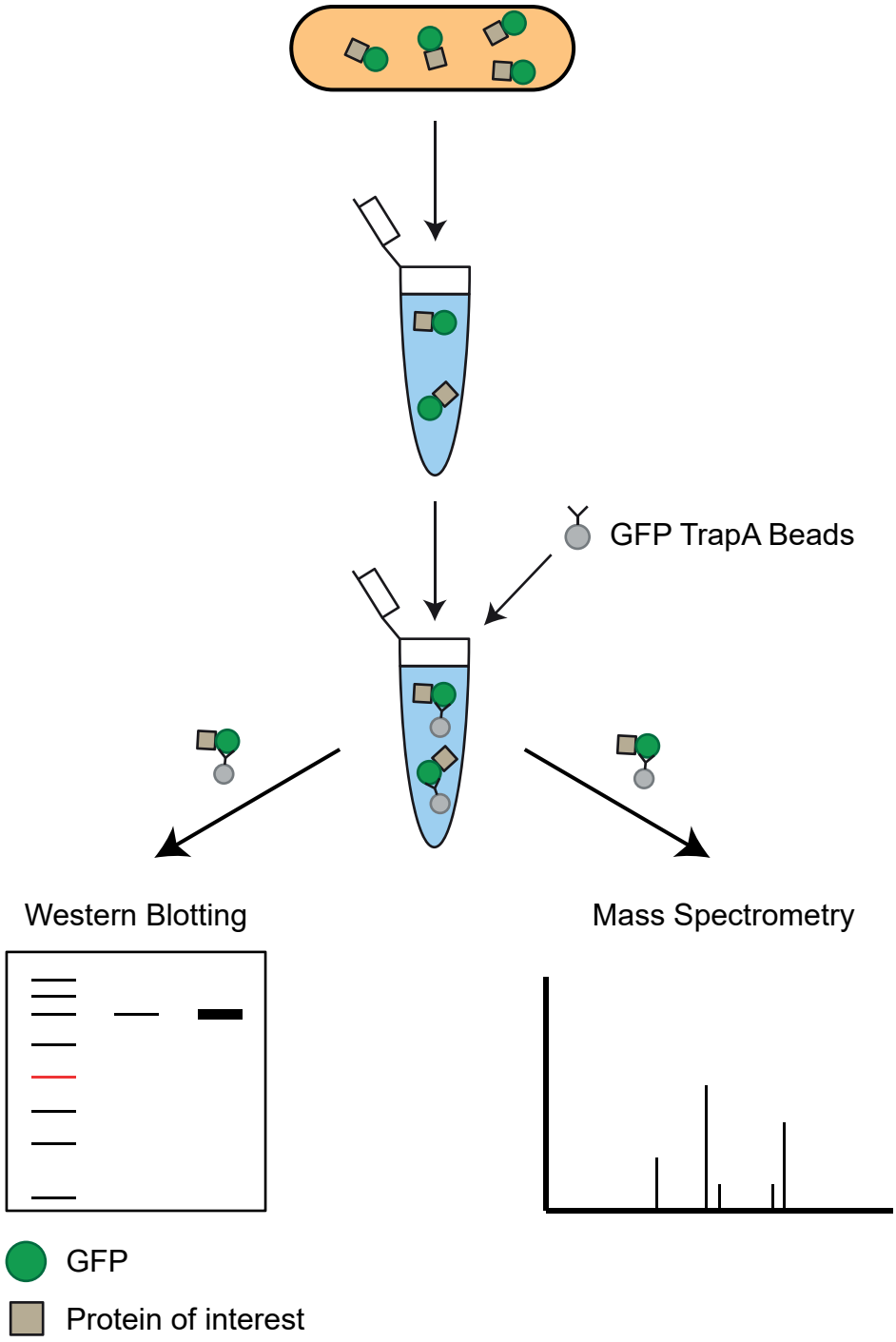

Figure 5.1: GFP-TRAP method in *S. pombe*. Strains expressing GFP-tagged proteins of interest were lysed and mixed with Chromotek GFP-TRAP A beads. After overnight incubation, 10% of the total beads were analysed by western blotting to verify success of pull-down. The remaining beads were sent for mass spectrometry analysis.

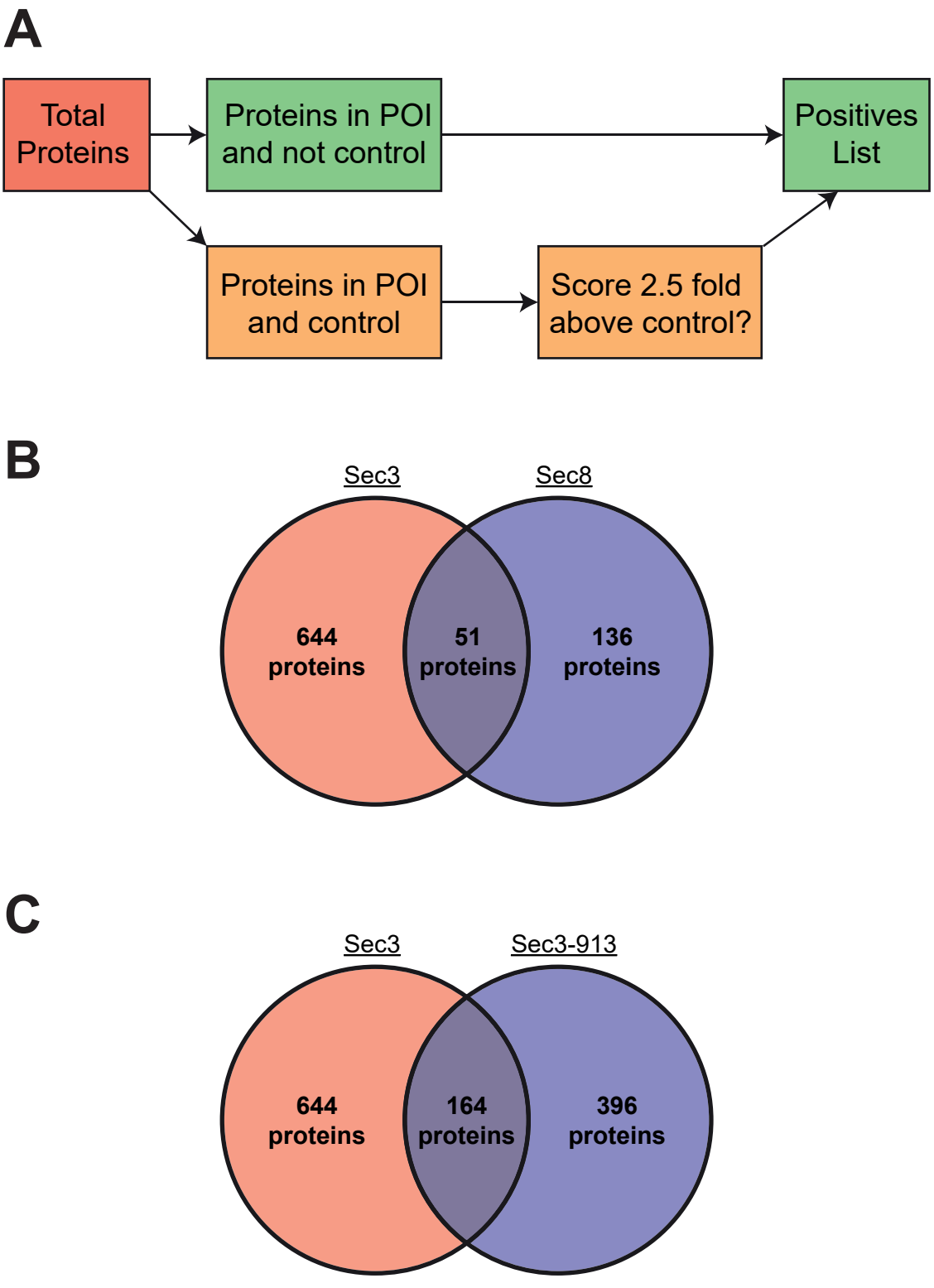

Figure 5.2: Filtering and final number of positive interactors for each pulldown. [A] Mass spectrometry output of each protein of interest (POI) were sorted using the following criteria: proteins that came down in both the control and POI traps were accepted as true hits if their proteins score was at least 2.5-fold higher than the control. **[B]** Total positive interactors in Sec3 and Sec8, and number of proteins that came down in both. **[C]** Total positive interactors in Sec3 and Sec3-913, and number of proteins that came down in both.

After filtering, a positives list for each exocyst protein was created. The lists were then compared to view overlap of positives between the exocyst members. Sec3 was found to have the largest number of positives with 644 proteins being identified (Figure 5.2b), Sec8 pulled down 136 positive hits and Sec3-913 had 396 positive interactors (Figure 5.2 b and c). Of these positive interactors Sec3 shared 51 similar proteins with Sec8 (Figure 5.2b), and 164 with Sec3-913 (Figure 5.2c). These lists were then used to identify biological processes that each protein may be involved in, and also to determine whether the differences between Sec3 and Sec3-913 may reveal evidence towards the phenotypes seen in *sec3-913*.

5.2.2 Functional annotation clustering reveals that exocyst interactors are associated with known and previously undescribed cellular processes

Functional clustering of proteins from each exocyst positives list could help to better understand known processes the exocyst is involved in, but also elucidate novel interactions for the exocyst members. Proteins were clustered using the STRING database to generate interaction webs and lists of significantly enriched gene ontology terms (GO:Terms) which were then highlighted on the webs. The positives list of Sec3 revealed several significantly enriched clusters including the exocyst complex, where all members were identified (Figure 5.3). This was reassuring as it provides robust evidence that the pull down of Sec3 was successful and known interactors were identified.

Other enriched clusters included the cell cortex, inner mitochondrial membrane protein complex, mitochondrial part, and mitochondrial protein complex (Figure 5.3). Due to the number of positives being larger for Sec3 it was possible that this would generate noise that might make it hard to see more focussed clusters. The lists of Sec3 positive proteins that clustered into the mitochondrial protein complex and cell cortex GO:Terms were analysed again in STRING to view more focused clusters. Analysis of the cell cortex cluster of Sec3 positives showed 3 clusters which were annotated as cortical cytoskeleton, actin cytoskeleton organisation and exocytosis (Figure 5.4). The mitochondrial protein complex cluster revealed a web with 3 clear clusters that were annotated as mitochondrial inner membrane protein complex, mitochondrial outer membrane complex and mitochondrial gene expression (Figure 5.4). These data reveal that Sec3 may

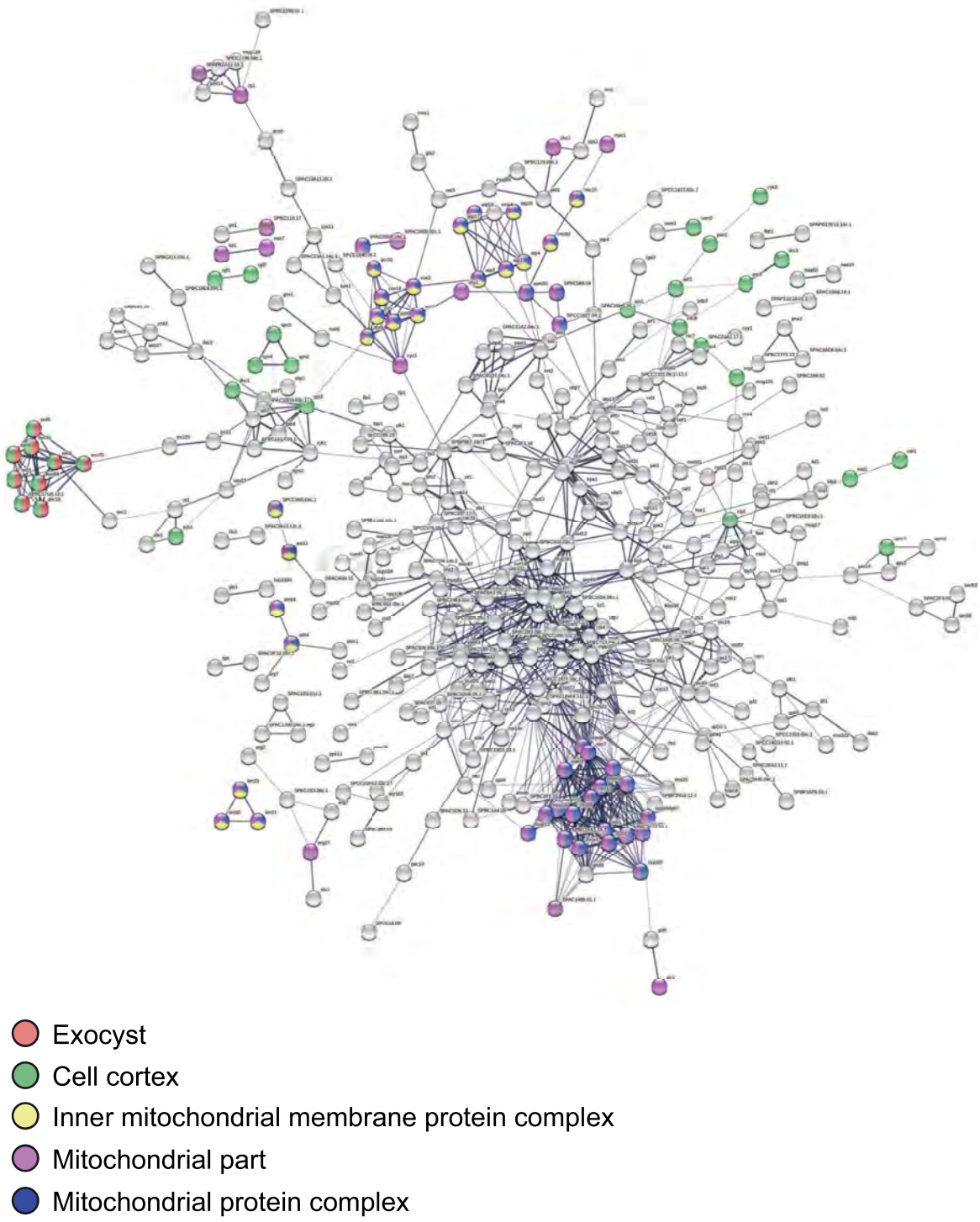

Figure 5.3: Sec3 interacts with proteins involved in multiple cellular processes. The 642 positive interactors identified in the Sec3 GFP-Trap were analysed using the STRING web resource. Significantly enriched Gene Ontology (GO) terms were coloured as indicated.

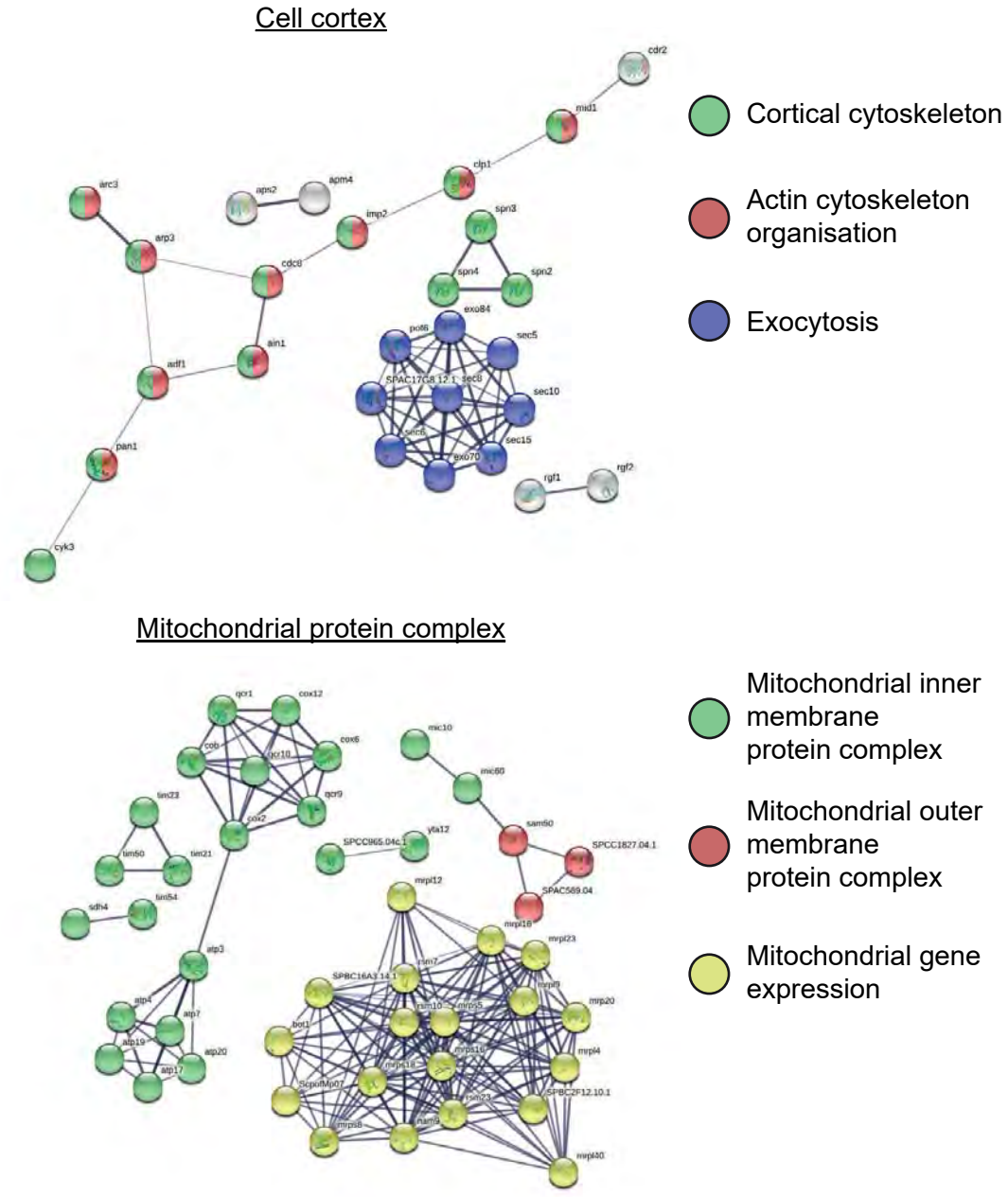

Figure 5.4: Focused clustering of putative Sec3 interactors reveals associations with actin and mitochondria . The list of proteins from the GO terms identified in Figure 5.3 were re-analysed using the STRING web resource to identify more focused clusters.

interact with proteins involved in the actin organisation and also complexes associated with the mitochondrion.

To create a more robust picture of interactors of the exocyst complex as a whole, positive interactors of the exocyst member Sec8 were also sorted by STRING analysis. Positive interactors of Sec8 were found to cluster into GO:Terms of proteins involved in the regulation of biological processes, exocytosis, and nucleocytoplasmic import (Figure 5.5). The exocytosis cluster contained the whole exocyst complex also highlighting that pull down of Sec8 was successful (Figure 5.5). These data show that Sec8 may play a role at the nucleus, but may also function with regulators of many biological processes which could explain why mutants of the exocyst exhibit multiple phenotypes.

As Sec8 appeared to interact with proteins involved in different processes to Sec3, it was interesting to see the similarities between the positive interactors of Sec3 and Sec8. The 51 proteins that appeared in the positives lists of both Sec3 and Sec8 were analysed by STRING. Clustering revealed that the only significant GO:Term that was enriched in the shared positives of Sec3 and Sec8 was the exocyst complex (Figure 5.6). This shows that Sec3 and Sec8 both pulled down the whole exocyst, but do not appear to interact with proteins that share similar functions.

To further assess the interactors of Sec3 it was important to see what positive interactors were pulled down when Sec3 was mutated in the Sec3-913 strains. STRING analysis of the positive interactors of Sec3-913 showed only one significantly enriched GO:Term, which was annotated as catalytic activity (Figure 5.7).This shows that the interactors of Sec3-913 do not significantly cluster into many different biological processes, meaning it is unlikely that the phenotypes seen in *sec3* mutants is due to a gain of function.

To further assess the differences between Sec3 and Sec3-913, the 164 positive interactors that were pulled down by both Sec3 and Sec3-913 were analysed using STRING. Interestingly this analysis revealed common interactors of Sec3 and Sec3-913 are not significantly enriched in any GO:Term (Figure 5.8). These data show that mutation of Sec3 appears to change its ability to interact proteins involved in difference biological processes.

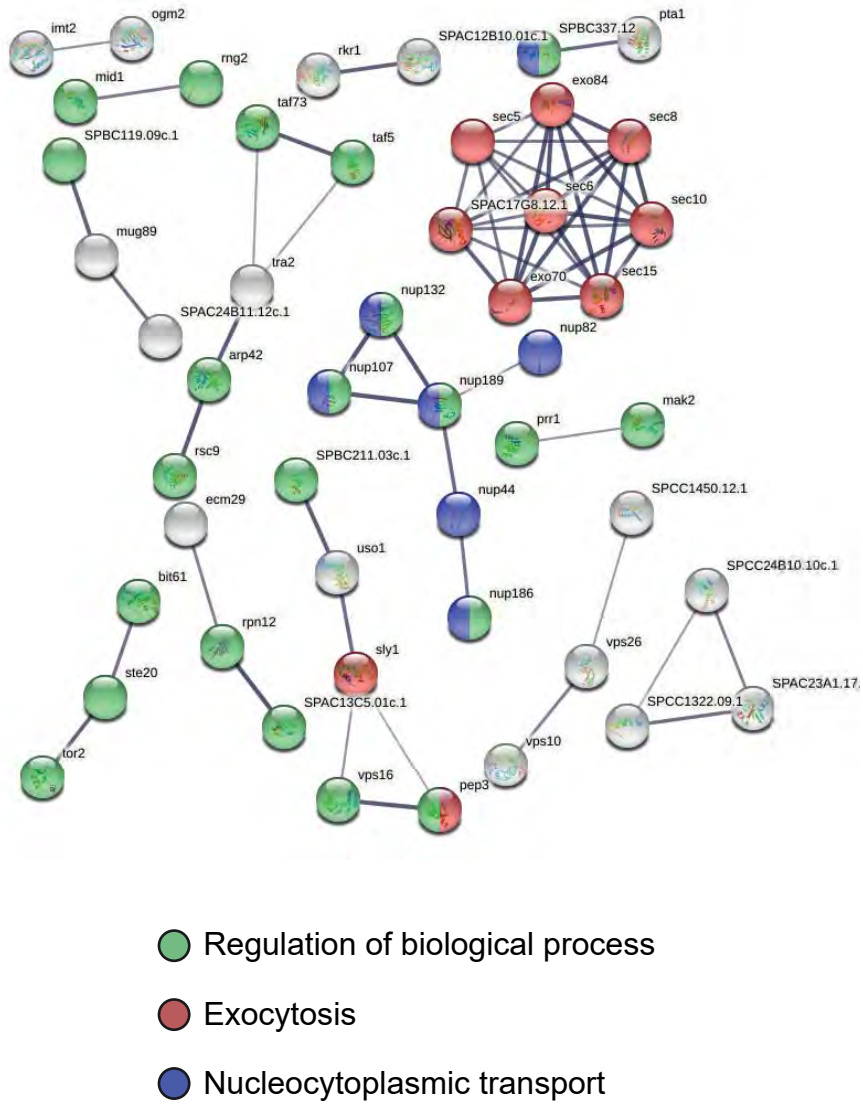

Figure 5.5: GFP-Trap of Sec8 reveals putative interactions with nuclear proteins, and a role for Sec8 in the regulation of biological processes. The 136 positive interactors detected in the Sec8 GFP-Trap were analysed using the STRING web resource. The complete exocyst was identified (red), and many proteins implicated in nucleocytoplasmic transport (blue) and regulation of biological processes (green) were enriched in the Sec8 dataset.

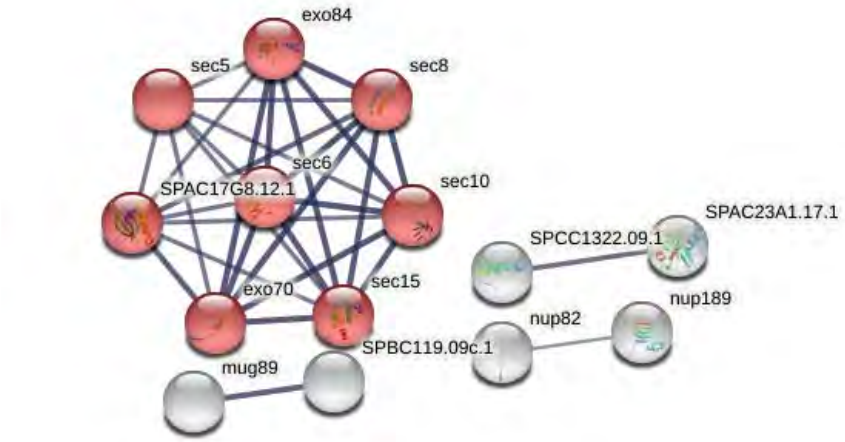

Figure 5.6: Comparison of putative Sec3 and Sec8 interactors reveals a difference in function of different exocyst members. Positive interactors that were found in both the Sec3 and Sec8 GFP-Traps were analysed using the STRING web resource. Of these 51 proteins, enrichment analysis revealed that the exocyst was the only shared cluster between the two exocyst members.

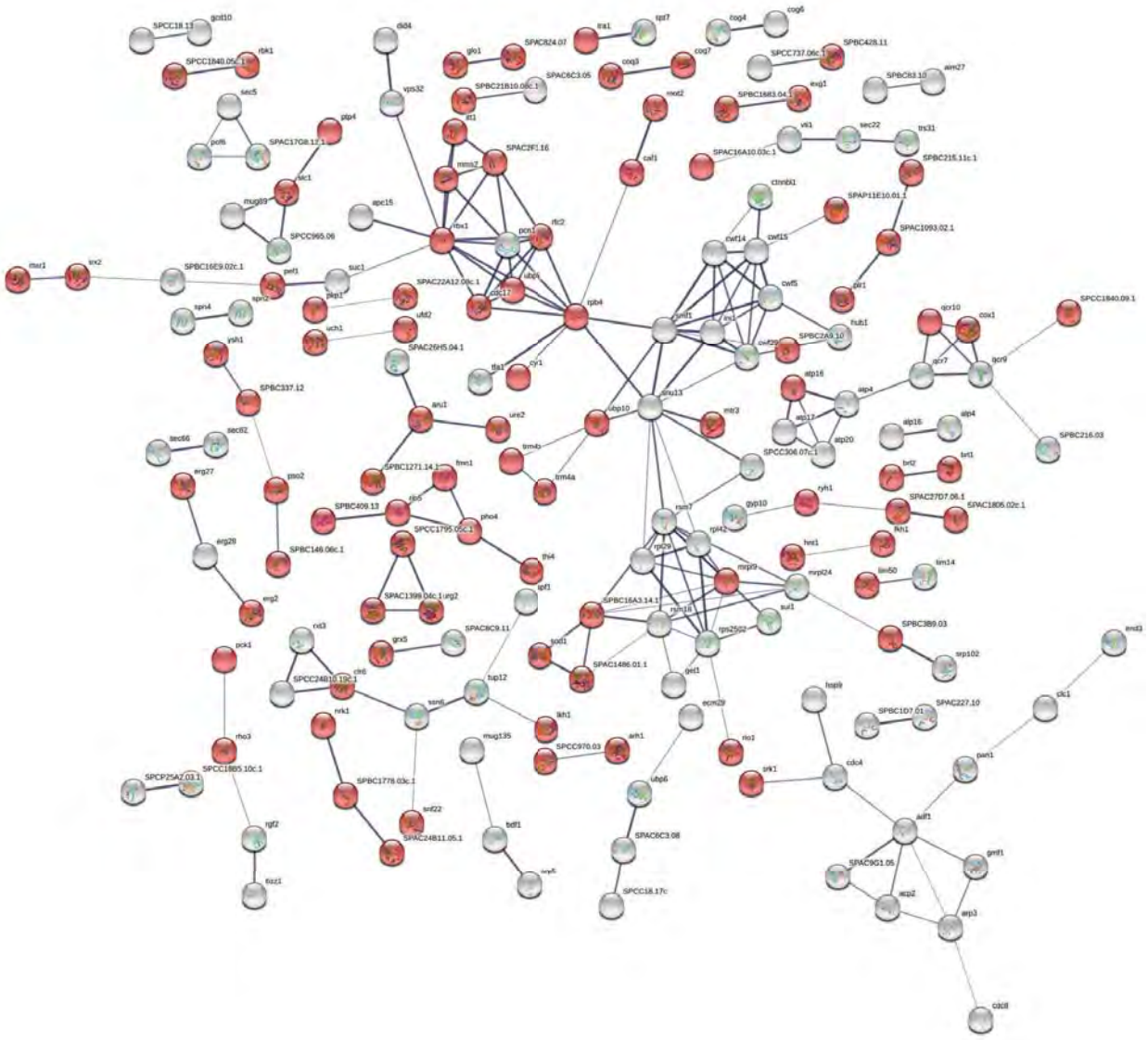

Catalytic activity

Figure 5.7: Analysis of putative Sec3-913 interactors reveals enrichment of proteins involved in catalytic processes. The 396 positive interactors pulled down in the Sec3-913 GFP-Trap were analysed using the STRING web resource. This revealed that the only enriched GO term was “catalytic activity” (red).

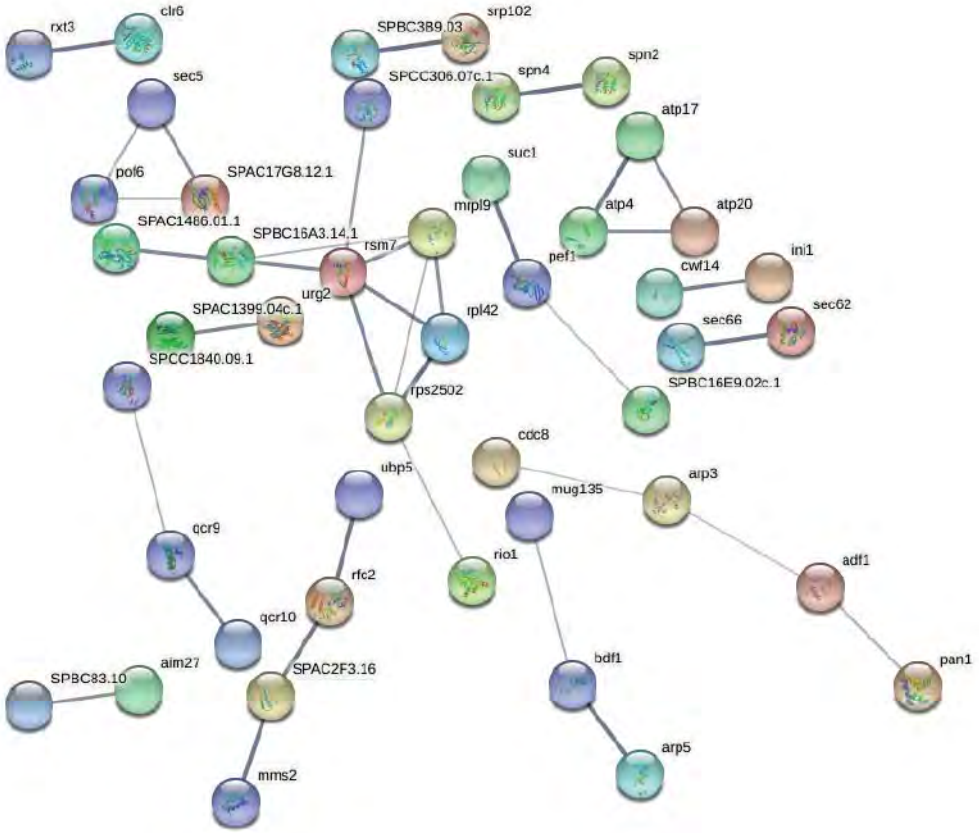

Figure 5.8: STRING analysis of the positive interactors found in both Sec3 and Sec3-913 shows no enriched clusters. The lists of positive interactors detected in the Sec3 and Sec3-913 GFP-Traps were compared. Proteins that appeared in both lists were analysed using the STRING web resource, but no enriched clusters were found.

5.2.3 Sec3 mutation results in loss of interaction with proteins involved in endocytosis, mitochondrial ribosomal and protein complexes, and also other exocyst subunits.

The positives pulled down by Sec3-913 showed no commonality with Sec3, so it was important to see whether the mutation of Sec3 caused it to gain interactors not found in Sec3, and whether these gained interactions show any biological relevance that could account for the phenotypes seen in *sec3-913*. To achieve this, a list of positive interactors found in the Sec3-913 pull down but not in Sec3 were analysed by STRING. STRING analysis showed that most of these proteins were not linked to each other, and no significant enrichment could be seen (Figure 5.9). These data show that the phenotypes seen in *sec3-913* are unlikely to be due to a gain of function with proteins in other biological processes therefore it can be assumed that the phenotypes in *sec3-913* are due to a loss of interactions with proteins.

As a gain of function role for *sec3-913* was shown to be unlikely, it was possible that the mutation of *sec3* causes it to lose interactions with proteins involved in specific cellular functions. A list of positives pulled down by Sec3 but not Sec3-913 were generated and analysed by STRING. Analysis revealed several enriched clusters including the spindle pole, mitochondrial protein complex and ribosome, and also the exocyst (Figure 5.10). These data suggest that mutation of Sec3 causes a loss of interaction with proteins involved at the spindle pole, mitochondrial ribosomal and protein complexes, and even other members of the exocyst.

The loss of interaction between Sec3-913 and the exocyst prompted the investigation of which exocyst members are lost or retained when Sec3 is mutated. Analysis of the exocyst clusters found by STRING analysis for all three proteins showed that Sec3 and Sec8 both pulled down the whole exocyst complex (Figure 5.11). Interestingly, Sec3-913 lost interaction with all the exocyst components except Sec5 (Figure 5.11). This shows that mutation of Sec3 stops it from integrating into the full exocyst complex, but it still retains an interaction with Sec5. A recent study into the overall architecture of the budding yeast exocyst revealed that Sec3 binds strongly to only Sec5 but not other members of the exocyst (Heider et al., 2016), which could explain why Sec3-913 retains this interaction.

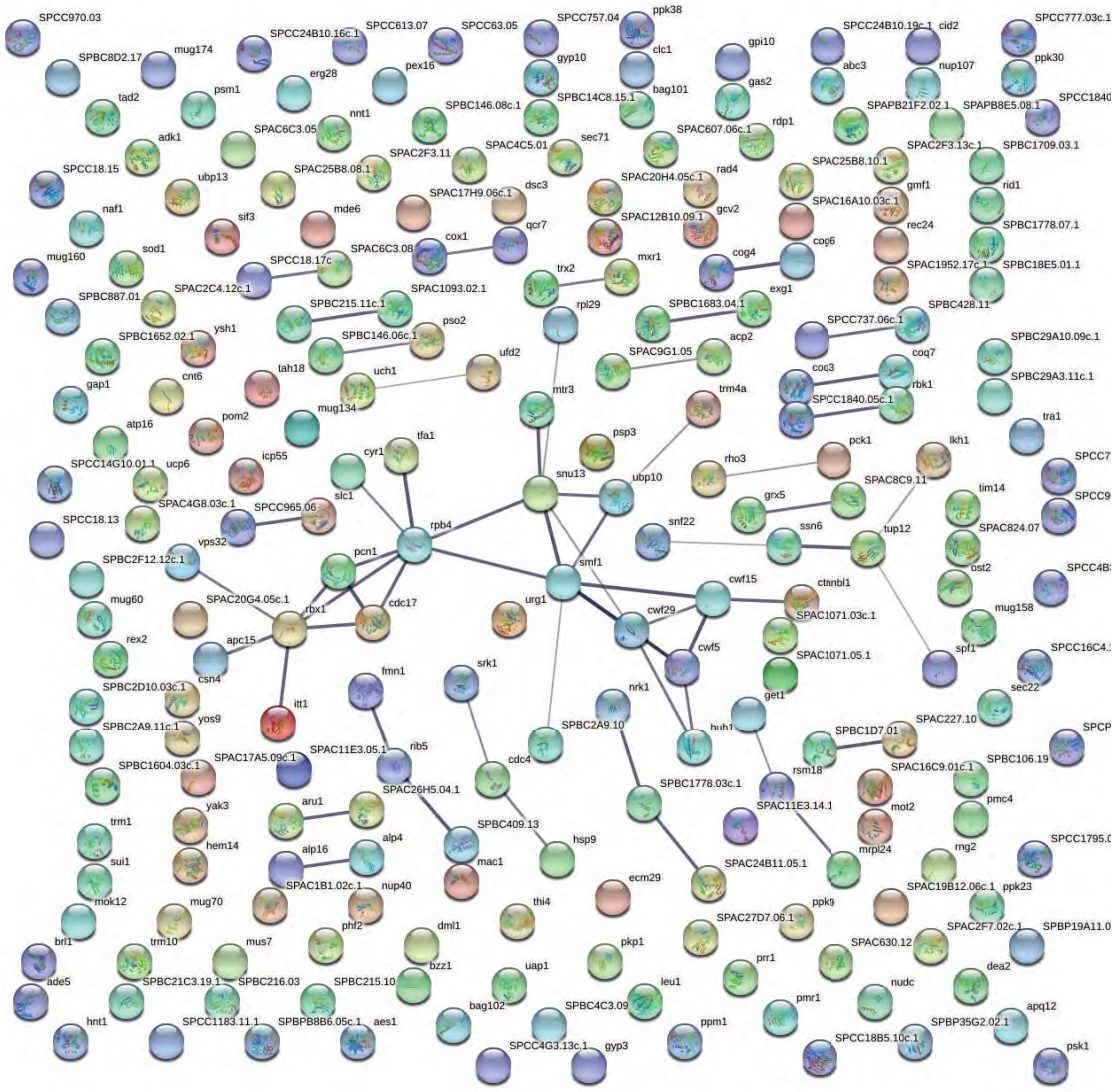

Figure 5.9: Protein interactors gained in the Sec3-913 mutant showed no enrichment for specific clusters. Positive interactors that were detected in the Sec3-913 GFP-Trap (but not the Sec3 GFP-Trap) were analysed using the STRING web resource. No enriched clusters were found.

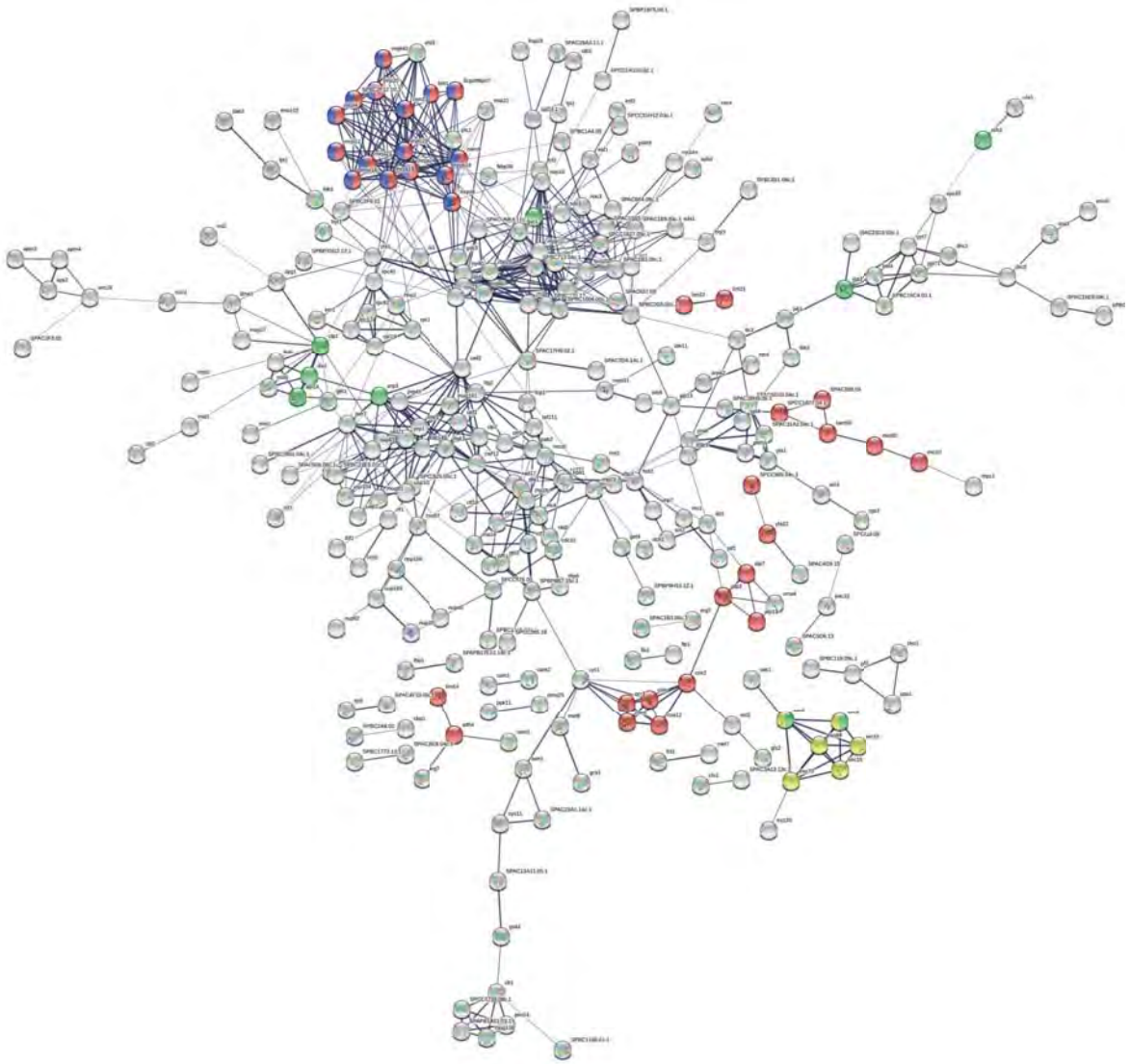

Spindle pole

Mitochondrial protein complex

Exocyst

Mitochondrial ribosome

Figure 5.10: Mutation of Sec3 causes a loss of interaction with members of the exocyst, as well as proteins at the mitochondria. A list of the positive interactors that were found in the Sec3-GFP-Trap, but lost in the Sec3-913 GFP-Trap, was generated. Members of the exocyst complex were lost, as well as many mitochondrial proteins and spindle pole proteins.

Figure 5.11: Sec3-913 loses associations with the majority of exocyst subunits. Diagram showing the detection of exocyst proteins in GFP-TRAPs of mutliple exocyst strains. Proteins detected as positive interactors are indicated by a green box. A red box indicates no interaction was detected.

STRING analysis of Sec3 revealed enriched cluster of proteins involved in actin cytoskeleton organisation (Figure 5.4). Mutation of Sec3 results in a delocalisation of endocytic actin patch machinery (Jourdain et al., 2012), and because of this these proteins were investigated further. The endocytic proteins that Sec3 pulled down were found to be proteins that play a role in the early part of the endocytic patch lifetime (Figure 5.12 green). Two out of the 7 proteins that comprise the actin branching Arp2/3 complex were also pulled down by Sec3 (Figure 5.12 yellow). The actin depolymerising protein Adf1/Cofilin was also identified as a possible interactor of Sec3 (Figure 5.12 red). Mutation of Sec3 caused a loss of nearly all early patch proteins except Pan1 and End3, and a loss of the Arp2/3 complex component Arc3 (Figure 5.12). In contrast, Sec8 was not found to show any interactions with the endocytic actin machinery by mass spectrometry (Figure 5.12). These data indicate that Sec3 and not Sec8 may link the exocyst complex to the endocytic actin cytoskeleton, and that mutation of Sec3 may cause a loss of this interaction.

The interactors of Sec3 suggested the existence of a novel interaction between the exocyst and mitochondria (Figure 5.4). Because of the novelty of this, these mitochondrial proteins were examined further by STRING. Outer membrane complexes were prioritised as it is unlikely that the exocyst would be present on the mitochondrial inner membrane. Outer membrane complexes that were enriched in Sec3 were found to be the mitochondrial contact site and cristae organising system (MICOS) complex and the sorting and assembling machinery (SAM) complex (Figure 5.13). Sec3 was found to interact with Mic10 and Mic60 of the MICOS complex and Mtx1 and Sam50 of the SAM complex (Figure 5.13). Also included on this list was unidentified protein SPCC63.03 which is predicted to be the *S. pombe* orthologue of mammalian DNAJC11 and which also interacts with these complexes (Xie et al., 2007). Both Sec8 and Sec3-913 did not pull down any of these complexes (Figure 5.13). These data show that Sec3 may interact with the outer membrane of mitochondria via the MICOS and SAM complexes, and that this interaction may be lost when Sec3 is mutated. These data also show that Sec8 does not appear to interact with mitochondrial proteins.

Co-immunoprecipitation analyses between Sec3 and members of the MICOS complex were performed but could not confirm the possibility of a novel exocyst-mitochondria interaction (data not shown). As biochemistry could not confirm an

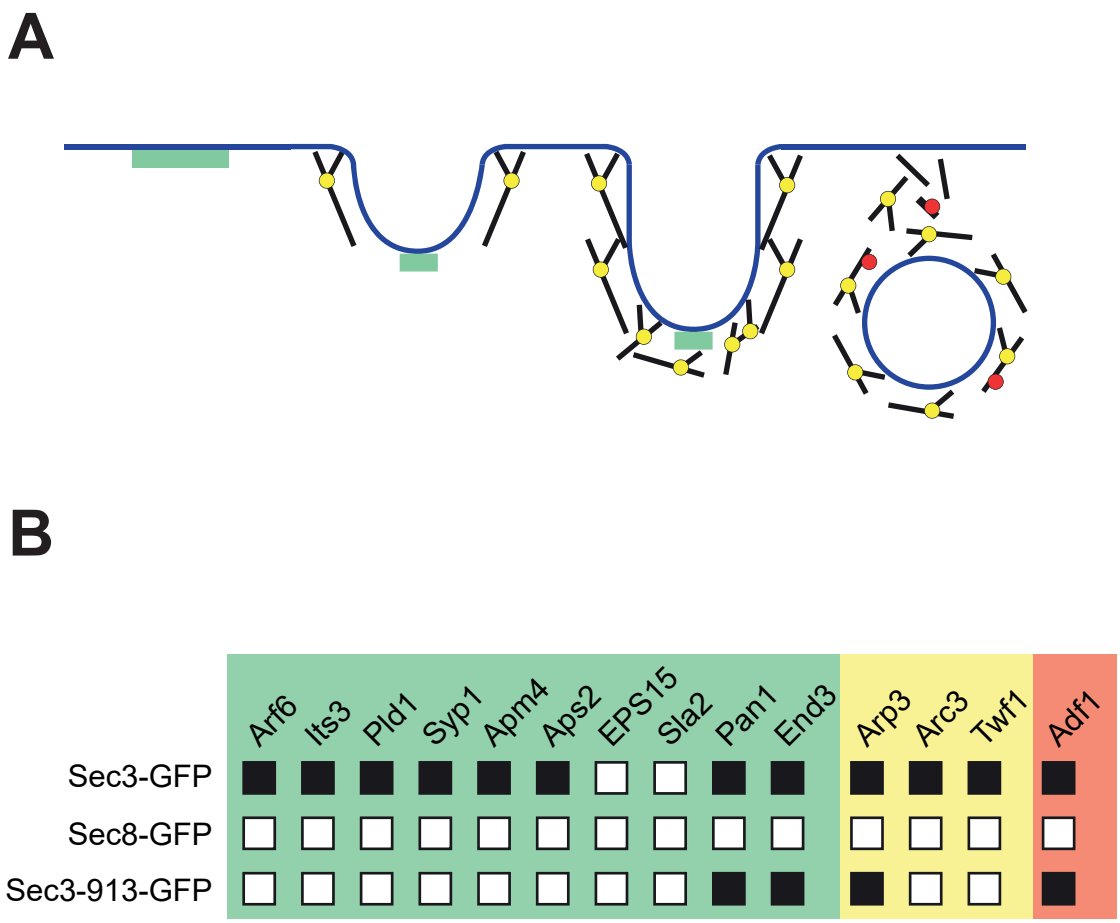

Figure 5.12: Protein constituents of the cortical actin patch are putative Sec3 interactors. [A] Cartoon to show the protein constituents of endocytic actin patches, and **[B]** their detection in GFP-TRAPs of multiple exocyst strains. Cortical actin patch components are shown in green, and members of the Arp2/3 complex shown in yellow. Actin depolymerising factor 1 (Adf1) is shown in red. Proteins detected as positive interactors are indicated by a black box. A white box indicates no interaction was detected.

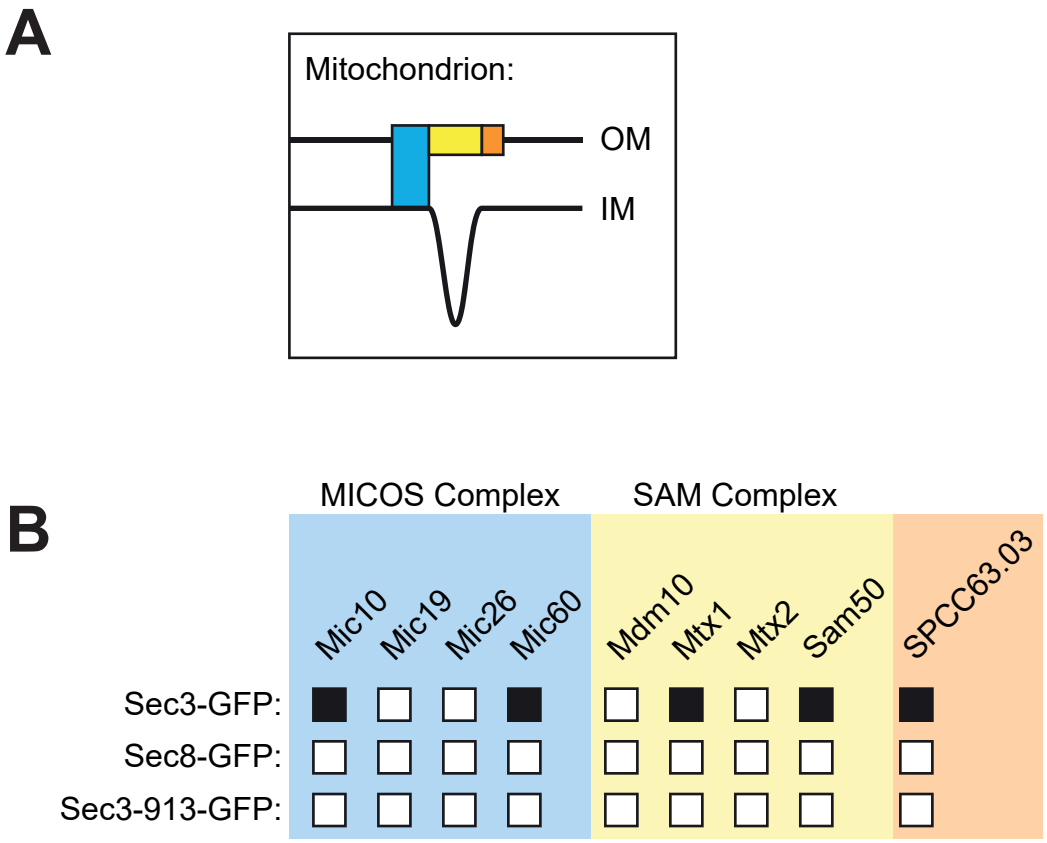

Figure 5.13: Protein complexes of the inner and outer mitochondrial membranes are putative Sec3 interactors. [A] Cartoon to show the MICOS (blue) and SAM (yellow) complexes, as well as an uncharacterised mitochondrial membrane protein (orange). **[B]** Diagram showing their detection in GFP-TRAPs of multiple exocyst strains. Colours correspond to panel A. Proteins detected as positive interactors are indicated by a black box. A white box indicates no interaction was detected.

interaction I decided to examine the morphology of mitochondria in *sec3* mutants using fluorescence microscopy.

Wild-type and *sec3* mutants possessing endogenously labelled Cox4-dsRed were grown overnight in minimal media and imaged on the morning. Cox4 is a part of the electron transport chain and is a good marker label for mitochondria. Z stacks of each strain were imaged. The wild type mitochondria were organised as short strands (Figure 5.14a). The mitochondria of *sec3-913* appeared elongated with aberrant directionality, and this was found to get progressively worse in the more aggressive *sec3-916* strain (Figure 5.14a). Mitochondria are highly dynamic organelles which constantly either join to each other by fusion, or break apart by fission (Bleazard et al., 1999; Chen et al., 2003). The elongated phenotype could possibly be due to either a reduction in fission, or an increase in fusion events. To test this z stack images were taken of each strain at 30 second intervals for 10 minutes and fission and fusion events were counted when mitochondria were seen to break apart or join together. The wild type over 10 minutes had an average of 5 fission and 4 fusion events equating to 0.5 fission and 0.4 fusion events per minute (Figure 5.14b). The *sec3-913* strain showed a significant reduction in fission events (Kruskal-Wallis, P = <0.001), with 0.4 fission events a minute (Figure 5.14b). A slight but non-significant reduction in fusion was also seen in *sec3-913* (Figure 5.14b). The more aggressive *sec3-916* mutant showed a more pronounced reduction in fission and fusion events than the wild type than the *sec3-913* strain (Figure 5.14b). The fission events in *sec3-916* were significantly reduced compared to the wild type at ~0.25 fission events per minute (Figure 5.14b, N = approx. 50 cells per strain over 2 replicates, Kruskal-Wallis, P = < 0.001). Fusion events were also found to be significantly decreased compared to the wild type at ~0.25 fusion events per minute (Figure 5.14b, Kruskal-Wallis, P = < 0.001). Taken together these data show that mutation of *sec3* alters mitochondrial organisation dynamics through simultaneous reduction of both fission and fusion events.

5.2.4 Sec3 may interact with a minority of amino acid importers, including Cat1

Due to the leucine sensitivity of exocyst mutants and that Cat1 appears to be overexpressed at the plasma membrane of *sec3-913* (Figure 3.13), interactions between the exocyst and amino acid importers was investigated. Of the 38 proteins cited to be amino acid transporters in *S. pombe*, the exocyst was found

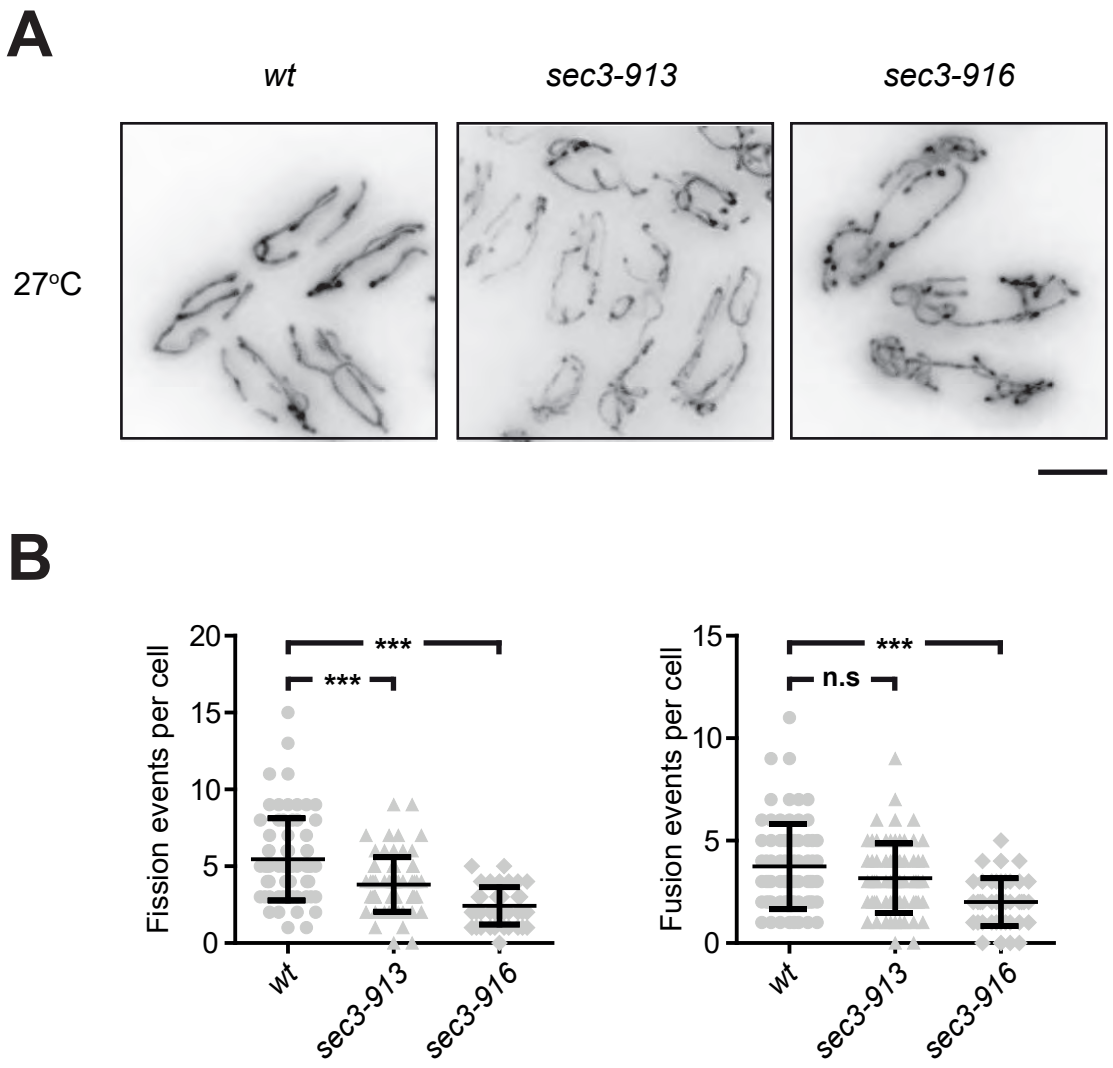

Figure 5.14: Mutation of Sec3 affects mitochondrial dynamics. [A] Wild-type and *sec3* mutant strains expressing cox4-dsRed were grown in EMM overnight at 27 °C to mid-log phase, and z-stack images were taken. The wild type (*wt*) had classic strands of mitochondria, whereas mutation of *sec3* appeared to cause elongation of the mitochondria. Scale bar represents 5 µm. **[B]** Z-stack images of the strains in panel A were taken every 30 seconds for 10 minutes at 27 °C, and the number of fission and fusion events per cell were calculated. Both *sec3-913* and *sec3-916* showed a simultaneous reduction in both fission and fusion events (Shapiro-Wilk, Kruskal-Wallis with Turkeys post-hoc, p = <0.0001, N = >73 cells per condition.)

to interact with only 5 of these proteins (Figure 5.15). Sec3 pulled down the cationic transporter Cat1 and 2 other uncharacterised importers (Figure 5.15). Sec3-913 also interacted with Cat1 and the uncharacterised protein SPBC460.01c, but showed a possible interaction with the 2 other importers Ort1 and SPBC1652.02 (Figure 5.15). Sec3 has previously been implicated in the trafficking of glucose transporters in higher eukaryotes (Inoue et al., 2003). Because of this, carbohydrate importers were also investigated. Sec3 pulled down 2 out of 6 annotated carbohydrate importers, Ght2 and Ght5 (Figure 5.16). Pull down of Sec3-913 also showed an interaction Ght2 but not Ght5 (Figure 5.16). STRING analysis of Sec8 revealed no interaction with amino acid or carbohydrate transporters (Figures 5.15 and 5.16). These data show that nutrient importers are likely to be a cargo that Sec3 traffics, and that these interactions do not appear to be lost when *sec3* is mutated. Furthermore Sec8 did not appear to interact with nutrient transporters, hinting that Sec3 may interact more strongly than Sec8 with this family of proteins.

5.2.5 There is unlikely to be a physical interaction between the exocyst and TOR complexes.

The temperature sensitive phenotype of *sec3-913* can be rescued by rapamycin and mutation of *tor1*, highlighting a genetic interaction between the exocyst and TOR (Figure 4.8). This interaction could also be physical and therefore the exocyst GFP trap data was analysed to find possible interactions with the TOR signalling network. Of the seven proteins that comprise TORC1, two were pulled down across all 3 exocyst members (Figure 5.17). The protein Psk1 was pulled down by *sec3-913* and is mentioned here as it is the pombe S6 kinase homologue that is a downstream target of TORC1 (Nakashima et al., 2012). Sec8 was only found to pull down the main kinase of TORC1, Tor2 (Figure 5.17). Of the 8 members of TORC2, only Sec8 was found to pull down two of them, Bit61 and Ste20 (Figure 5.17). Thus, it is unlikely that the exocyst interacts physically with the TOR complexes.

Regulation of TORC1 and TORC2 is also important for their function, and it could be possible that the exocyst may interact with this part of the TOR signalling cascade. Due to how TORC2 is regulated still remaining unclear, the TORC1 regulating Rag GTPases were searched for. Sec3 was found to pull down 1 out of 4 Lam proteins (Lam2) and 1 out of 2 Rag GTPases (Gtr1) (Figure 5.17). Lam

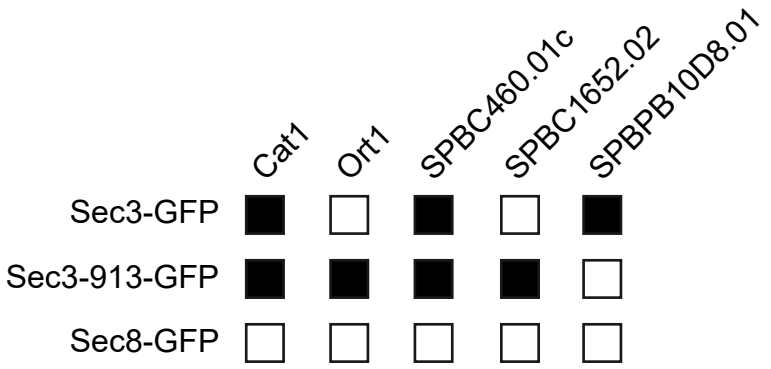

Figure 5.15: Sec3 may traffic a minority of amino acid importers. Diagram showing the detection of amino acid transporters in GFP-TRAPs of mutliple exocyst strains. Proteins detected as positive interactors are indicated by a black box. A white box indicates no interaction was detected.

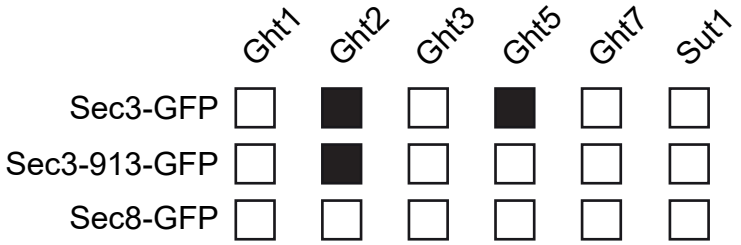

Figure 5.16: Sec3 did not interact with many carbohydrate importers. Legend. Diagram showing the detection of carbohydrate importers in GFP-TRAPs of mutliple exocyst strains. Proteins detected as positive interactors are indicated by a black box. A white box indicates no interaction was detected.

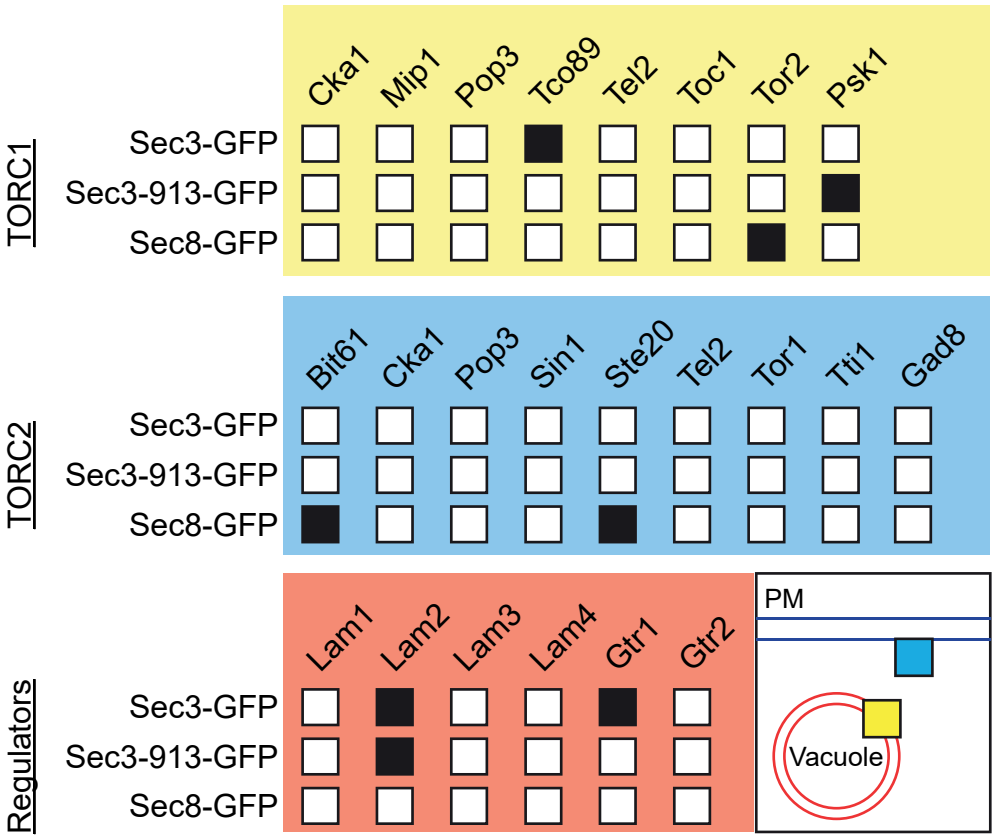

Figure 5.17: The exocyst may have a very weak interaction with proteins involved in TOR signalling. Diagram showing the detection of TOR signalling components in GFP-TRAPs of mutliple exocyst strains. Colours correspond to the diagram (bottom-right). Proteins detected as positive interactors are indicated by a black box. A white box indicates no interaction was detected.

proteins belong to the LAMTOR complex which acts as a guanine exchange factor (GEF) for the Rag GTPases (Bar-Peled et al., 2012). Positives of Sec3-913 were found to contain only Lam2 and Sec8 did not appear to pull down any regulators of TORC1 signalling (Figure 5.17). These findings show that it is unlikely the exocyst helps to regulate TOR signalling at the vacuole.

5.2.6 GFP-Trap reveal possible interactions between Sec3 and small GTPases controlling growth signalling.

In contrast, it is possible that Sec3 may regulate growth signalling via interactions with small GTPases (Figure 5.18). Analysis of GTPases in all three strains showed that Sec3 interacted multiple families of GTPases while Sec8 did not (Figure 5.18).

The ADP-ribosylation family (Arf) of GTPases appear to be involved in the establishment of polarity in *S. pombe*, particularly in the initiation of new end take off (Fujita, 2008; Fujita and Misumi, 2009). In conjunction with the Arfs, the Rab family of GTPases regulate the secretory and endocytic trafficking of vesicles (Craighead et al., 1993; Lipatova et al., 2008). Of these families, proteomics of Sec3 revealed potential interactions with Arf6 and the Rabs Ypt3, 7, and 71 (Figure 5.18). Furthermore the mutation sites in Sec3-913 may ablate this potential binding to polarity and trafficking factors as no Arf or Rab GTPases were found to associate with Sec3-913 (Figure 5.18). This analysis suggests that Sec3 is regulated by the Arf and Rab family of GTPases potentially to position the exocyst at the correct site in fission yeast (Boyd et al., 2004), and mutation of Sec3 may prevent efficient targeting of the exocyst via a loss of regulation.

Regulation of Tor growth signalling is also dependent on GTPases with the Ras-family protein Rheb (Rhb1) and the Rab-family GTPase Ryh1 activating TORC1 and TORC2 signalling complexes respectively (Bai et al., 2007; Hatano et al., 2015). Sec3 bound to both Rhb1 and Ryh1, the latter of which was also found to interact with Sec3-913 (Figure 5.18). This data provides evidence of a possible regulatory role of both TORC1 and TORC2 via exocyst interactions with key small GTPases.

5.2.7 Is it all about membrane tension?

Taken together the proteomics of Sec3 has identified potential binding partners that function in cortical actin patches, activation of TORC2 signalling, and the

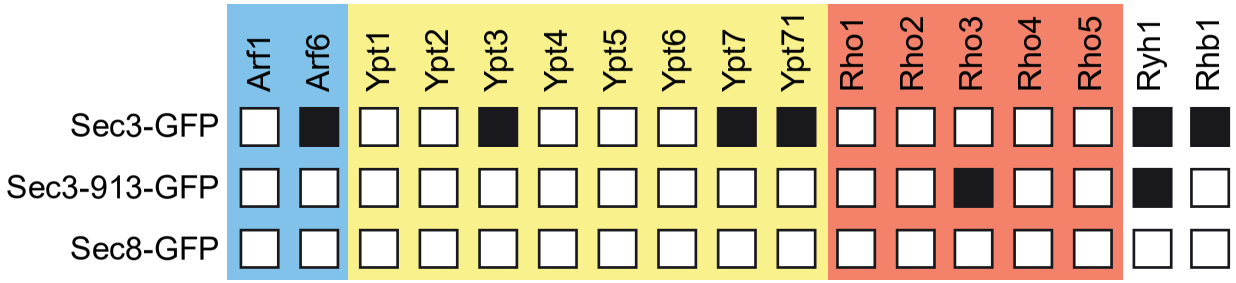

Figure 5.18: Sec3 may interact with members of the Arf and Rab families of small GTPases, as well as activators of TOR signalling. Diagram showing the detection of Arf (blue), Rab (yellow) and Rho (red) family small GTPases, as well as small GTPase activators of TOR signalling, in GFP-TRAPs of mutliple exocyst strains. Proteins detected as positive interactors are indicated by a black box. A white box indicates no interaction was detected.

establishment of polarity in vesicle trafficking. These clusters align well with the phenotypes seen in the *sec3* mutant strains which include delocalised actin patches, perturbed cell morphology (Jourdain et al., 2012), and a novel phenotype presented in chapter of delocalised sterols. All of these clusters also feed into the regulation of membrane tension. This positions Sec3 as a possible master regulator of membrane tension in multiple cellular contexts

Therefore I tested this hypothesis by examining the effect of the manipulation of TORC2 signalling on the cortical actin patch, and sterol distribution defects seen in the *sec3* mutants.

Mutation of *sec3* has been shown to cause delocalisation of the cortical endocytic actin patches (Jourdain et al., 2012). The GFP trap data of Sec3-GFP showed a pull down of many proteins involved in the endocytic patch (Figure 5.12). TORC2 has also been shown to regulate the arrangement of the actin cytoskeleton (Niles and Powers, 2014). This means it is possible that the rescue of *sec3* mutants by mutation of *tor1* kinase may be due to interplay of both proteins at the actin cytoskeleton. To test whether the endocytic patch phenotype of *sec3* is restored by mutation of *tor1* kinase, strains were grown in YE5S at the permissive temperature, fixed with 4% paraformaldehyde (PFA), and stained with bodipy-phallicidin to label actin structures. Staining of the wild type showed polarised endocytic actin patches at the tips and septum, and cables emanating from the tip confirming that the staining protocol preserved the actin efficiently (Figure 5.19). The *sec3-916* strain had delocalised actin patches as expected and aberrant cable morphology, however no cytokinetic actin rings (CAR) could be seen (Figure 5.19). Mutation of *tor1* kinase did not delocalise endocytic patches and CAR morphology appeared to be similar to the *WT* (Figure 5.19). The *sec3-916 tor1-L2045D* dual mutant retained the delocalised patch phenotype of the *sec3-916* strain, however more often than not, the CAR appeared to form (Figure 5.19).The cables also appeared more polarised (Figure 5.19). These data show that the rescue of *sec3-916* by *tor1-L2045D* is unlikely to be due to endocytic patch re-localisation.

The sterol trafficking defect seen in *sec3-916* could lead to a higher PM sterol content thus leading to a lower membrane tension. Turning off TORC2 would reduce sterol biosynthesis (Muir et al., 2014), and potentially rescue *sec3-916* by reducing membrane sterol content. To see if reduced sterol production rescued

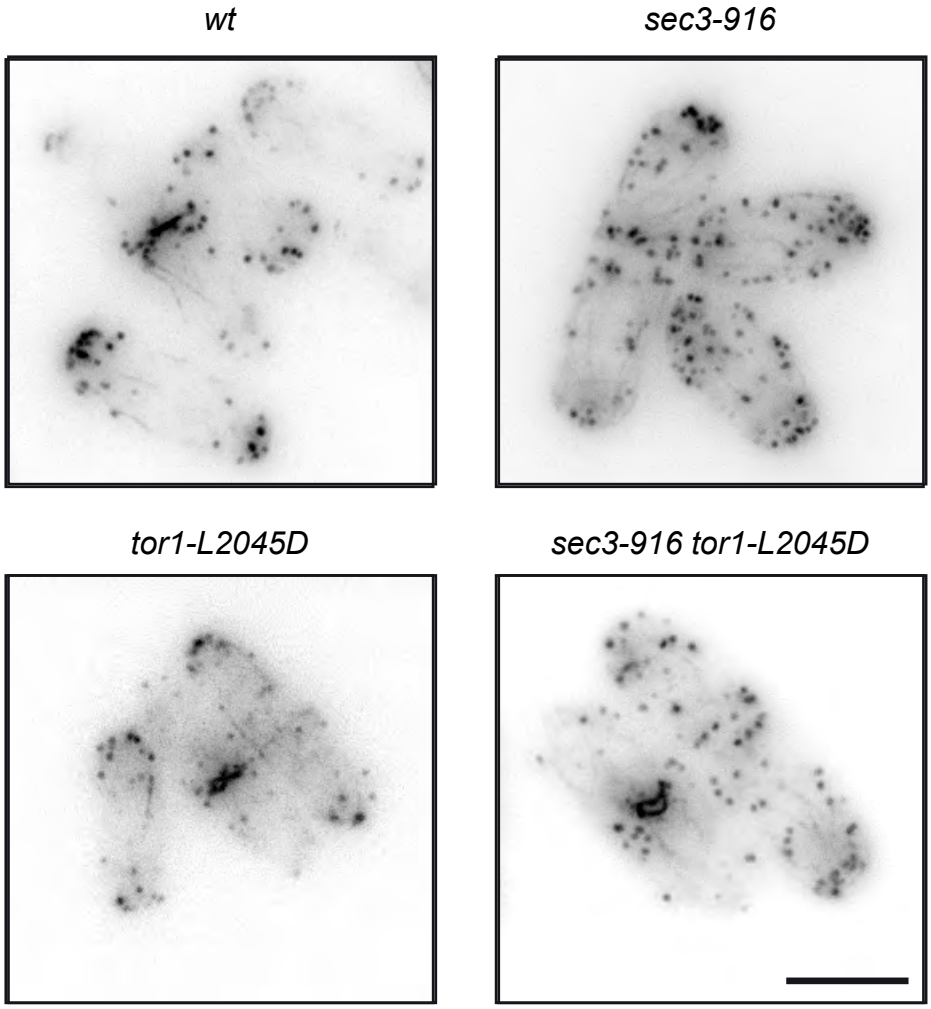

Figure 5.19: Mutation of *tor1* does not restore actin localisation in *sec3-916*. Strains were grown to mid-log in YE5S and then fixed with 4% PFA. Strains were then stained with bodipy-phallicidin 488, and imaged. Scale bar = 5 μm.

the *sec3* and *tor1* mutants, strains were spotted in ten-fold dilutions on YE5S containing 0.8 and 0.9 μM myriocin or equal volume methanol. The *sec3* mutants showed no sensitivity to the drug (Figure 5.20). The *tor1* mutant did show sensitivity with a dose dependent reduction in growth seen with the addition of myriocin (Figure 5.20). The same amount of sensitivity was seen in the *tor1 sec3* dual mutants, showing no interaction between the two proteins and sterol biosynthesis (Figure 5.20). These data show that *tor1* is sensitive to myriocin but mutations in *sec3* are not affected by sterol biosynthesis.

To further verify this I assessed the sensitivity of the strains to the anti-fungal drug Amphotericin B (AmB). AmB targets PM ergosterol and creates pores in the membrane to cause cell death (Andreoli, 1974). Sec3 and Tor1 mutant strains were spotted on rich medium containing 0.1 μg/ml AmB or the equivalent volume DMSO. At the permissive temperature, *sec3-916* was more sensitive to AmB than *sec3-913* and the wild type (Figure 5.21). The *tor1-L2045D* strain did not appear to show sensitivity to the drug, but interestingly both the *tor1* and *sec3* mutant dual strains appeared more sensitive to the drug than the respective single mutant strains suggesting these strains have an increased plasma membrane sterol content (Figure 5.21). At the restrictive temperature of 34 ^{o}C, both the *tor1-L2045D* with and without the *sec3-913* gene exhibited the same sensitivity to AmB (Figure 5.21). Treatment of the strains AmB revealed that mutations in both the exocyst and TORC2 increases the concentration of plasma membrane sterol content.

Fission yeast that lack the endocytic myosin MyoI phenocopy the depolarised sterol phenotype seen in the *sec3* mutants (Takeda and Chang, 2005). Furthermore, MyoI has also been shown to regulate membrane tension (Nambiar et al., 2009). To determine if Sec3 and MyoI genetically interact wild-type and *sec3-913* strains lacking MyoI were spotted on YE5S with either DMSO or 25 ng/ml rapamycin. All strains exhibited normal growth at the permissive temperature of 27 ^{o}C (Figure 5.22). Both the *sec3-913* and *myoI*Δ strain were ts at the restrictive temperature, however the growth of the *myoI*Δ strain was greater than expected, suggesting the strain may harbour a suppressor which partially rescues it's growth. Growth of the *sec3-913 myoI*Δ dual mutant was similar to the wild type at 36 ^{o}C (Figure 5.22). Rapamycin rescued both the *sec3-913* and *myoI*Δ strains, however due to the dual mutant being fully rescued rapamycin did

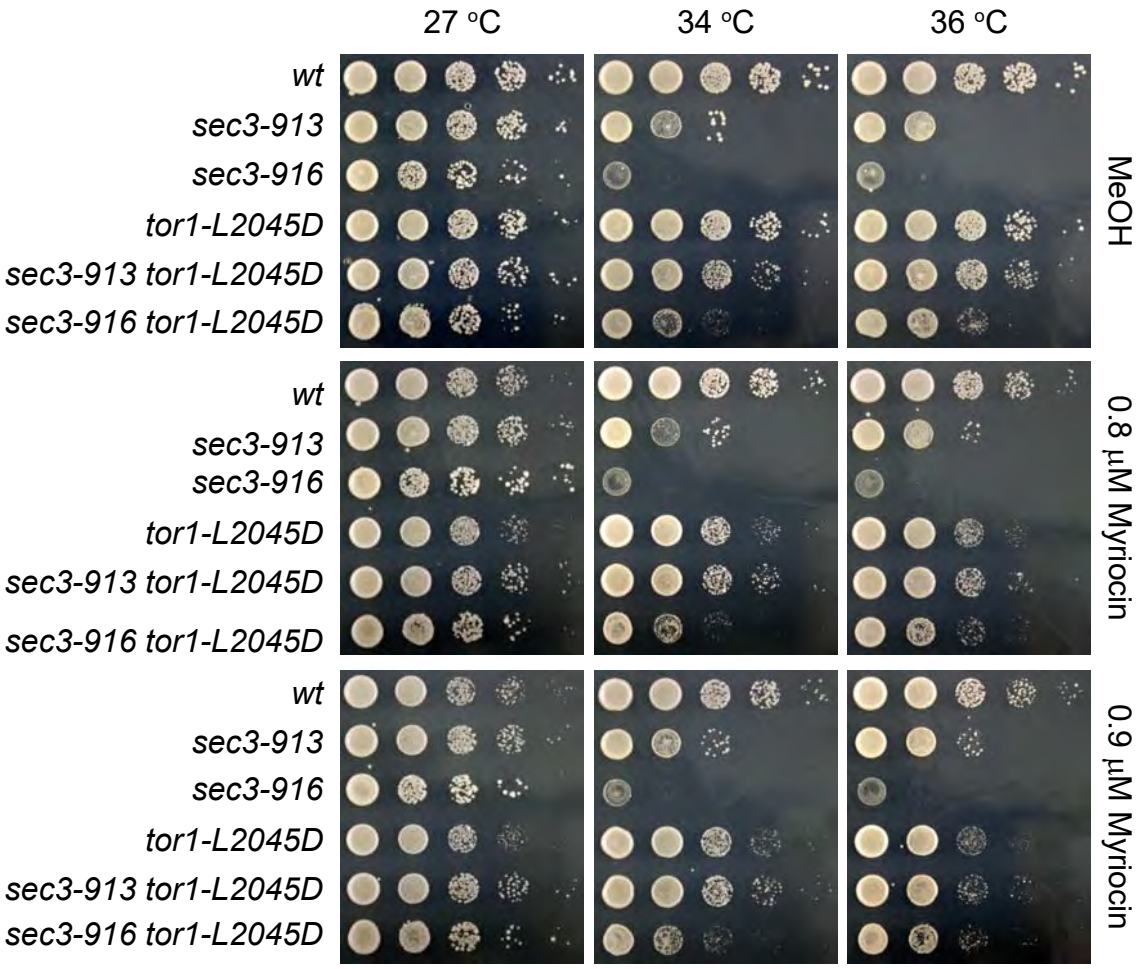

Figure 5.20: Sec3 mutants are not sensitive to inhibition of ergosterol biosynthesis. Strains were grown to mid-log phase in YE5S and adjusted to the same density. Cells were then spotted in ten-fold dilutions on YE5S containing the sterol biosynthesis inhibitor myriocin at the shown concentrations, or the same volume of methanol (MeOH). The *tor1* mutant showed sensitivity to the drug, whereas the *sec3* mutants did not.

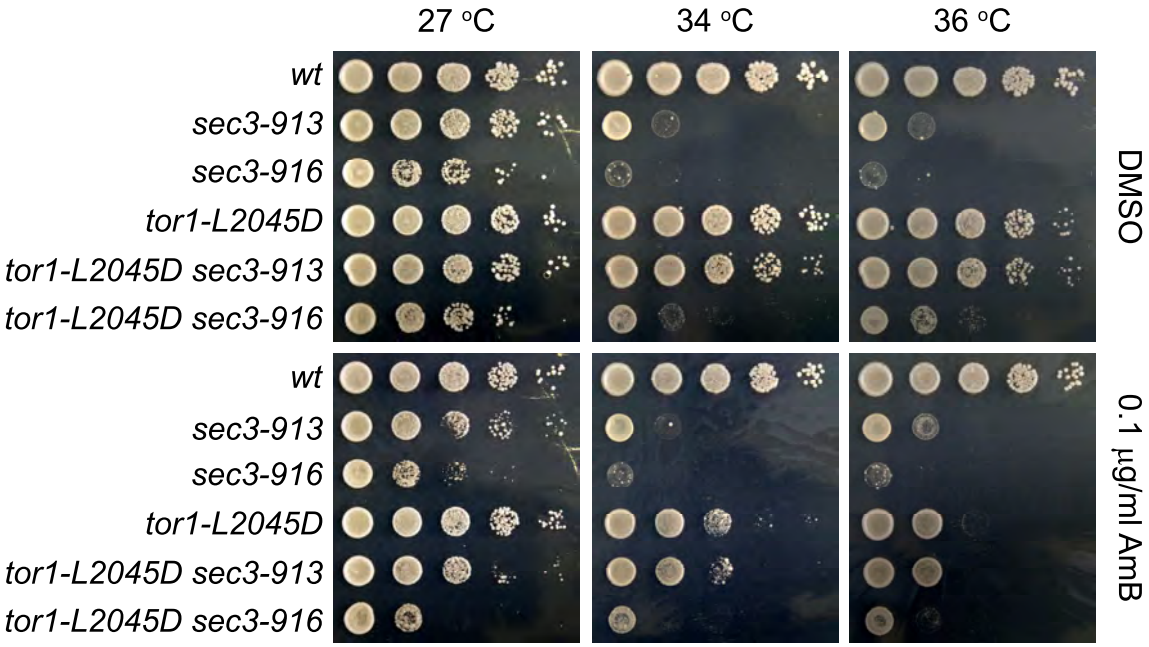

Figure 5.21: Mutation of Sec3 does not increase plasma membrane ergosterol content. Serial dilutions of wild-type (*wt*) and mutant strains shown were spotted on YE5S agar medium containing no (DMSO) or 0.1 µg/ml of the ergosterol targeting drug Amphotericin B (AmB). Plates were incubated at the permissive (27 °C), semi-restrictive (34 °C), and restrictive (36 °C) temperatures.

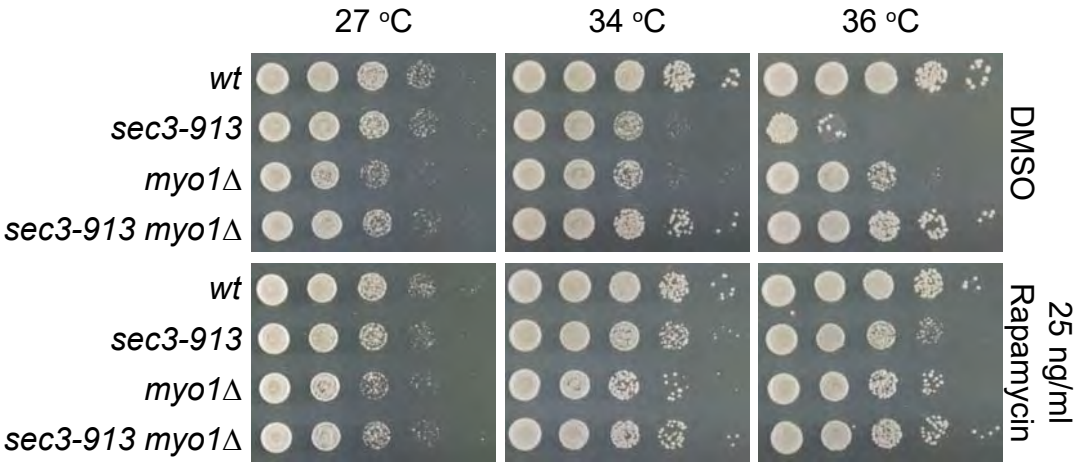

Figure 5.22: The growth of *sec3-913* is rescued by deletion of myosin 1. Serial dilutions of wild-type (*wt*), *sec3-913, myo1*Δ and *sec3-913 myo1*Δ cells were spotted on YE5S agar medium containing no (DMSO) or 25 ng/ml of rapamycin. Plates were incubated at the permissive (27 °C), semi-restrictive (34 °C) or restrictive (36 °C) temperatures. Growth of *sec3-913* was reduced at the restricitve temperature, but deletion of *myo1* rescues this. Addition of rapamycin rescued the growth of both *sec3-913* and *myo1*Δ, but the double mutant was unaffected.

not affect the growth of this strain (Figure 5.22). These data show that deletion of Myo1 may rescue the growth of *sec3-913*, suggesting Sec3 may genetically interact with Myo1. However, this must be repeated using a re-isolated *myo1Δ* strain lacking a suppressor.

5.3 Discussion

To assess the mechanism by which Sec3 may interact with the TOR signalling network, the direct binding partners of the exocyst were evaluated using the GFP Trap method of immunoprecipitation. The mass spectrometry output for each of the exocyst proteins was sorted stringently to generate a list of possible positive interactors. The list of positives for Sec3 contained 644 proteins, which seemed quite high considering that *S. pombe* is predicted to have a maximum of 4940 proteins coding genes (Wood et al., 2002). This was due to the fact that the number of shared positives between the two replicates of the Sec3 GFP Trap came to less than 20 double positives. It was possible that if only those 20 positives were investigated, that some real interactions may be missed. Biological relevance of interactors was considered for Sec3 by finding proteins that have already been cited to interact with Sec3 in the literature and using their protein score to determine a suitable cut off.

Both Sec3 and Sec8 pulled down the entire exocyst complex. This was a good internal control for the experiment as the exocyst complex has been shown to always be assembled at 1:1 stoichiometry in *S. cerevisiae* (Heider et al., 2016). It was not possible to determine whether the *S. pombe* exocyst came out at 1:1 stoichiometry as the GFP trap method is not quantitative like other methods such as SILAC (Mann, 2006). However, this result verified that the pull downs had been successful and the data sets could be trusted.

The comparison of positives between Sec3 and Sec3-913 revealed that mutating Sec3 appears to stop it from being able to incorporate into a functional exocyst complex but retains its interaction with Sec5 (Figure 5.11). This finding fits with the proposed holocomplex model of the *S. cerevisiae* exocyst where Sec3 shows a very strong pairwise interaction with Sec5 in the 4-subunit module that also contains Sec6 and Sec8 (Heider et al., 2016). There is some functional redundancy between Sec3 and Exo70 as they both contain a PH domain to dock

the complex to the PM (Baek et al., 2010; He et al., 2007; Yamashita et al., 2010). This means that from my data set I cannot determine whether the exocyst complex is completely disassembled, or whether a semi functional exocyst complex that lacks Sec3 and possibly Sec5 can form when Sec3 is mutated. Exocytosis and endocytosis has been shown to be perturbed in *sec3-913* (Jourdain et al., 2012), and this could be due to the lack of a functional exocyst complex. However, the GFP trap data also suggest that individual members of the exocyst may play roles in different biological processes, and that Sec3 may be the key connector to the actin cytoskeleton.

Sec3 has previously been shown to affect the localisation of endocytic actin patches and components including Sla2 and ArpC3 (Jourdain et al., 2012). The GFP trap of Sec3 in this chapter revealed an interaction with many components of the actin cytoskeleton as expected (Figure 5.4). Further investigation into this cluster of interactors showed that all of these proteins function at the early endocytic patch. This is an interesting result as due to the exocyst's reliance on formin nucleated cables and the movement via MyosinV for its main role in exocytosis (Jin et al., 2011), some interactors of the actin transport machinery would have been pulled down too. Controversially the data presented here hints that Sec3 is predominantly an endocytic protein.

Intriguingly, the positive interactors of Sec8 did not contain any proteins involved in the actin cytoskeleton. This raises the question of whether different exocyst components interact with different biological processes individually or as a complex. One study that adds weight to this argument showed that the staining of mammalian Sec6 with antibodies generated towards multiple epitopes of the same protein shows that it colocalises with many different structures including intermediate filaments (Inamdar et al., 2016). Due to the 1:1 stoichiometry it could be possible that depending on the location in the cell, different exocyst members perform different roles. As seen in the GFP trap data Sec3 predominantly interacts with mitochondrial protein complexes, whereas Sec8 showed preferences towards nuclear import proteins. This is possibly the first time a novel interaction has been shown between Sec3 and the mitochondria, but also Sec8 and the nucleus.

Another explanation for this differential function of the exocyst could be due to interaction with external regulators. The actin branching nucleator complex

Arp2/3 is classically involved in the branching of actin at the plasma membrane (Amann and Pollard, 2001). This function has been shown to be regulated by the nucleation promoting factor (NPF) WAVE (Suetsugu et al., 1999). However recent work has revealed a role for Arp2/3 in vesicular trafficking, and this function occurs when Arp2/3 is regulated by the WASH complex (Duleh and Welch, 2010; Zhou et al., 2015). This shows that protein complexes alter their function and cellular localisation depending on how they are regulated. The data presented in this chapter revealed that Sec3 pulled down multiple GTPases from different families, which could account for the diverse clusters of biological clusters identified. The finding that Sec8 did not pull down any GTPases could be explained by the fact that, unlike Sec3, Exo70, and Exo84, it does not possess binding domains for regulators (Moskalenko et al., 2003; Wu et al., 2010; Yamashita et al., 2010). However this could also mean that the complex pulled down may also be differentially regulated to the one pulled down in Sec3, explaining why they interact with different cellular compartments.

The positive interactors of Sec3 were shown to be significantly enriched in mitochondrial GO:Terms. This was surprising as the exocyst is primarily located at the plasma membrane and has never been shown to interact with mitochondria. A further investigation of these protein clusters showed that two outer complexes of mitochondria came down in the trap (Figure 5.4). These complexes were identified as the MICOS and SAM complex. The MICOS complex is primarily involved in the positioning of the mitochondrial cristae (Tarasenko et al., 2017). The SAM complex is required for the import and integration of other outer membrane proteins including the TOM complex (Kozjak et al., 2003). Both these complexes have also been cited as being important for contact sites between mitochondria and the endoplasmic reticulum (ER) through an interaction with the ER bound ERMES complex (Hoppins et al., 2011). This interaction is important for the movement of lipids from the ER to the mitochondria (Wideman and Muñoz-Gómez, 2016). Due to the interaction between Sec3 and mitochondria being novel and unexpected, coimmunoprecipitations of Sec3 and members of the MICOS complex were performed but inconclusive (data not shown). It is possible that an interaction between the exocyst and mitochondria may be a minor occurrence in the cell, and therefore undetectable. Further evidence for an exocyst-mitochondria interaction was also found in GFP traps of GFP-Sec3 and GFP-Sec8 in mouse embryonic fibroblasts where the MICOS

complex was pulled down by both exocyst proteins (unpublished data, Dawe lab). While the data here indicate a potentially novel and conserved interaction between the exocyst and mitochondria, attempts to verify the interaction by co-immunoprecipitation were unsuccessful.

The finding that *sec3-913* is rescued by an inactive mutant of Tor1 kinase would suggest that Sec3 may operate within the TOR signal transduction pathway through TORC2. The GFP trap data for Sec3 did not seem to correlate with this hypothesis with Sec3 only pulling down TORC1 specific proteins. Contrastingly pull down of Sec8 showed a possible interaction with three proteins involved in TOR signalling; Bit61, Ste20, and Tor2 kinase. Both Ste20 and Bit61 are members of the TORC2 complex, while Tor2 kinase is the key component of the TORC1 complex (Loewith et al., 2002). The temperature sensitive phenotype of both Sec3 and Sec8 were found to be rescued by rapamycin, so it is possible that Sec8 but not Sec3 interacts directly with members of TORC2 accounting for this rescue. However, the fact that only 2 proteins out of the 8 that comprise TORC2 were pulled down by Sec8 means that it is unlikely that an interaction is with the complete TORC2 complex.

It is established that Sec3 interacts with the Rho family of GTPases which are indispensable for the establishment of polarity in fission yeast (Bendezú and Martin, 2011; Zhang et al., 2001). While the known Rho interactors of Sec3 including Cdc42 were not identified by GFP-Trap, other families including the Arfs and Rabs were (see Figure 5.18). Proteomics of Sec3 revealed a possible interaction with Arf6 which has shown to be involved in the activation of new tip growth during the NETO phase of the fission yeast cell cycle (Fujita, 2008; Fujita and Misumi, 2009). To the authors knowledge there has been no described interaction between the exocyst and Arfs in fission yeast, however one study in the mammalian HeLa cell line has shown that a potential Exo70-Arf6 interaction may position the components needed for cytokinesis (Fielding et al., 2005).

Due to the wide range of cellular processes that TOR signalling affects, it is possible that Sec3 may play a role in the signalling feedback loops the repress TOR. Evidence from the GFP trap data suggest that it is possible that this may be at an organelle level with Sec3 and Sec8 possibly interacting with mitochondria and nucleus respectively. Active TOR signalling promotes mitochondrial biogenesis, presumably so that more ATP can generated while the

cell is in a nutrient rich environment (Wu et al., 2006). When mitochondrial lipids become damaged through reactive oxygen species (ROS) generation, these are removed through selective autophagy or mitophagy in the case of mitochondria (Xiao et al., 2017). Autophagy is also controlled by both the Tor signalling and the exocyst complex (Bodemann et al., 2011; Kamada et al., 2010; Kulich et al., 2013; Singh et al., 2019). This means it is possible that Sec3 may feedback to Tor to control organelle homeostasis, and that disruption to this axis might underlie some of the cellular phenotypes described in exocyst mutants.

Chapter 6: **General Discussion**

In this thesis the relationship between the exocyst complex member Sec3 and nutrient sensing was established. Mutants of the exocyst grow better on minimal media than they do on rich medium. Of the components of media it was found that the amino acid leucine particularly affected the growth of both Sec3 and Sec8 mutants. Due to the established role of leucine in promoting growth through activation of the Tor signalling axis, the possible interaction between the exocyst and Tor was investigated. The inhibitor of TOR, rapamycin, was found to rescue the temperature sensitive phenotype of both *sec3* and *sec8* mutants. This was found to be due to a genetic interaction between Sec3 and the TORC2 specific kinase Tor1. From this it was hypothesised that Sec3 and TORC2 may function together to regulate membrane tension in fission yeast.

6.1 Localisation of TORC2 to the plasma membrane is not dependent on Sec3

The localisation of TORC2 is integral for its function. In budding and fission yeast, TORC2 has been shown to be localised to the plasma membrane (Berchtold and Walther, 2009; Fadri et al., 2005). While TORC2 senses glucose (Cohen et al., 2014; Hatano et al., 2015), it also serves to sense and regulate plasma membrane tension (Riggi et al., 2018). When plasma membrane tension is high TORC2 is activated stimulating the production of sterols via phosphorylation of Gad8 (Muir et al., 2014). The sterols are then incorporated into the PM increasing fluidity and thus reducing membrane tension. One hypothesis was that Sec3 may be responsible for the trafficking and/or tethering of TORC2 at the plasma membrane. Analysis of a fluorescently labelled RICTOR/Ste20 showed no difference in the localisation of TORC2 between the wild type and *sec3-916* showing that Sec3 does not regulate the position of TORC2 at the plasma membrane. This was not surprising as the components of TORC2 in *S. cerevisiae* were shown to localise to the plasma membrane independently of PIP_2 rich regions, even though they all possess a pleckstrin homology domain (Martinez Marshall et al., 2019). As Sec3 is also localised to the PM via a PH domain (Baek et al., 2010; Bendezú and Martin, 2011; Yamashita et al., 2010), the data presented here fits with the idea that TORC2 is localised independently of proteins localising to PIP_2 rich domains in the PM.

While Sec3 may not serve to bring TORC2 to the plasma membrane, it is possible that it could help to inactivate it. An increase in plasma membrane tension causes phase separation of PIP_2 into specific domains, and recruitment of TORC2 to these regions is thought to be how the complex is deactivated (Riggi et al., 2018). The exocyst binds to PIP_2 rich regions of the PM via Exo70 and Sec3 (Boyd et al., 2004; He et al., 2007; Zhang et al., 2008). Also the GFP trap of Sec8 in Chapter 5 showed a possible interaction with to TORC2 members Ste20 and Bit61. Therefore it is not unreasonable to suggest that the exocyst may play a role in deactivation of TORC2. Furthermore deactivation of TORC2 signalling by both rapamycin and mutation of *tor1* kinase rescues the growth of *sec3* mutants. This gives weight to the notion that Sec3 and possibly the whole exocyst may be a negative regulator of TORC2 signalling, and this may possibly be through tethering TORC2 to PIP_2 rich domains.

Recent work in higher eukaryotic organisms has provided evidence for TORC2 gaining a more complex role throughout evolution. TORC2 has been shown to not only be at the plasma membrane, but has also been found to localise to other cellular compartments including the outer mitochondrial membrane and a subpopulation of endosomal vesicles in mammalian cells (Ebner et al., 2017). Although this localisation has not been seen in *S. pombe*, it is tempting to speculate that the mitochondrial and vacuolar phenotypes seen in *sec3* mutants may be due to a loss of TORC2 localisation to specific cellular compartments rather than the plasma membrane. However due to the fact that the neither the exocyst or TORC2 can be seen to localise to these compartments in *S. pombe*, this hypothesis was not pursued.

6.2 How might TORC2 and Sec3 regulate membrane tension?

6.2.1 Sterols

Previous research has shown that the Ts phenotype of *sec3-913* can be rescued by the addition of sorbitol to the medium (Bendezú et al., 2012). This was cited to be due sorbitol ameliorating the membrane tension defects possibly caused by a loss of exocyst function (Bendezú et al., 2012). However sorbitol also changes the osmotic gradient of the surrounding media. The application of the salt potassium chloride (KCl) to *sec3* mutants was shown to rescue growth. Both Sorbitol and KCl create an osmotic gradient in favour of water transport from the cell to the environment (Shen et al., 1999). This would reduce membrane tension

as the internal pressure of the cell is reduced (Colom et al., 2018). Either way the data here suggest that the environmental manipulation of membrane tension affects growth of *sec3* mutants. One possible explanation for this could be the effect Sec3 has on membrane sterol localisation.

The genetic interaction between Sec3 and TORC2 prompted the hypothesis that both proteins may play a role in membrane sterol homeostasis, due to the role of TORC2 in maintaining plasma membrane sterol homeostasis (Berchtold and Walther, 2009; Roelants et al., 2018). Sterols only accumulate at the growing tip and division plane in *S. pombe* (Wachtler et al., 2003). Staining with the fluorescently labelled sterol specific compound filipin revealed that mutation of both *sec3* and *tor1* kinase results in complete loss of sterol polarisation with signal seen over the complete plasma membrane. To further investigate whether this localisation was due to an increase in sterol content, growth of the mutants was assessed on media containing the ergosterol specific drug Amphotericin B to look for increased sensitivity which would mean increased ergosterol, however this data was inconclusive. Loss of polarisation of sterols may affect membrane fluidity and thus tension. One way PM tension has been viewed in *S. cerevisiae* was through the use of the FliptR probe (Colom et al., 2018). The probe fluoresces either green or red depending on the force exerted by phospholipids either side of the probe (Colom et al., 2018). This probe has not been used in fission yeast yet, and if there was more time on the project it would have been interesting to use this tool to visualise membrane tension in *sec3* mutants.

A similar sterol delocalisation phenotype is seen in *S. pombe* upon the deletion of the endocytic myosin Myo1 (Takeda and Chang, 2005). Myo1 is the sole endocytic myosin in the fission yeast (Attanapola et al., 2009; Lee et al., 2000), and the sterol delocalisation in the delete strain has been shown to be due to an inability to endocytose these sterol rich domains (Takeda and Chang, 2005). Mutation of *sec3* causes a defect in both secretion and endocytosis (Jourdain et al., 2012), therefore it was interesting to see which of these contributed to the sterol localisation. Inhibition of sterol biosynthesis with the drug Myriocin caused a loss of sterols at the plasma membrane in *sec3-916* showing that endocytosis of sterols appears to still be functional in the *sec3* mutant. This would suggest that it is the trafficking and localisation of sterols to the membrane that appears

to perturbed in exocyst mutants, rather than the endocytosis of sterol rich domains.

6.3 Endocytosis

As mentioned above, endocytosis is an important part of the maintenance of membrane tension through the removal of sterols (Takeda and Chang, 2005). What governs the retrograde trafficking of sterols from the membrane into the cell still remains elusive. Mutation of *sec3* alters the localisation of both endocytic actin patches and as shown in this thesis, sterols (Jourdain et al., 2012). Interplay between both actin and sterols is required for endocytosis (Hyman et al., 2006; Kim et al., 2017). Sterols are needed to create fluidity of the membrane allowing endocytic invaginations to push into the cell, where they are then pulled in by Arp2/3 mediated polymerisation of the actin cytoskeleton (Hirama et al., 2017; Sun et al., 2015). This poses the question is the endocytic defect caused by mislocalisation of sterols, or are the sterols delocalised due to perturbed endocytosis in *sec3* mutants?

To assess potential binding partners of Sec3 a GFP trap method was employed. Analysis of the mass spectrometry data showed that Sec3 may interact with many proteins annotated as cortical actin patch components. Further analysis showed that the majority of these proteins fell into the category of early patch components that are important for position and initiation of the endocytic patch (Kovar et al., 2011). Exo70, another exocyst member, was also found to interact with the endocytic Arp2/3 complex (Zuo et al., 2006). This provides further evidence for an interaction between the exocyst and endocytic patch components. If these results are trusted then this positions Sec3 as a possible early patch component, and possibly involved in the establishment of patch localisation. However analysis of the patch component Sla2 in *sec3-913* showed that endocytosis is still completed, but at a slower rate (Jourdain et al., 2012). This lends itself to the idea that the sterol content may be the cause of slow endocytosis in *sec3* mutants.

6.4 Cell Wall

Another determinant of cell membrane tension that is important in cellular growth and survival is the fungal cell wall. The cell wall helps to maintain the cellular osmotic gradient across the plasma membrane (Ene et al., 2015; Pérez and Ribas, 2004). The osmotic gradient is important for maintaining intracellular

pressures which also contributes to homeostasis of membrane tension (Colom et al., 2018). It was determined that the pressure that *S. pombe* exerts on its plasma membrane is similar to a racing bike tire, around 1-1.5 MPa (Basu et al., 2014). This means that the integrity of the cell wall is paramount for cellular shape, growth, and survival.

In fission yeast growth the cell wall is incredibly dynamic at the polar tips showing fluctuations in thickness (Davì et al., 2018). These changes in thickness were also shown to be part of a feedback loop controlling growth with thinning of the cell wall negatively regulating growth and vice versa (Davì et al., 2018). Remodelling is entirely dependent on the secretion of enzymes across the plasma membrane that build or breakdown cell wall components such as beta-3-glucan (Martín-Cuadrado et al., 2003). Due to the secretion defects found in the exocyst it is reasonable to suggest that cell wall remodelling and thus osmotic gradients are defective in *sec3* mutants. The osmotic stressors sorbitol and KCl have both been found to rescue *sec3-913* which further reinforces this idea (Bendezú et al., 2012). This suggests that Sec3 may interact with TORC2 indirectly through the regulation of membrane tension via osmotic gradients.

The osmotic stress pathway also signals through the MAPK pathway but via the activation of the MAP kinase Sty1 instead of Pmk1 (Asp et al., 2008). Sty1 and the TOR component Tor1 have been shown to link the MAPK and TOR signalling pathways (Hartmuth and Petersen, 2009). The TORC2-Gad8 axis has also been found to crosstalk with Pmk1, showing that MAPK and TOR signalling are heavily entwined (Madrid et al., 2016). Sty1 activation is also promoted during osmotic stress from salts such as KCL and Sorbitol. Osmotic stress and mutation of Tor1 kinase were found to rescue both *sec3-913* and *sec3-916*. Both these conditions would lead to an increase in Sty1 activation (Asp et al., 2008; Hartmuth and Petersen, 2009)(Berchtold and Walther, 2009). Therefore it is possible that mutation of Sec3 affects Sty1 activation in pombe, and this is rescued by TORC2 inactivation by mutation of Tor1 kinase or addition of rapamycin.

Further evidence for an exocyst – MAPK interaction has been seen in higher eukaryotes. The exocyst member Sec10 was found to activate MAPK signalling via the endocytosis of the epidermal growth factor receptor EGFR in renal tubule cells (Fogelgren et al., 2014). Sec8 has also been found to promote MAPK signalling through ERK and p38 in the regulation of intermediate filament

assembly during cell migration in higher eukaryotes (Tanaka and Iino, 2015). These findings add further weight to the idea that the fission yeast exocyst could be modulating membrane tension through a conserved interaction with the MAPK pathway, and that TORC2 genetically interacts with Sec3 by intersecting with the MAPK pathway.

6.5 Implications for fission yeast physiology

Characterisation of Sec3 and Exo70 in *S. pombe* revealed that strains with mutations or deletions in these proteins can be rescued by the presence of an osmotic stabiliser such as sorbitol (Bendezú et al., 2012). The reduction in internal turgor pressure is thought to be the cause of rescue in these strains, as lower turgor pressure reduces membrane tension making membrane remodelling easier (Bendezú et al., 2012). Here I show that the membrane tension sensing TORC2 complex shares a genetic interaction with the exocyst member Sec3 presumably through a similar membrane tension phenotype. This interaction could be through the endocytic myosin MyoI. Deletion of MyoI rescued the Ts phenotype of *sec3-913* completely on rich media. Furthermore Sec3 polarises actin patches (Jourdain et al., 2012), and pulled down binding partners associated with endocytosis showing that Sec3 may localised to a similar cellular compartment to MyoI. The TORC2 complex plays a role in endocytosis and this appears to through the component Ste20 (Baker et al., 2019; Bourgoint et al., 2018; Wut et al., 1996). I propose a model in which Sec3 and TORC2 intersect at MyoI to regulate membrane tension. MyoI has already been implicated in the regulation of membrane tension (Dai et al., 1999; Nambiar et al., 2009). Therefore MyoI could link the plasma membrane and secretory pathway in the regulation of membrane tension.

Rapamycin is a macrolide compound that inhibits TORC1 signalling by binding to FKBP12 and inhibiting Tor2 kinase (Vilella-Bach et al., 1999). The temperature sensitive phenotype of the *sec3* mutants were found to be rescued by the addition of rapamycin, suggesting that Sec3 may help to regulate TORC1 signalling in fission yeast. However mutation of TORC2 and not TORC1 was found to copy the rescue seen with rapamycin. This was surprising as TORC2 is cited to be rapamycin insensitive (Loewith et al., 2002). Using the budding yeast *S. cerevisiae* as a model, it was found that the TORC2 complex component Avo3 is responsible for this insensitivity (Gaubitz et al., 2015). The mechanism for this

was shown to be that the C terminal of Avo3 blocks the FKBP12 binding pocket of scTor2/spTor1 kinase (Gaubitz et al., 2015). Avo3 has similarities to the pombe RICTOR homologue Ste20 (Hayashi et al., 2007). GFP trap of the exocyst revealed that Sec8 may interact with Ste2. Because of this one would assume that the exocyst may help couple Ste20 to Tor1 kinase, and because of this the TORC2 complex becomes sensitive to rapamycin. However localisation of Ste20 was found to be unaffected when Sec3 is mutated. These data raise new questions about the fundamental mechanics of the relationship between Ste20 and Tor1 in the TORC2 complex in fission yeast. Rapamycin was found to inhibit mammalian TORC2 formation after prolonged exposure (Sarbassov et al., 2006). The rescue of *sec3* mutants by rapamycin in this thesis was observed on agar plates which were incubated for multiple days. This means the prolonged exposure could explain why both rapamycin and the *tor1-L2045D* were found to *sec3-913* and *sec3-916*.

6.6 Wider implications – Health and disease

Correct regulation of signalling from both TORC1 and TORC2 is imperative for cell survival, and many diseases are caused by mis-regulation of this signalling axis (Saxton and Sabatini, 2017). This thesis presents a novel genetic interaction between the exocyst member Sec3 and the TORC2 signalling complex. As deactivation of TORC2 was found to rescue *sec3-913* and *sec3-916*, this positions Sec3 and the exocyst as a potential regulator of TORC2 signalling.

Negative regulation of TOR signalling is important for cancer. Due to TOR's promotion of cellular growth and proliferation, a continually active signalling axis promotes tumour growth and metastasis (Beauchamp and Platanias, 2013). Drugs that target and inhibit both TORC1 and TORC2 are currently the centre of much research due the prominent role that TOR plays in cancer (Li et al., 2014; Weisman et al., 2014). Investigations into combinatorial therapies using current anti-cancer drugs and TOR inhibitors have shown promise in the treatment of tumour (Conciatori et al., 2018). If Sec3 is indeed a negative regulator of TORC2 signalling, this could add new avenues for the progression of TORC2 inhibitor drugs in the treatment of cancer.

Mammalian TORC2 has been shown to promote cellular senescence through via Akt mediated signalling networks (Yang et al., 2018). This places TOR signalling

upstream as controller of one of the key events that causes aging (McHugh and Gil, 2018). Studies in yeast have shown that inhibition of TOR signalling through growth of cells on medium containing rapamycin and caffeine promotes longevity (Rallis et al., 2013). Inhibition of TORC1 signalling provides the best route for anti-ageing therapies as side effects caused by TORC2 inhibition can be detrimental to health (Boutouja et al., 2019). Because of this, research into targeted inhibition of TORC1 and not TORC2 has become the main focus in the reduction of side effects. The findings of this thesis show that Sec3 shares a genetic interaction with TORC2 only, and not TORC1. This means that the exocyst complex may provide a future target for ways of regulating TORC2 signalling whilst inhibiting TORC1, potentially leading for future avenues for anti-ageing therapies.

Chapter 7: **References**

Achleitner, G., Gaigg, B., Krasser, A., Kainersdorfer, E., Kohlwein, S. D., Perktold, A., Zellnig, G. and Daum, G. (1999). Association between the endoplasmic reticulum and mitochondria of yeast facilitates interorganelle transport of phospholipids through membrane contact. *Eur. J. Biochem.* **264**, 545–553.

Ahmed, S. M. and MacAra, I. G. (2017). The Par3 polarity protein is an exocyst receptor essential for mammary cell survival. *Nat. Commun.* **8**, 14867.

Ahmed, S. M., Nishida-Fukuda, H., Li, Y., McDonald, W. H., Gradinaru, C. C. and Macara, I. G. (2018). Exocyst dynamics during vesicle tethering and fusion. *Nat. Commun.* **9**, 5140.

Akram, M. (2013). Mini-review on glycolysis and cancer. *J. Cancer Educ.* **28**, 454–457.

Akram, M. (2014). Citric Acid Cycle and Role of its Intermediates in Metabolism. *Cell Biochem. Biophys.* **68**, 475–478.

Albeg, A., Smith, C. J., Chatzigeorgiou, M., Feitelson, D. G., Hall, D. H., Schafer, W. R., Miller, D. M. and Treinin, M. (2011). C. elegans multi-dendritic sensory neurons: Morphology and function. *Mol. Cell. Neurosci.* **46**, 308–317.

Amann, K. J. and Pollard, T. D. (2001). The Arp2/3 complex nucleates actin filament branches from the sides of pre-existing filaments. *Nat. Cell Biol.* **3**, 306–310.

Andersen, N. J. and Yeaman, C. (2010). Sec3-containing exocyst complex is required for desmosome assembly in mammalian epithelial cells. *Mol. Biol. Cell* **21**, 152–164.

Andreoli, T. E. (1974). The structure and function of amphotericin B-cholesterol pores in lipid bilayer membranes. *Ann. N. Y. Acad. Sci.* **235**, 448–468.

Asp, E., Nilsson, D. and Sunnerhagen, P. (2008). Fission yeast mitogen-activated protein kinase Sty1 interacts with translation factors. *Eukaryot. Cell* **7**, 328–338.

Aspuria, P. J. and Tamanoi, F. (2008). The Tsc/Rheb signaling pathway controls basic amino acid uptake via the Cat1 permease in fission yeast. *Mol. Genet. Genomics* **279**, 441–450.

Attanapola, S. L., Alexander, C. J. and Mulvihill, D. P. (2009). Ste20-kinase-dependent TEDS-site phosphorylation modulates the dynamic localisation and endocytic function of the fission yeast class I myosin, Myo1. *J. Cell Sci.* **122**, 3856–

3861.

Ayscough, K. R. (2000). Endocytosis and the development of cell polarity in yeast require a dynamic F-actin cytoskeleton. *Curr. Biol.* **10**, 1587–1590.

Babbey, C. M., Bacallao, R. L. and Dunn, K. W. (2010). Rab10 associates with primary cilia and the exocyst complex in renal epithelial cells. *Am. J. Physiol. - Ren. Physiol.* **299**, F495-F506.

Baek, K., Knödler, A., Lee, S. H., Zhang, X., Orlando, K., Zhang, J., Foskett, T. J., Guo, W. and Dominguez, R. (2010). Structure-function study of the N-terminal domain of exocyst subunit Sec3. *J. Biol. Chem.* **285**, 10424–10433.

Bähler, J., Wu, J. Q., Longtine, M. S., Shah, N. G., McKenzie, A., Steever, A. B., Wach, A., Philippsen, P. and Pringle, J. R. (1998). Heterologous modules for efficient and versatile PCR-based gene targeting in *Schizosaccharomyces pombe*. *Yeast* **14**, 943–951.

Bai, X., Ma, D., Liu, A., Shen, X., Wang, Q. J., Liu, Y. and Jiang, Y. (2007). Rheb activates mTOR by antagonizing its endogenous inhibitor, FKBP38. *Science* **318**, 977–980.

Baker, K., Gyamfi, I. A., Mashanov, G. I., Molloy, J. E., Geeves, M. A. and Mulvihill, D. P. (2019). TORC2-GAD8 dependent myosin phosphorylation modulates regulation by calcium. *Elife* **8**, 1–42.

Baker, K., Kirkham, S., Halova, L., Atkin, J., Franz-Wachtel, M., Cobley, D., Krug, K., Maček, B., Mulvihill, D. P. and Petersen, J. (2016). TOR complex 2 localises to the cytokinetic actomyosin ring and controls the fidelity of cytokinesis. *J. Cell Sci.* **129**, 2613–2624.

Bar-Peled, L., Schweitzer, L. D., Zoncu, R. and Sabatini, D. M. (2012). Ragulator is a GEF for the rag GTPases that signal amino acid levels to mTORC1. *Cell* **150**, 1196–1208.

Barbet, N. C., Schneider, U., Helliwell, S. B., Stansfield, I., Tuite, M. F. and Hall, M. N. (1996). TOR controls translation initiation and early G1 progression in yeast. *Mol. Biol. Cell* **7**, 25–42.

Basu, R., Munteanu, E. L. and Chang, F. (2014). Role of turgor pressure in endocytosis in fission yeast. *Mol. Biol. Cell* **25**, 679–687.

Beauchamp, E. M. and Platanias, L. C. (2013). The evolution of the TOR pathway and

its role in cancer. *Oncogene* **32**, 3923–3932.

Bendezú, F. O. and Martin, S. G. (2011). Actin cables and the exocyst form two independent morphogenesis pathways in the fission yeast. *Mol. Biol. Cell* **22**, 44–53.

Bendezú, F. O., Vincenzetti, V. and Martin, S. G. (2012). Fission yeast Sec3 and Exo70 are transported on actin cables and localize the exocyst complex to cell poles. *PLoS One* **7**, e40248.

Berchtold, D. and Walther, T. C. (2009). TORC2 plasma membrane localization is essential for cell viability and restricted to a distinct domain. *Mol. Biol. Cell* **20**, 1565–1575.

Berchtold, D., Piccolis, M., Chiaruttini, N., Riezman, I., Riezman, H., Roux, A., Walther, T. C. and Loewith, R. (2012). Plasma membrane stress induces relocalization of Slm proteins and activation of TORC2 to promote sphingolipid synthesis. *Nat. Cell Biol.* **14**, 542–547.

Betz, C., Stracka, D., Prescianotto-Baschong, C., Frieden, M., Demaurex, N. and Hall, M. N. (2013). MTOR complex 2-Akt signaling at mitochondria-associated endoplasmic reticulum membranes (MAM) regulates mitochondrial physiology. *Proc. Natl. Acad. Sci. U. S. A.* **110**, 12526–12534.

Binda, M., Péli-Gulli, M.-P. P., Bonfils, G., Panchaud, N., Urban, J., Sturgill, T. W., Loewith, R. and De Virgilio, C. (2009). The Vam6 GEF Controls TORC1 by activating the EGO Complex. *Mol. Cell* **35**, 563–573.

Biondini, M., Sadou-Dubourgnoux, A., Paul-Gilloteaux, P., Zago, G., Arslanhan, M. D., Waharte, F., Formstecher, E., Hertzog, M., Yu, J., Guerois, R., et al. (2016). Direct interaction between exocyst and Wave complexes promotes cell protrusions and motility. *J. Cell Sci.* **129**, 3756–3769.

Bleazard, W., McCaffery, J. M., King, E. J., Bale, S., Mozdy, A., Tieu, Q., Nunnari, J. and Shaw, J. M. (1999). The dynamin-related GTPase Dnm1 regulates mitochondrial fission in yeast. *Nat. Cell Biol.* **1**, 298–304.

Bliss, T. V. P. and Collingridge, G. L. (1993). A synaptic model of memory: Long-term potentiation in the hippocampus. *Nature* **361**, 31–39.

Bodemann, B. O., Orvedahl, A., Cheng, T., Ram, R. R., Ou, Y. H., Formstecher, E., Maiti, M., Hazelett, C. C., Wauson, E. M., Balakireva, M., et al. (2011). RalB and the exocyst mediate the cellular starvation response by direct activation of

autophagosome assembly. *Cell* **144**, 253–267.

Boehm, C. M., Obado, S., Gadelha, C., Kaupisch, A., Manna, P. T., Gould, G. W., Munson, M., Chait, B. T., Rout, M. P. and Field, M. C. (2017). The trypanosome exocyst: a conserved structure revealing a new role in endocytosis. *PLoS Pathog.* **13**, e1006063.

Bourgoint, C., Rispal, D., Berti, M., Filipuzzi, I., Helliwell, S. B., Prouteau, M. and Loewith, R. (2018). Target of rapamycin complex 2– dependent phosphorylation of the coat protein Pan1 by Akl1 controls endocytosis dynamics in *Saccharomyces cerevisiae*. *J. Biol. Chem.* **293**, 12043–12053.

Boutouja, F., Stiehm, C. M. and Platta, H. W. (2019). mTOR: A Cellular Regulator Interface in Health and Disease. *Cells* **8**, 18.

Boyd, C., Hughes, T., Pypaert, M. and Novick, P. (2004). Vesicles carry most exocyst subunits to exocytic sites marked by the remaining two subunits, Sec3p and Exo70p. *J. Cell Biol.* **167**, 889–901.

Brown, E. J., Albers, M. W., Bum Shin, T., Ichikawa, K., Keith, C. T., Lane, W. S. and Schreiber, S. L. (1994). A mammalian protein targeted by G1-arresting rapamycin-receptor complex. *Nature* **369**, 756–758.

Byrne, S. M. and Hoffman, C. S. (1993). Six git genes encode a glucose-induced adenylate cyclase activation pathway in the fission yeast *Schizosaccharomyces pombe*. *J. Cell Sci.* **105**, 1095–1100.

Carrillo, D., Vicente-Soler, J. and Gacto, M. (1994). Cyclic AMP signalling pathway and trehalase activation in the fission yeast *Schizosaccharomyces pombe*. *Microbiology* **140**, 1467–1472.

Castanho, M. A. R. B., Prieto, M. and Jameson, D. M. (1999). The pentaene macrolide antibiotic filipin prefers more rigid DPPC bilayers: A fluorescence pressure dependence study. *Biochim. Biophys. Acta - Biomembr.* **1419**, 1–14.

Chantranupong, L., Wolfson, R. L., Orozco, J. M., Saxton, R. A., Scaria, S. M., Bar-Peled, L., Spooner, E., Isasa, M., Gygi, S. P. and Sabatini, D. M. (2014). The sestrins interact with GATOR2 to negatively regulate the amino-acid-sensing pathway upstream of mTORC1. *Cell Rep.* **9**, 1–8.

Chen, H., Detmer, S. A., Ewald, A. J., Griffin, E. E., Fraser, S. E. and Chan, D. C. (2003). Mitofusins Mfn1 and Mfn2 coordinately regulate mitochondrial fusion and are essential for embryonic development. *J. Cell Biol.* **160**, 189–200.

Chen, X. W., Inoue, M., Hsu, S. C. and Saltiel, A. R. (2006). RalA-exocyst-dependent recycling endosome trafficking is required for the completion of cytokinesis. *J. Biol. Chem.* **281**, 38609–38616.

Cherry, J. R., Johnson, T. R., Dollard, C., Shuster, J. R. and Denis, C. L. (1989). Cyclic AMP-dependent protein kinase phosphorylates and inactivates the yeast transcriptional activator ADR1. *Cell* **56**, 409–419.

Chia, K. H., Fukuda, T., Sofyantoro, F., Matsuda, T., Amai, T. and Shiozaki, K. (2017). Ragulator and GATOR1 complexes promote fission yeast growth by attenuating TOR complex 1 through rag GTPases. *Elife* **6**, e30880.

Chica, N., Rozalén, A. E., Pérez-Hidalgo, L., Rubio, A., Novak, B. and Moreno, S. (2016). Nutritional control of cell size by the greatwall-endosulfine-PP2A·B55 pathway. *Curr. Biol.* **26**, 319–330.

Chiron, S., Gaisne, M., Guillou, E., Belenguer, P., Clark-Walker, G. D. and Bonnefoy, N. (2007). Studying mitochondria in an attractive model: *Schizosaccharomyces pombe*. *Methods Mol. Biol.* **372**, 91–105.

Chung, J., Kuo, C. J., Crabtree, G. R. and Blenis, J. (1992). Rapamycin-FKBP specifically blocks growth-dependent activation of and signaling by the 70 kd S6 protein kinases. *Cell* **69**, 1227–1236.

Cohen, A., Kupiec, M. and Weisman, R. (2014). Glucose activates TORC2-Gad8 protein via positive regulation of the cAMP/cAMP-dependent Protein Kinase A (PKA) pathway and negative regulation of the Pmk1 protein-mitogen-activated protein kinase pathway. *J. Biol. Chem.* **289**, 21727–21737.

Colom, A., Derivery, E., Soleimanpour, S., Tomba, C., Molin, M. D., Sakai, N., González-Gaitán, M., Matile, S. and Roux, A. (2018). A fluorescent membrane tension probe. *Nat. Chem.* **10**, 1118-1125.

Conciatori, F., Ciuffreda, L., Bazzichetto, C., Falcone, I., Pilotto, S., Bria, E., Cognetti, F. and Milella, M. (2018). MTOR cross-talk in cancer and potential for combination therapy. *Cancers (Basel).* **10**, 23.

Consortium (1993). Identification and characterization of the tuberous sclerosis gene on chromosome 16. *Cell* **75**, 1305-1315.

Craighead, M. W., Bowden, S., Watson, R. and Armstrong, J. (1993). Function of the *ypt2* gene in the exocytic pathway of *Schizosaccharomyces pombe*. *Mol. Biol. Cell* **4**, 1069–1076.

Dai, J., Ting-Beall, H. P., Hochmuth, R. M., Sheetz, M. P. and Titus, M. A. (1999). Myosin I contributes to the generation of resting cortical tension. *Biophys. J.* **77**, 1168–1176.

Davì, V., Tanimoto, H., Ershov, D., Haupt, A., De Belly, H., Le Borgne, R., Couturier, E., Boudaoud, A. and Minc, N. (2018). Mechanosensation dynamically coordinates polar growth and cell wall assembly to promote cell survival. *Dev. Cell* **45**, 170-182.e7.

De Montigny, J., Straub, M. L., Wagner, R., Bach, M. L. and Chevallier, M. R. (1998). The uracil permease of *Schizosaccharomyces pombe*: A representative of a family of 10 transmembrane helix transporter proteins of yeasts. *Yeast* **14**, 1051–1059.

Dever, T. E., Feng, L., Wek, R. C., Cigan, A. M., Donahue, T. F. and Hinnebusch, A. G. (1992). Phosphorylation of initiation factor 2α by protein kinase GCN2 mediates gene-specific translational control of GCN4 in yeast. *Cell* **68**, 585–596.

Dokudovskaya, S. and Rout, M. P. (2011). A novel coatomer-related SEA complex dynamically associates with the vacuole in yeast and is implicated in the response to nitrogen starvation. *Autophagy* **7**, 1392–1393.

Du, W., Hálová, L., Kirkham, S., Atkin, J., Petersen, J., Há, L., Kirkham, S., Atkin, J. and Petersen, J. (2012). TORC2 and the AGC kinase Gad8 regulate phosphorylation of the ribosomal protein S6 in fission yeast. *Biol. Open* **1**, 884–888.

Du, W., Forte, G. M., Smith, D. and Petersen, J. (2016). Phosphorylation of the amino-terminus of the AGC kinase Gad8 prevents its interaction with TORC2. *Open Biol.* **6**, 150189.

Dubuke, M. L., Maniatis, S., Shaffer, S. A. and Munson, M. (2015). The exocyst subunit Sec6 interacts with assembled exocytic SNARE complexes. *J. Biol. Chem.* **290**, 28245–28256.

Duleh, S. N. and Welch, M. D. (2010). WASH and the Arp2/3 complex regulate endosome shape and trafficking. *Cytoskeleton* **67**, 193–206.

Duncan, C. D. S., Rodríguez-López, M., Ruis, P., Bähler, J. and Mata, J. (2018). General amino acid control in fission yeast is regulated by a nonconserved transcription factor, with functions analogous to Gcn4/Atf4. *Proc. Natl. Acad. Sci. U. S. A.* **115**, E1829E1838.

Düvel, K., Yecies, J. L., Menon, S., Raman, P., Lipovsky, A. I., Souza, A. L., Triantafellow, E., Ma, Q., Gorski, R., Cleaver, S., et al. (2010). Activation of a

metabolic gene regulatory network downstream of mTOR complex 1. *Mol. Cell* **39**, 171–183.

Eaton, C.J., Jourdain, I., Foster, S.J., Hyams, J.S. and Scott, B. (2008). Functional analysis of a fungal endophyte stress-activated MAP kinase. *Curr. Genet*. **53**, 163–174.

Ebner, M., Sinkovics, B., Szczygieł, M., Ribeiro, D. W. and Yudushkin, I. (2017). Localization of mTORC2 activity inside cells. *J. Cell Biol.* **216**, 343–353.

Eby, J. J., Holly, S. P., Van Drogen, F., Grishin, A. V., Peter, M., Drubin, D. G. and Blumer, K. J. (1998). Actin cytoskeleton organization regulated by the PAK family of protein kinases. *Curr. Biol.* **8**, 967-970.

Elias, M., Drdova, E., Ziak, D., Bavlnka, B., Hala, M., Cvrckova, F., Soukupova, H. and Zarsky, V. (2003). The exocyst complex in plants. *Cell Biol. Int.* **27**, 199–201.

Ene, I. V., Walker, L. A., Schiavone, M., Lee, K. K., Martin-Yken, H., Dague, E., Gow, N. A. R., Munro, C. A. and Brown, A. J. P. (2015). Cell wall remodeling enzymes modulate fungal cell wall elasticity and osmotic stress resistance. *MBio* **6**, e00986-15.

Ewart, M. A., Clarke, M., Kane, S., Chamberlain, L. H. and Gould, G. W. (2005). Evidence for a role of the exocyst in insulin-stimulated Glut4 trafficking in 3T3-L1 adipocytes. *J. Biol. Chem.* **280**, 3812–3816.

Fadri, M., Daquinag, A., Wang, S., Xue, T. and Kunz, J. (2005). The pleckstrin homology domain proteins Slm1 and Slm2 are required for actin cytoskeleton organization in yeast and bind phosphatidylinositol-4,5- bisphosphate and TORC2. *Mol. Biol. Cell* **16**, 1883–1900.

Fantes, P. and Nurse, P. (1977). Control of cell size at division in fission yeast by a growth-modulated size control over nuclear division. *Exp. Cell Res.* **107**, 377–386.

Feierbach, B. and Chang, F. (2001). Roles of the fission yeast formin For3p in cell polarity, actin cable formation and symmetric cell division. *Curr. Biol.* **11**, 1656–1665.

Fielding, A. B., Schonteich, E., Matheson, J., Wilson, G., Yu, X., Hickson, G. R. X., Srivastava, S., Baldwin, S. A., Prekeris, R. and Gould, G. W. (2005). Rab11-FIP3 and FIP4 interact with Arf6 and the exocyst to control membrane traffic in cytokinesis. *EMBO J.* **24**, 3389–3399.

Fingar, D. C., Salama, S., Tsou, C., Harlow, E. and Blenis, J. (2002). Mammalian cell size is controlled by mTOR and its downstream targets S6K1 and 4EBP1/eIF4E. *Genes Dev.* **16**, 1472–1487.

Finger, F. P., Hughes, T. E. and Novick, P. (1998). Sec3p is a spatial landmark for polarized secretion in budding yeast. *Cell* **92**, 559–571.

Finger, F. P. and Novick, P. (1997). Sec3p is involved in secretion and morphogenesis in *Saccharomyces cerevisiae*. *Mol. Biol. Cell* **8**, 647–662.

Fogelgren, B., Zuo, X., Buonato, J. M., Vasilyev, A., Baek, J. I., Choi, S. Y., Chacon-Heszele, M. F., Palmyre, A., Polgar, N., Drummond, I., et al. (2014). Exocyst Sec10 protects renal tubule cells from injury by EGFR/MAPK activation and effects on endocytosis. *Am. J. Physiol. - Ren. Physiol.* **307**, F1334–F1341.

Forsburg, S. L. and Rhind, N. (2006). Basic methods for fission yeast. *Yeast* **23**, 173–183.

Fujita, A. (2008). ADP-ribosylation factor arf6p may function as a molecular switch of new end take off in fission yeast. *Biochem. Biophys. Res. Commun.* **366**, 193–198.

Fujita, A. and Misumi, Y. (2009). Fission yeast Syt22 protein, a putative Arf guanine nucleotide exchange factor, is necessary for new end take off. *FEMS Microbiol. Lett.* **294**, 191-197.

Gachet, Y. and Hyams, J. S. (2005). Endocytosis in fission yeast is spatially associated with the actin cytoskeleton during polarised cell growth and cytokinesis. *J. Cell Sci.* **118**, 4231–4242.

Ganley, I. G., Lam, D. H., Wang, J., Ding, X., Chen, S. and Jiang, X. (2009). ULK1·ATG13·FIP200 complex mediates mTOR signaling and is essential for autophagy. *J. Biol. Chem.* **284**, 12297–12305.

Gaubitz, C., Oliveira, T. M., Prouteau, M., Leitner, A., Karuppasamy, M., Konstantinidou, G., Rispal, D., Eltschinger, S., Robinson, G. C., Thore, S., et al. (2015). Molecular basis of the rapamycin insensitivity of target of rapamycin complex 2. *Mol. Cell* **58**, 977–988.

Gelmetti, V., De Rosa, P., Torosantucci, L., Marini, E. S., Romagnoli, A., Di Rienzo, M., Arena, G., Vignone, D., Fimia, G. M. and Valente, E. M. (2017). PINK1 and BECN1 relocalize at mitochondria-associated membranes during mitophagy and promote ER-mitochondria tethering and autophagosome formation. *Autophagy* **13**, 654–669.

Georis, I., Feller, A., Tate, J. J., Cooper, T. G. and Dubois, E. (2009). Nitrogen catabolite repression-sensitive transcription as a readout of Tor pathway regulation: The genetic background, reporter gene and GATA factor assayed determine the outcomes. *Genetics* **181**, 861–874.

Gerges, N. Z., Backos, D. S., Rupasinghe, C. N., Spaller, M. R. and Esteban, J. A. (2006). Dual role of the exocyst in AMPA receptor targeting and insertion into the postsynaptic membrane. *EMBO J.* **25**, 1623–1634.

González, A., Shimobayashi, M., Eisenberg, T., Merle, D. A., Pendl, T., Hall, M. N. and Moustafa, T. (2015). TORC1 promotes phosphorylation of ribosomal protein S6 via the AGC Kinase Ypk3 in *Saccharomyces cerevisiae*. *PLoS One* **10**, e0120250.

Goldstein, J. L. and Brown, M. S. (1990). Regulation of the mevalonate pathway. *Nature* **343**, 425–430.

Goode, B. L., Eskin, J. A. and Wendland, B. (2014). Actin and endocytosis in budding yeast. *Genetics* **199**, 315–358.

Govindan, B., Bowser, R. and Novick, P. (1995). The role of Myo2, a yeast class V myosin, in vesicular transport. *J. Cell Biol.* **128**, 1055–1068.

Gromley, A., Yeaman, C., Rosa, J., Redick, S., Chen, C. T., Mirabelle, S., Guha, M., Sillibourne, J. and Doxsey, S. J. (2005). Centriolin anchoring of exocyst and SNARE complexes at the midbody is required for secretory-vesicle-mediated abscission. *Cell* **123**, 75–87.

Grote, E., Carr, C. M. and Novick, P. J. (2000). Ordering the final events in yeast exocytosis. *J. Cell Biol.* **151**, 439–451.

Guichard, A., McGillivray, S. M., Cruz-Moreno, B., Van Sorge, N. M., Nizet, V. and Bier, E. (2010). Anthrax toxins cooperatively inhibit endocytic recycling by the Rab11/Sec15 exocyst. *Nature* **467**, 854–858.

Guichard, A., Cruz-Moreno, B. C., Aguilar, B., Van Sorge, N. M., Kuang, J., Kurkciyan, A. A., Wang, Z., Hang, S., Pineton De Chambrun, G. P., McCole, D. F., et al. (2013). Cholera toxin disrupts barrier function by inhibiting exocyst-mediated trafficking of host proteins to intestinal cell junctions. *Cell Host Microbe* **14**, 294–305.

Guo, W., Grant, A. and Novick, P. (1999). Exo84p is an exocyst protein essential for secretion. *J. Biol. Chem.* **274**, 23558–23564.

Guo, W., Tamanoi, F. and Novick, P. (2001). Spatial regulation of the exocyst complex by Rho1 GTPase. *Nat. Cell Biol.* **3**, 353–360.

Hachet, O. and Simanis, V. (2008). Mid1p/anillin and the septation initiation network orchestrate contractile ring assembly for cytokinesis. *Genes Dev.* **22**, 3205–3216.

Hála, M., Cole, R., Synek, L., Drdová, E., Pečenková, T., Nordheim, A., Lamkemeyer, T., Madlung, J., Hochholdinger, F., Fowler, J. E., et al. (2008). An exocyst complex functions in plant cell growth in *Arabidopsis* and tobacco. *Plant Cell* **20**, 1330–1345.

Hall, Z. W. and Sanes, J. R. (1993). Synaptic structure and development: The neuromuscular junction. *Cell* **72**, 99–121.

Hara, K., Yonezawa, K., Weng, Q. P., Kozlowski, M. T., Belham, C. and Avruch, J. (1998). Amino acid sufficiency and mTOR regulate p70 S6 kinase and eIF-4E BP1 through a common effector mechanism. *J. Biol. Chem.* **273**, 14484–14494.

Hara, K., Maruki, Y., Long, X., Yoshino, K. ichi, Oshiro, N., Hidayat, S., Tokunaga, C., Avruch, J. and Yonezawa, K. (2002). Raptor, a binding partner of target of rapamycin (TOR), mediates TOR action. *Cell* **110**, 177–189.

Hartmuth, S. and Petersen, J. (2009). Fission yeast Tor1 functions as part of TORC1 to control mitotic entry through the stress MAPK pathway following nutrient stress. *J. Cell Sci.* **122**, 1737–1746.

Hatanaka, M. and Shimoda, C. (2001). The cyclic AMP/PKA signal pathway is required for initiation of spore germination in *Schizosaccharomyces pombe*. *Yeast* **18**, 207–217.

Hatano, T., Morigasaki, S., Tatebe, H., Ikeda, K. and Shiozaki, K. (2015). Fission yeast Ryh1 gtpase activates Tor complex 2 in response to glucose. *Cell Cycle* **14**, 848–856.

Hayashi, T., Hatanaka, M., Nagao, K., Nakaseko, Y., Kanoh, J., Kokubu, A., Ebe, M. and Yanagida, M. (2007). Rapamycin sensitivity of the *Schizosaccharomyces pombe tor2* mutant and organization of two highly phosphorylated TOR complexes by specific and common subunits. *Genes to Cells* **12**, 1357–1370.

Hazuka, C. D., Foletti, D. L., Hsu, S. C., Kee, Y., Hopf, F. W. and Scheller, R. H. (1999). The Sec6/8 complex is located at neurite outgrowth and axonal synapse-assembly domains. *J. Neurosci.* **19**, 1324–1334.

He, B., Xi, F., Zhang, X., Zhang, J. and Guo, W. (2007). Exo70 interacts with phospholipids and mediates the targeting of the exocyst to the plasma membrane. *EMBO J.* **26**, 4053–4065.

Heider, M. R., Gu, M., Duffy, C. M., Mirza, A. M., Marcotte, L. L., Walls, A. C., Farrall, N., Hakhverdyan, Z., Field, M. C., Rout, M. P., et al. (2016). Subunit connectivity, assembly determinants and architecture of the yeast exocyst complex. *Nat. Struct. Mol. Biol.* **23**, 59–66.

Heiland, S., Radovanovic, N., Höfer, M., Winderickx, J. and Lichtenberg, H. (2000). Multiple hexose transporters of *Schizosaccharomyces pombe*. *J. Bacteriol.* **182**, 2153–2162.

Heitman, J., Movva, N. R. and Hall, M. N. (1991). Targets for cell cycle arrest by the immunosuppressant rapamycin in yeast. *Science* **253**, 905–909.

Helms, J. B. and Zurzolo, C. (2004). Lipids as targeting signals: Lipid rafts and intracellular trafficking. *Traffic* **5**, 247–254.

Hill, E., Broadbent, I. D., Chothia, C. and Pettitt, J. (2001). Cadherin superfamily proteins in *Caenorhabditis elegans* and *Drosophila melanogaster*. *J. Mol. Biol.* **305**, 1011–1024.

Hinnebusch, A. G. (2005). Translational regulation of *gcn4* and the general amino acid control of yeast . *Annu. Rev. Microbiol.* **59**, 407–450.

Hirama, T., Lu, S. M., Kay, J. G., Maekawa, M., Kozlov, M. M., Grinstein, S. and Fairn, G. D. (2017). Membrane curvature induced by proximity of anionic phospholipids can initiate endocytosis. *Nat. Commun.* **8**, 1393.

Hoppins, S., Collins, S. R., Cassidy-Stone, A., Hummel, E., DeVay, R. M., Lackner, L. L., Westermann, B., Schuldiner, M., Weissman, J. S. and Nunnari, J. (2011). A mitochondrial-focused genetic interaction map reveals a scaffold-like complex required for inner membrane organization in mitochondria. *J. Cell Biol.* **195**, 323–340.

Horák, J. (1986). Amino acid transport in eucaryotic microorganisms. *BBA - Rev. Biomembr.* **864**, 223–256.

Horák, J. and Ŕíhová, L. (1982). L-Proline transport in *Saccharomyces cerevisiae*. *BBA - Biomembr.* **691**, 144–150.

Hosokawa, N., Hara, T., Kaizuka, T., Kishi, C., Takamura, A., Miura, Y., Iemura, S.

I., Natsume, T., Takehana, K., Yamada, N., et al. (2009). Nutrient-dependent mTORCl association with the ULK1-Atg13-FIP200 complex required for autophagy. *Mol. Biol. Cell* **20**, 1981–1991.

Hsu, S. C., Ting, A. E., Hazuka, C. D., Davanger, S., Kenny, J. W., Kee, Y. and Scheller, R. H. (1996). The mammalian brain rsec6/8 complex. *Neuron* **17**, 1209–1219.

Hyman, T., Shmuel, M. and Altschuler, Y. (2006). Actin is required for endocytosis at the apical surface of Madin-Darby canine kidney cells where ARF6 and clathrin regulate the actin cytoskeleton. *Mol. Biol. Cell* **17**, 427–437.

Ichihara, A. and Koyama, E. (1966). Transaminase of branched chain amino acids: I. branched chain amino acids-α-ketoglutarate transaminase. *J. Biochem.* **59**, 160–169.

Ikai, N., Nakazawa, N., Hayashi, T. and Yanagida, M. (2011). The reverse, but coordinated, roles of Tor2 (TORC1) and Tor1 (TORC2) kinases for growth, cell cycle and separase-mediated mitosis in *Schizosaccharomyces pombe*. *Open Biol.* **1**, 110007.

Ikeda, K., Morigasaki, S., Tatebe, H., Tamanoi, F. and Shiozaki, K. (2008). Fission yeast TOR complex 2 activates the AGC-family Gad8 kinase essential for stress resistance and cell cycle control. *Cell Cycle* **7**, 358–364.

Inamdar, S. M., Hsu, S.-C. and Yeaman, C. (2016). Probing functional changes in exocyst configuration with monoclonal antibodies. *Front. Cell Dev. Biol.* **4**, 51.

Inoki, K., Li, Y., Xu, T. and Guan, K. L. (2003). Rheb GTPase is a direct target of TSC2 GAP activity and regulates mTOR signaling. *Genes Dev.* **17**, 1829–1834.

Inoue, M., Chang, L., Hwang, J., Chiang, S. H. and Saltiel, A. R. (2003). The exocyst complex is required for targeting of Glut4 to the plasma membrane by insulin. *Nature* **422**, 629–633.

Inoue, M., Chiang, S. H., Chang, L., Chen, X. W. and Saltiel, A. R. (2006). Compartmentalization of the exocyst complex in lipid rafts controls Glut4 vesicle tethering. *Mol. Biol. Cell* **17**, 2303–2311.

Iwaki, T., Iefuji, H., Hiraga, Y., Hosomi, A., Morita, T., Giga-Hama, Y. and Takegawa, K. (2008). Multiple functions of ergosterol in the fission yeast *Schizosaccharomyces pombe*. *Microbiology* **154**, 830–841.

Jafar-Nejad, H., Andrews, H. K., Acar, M., Bayat, V., Wirtz-Peitz, F., Mehta, S. Q., Knoblich, J. A. and Bellen, H. J. (2005). Sec15, a component of the exocyst, promotes notch signaling during the asymmetric division of *Drosophila* sensory organ precursors. *Dev. Cell* **9**, 351–363.

Jin, Y., Sultana, A., Gandhi, P., Franklin, E., Hamamoto, S., Khan, A. R., Munson, M., Schekman, R. and Weisman, L. S. (2011). Myosin V transports secretory vesicles via a Rab GTPase cascade and interaction with the exocyst complex. *Dev. Cell* **21**, 1156–1170.

Jiu, Y., Jin, C., Liu, Y., Holmberg, C. I. and Jäntti, J. (2012). Exocyst subunits Exo70 and Exo84 cooperate with small GTPases to regulate behavior and endocytic trafficking in *C. elegans*. *PLoS One* **7**, e32077.

Jourdain, I., Dooley, H. C. and Toda, T. (2012). Fission yeast Sec3 bridges the exocyst complex to the actin cytoskeleton. *Traffic* **13**, 1481–1495.

Kamada, Y., Yoshino, K. -i., Kondo, C., Kawamata, T., Oshiro, N., Yonezawa, K. and Ohsumi, Y. (2010). Tor directly controls the Atg1 kinase complex to regulate autophagy. *Mol. Cell. Biol.* **30**, 1049–1058.

Kampmeyer, C., Karakostova, A., Schenstrøm, S. M., Abildgaard, A. B., Lauridsen, A. M., Jourdain, I. and Hartmann-Petersen, R. (2017). The exocyst subunit Sec3 is regulated by a protein quality control pathway. *J. Biol. Chem.* **292**, 15240–15253.

Kandt, R. S., Haines, J. L., Smith, M., Northrup, H., Gardner, R. J. M., Short, M. P., Dumars, K., Roach, E. S., Steingold, S., Wall, S., et al. (1992). Linkage of an important gene locus for tuberous sclerosis to a chromosome 16 marker for polycystic kidney disease. *Nat. Genet.* **2**, 37–41.

Karagiannis, J., Saleki, R. and Young, P. G. (1999). The Pub1 E3 ubiquitin ligase negatively regulates leucine uptake in response to NH4+ in fission yeast. *Curr. Genet.* **35**, 593–601.

Kashiwazaki, J., Iwaki, T., Takegawa, K., Shimoda, C. and Nakamura, T. (2009). Two fission yeast Rab7 homologs, Ypt7 and Ypt71, play antagonistic roles in the regulation of vacuolar morphology. *Traffic* **10**, 912–924.

Kawai, M., Nakashima, A., Ueno, M., Ushimaru, T., Aiba, K., Doi, H. and Uritani, M. (2001). Fission yeast Tor1 functions in response to various stresses including nitrogen starvation, high osmolarity, and high temperature. *Curr. Genet.* **39**, 166–174.

Kilberg, M. S., Shan, J. and Su, N. (2009). ATF4-dependent transcription mediates signaling of amino acid limitation. *Trends Endocrinol. Metab.* **20**, 436–443.

Kilberg, M. S., Balasubramanian, M., Fu, L. and Shan, J. (2012). The transcription factor network associated with the amino acid response in mammalian cells. *Adv. Nutr.* **3**, 295–306.

Kim, D. H., Sarbassov, D. D., Ali, S. M., King, J. E., Latek, R. R., Erdjument-Bromage, H., Tempst, P. and Sabatini, D. M. (2002). mTOR interacts with raptor to form a nutrient-sensitive complex that signals to the cell growth machinery. *Cell* **110**, 163-175.

Kim, D. U., Hayles, J., Kim, D., Wood, V., Park, H. O., Won, M., Yoo, H. S., Duhig, T., Nam, M., Palmer, G., et al. (2010). Analysis of a genome-wide set of gene deletions in the fission yeast *Schizosaccharomyces pombe*. *Nat. Biotechnol.* **28**, 617–623.

Kim, J. H., Roy, A., Jouandot, D. and Cho, K. H. (2013). The glucose signaling network in yeast. *Biochim. Biophys. Acta - Gen. Subj.* **1830**, 5204–5210.

Kim, J. H., Singh, A., Poeta, M. Del, Brown, D. A. and London, E. (2017). The effect of sterol structure upon clathrin-mediated and clathrin-independent endocytosis. *J. Cell Sci.* **130**, 2682–2695.

Kimball, S. R., Gordon, B. S., Moyer, J. E., Dennis, M. D. and Jefferson, L. S. (2016). Leucine induced dephosphorylation of Sestrin2 promotes mTORC1 activation. *Cell. Signal.* **28**, 896–906.

Kira, S., Kumano, Y., Ukai, H., Takeda, E., Matsuura, A. and Noda, T. (2016). Dynamic relocation of the TORC1-Gtr1/2-Ego1/2/3 complex is regulated by Gtr1 and Gtr2. *Mol. Biol. Cell* **27**, 382–396.

Kitayama, C., Sugimoto, A. and Yamamoto, M. (1997). Type II myosin heavy chain encoded by the *myo2* gene composes the contractile ring during cytokinesis in *Schizosaccharomyces pombe*. *J. Cell Biol.* **137**, 1309–1319.

Koumandou, V. L., Dacks, J. B., Coulson, R. M. R. and Field, M. C. (2007). Control systems for membrane fusion in the ancestral eukaryote; Evolution of tethering complexes and SM proteins. *BMC Evol. Biol.* **7**, 29.

Kovar, D. R., Sirotkin, V. and Lord, M. (2011). Three's company: The fission yeast actin cytoskeleton. *Trends Cell Biol.* **21**, 177–187.

Kozjak, V., Wiedemann, N., Milenkovic, D., Lohaus, C., Meyer, H. E., Guiard, B.,

Meisinger, C. and Pfanner, N. (2003). An essential role of Sam50 in the protein sorting and assembly machinery of the mitochondrial outer membrane. *J. Biol. Chem.* **278**, 48520–48523.

Kulich, I., Pečenková, T., Sekereš, J., Smetana, O., Fendrych, M., Foissner, I., Höftberger, M. and Žárský, V. (2013). Arabidopsis exocyst subcomplex containing subunit EXO70B1 is involved in autophagy-related transport to the vacuole. *Traffic* **14**, 1155–1165.

Kunz, J., Henriquez, R., Schneider, U., Deuter-Reinhard, M., Movva, N. R. and Hall, M. N. (1993). Target of rapamycin in yeast, TOR2, is an essential phosphatidylinositol kinase homolog required for G1 progression. *Cell* **73**, 585–596.

Lalli, G. (2009). RalA and the exocyst complex influence neuronal polarity through PAR-3 and aPKC. *J. Cell Sci.* **122**, 1499–1506.

Lappalainen, P. and Drubin, D. G. (1997). Cofilin promotes rapid actin filament turnover in vivo. *Nature* **388**, 78–82.

Lee, W. L., Bezanilla, M. and Pollard, T. D. (2000). Fission yeast myosin-I, Myo1p, stimulates actin assembly by Arp2/3 complex and shares functions with WASP. *J. Cell Biol.* **151**, 789–799.

Lesage, G., Shapiro, J., Specht, C. A., Sdicu, A. M., Ménard, P., Hussein, S., Tong, A. H. Y., Boone, C. and Bussey, H. (2005). An interactional network of genes involved in chitin synthesis in *Saccharomyces cerevisiae*. *BMC Genet.* **6**, 8.

Li, J., Kim, S. G. and Blenis, J. (2014). Rapamycin: One drug, many effects. *Cell Metab.* **19**, 373–379.

Li, Z. and Sheng, M. (2003). Some assembly required: The development of neuronal synapses. *Nat. Rev. Mol. Cell Biol.* **4**, 833–841.

Lipatova, Z., Tokarev, A. A., Jin, Y., Mulholland, J., Weisman, L. S. and Segev, N. (2008). Direct interaction between a myosin v motor and the Rab GTPases Ypt31/32 is required for polarized secretion. *Mol. Biol. Cell* **19**, 4177–4187.

Liu, X. and Klionsky, D. J. (2016). The Atg17-Atg31-Atg29 complex and Atg11 regulate autophagosome-vacuole fusion. *Autophagy* **12**, 894–895.

Liu, J., Yue, P., Artym, V. V., Mueller, S. C. and Guo, W. (2009). The role of the exocyst in matrix metalloproteinase secretion and actin dynamics during tumor cell invadopodia formation. *Mol. Biol. Cell* **20**, 3763–3771.

Liu, Q., Ma, Y., Zhou, X. and Furuyashiki, T. (2015). Constitutive Tor2 activity promotes retention of the amino acid transporter Agp3 at trans-golgi/endosomes in fission yeast. *PLoS One* **10**, e0139045.

Liu, D., Li, X., Shen, D. and Novick, P. (2018). Two subunits of the exocyst, Sec3p and Exo70p, can function exclusively on the plasma membrane. *Mol. Biol. Cell* **29**, 736–750.

Loewith, R., Jacinto, E., Wullschleger, S., Lorberg, A., Crespo, J. L., Bonenfant, D., Oppliger, W., Jenoe, P. and Hall, M. N. (2002). Two TOR complexes, only one of which is rapamycin sensitive, have distinct roles in cell growth control. *Mol. Cell* **10**, 457-468.

Long, X., Lin, Y., Ortiz-Vega, S., Yonezawa, K. and Avruch, J. (2005). Rheb binds and regulates the mTOR kinase. *Curr. Biol.* **15**, 702-713.

Lu, H., Liu, J., Liu, S., Zeng, J., Ding, D., Carstens, R. P., Cong, Y., Xu, X. and Guo, W. (2013). Exo70 isoform switching upon epithelial-mesenchymal transition mediates cancer cell invasion. *Dev. Cell* **27**, 560–573.

Lynch, C. J., Halle, B., Fujii, H., Vary, T. C., Wallin, R., Damuni, Z. and Hutson, S. M. (2003). Potential role of leucine metabolism in the leucine-signaling pathway involving mTOR. *Am. J. Physiol. - Endocrinol. Metab.* **285**, E854-E863.

Mach, K. E., Furge, K. A. and Albright, C. F. (2000). Loss of Rhb1, a Rheb-related GTPase in fission yeast, causes growth arrest with a terminal phenotype similar to that caused by nitrogen starvation. *Genetics* **155**, 611–22.

Madrid, M., Soto, T., Hou, K. K., Franco, A., Vicente, J., Pérez, P., Gacto, M. and Cansado, J. (2006). Stress-induced response, localization, and regulation of the Pmk1 cell integrity pathway in *Schizosaccharomyces pombe*. *J. Biol. Chem.* **281**, 2033–2043.

Madrid, M., Vázquez-Marín, B., Franco, A., Soto, T., Vicente-Soler, J., Gacto, M. and Cansado, J. (2016). Multiple crosstalk between TOR and the cell integrity MAPK signaling pathway in fission yeast. *Sci. Rep.* **6**, 37515.

Magnuson, B., Ekim, B. and Fingar, D. C. (2012). Regulation and function of ribosomal protein S6 kinase (S6K) within mTOR signalling networks. *Biochem. J.* **441**, 1–21.

Makushok, T., Alves, P., Huisman, S. M., Kijowski, A. R. and Brunner, D. (2016). Sterol-rich membrane domains define fission yeast cell polarity. *Cell* **165**, 1182–1196.

Malecki, M., Bitton, D. A., Rodríguez-López, M., Rallis, C., Calavia, N. G., Smith, G. C. and Bähler, J. (2016). Functional and regulatory profiling of energy metabolism in fission yeast. *Genome Biol.* **17**.

Mann, M. (2006). Functional and quantitative proteomics using SILAC. *Nat. Rev. Mol. Cell Biol.* **7**, 952-958.

Marshall, R. S. and Vierstra, R. D. (2018). Autophagy: The master of bulk and selective recycling. *Annu. Rev. Plant Biol.* **69**, 173-208.

Martín-Cuadrado, A. B., Dueñas, E., Sipiczki, M., Vázquez de Aldana, C. R. and del Rey, F. (2003). The endo-β-1,3-glucanase Eng1p is required for dissolution of the primary septum during cell separation in *Schizosaccharomyces pombe*. *J. Cell Sci.* **116**, 1689–1698.

Martín-Cuadrado, A. B., Morrell, J. L., Konomi, M., An, H., Petit, C., Osumi, M., Balasubramanian, M., Gould, K. L., Del Rey, F. and Vázquez De Aldana, C. R. (2005). Role of septins and the exocyst complex in the function of hydrolytic enzymes responsible for fission yeast cell separation. *Mol. Biol. Cell* **16**, 4867–4881.

Martín-García, R., Coll, P. M. and Pérez, P. (2014). F-BAR domain protein Rga7 collaborates with Cdc15 and Imp2 to ensure proper cytokinesis in fission yeast. *J. Cell Sci.* **127**, 4146-4158.

Martin, S. G., McDonald, W. H., Yates, J. R. and Chang, F. (2005). Tea4p links microtubule plus ends with the formin For3p in the establishment of cell polarity. *Dev. Cell* **8**, 479–491.

Martinez Marshall, M. N., Emmerstorfer-Augustin, A., Leskoske, K. L., Zhang, L. H., Li, B. and Thorner, J. (2019). Analysis of the roles of phosphatidylinositol-4,5-bisphosphate and individual subunits in assembly, localization, and function of *Saccharomyces cerevisiae* target of rapamycin complex 2. *Mol. Biol. Cell* **30**, 1555–1574.

Matsuo, T., Otsubo, Y., Urano, J., Tamanoi, F. and Yamamoto, M. (2007). Loss of the TOR Kinase Tor2 Mimics nitrogen starvation and activates the sexual development pathway in fission yeast. *Mol. Cell. Biol.* **27**, 3154–3164.

Matsuyama, A., Shirai, A. and Yoshida, M. (2008), A series of promoters for constitutive expression of heterologous genes in fission yeast. *Yeast* **25**, 371-376.

Mayer, C., Zhao, J., Yuan, X. and Grummt, I. (2004). mTOR-dependent activation of

the transcription factor TIF-IA links rRNA synthesis to nutrient availability. *Genes Dev.* **18**, 423–434.

McHugh, D. and Gil, J. (2018). Senescence and aging: Causes, consequences, and therapeutic avenues. *J. Cell Biol.* **217**, 65–77.

Mehta, S. Q., Hiesinger, P. R., Beronja, S., Zhai, R. G., Schulze, K. L., Verstreken, P., Cao, Y., Zhou, Y., Tepass, U., Crair, M. C., et al. (2005). Mutations in *Drosophila sec15* reveal a function in neuronal targeting for a subset of exocyst components. *Neuron* **46**, 219–232.

Miettinen, T. A. and Penttilä, I. M. (1968). Leucine and mevalonate as precursors of serum cholesterol in man. *Acta Med. Scand.* **184**, 159–164.

Miller, P. J. and Johnson, D. I. (1994). Cdc42p GTPase is involved in controlling polarized cell growth in *Schizosaccharomyces pombe*. *Mol. Cell. Biol.* **14**, 1075–1083.

Mitchison, J. M. and Nurse, P. (1985). Growth in cell length in the fission yeast *Schizosaccharomyces pombe*. *J. Cell Sci.* **75**, 357–376.

Mizuno, S., Takami, K., Daitoku, Y., Tanimoto, Y., Dinh, T. T. H., Mizuno-Iijima, S., Hasegawa, Y., Takahashi, S., Sugiyama, F. and Yagami, K. I. (2015). Peri-implantation lethality in mice carrying megabase-scale deletion on 5qc3.3 is caused by Exoc1 null mutation. *Sci. Rep.* **5**, 13632.

Moloughney, J. G., Kim, P. K., Vega-Cotto, N. M., Wu, C. C., Zhang, S., Adlam, M., Lynch, T., Chou, P. C., Rabinowitz, J. D., Werlen, G., et al. (2016). mTORC2 responds to glutamine catabolite levels to modulate the hexosamine biosynthesis enzyme GFAT1. *Mol. Cell* **63**, 811–826.

Monteiro, P., Rossé, C., Castro-Castro, A., Irondelle, M., Lagoutte, E., Paul-Gilloteaux, P., Desnos, C., Formstecher, E., Darchen, F., Perrais, D., et al. (2013). Endosomal WASH and exocyst complexes control exocytosis of MT1-MMP at invadopodia. *J. Cell Biol.* **203**, 1063–1079.

Moreno, S., Klar, A. and Nurse, P. (1991). Molecular genetic analysis of fission yeast *Schizosaccharomyces pombe*. *Methods Enzymol.* **194**, 795–823.

Morgera, F., Sallah, M. R., Dubuke, M. L., Gandhi, P., Brewer, D. N., Carr, C. M. and Munson, M. (2012). Regulation of exocytosis by the exocyst subunit Sec6 and the SM protein Sec1. *Mol. Biol. Cell* **23**, 337–346.

Morita, T. and Takegawa, K. (2004). A simple and efficient procedure for transformation of *Schizosaccharomyces pombe*. *Yeast* **21**, 613–617.

Moseley, J. B., Mayeux, A., Paoletti, A. and Nurse, P. (2009). A spatial gradient coordinates cell size and mitotic entry in fission yeast. *Nature* **459**, 857–860.

Moskalenko, S., Tong, C., Rosse, C., Mirey, G., Formstecher, E., Daviet, L., Camonis, J. and White, M. A. (2003). Ral GTPases regulate exocyst assembly through dual subunit interactions. *J. Biol. Chem.* **278**, 51743–51748.

Muir, A., Ramachandran, S., Roelants, F. M., Timmons, G. and Thorner, J. (2014). TORC2-dependent protein kinase Ypk1 phosphorylates ceramide synthase to stimulate synthesis of complex sphingolipids. *Elife* **3**, e03779.

Mukaiyama, H., Nakase, M., Nakamura, T., Kakinuma, Y. and Takegawa, K. (2010). Autophagy in the fission yeast *Schizosaccharomyces pombe*. *FEBS Lett.* **584**, 1327–1334.

Mukherjee, S. and Maxfield, F. R. (2000). Role of membrane organization and membrane domains in endocytic lipid trafficking. *Traffic* **1**, 203–211.

Munson, M. and Novick, P. (2006). The exocyst defrocked, a framework of rods revealed. *Nat. Struct. Mol. Biol.* **13**, 577–581.

Murthy, M., Garza, D., Scheller, R. H. and Schwarz, T. L. (2003). Mutations in the exocyst component Sec5 disrupt neuronal membrane traffic, but neurotransmitter release persists. *Neuron* **37**, 433–447.

Nakase, M., Nakase, Y., Chardwiriyapreecha, S., Kakinuma, Y., Matsumoto, T. and Takegawa, K. (2012). Intracellular trafficking and ubiquitination of the *Schizosaccharomyces pombe* amino acid permease Aat1p. *Microbiology* **158**, 659–673.

Nakashima, A. and Tamanoi, F. (2010). Conservation of the Tsc/Rheb/TORC1/S6K/S6 signaling in fission yeast. *Enzymes* **28**, 167–187.

Nakashima, A., Sato, T. and Tamanoi, F. (2010). Fission yeast TORC1 regulates phosphorylation of ribosomal S6 proteins in response to nutrients and its activity is inhibited by rapamycin. *J. Cell Sci.* **123**, 777–786.

Nakashima, A., Otsubo, Y., Yamashita, A., Sato, T., Yamamoto, M. and Tamanoi, F. (2012). Psk1, an AGC kinase family member in fission yeast, is directly phosphorylated and controlled by TORC1 and functions as S6 kinase. *J. Cell Sci.*

125, 5840–5849.

Nakashima, A., Kamada, S., Tamanoi, F. and Kikkawa, U. (2014). Fission yeast arrestin-related trafficking adaptor, Arn1/Any1, is ubiquitinated by Pub1 E3 ligase and regulates endocytosis of Cat1 amino acid transporter. *Biol. Open* **3**, 542–552.

Nambiar, R., McConnell, R. E. and Tyska, M. J. (2009). Control of cell membrane tension by myosin-I. *Proc. Natl. Acad. Sci. U. S. A.* **106**, 11972–11977.

Naqvi, S. N., Zahn, R., Mitchell, D. A., Stevenson, B. J. and Munn, A. L. (1998). The WASp homologue Las17p functions with the WIP homologue End5p/verprolin and is essential for endocytosis in yeast. *Curr. Biol.* **8**, 959–962.

Newsholme, P., Stenson, L., Sulvucci, M., Sumayao, R. and Krause, M. (2011). Amino Acid Metabolism. In *Comprehensive Biotechnology, Second Edition*, pp. 3–14.

Niles, B. J. and Powers, T. (2014). TOR complex 2-Ypk1 signaling regulates actin polarization via reactive oxygen species. *Mol. Biol. Cell* **25**, 3962–3972.

Noda, T. and Ohsumi, Y. (1998). Tor, a phosphatidylinositol kinase homologue, controls autophagy in yeast. *J. Biol. Chem.* **273**, 3963–3966.

Nollet, F., Kools, P. and Van Roy, F. (2000). Phylogenetic analysis of the cadherin superfamily allows identification of six major subfamilies besides several solitary members. *J. Mol. Biol.* **299**, 551–572.

Novick, P., Field, C. and Schekman, R. (1980). Identification of 23 complementation groups required for post-translational events in the yeast secretory pathway. *Cell* **21**, 205–215.

O'Donnell, M., Chance, R. K. and Bashaw, G. J. (2009). Axon growth and guidance: receptor regulation and signal transduction. *Annu. Rev. Neurosci.* **32**, 383–412.

Özcan, S. (2002). Two different signals regulate repression and induction of gene expression by glucose. *J. Biol. Chem.* **277**, 46993–46997.

Özcan, S., Dover, J., Rosenwald, A. G., Wölfl, S. and Johnston, M. (1996). Two glucose transporters in *Saccharomyces cerevisiae* are glucose sensors that generate a signal for induction of gene expression. *Proc. Natl. Acad. Sci. U. S. A.* **93**, 12428–12432.

Oztan, A., Silvis, M., Weisz, O. A., Bradbury, N. A., Hsu, S. C., Goldenring, J. R., Yeaman, C. and Apodaca, G. (2007). Exocyst requirement for endocytic traffic

directed toward the apical and basolateral poles of polarized MDCK cells. *Mol. Biol. Cell* **18**, 3978–3992.

Penkett, C. J., Birtle, Z. and Bähler, J. (2006). Simplified primer design for PCR-based gene targeting and microarray primer database: Two web tools for fission yeast. *Yeast* **23**, 921–928.

Pérez, P. and Ribas, J. C. (2004). Cell wall analysis. *Methods* **33**, 245–251.

Pérez, P., Portales, E. and Santos, B. (2015). Rho4 interaction with exocyst and septins regulates cell separation in fission yeast. *Microbiol. (United Kingdom)* **161**, 948–959.

Petersen, J. and Hagan, I. M. (2005). Polo kinase links the stress pathway to cell cycle control and tip growth in fission yeast. *Nature* **435**, 507–512.

Petersen, J. and Nurse, P. (2007). TOR signalling regulates mitotic commitment through the stress MAP kinase pathway and the Polo and Cdc2 kinases. *Nat. Cell Biol.* **9**, 1263–1272.

Porstmann, T., Santos, C. R., Griffiths, B., Cully, M., Wu, M., Leevers, S., Griffiths, J. R., Chung, Y. L. and Schulze, A. (2008). SREBP activity is regulated by mTORC1 and contributes to Akt-dependent cell growth. *Cell Metab.* **8**, 224–236.

Pu, K. M., Akamatsu, M. and Pollard, T. D. (2015). The septation initiation network controls the assembly of nodes containing Cdr2p for cytokinesis in fission yeast. *J. Cell Sci.* **128**, 441–446.

Raitt, D. C. (2000). Yeast Cdc42 GTPase and Ste20 PAK-like kinase regulate Sho1-dependent activation of the Hog1 MAPK pathway. *EMBO J.* **19**, 4623–4631.

Rallis, C., Codlin, S. and Bähler, J. (2013). TORC1 signaling inhibition by rapamycin and caffeine affect lifespan, global gene expression, and cell proliferation of fission yeast. *Aging Cell* **12**, 563–573.

Regenberg, B., Düring-Olsen, L., Kielland-Brandt, M. C. and Holmberg, S. (1999). Substrate specificity and gene expression of the amino acid permeases in *Saccharomyces cerevisiae*. *Curr. Genet.* **36**, 317–328.

Riggi, M., Niewola-Staszkowska, K., Chiaruttini, N., Colom, A., Kusmider, B., Mercier, V., Soleimanpour, S., Stahl, M., Matile, S., Roux, A., et al. (2018). Decrease in plasma membrane tension triggers PtdIns(4,5)P 2 phase separation to inactivate TORC2. *Nat. Cell Biol.* **20**, 1043–1051.

Roelants, F. M., Chauhan, N., Muir, A., Davis, J. C., Menon, A. K., Levine, T. P. and Thorner, J. (2018). TOR complex 2-regulated protein kinase Ypk1 controls sterol distribution by inhibiting StARkin domain-containing proteins located at plasma membrane-endoplasmic reticulum contact sites. *Mol. Biol. Cell* **29**, 2128–2136.

Rogers, K. K., Wilson, P. D., Snyder, R. W., Zhang, X., Guo, W., Burrow, C. R. and Lipschutz, J. H. (2004). The exocyst localizes to the primary cilium in MDCK cells. *Biochem. Biophys. Res. Commun.* **319**, 138–143.

Rolland, F., Winderickx, J. and Thevelein, J. M. (2002). Glucose-sensing and signalling mechanisms in yeast. In *FEMS Yeast Research* **2**, 183–201.

Rosenthal, G. A. (1977). The biological effects and mode of action of L-canavanine, a structural analogue of L-arginine. *Q. Rev. Biol.* **52**, 155–178.

Rosse, C., Hatzoglou, A., Parrini, M.-C., White, M. A., Chavrier, P. and Camonis, J. (2006). RalB mobilizes the exocyst to drive cell migration. *Mol. Cell. Biol.* **26**, 727–734.

Rossi, G., Salminen, A., Rice, L. M., Brünger, A. T. and Brennwald, P. (1997). Analysis of a yeast SNARE complex reveals remarkable similarity to the neuronal SNARE complex and a novel function for the C terminus of the SNAP- 25 homolog, Sec9. *J. Biol. Chem.* **272**, 16610–16617.

Russell, P. and Nurse, P. (1986). Cdc25+ functions as an inducer in the mitotic control of fission yeast. *Cell* **45**, 145–153.

Ryuko, S., Ma, Y., Ma, N., Sakaue, M. and Kuno, T. (2012). Genome-wide screen reveals novel mechanisms for regulating cobalt uptake and detoxification in fission yeast. *Mol. Genet. Genomics* **287**, 651–62.

Sabatini, D. M., Pierchala, B. A., Barrow, R. K., Schell, M. J. and Snyder, S. H. (1995). The rapamycin and FKBP12 target (RAFT) displays phosphatidylinositol 4-kinase activity. *J. Biol. Chem.* **270**, 20875–20878.

Sabers, C. J., Martin, M. M., Brunn, G. J., Williams, J. M., Dumont, F. J., Wiederrecht, G. and Abraham, R. T. (1995). Isolation of a protein target of the FKBP12-rapamycin complex in mammalian cells. *J. Biol. Chem.* **270**, 815–822.

Saito, T., Shibasaki, T. and Seino, S. (2008). Involvement of Exoc31, a protein structurally related to the exocyst subunit Sec6, in insulin secretion. *Biomed. Res.* **29**, 85–91.

Saliba, E., Evangelinos, M., Gournas, C., Corrillon, F., Georis, I. and André, B. (2018). The yeast H^+-ATPase Pma1 promotes Rag/Gtr-dependent TORC1 activation in response to H^+-coupled nutrient uptake. *Elife* **7**, e31981.

Sancak, Y., Peterson, T. R., Shaul, Y. D., Lindquist, R. A., Thoreen, C. C., Bar-Peled, L. and Sabatini, D. M. (2008). The rag GTPases bind raptor and mediate amino acid signaling to mTORC1. *Science* **320**, 1496–1501.

Sancak, Y., Bar-Peled, L., Zoncu, R., Markhard, A. L., Nada, S. and Sabatini, D. M. (2010). Ragulator-Rag complex targets mTORC1 to the lysosomal surface and is necessary for its activation by amino acids. *Cell* **141**, 290–303.

Sans, N., Prybylowski, K., Petralia, R. S., Chang, K., Wang, Y. X., Racca, C., Vicini, S. and Wenthold, R. J. (2003). NMDA receptor trafficking through an interaction between PDZ proteins and the exocyst complex. *Nat. Cell Biol.* **5**, 520–530.

Sarbassov, D. D., Ali, S. M., Sengupta, S., Sheen, J. H., Hsu, P. P., Bagley, A. F., Markhard, A. L. and Sabatini, D. M. (2006). Prolonged rapamycin treatment inhibits mTORC2 assembly and Akt/PKB. *Mol. Cell* **22**, 159–168.

Saxton, R. A. and Sabatini, D. M. (2017). mTOR signaling in growth, metabolism, and disease. *Cell* **168**, 960–976.

Schreve, J. L. and Garrett, J. M. (2004). Yeast Agp2p and Agp3p function as amino acid permeases in poor nutrient conditions. *Biochem. Biophys. Res. Commun.* **313**, 745–751.

Sekereš, J., Pejchar, P., Šantrůček, J., Vukasinovic, N., Žárský, V. and Potocký, M. (2017). Analysis of exocyst subunit EXO70 family reveals distinct membrane polar domains in tobacco pollen tubes. *Plant Physiol.* **173**, 1659–1675.

Settembre, C., De Cegli, R., Mansueto, G., Saha, P. K., Vetrini, F., Visvikis, O., Huynh, T., Carissimo, A., Palmer, D., Jürgen Klisch, T., et al. (2013). TFEB controls cellular lipid metabolism through a starvation-induced autoregulatory loop. *Nat. Cell Biol.* **15**, 647–658.

Shang, L., Chen, S., Du, F., Li, S., Zhao, L. and Wang, X. (2011). Nutrient starvation elicits an acute autophagic response mediated by Ulk1 dephosphorylation and its subsequent dissociation from AMPK. *Proc. Natl. Acad. Sci. U. S. A.* **108**, 4788–4793.

Shen, B., Hohmann, S., Jensen, R. G. and Bohnert, H. J. (1999). Roles of sugar alcohols in osmotic stress adaptation. Replacement of glycerol by mannitol and

sorbitol in yeast. *Plant Physiol.* **121**, 45–52.

Singh, S., Kumari, R., Chinchwadkar, S., Aher, A., Matheshwaran, S. and Manjithaya, R. (2019). Exocyst subcomplex functions in autophagosome biogenesis by regulating Atg9 trafficking. *J. Mol. Biol.* **431**, 2821–2834.

Sirotkin, V., Beltzner, C. C., Marchand, J. B. and Pollard, T. D. (2005). Interactions of WASp, myosin-I, and verprolin with Arp2/3 complex during actin patch assembly in fission yeast. *J. Cell Biol.* **170**, 637–648.

Smaczynska-de Rooij, I. I., Allwood, E. G., Aghamohammadzadeh, S., Hettema, E. H., Goldberg, M. W. and Ayscough, K. R. (2010). A role for the dynamin-like protein Vps1 during endocytosis in yeast. *J. Cell Sci.* **123**, 3496–3506.

Sommer, B., Oprins, A., Rabouille, C. and Munro, S. (2005). The exocyst component Sec5 is present on endocytic vesicles in the oocyte of *Drosophila melanogaster*. *J. Cell Biol.* **169**, 953–963.

Suetsugu, S., Miki, H. and Takenawa, T. (1999). Identification of two human WAVE/SCAR homologues as general actin regulatory molecules which associate with the Arp2/3 complex. *Biochem. Biophys. Res. Commun.* **260**, 296–302.

Sugihara, K., Asano, S., Tanaka, K., Iwamatsu, A., Okawa, K. and Ohta, Y. (2002). The exocyst complex binds the small GTPase RalA to mediate filopodia formation. *Nat. Cell Biol.* **4**, 73–78.

Sun, Y., Leong, N. T., Wong, T. and Drubin, D. G. (2015). A Pan1/End3/Sla1 complex links Arp2/3-mediated actin assembly to sites of clathrinmediated endocytosis. *Mol. Biol. Cell* **26**, 3841–3856.

Svitkina, T. M. and Borisy, G. G. (1999). Arp2/3 complex and actin depolymerizing factor/cofilin in dendritic organization and treadmilling of actin filament array in lamellipodia. *J. Cell Biol.* **145**, 1009–1026.

Synek, L., Schlager, N., Eliáš, M., Quentin, M., Hauser, M. T. and Žárský, V. (2006). AtEXO70A1, a member of a family of putative exocyst subunits specifically expanded in land plants, is important for polar growth and plant development. *Plant J.* **48**, 54–72.

Szklarczyk, D., Morris, J. H., Cook, H., Kuhn, M., Wyder, S., Simonovic, M., Santos, A., Doncheva, N. T., Roth, A., Bork, P., et al. (2017). The STRING database in 2017: Quality-controlled protein-protein association networks, made broadly accessible. *Nucleic Acids Res.* **45**, D362–D368.

Takahashi, H., Sun, X., Hamamoto, M., Yashiroda, Y. and Yoshida, M. (2012). The SAGA histone acetyltransferase complex regulates leucine uptake through the Agp3 permease in fission yeast. *J. Biol. Chem.* **287**, 38158–38167.

Takaine, M. and Mabuchi, I. (2007). Properties of actin from the fission yeast *Schizosaccharomyces pombe* and interaction with fission yeast profilin. *J. Biol. Chem.* **282**, 21683–21694.

Takayama, K., Muto, A. and Kikuchi, Y. (2018). Leucine/glutamine and v-ATPase/lysosomal acidification via mTORC1 activation are required for position-dependent regeneration. *Sci. Rep.* **8**, 8278.

Takeda, T. and Chang, F. (2005). Role of fission yeast myosin I in organization of sterol-rich membrane domains. *Curr. Biol.* **15**, 1331–1336.

Tanaka, T. and Iino, M. (2015). Sec8 regulates cytokeratin8 phosphorylation and cell migration by controlling the ERK and p38 MAPK signalling pathways. *Cell. Signal.* **27**, 1110–1119.

Tarasenko, D., Barbot, M., Jans, D. C., Kroppen, B., Sadowski, B., Heim, G., Möbius, W., Jakobs, S. and Meinecke, M. (2017). The MICOS component Mic60 displays a conserved membrane-bending activity that is necessary for normal cristae morphology. *J. Cell Biol.* **216**, 889–899.

Tatebe, H. and Shiozaki, K. (2010). Rab small GTPase emerges as a regulator of TOR complex 2. *Small GTPases* **1**, 180-182.

Tatebe, H., Morigasaki, S., Murayama, S., Zeng, C. T. and Shiozaki, K. (2010). Rab-Family GTPase regulates TOR complex 2 signaling in fission yeast. *Curr. Biol.* **20**, 1975–1982.

Tay, Y. D., Leda, M., Spanos, C., Rappsilber, J., Goryachev, A. B. and Sawin, K. E. (2019). Fission yeast NDR/LATS kinase Orb6 regulates exocytosis via phosphorylation of the exocyst complex. *Cell Rep.* **26**, 1654-1667.e7.

Taylor, C. A., Yan, J., Howell, A. S., Dong, X. and Shen, K. (2015). RAB-10 regulates dendritic branching by balancing dendritic transport. *PLoS Genet.* **11**, e1005695.

TerBush, D. R., Maurice, T., Roth, D. and Novick, P. (1996). The Exocyst is a multiprotein complex required for exocytosis in *Saccharomyces cerevisiae*. *EMBO J.* **15**, 6483–6494.

Thevelein, J. M. (1984). Cyclic-AMP content and trehalase activation in vegetative cells

and ascospores of yeast. *Arch. Microbiol.* **138**, 64–67.

Thwaites, D. T., McEwan, G. T. A. and Simmons, N. L. (1995). The role of the proton electrochemical gradient in the transepithelial absorption of amino acids by human intestinal Caco-2 cell monolayers. *J. Membr. Biol.* **145**, 245–256.

Tucker, K. A., Reggiori, F., Dunn, W. A. and Klionsky, D. J. (2003). Atg23 is essential for the cytoplasm to vacuole targeting pathway and efficient autophagy but not pexophagy. *J. Biol. Chem.* **278**, 48445–48452.

Valbuena, N., Rozalén, A. E. and Moreno, S. (2012). Fission yeast TORC1 prevents eIF2α phosphorylation in response to nitrogen and amino acids via Gcn2 kinase. *J. Cell Sci.* **125**, 5955–5959.

Van Slegtenhorst, M., De Hoogt, R., Hermans, C., Nellist, M., Janssen, B., Verhoef, S., Lindhout, D., Van Den Ouweland, A., Halley, D., Young, J., et al. (1997). Identification of the tuberous sclerosis gene TSC1 on chromosome 9q34. *Science* **277**, 805–808.

Vik-Mo, E. O., Oltedal, L., Hoivik, E. A., Kleivdal, H., Eidet, J. and Davanger, S. (2003). Sec6 is localized to the plasma membrane of mature synaptic terminals and is transported with secretogranin II-containing vesicles. *Neuroscience* **119**, 73–85.

Vilella-Bach, M., Nuzzi, P., Fang, Y. and Chen, J. (1999). The FKBP12-rapamycin-binding domain is required for FKBP12-rapamycin- associated protein kinase activity and G1 progression. *J. Biol. Chem.* **274**, 4266–4272.

Volkmann, N., Amann, K. J., Stoilova-McPhie, S., Egile, C., Winter, D. C., Hazelwood, L., Heuser, J. E., Li, R., Pollard, T. D. and Hanein, D. (2001). Structure of Arp2/3 complex in its activated state and in actin filament branch junctions. *Science* **293**, 2456–2459.

Wachtler, V., Rajagopalan, S. and Balasubramanian, M. K. (2003). Sterol-rich plasma membrane domains in the fission yeast *Schizosaccharomyces pombe*. *J. Cell Sci.* **116**, 867–874.

Wan, P., Zheng, S., Chen, L., Wang, D., Liao, T., Yan, X. and Wang, X. (2019). The exocyst component Sec3 controls egg chamber development through Notch during *Drosophila* oogenesis. *Front. Physiol.* **10**, 345.

Wang, H., Tang, X., Liu, J., Trautmann, S., Balasundaram, D., McCollum, D. and Balasubramanian, M. K. (2002). The multiprotein exocyst complex is essential for cell separation in *Schizosaccharomyces pombe*. *Mol. Biol. Cell* **13**, 515–529.

Wang, H., Tang, X. and Balasubramanian, M. K. (2003). Rho3p regulates cell separation by modulating exocyst function in *Schizosaccharomyces pombe*. *Genetics* **164**, 1323–1331.

Wang, R., Jiao, H., Zhao, J., Wang, X. and Lin, H. (2018). L-arginine enhances protein synthesis by phosphorylating mTOR (Thr 2446) in a nitric oxide-dependent manner in C2C12 cells. *Oxid. Med. Cell. Longev.* **2018**, 1-13.

Watson, R. T., Shigematsu, S., Chiang, S. H., Mora, S., Kanzaki, M., Macara, I. G., Saltiel, A. R. and Pessin, J. E. (2001). Lipid raft microdomain compartmentalization of TC10 is required for insulin signaling and Glut4 translocation. *J. Cell Biol.* **154**, 829–840.

Weisman, R., Finkelstein, S. and Choder, M. (2001). Rapamycin blocks sexual development in fission yeast through inhibition of the cellular function of an FKBP12 homolog. *J. Biol. Chem.* **276**, 24736–24742.

Weisman, R., Roitburg, I., Nahari, T. and Kupiec, M. (2005). Regulation of leucine uptake by *tor1+* in *Schizosaccharomyces pombe* is sensitive to rapamycin. *Genetics* **169**, 539–550.

Weisman, R., Cohen, A. and Gasser, S. M. (2014). TORC 2—a new player in genome stability . *EMBO Mol. Med.* **6**, 995–1002.

Welton, R. M. and Hoffman, C. S. (2000). Glucose monitoring in fission yeast via the Gpa2 Gα, the Git5 Gβ and the Git3 putative glucose receptor. *Genetics* **156**, 513–521.

Wideman, J. G. and Muñoz-Gómez, S. A. (2016). The evolution of ERMIONE in mitochondrial biogenesis and lipid homeostasis: An evolutionary view from comparative cell biology. *Biochim. Biophys. Acta - Mol. Cell Biol. Lipids* **1861**, 900–912.

Wiederkehr, A., Du, Y., Pypaert, M., Ferro-Novick, S. and Novick, P. (2003). Sec3p is needed for the spatial regulation of secretion and for the inheritance of the cortical endoplasmic reticulum. *Mol. Biol. Cell* **14**, 4770–4782.

Wiemken, A. and Dürr, M. (1974). Characterization of amino acid pools in the vacuolar compartment of *Saccharomyces cerevisiae*. *Arch. Microbiol.* **101**, 45–57.

Wilkinson, M. G., Samuels, M., Takeda, T., Mark Toone, W., Shieh, J. C., Toda, T., Millar, J. B. A. and Jones, N. (1996). The Atf1 transcription factor is a target for the Sty1 stress-activated MAP kinase pathway in fission yeast. *Genes Dev.* **10**,

2289–2301.

Wood, E. and Nurse, P. (2015). Sizing up to divide: Mitotic cell-size control in fission yeast. *Annu. Rev. Cell Dev. Biol.* **31**, 11–29.

Wood, V., Gwilliam, R., Rajandream, M. A., Lyne, M., Lyne, R., Stewart, A., Sgouros, J., Peat, N., Hayles, J., Baker, S., et al. (2002). The genome sequence of *Schizosaccharomyces pombe*. *Nature* **415**, 871–880.

Woods, A., Sherwin, T., Sasse, R., MacRae, T. H., Baines, A. J. and Gull, K. (1989). Definition of individual components within the cytoskeleton of *Trypanosoma brucei* by a library of monoclonal antibodies. *J. Cell Sci.* **93**, 491–500.

Wu, B. and Guo, W. (2015). The exocyst at a glance. *J. Cell Sci.* **128**, 2957–2964.

Wu, Z., Huang, X., Feng, Y., Handschin, C., Feng, Y., Gullicksen, P. S., Bare, O., Labow, M., Spiegelman, B. and Stevenson, S. C. (2006). Transducer of regulated CREB-binding proteins (TORCs) induce PGC-1α transcription and mitochondrial biogenesis in muscle cells. *Proc. Natl. Acad. Sci. U. S. A.* **103**, 14379–14384.

Wu, H., Turner, C., Gardner, J., Temple, B. and Brennwald, P. (2010). The Exo70 subunit of the exocyst is an effector for both Cdc42 and Rho3 function in polarized exocytosis. *Mol. Biol. Cell* **21**, 430–442.

Wut, C., Lee, S. F., Furmaniak-Kazmierczak, E., Côté, G. P., Thomas, D. Y. and Leberer, E. (1996). Activation of myosin-I by members of the Ste20p protein kinase family. *J. Biol. Chem.* **271**, 31787–31790.

Xiao, B., Goh, J. Y., Xiao, L., Xian, H., Lim, K. L. and Liou, Y. C. (2017). Reactive oxygen species trigger Parkin/PINK1 pathway–dependent mitophagy by inducing mitochondrial recruitment of Parkin. *J. Biol. Chem.* **292**, 16697–16708.

Xie, J., Marusich, M. F., Souda, P., Whitelegge, J. and Capaldi, R. A. (2007). The mitochondrial inner membrane protein Mitofilin exists as a complex with SAM50, metaxins 1 and 2, coiled-coil-helix coiled-coil-helix domain-containing protein 3 and 6 and DnaJC11. *FEBS Lett.* **581**, 3545–3549.

Xiong, X., Xu, Q., Huang, Y., Singh, R. D., Anderson, R., Leof, E., Hu, J. and Ling, K. (2012). An association between type Iγ PI4P 5-kinase and Exo70 directs E-cadherin clustering and epithelial polarization. *Mol. Biol. Cell* **23**, 87–98.

Xu, D., Shimkus, K. L., Lacko, H. A., Kutzler, L., Jefferson, L. S. and Kimball, S. R. (2019). Evidence for a role for Sestrin1 in mediating leucine-induced activation of

mTORC1 in skeletal muscle. *Am. J. Physiol. - Endocrinol. Metab.* **316**, E817–E828.

Yamashita, M., Kurokawa, K., Sato, Y., Yamagata, A., Mimura, H., Yoshikawa, A., Sato, K., Nakano, A. and Fukai, S. (2010). Structural basis for the Rho-and phosphoinositide-dependent localization of the exocyst subunit Sec3. *Nat. Struct. Mol. Biol.* **17**, 180–186.

Yang, H. wei, Hong, H. ling, Luo, W. wei, Dai, C. mei, Chen, X. yi, Wang, L. ping, Li, Q., Li, Z. qing, Liu, P. qing and Li, Z. ming (2018). mTORC2 facilitates endothelial cell senescence by suppressing Nrf2 expression via the Akt/GSK-3β/C/EBPα signaling pathway. *Acta Pharmacol. Sin.* **39**, 1837–1846.

Yeaman, C., Grindstaff, K. K., Wright, J. R. and James Nelson, W. (2001). Sec6/8 complexes on trans-Golgi network and plasma membrane regulate late stages of exocytosis in mammalian cells. *J. Cell Biol.* **155**, 593–604.

Yeaman, C., Grindstaff, K. K. and Nelson, W. J. (2004). Mechanism of recruiting Sec6/8 (exocyst) complex to the apical junctional complex during polarization of epithelial cells. *J. Cell Sci.* **117**, 559–570.

Young, P. G. and Fantes, P. A. (1987). *Schizosaccharomyces pombe* mutants affected in their division response to starvation. *J. Cell Sci.* **88**, 295–304.

Yu, B., Wang, Y., Liu, Y., Liu, Y., Li, X., Wu, D., Zong, Z., Zhang, J. and Yu, D. (2005). Protein kinase A regulates cell cycle progression of mouse fertilized eggs by means of MPF. *Dev. Dyn.* **232**, 98–105.

Yue, P., Zhang, Y., Mei, K., Wang, S., Lesigang, J., Zhu, Y., Dong, G. and Guo, W. (2017). Sec3 promotes the initial binary t-SNARE complex assembly and membrane fusion. *Nat. Commun.* **8**, 14236.

Zhang, X., Bi, E., Novick, P., Du, L., Kozminski, K. G., Lipschutz, J. H. and Guo, W. (2001). Cdc42 interacts with the exocyst and regulates polarized secretion. *J. Biol. Chem.* **276**, 46745–46750.

Zhang, X., Orlando, K., He, B., Xi, F., Zhang, J., Zajac, A. and Guo, W. (2008). Membrane association and functional regulation of Sec3 by phospholipids and Cdc42. *J. Cell Biol.* **180**, 145–158.

Zhang, D., Dubey, J., Koushika, S. P. and Rongo, C. (2016). RAB-6.1 and RAB-6.2 promote retrograde transport in *C. elegans*. *PLoS One* **11**, e0149314.

Zhou, K., Sumigray, K. D. and Lechler, T. (2015). The Arp2/3 complex has essential

roles in vesicle trafficking and transcytosis in the mammalian small intestine. *Mol. Biol. Cell* **26**, 1995–2004.

Zou, W., Yadav, S., DeVault, L., Nung Jan, Y. and Sherwood, D. R. (2015). RAB-10-dependent membrane transport is required for dendrite arborization. *PLoS Genet.* **11**, e1005484.

Zuo, X., Zhang, J., Zhang, Y., Hsu, S. C., Zhou, D. and Guo, W. (2006). Exo70 interacts with the Arp2/3 complex and regulates cell migration. *Nat. Cell Biol.* **8**, 1383–1388.

Zuo, X., Guo, W. and Lipschutz, J. H. (2009). The exocyst protein Sec10 is necessary for primary ciliogenesis and cystogenesis in vitro. *Mol. Biol. Cell* **20**, 2522–2529.

Chapter 8: **Appendices**

Appendix Table 1.1: Positive Interactors in the Sec3-GFP Trap (Replicate 1)

Uniprot Accession	Area	Score	Peptides	Score in GFP Control	Fold Increase Over Control
O60121	7.913E6	5.87	3	0.00	5.86524E+12
O14079	0.000E0	3.96	1	0.00	3.95687E+12
O94414	0.000E0	3.87	1	0.00	3.87079E+12
O94590	7.205E6	3.00	2	0.00	2.9953E+12
Q10324	4.944E6	2.91	1	0.00	2.90693E+12
Q9Y810	0.000E0	2.48	1	0.00	2.48084E+12
Q9C0Z9	0.000E0	2.38	1	0.00	2.38452E+12
O94707	4.427E6	2.31	1	0.00	2.31413E+12
Q9URZ4	1.855E7	2.09	1	0.00	2.09285E+12
Q9P7C1	0.000E0	2.08	1	0.00	2.07723E+12
O60111	3.954E6	2.07	1	0.00	2.06598E+12
O74370	0.000E0	2.05	2	0.00	2.04776E+12
Q1MTQ5	4.561E6	2.01	3	0.00	2.00792E+12
O74846	0.000E0	1.98	4	0.00	1.97628E+12
Q9Y7X6	1.795E7	1.88	1	0.00	1.87652E+12
O74433	2.669E7	16.06	2	0.00	1.6061E+13
O94312	0.000E0	15.90	3	0.00	1.59024E+13
O13755	0.000E0	10.71	1	0.00	1.0712E+13
Q9HDZ0	3.798E6	10.02	3	0.00	1.00214E+13
Q9C1X5	7.380E5	9.57	3	0.00	9.57159E+12
Q9UT25	0.000E0	8.49	3	0.00	8.49058E+12
O94424	0.000E0	7.78	2	0.00	7.77522E+12
O74983	1.797E7	7.51	3	0.00	7.50824E+12
O94435	0.000E0	7.35	2	0.00	7.34549E+12
Q09673	1.215E7	6.89	4	0.00	6.88902E+12
Q9USH5	0.000E0	6.49	1	0.00	6.48859E+12
Q09774	0.000E0	6.46	1	0.00	6.45911E+12
Q9UUF1	0.000E0	6.43	3	0.00	6.42542E+12
Q9UTP3	0.000E0	4.80	1	0.00	4.79639E+12
O94624	0.000E0	4.75	2	0.00	4.75312E+12
O74731	3.068E6	4.69	2	0.00	4.69429E+12
Q9UTF6	0.000E0	4.67	2	0.00	4.66594E+12
Q9UUK0	2.664E6	4.36	2	0.00	4.36436E+12
Q9P7W0	0.000E0	4.31	1	0.00	4.30726E+12
Q9Y703	0.000E0	4.25	2	0.00	4.24873E+12
O13830	0.000E0	4.22	1	0.00	4.21927E+12
Q9URT2	5.890E6	4.13	6	0.00	4.13254E+12
O94437	0.000E0	4.06	3	0.00	4.05904E+12
Q9P7Q8	5.544E8	4.03	2	0.00	4.03073E+12
O14319	6.139E6	3.94	1	0.00	3.9369E+12
O94479	1.852E7	3.85	1	0.00	3.84547E+12
O94377	3.456E6	3.81	2	0.00	3.80548E+12
O94274	0.000E0	3.73	1	0.00	3.73352E+12
O74333	0.000E0	3.71	2	0.00	3.71486E+12
O74794	4.403E6	3.69	3	0.00	3.6858E+12
O94584	0.000E0	3.63	1	0.00	3.62902E+12
O74435	0.000E0	3.56	1	0.00	3.56449E+12
Q9USZ7	1.277E6	3.50	2	0.00	3.50116E+12
O13739	0.000E0	3.48	1	0.00	3.48471E+12
P87027	8.153E6	3.45	2	0.00	3.44781E+12
P53693	0.000E0	3.36	1	0.00	3.35591E+12

P47979	7.224E6	3.35	1	0.00	3.35391E+12
O13681	0.000E0	3.33	1	0.00	3.33439E+12
O74480	0.000E0	3.33	2	0.00	3.32888E+12
O14059	0.000E0	3.31	1	0.00	3.30896E+12
Q92353	4.809E7	3.30	3	0.00	3.30311E+12
Q9HE15	5.730E6	2.98	1	0.00	2.98012E+12
G2TRQ8	0.000E0	2.95	1	0.00	2.95375E+12
O14109	0.000E0	2.94	1	0.00	2.9427E+12
O59815	0.000E0	2.93	1	0.00	2.93222E+12
Q9USW3	0.000E0	2.89	1	0.00	2.89133E+12
Q9C1W8	0.000E0	2.88	1	0.00	2.88059E+12
Q9USH1	0.000E0	2.80	1	0.00	2.80422E+12
O13850	0.000E0	2.73	3	0.00	2.72785E+12
Q8TFH0	0.000E0	2.64	1	0.00	2.63565E+12
P79007	0.000E0	2.61	1	0.00	2.60836E+12
O42903	4.035E6	2.61	1	0.00	2.60594E+12
O94685	3.035E6	2.55	3	0.00	2.54743E+12
O13728	0.000E0	2.54	1	0.00	2.53702E+12
Q9P376	0.000E0	2.53	1	0.00	2.52874E+12
O14269	0.000E0	2.53	1	0.00	2.52675E+12
O74463	5.598E6	2.48	1	0.00	2.48174E+12
Q9UUD0	4.452E7	2.48	1	0.00	2.48086E+12
P40369	1.822E6	2.47	1	0.00	2.46533E+12
P87050	0.000E0	2.46	2	0.00	2.45603E+12
Q9C0Y8	0.000E0	2.45	1	0.00	2.45303E+12
O74561	0.000E0	2.39	3	0.00	2.38722E+12
Q9Y7K1	7.316E7	2.37	1	0.00	2.37436E+12
O94453	0.000E0	2.37	2	0.00	2.37303E+12
Q9HDZ5	0.000E0	2.36	2	0.00	2.36075E+12
O13997	0.000E0	2.35	1	0.00	2.35448E+12
O94298	0.000E0	2.34	1	0.00	2.34347E+12
Q9HFF0	0.000E0	2.34	1	0.00	2.33597E+12
Q9Y7K4	0.000E0	2.33	2	0.00	2.33137E+12
O14189	0.000E0	2.32	2	0.00	2.31724E+12
O42898	2.483E6	2.32	2	0.00	2.31506E+12
Q10488	0.000E0	2.31	1	0.00	2.30512E+12
Q9P6I4	0.000E0	2.29	1	0.00	2.29023E+12
O60068	0.000E0	2.29	1	0.00	2.28613E+12
O14353	0.000E0	2.26	2	0.00	2.26474E+12
O74827	1.783E7	2.26	1	0.00	2.2609E+12
O42957	0.000E0	2.26	1	0.00	2.25887E+12
O74541	0.000E0	2.25	1	0.00	2.25141E+12
O74732	9.313E6	2.25	1	0.00	2.24566E+12
O74969	3.446E7	2.18	1	0.00	2.17579E+12
C6Y4A3	0.000E0	2.14	1	0.00	2.1394E+12
Q6E434	0.000E0	2.13	1	0.00	2.12883E+12
Q10323	0.000E0	2.10	1	0.00	2.10358E+12
Q09116	1.017E7	2.08	1	0.00	2.07937E+12
O74871	0.000E0	2.07	2	0.00	2.0698E+12
O74386	0.000E0	2.06	1	0.00	2.06456E+12
Q10159	0.000E0	2.06	1	0.00	2.06312E+12
P08463	1.389E7	2.06	1	0.00	2.06011E+12
O59700	0.000E0	2.06	1	0.00	2.05615E+12
Q8WZK4	0.000E0	2.05	1	0.00	2.05062E+12
Q9P7X3	0.000E0	2.02	1	0.00	2.02408E+12
Q10172	4.915E6	2.01	1	0.00	2.013E+12
Q9URY8	0.000E0	2.00	1	0.00	2.00284E+12
Q10356	0.000E0	2.00	1	0.00	1.99506E+12
Q01682	1.189E7	1.95	2	0.00	1.94787E+12
O14032	0.000E0	1.93	1	0.00	1.92914E+12

Q04665	0.000E0	1.92	1	0.00	1.91608E+12
O74419	2.502E8	1.90	3	0.00	1.90446E+12
Q9P7J1	1.740E6	1.90	1	0.00	1.90172E+12
O59795	2.405E8	1.90	4	0.00	1.89918E+12
Q09718	0.000E0	1.90	1	0.00	1.89696E+12
O94694	7.079E6	1.89	1	0.00	1.89396E+12
Q9P7D6	0.000E0	1.88	1	0.00	1.87514E+12
O14361	6.579E6	1.87	1	0.00	1.86573E+12
O74876	5.764E6	1.86	1	0.00	1.85725E+12
O13787	1.455E7	1.85	3	0.00	1.85146E+12
O74428	0.000E0	1.84	1	0.00	1.83825E+12
O94487	0.000E0	1.83	1	0.00	1.83498E+12
P50531	0.000E0	1.80	1	0.00	1.79543E+12
P78871	1.179E7	1.79	1	0.00	1.79477E+12
G2TRS8	0.000E0	1.78	1	0.00	1.78149E+12
Q4LB35	0.000E0	1.77	3	0.00	1.76849E+12
O74944	0.000E0	1.75	2	0.00	1.75307E+12
P87227	6.224E6	1.72	1	0.00	1.71744E+12
Q9P7N9	5.144E6	1.71	1	0.00	1.71264E+12
O59710	4.432E6	1.71	2	0.00	1.70711E+12
Q09879	0.000E0	1.70	1	0.00	1.69955E+12
Q96UP3	8.822E7	1.70	1	0.00	1.69898E+12
O74772	1.145E6	1.70	1	0.00	1.69582E+12
O43020	5.943E6	1.69	1	0.00	1.69347E+12
Q10092	0.000E0	1.69	1	0.00	1.68612E+12
P87152	1.486E7	1.69	1	0.00	1.6858E+12
P49777	0.000E0	1.69	1	0.00	1.6851E+12
Q10302	5.063E6	1.68	1	0.00	1.68497E+12
O60142	0.000E0	1.67	1	0.00	1.66802E+12
O94522	5.417E6	1.67	1	0.00	1.66712E+12
P09202	0.000E0	1.66	1	0.00	1.6621E+12
Q9UTE5	0.000E0	1.66	1	0.00	1.66195E+12
Q9Y7Y1	0.000E0	1.64	2	0.00	1.64179E+12
O13987	0.000E0	1.62	2	0.00	1.61923E+12
O60131	0.000E0	1.60	1	0.00	1.60469E+12
Q9P7D2	0.000E0	1.60	1	0.00	1.60418E+12
Q6LA55	1.270E7	2.49	2	0.00	2.48933E+12
Q9Y7X9	0.000E0	2.44	3	0.00	2.44186E+12
O14047	0.000E0	2.17	1	0.00	2.16813E+12
O74956	3.126E7	2.07	1	0.00	2.06907E+12
O13744	0.000E0	2.02	1	0.00	2.02098E+12
O94598	6.057E8	1.62	3	0.00	1.61764E+12
Q9C0Y6	1.830E7	20.68	4	3.07	6.729369643
O74802	6.293E8	9.64	4	2.32	4.147603979
O13791	9.518E6	11.77	5	2.90	4.062024048
P78875	1.035E7	17.83	7	4.66	3.826168383
O94505	5.095E7	52.57	11	15.46	3.399323598
O94721	1.150E7	8.69	2	2.72	3.194678194
O42854	1.479E7	31.36	5	10.38	3.022388428
P78929	1.368E8	34.28	6	11.50	2.980719291
Q09751	3.119E7	16.44	5	5.82	2.822203257
O42650	7.426E6	20.47	9	7.36	2.780626845
Q9UQX0	3.443E7	29.71	6	11.29	2.63080026
O59725	5.815E6	15.94	3	6.25	2.552060197
O75006	6.646E5	18.67	5	7.46	2.504637793
O14209	3.220E7	11.91	5	0.00	1.19083E+13
P87128	5.955E6	7.66	3	0.00	7.66394E+12
O74500	0.000E0	6.17	2	0.00	6.16769E+12
O74749	0.000E0	5.68	1	0.00	5.67625E+12
O74343	0.000E0	4.59	1	0.00	4.58725E+12

P23566	1.041E8	4.57	1	0.00	4.56767E+12
O74482	8.879E6	4.35	2	0.00	4.34548E+12
Q9C0Y5	3.418E7	4.10	1	0.00	4.10206E+12
Q9HDZ2	5.256E6	4.07	2	0.00	4.0731E+12
Q9Y7X8	1.087E7	4.04	3	0.00	4.03999E+12
Q09882	2.618E6	3.79	2	0.00	3.79198E+12
O14132	2.480E7	3.69	2	0.00	3.69069E+12
O74456	2.480E7	3.69	1	0.00	3.69069E+12
Q9P7E0	2.619E7	3.55	1	0.00	3.55433E+12
Q9URX2	2.158E7	3.52	1	0.00	3.51682E+12
O13968	0.000E0	3.24	2	0.00	3.24089E+12
Q09833	2.969E7	3.20	2	0.00	3.20346E+12
O13735	4.994E6	3.15	2	0.00	3.14538E+12
O74563	3.975E8	2.93	1	0.00	2.93253E+12
Q10359	0.000E0	2.84	2	0.00	2.84264E+12
O14077	2.658E8	2.67	2	0.00	2.67068E+12
O14310	1.698E8	2.51	1	0.00	2.50693E+12
O43040	0.000E0	2.44	1	0.00	2.44128E+12
Q09683	0.000E0	2.32	1	0.00	2.31556E+12
Q9P6L8	2.331E7	2.10	2	0.00	2.09812E+12
Q09896	0.000E0	2.06	2	0.00	2.05564E+12
O94712	0.000E0	2.05	1	0.00	2.04557E+12
Q9C0V8	0.000E0	2.04	1	0.00	2.04427E+12
P21534	9.376E6	1.83	2	0.00	1.82895E+12
P05501	0.000E0	1.79	1	0.00	1.7944E+12
Q1MTR3	7.083E6	1.73	1	0.00	1.73459E+12
Q9HDV4	3.594E8	1.67	3	0.00	1.66612E+12
Q9UT55	1.254E7	1.65	3	0.00	1.64988E+12
O42975	3.105E8	1.62	1	0.00	1.61764E+12
P78763	1.339E7	1.62	2	0.00	1.61661E+12
Q9HGL4	7.104E6	26.70	6	2.12	12.6114792
O74856	1.962E7	12.96	5	1.79	7.218974597
O14008	0.000E0	9.90	3	1.69	5.86560393
Q9UTH9	1.401E7	12.37	7	2.17	5.714375916
Q10195	2.522E7	14.40	3	2.58	5.590723264
Q9UTK4	6.043E6	12.64	6	2.46	5.143605153
Q9UT27	3.044E7	19.24	4	3.92	4.913336096
O94346	6.501E6	11.16	3	2.34	4.772938001
O94497	2.440E7	66.78	12	14.07	4.746212149
Q9US43	1.012E8	12.19	6	2.73	4.459911366
P32390	4.924E7	74.33	13	17.21	4.318484897
Q9C0Y2	3.105E7	13.30	2	3.32	4.007411263
Q9Y7P1	7.955E6	6.44	5	1.66	3.88002859
Q9USL4	1.138E7	53.16	13	14.17	3.751819251
O14029	8.479E6	7.70	2	2.05	3.74962921
O94548	1.267E7	11.29	3	3.05	3.706871617
O74382	3.591E7	9.44	3	2.61	3.615502333
O74521	1.089E7	12.82	5	3.60	3.55942415
Q9UST8	1.228E7	6.43	1	1.87	3.431705573
P48008	8.084E6	11.51	6	3.36	3.425905724
O94373	2.854E7	20.18	5	6.00	3.364621084
Q9P7X1	2.584E7	32.77	12	9.94	3.295628649
Q9Y7J4	2.627E7	7.61	3	2.34	3.253536694
Q9USY2	6.372E8	6.16	2	1.92	3.217471952
P79009	2.338E8	24.22	4	7.63	3.172910823
O94675	6.089E7	7.64	3	2.41	3.172872434
Q9UU99	5.281E5	11.97	3	3.77	3.172163223
Q9UQY2	3.097E7	41.64	7	13.31	3.127457599
O13899	1.985E7	5.77	2	1.87	3.085607062
O36014	1.039E7	6.60	4	2.15	3.065516913

Q9UTH2	4.197E6	8.68	3	2.84	3.05423314
Q92356	1.212E7	12.15	2	4.03	3.017422181
Q09860	2.405E7	54.31	19	18.24	2.978132347
P78768	1.564E7	7.52	2	2.58	2.914470548
Q09720	2.515E7	22.91	3	7.87	2.910010275
O74975	1.061E7	11.92	2	4.21	2.830774537
P30655	8.582E6	11.80	4	4.28	2.756587823
Q9USJ1	2.160E8	5.00	2	1.82	2.744514577
Q10215	3.368E7	11.25	3	4.11	2.735537756
O74432	2.194E7	13.68	3	5.03	2.719890144
Q9P6K3	2.713E7	22.30	6	8.24	2.705000459
O60176	4.900E6	19.27	3	7.13	2.703245107
O74977	0.000E0	17.53	4	6.50	2.698258777
Q9Y7L1	1.314E7	7.77	3	2.88	2.694257075
P87113	1.967E7	4.64	2	1.75	2.66082283
Q10258	1.854E7	12.35	7	4.67	2.645857482
O00084	1.990E7	4.73	4	1.79	2.643659739
O74417	1.237E7	12.40	4	4.73	2.622631566
O13687	4.813E7	30.15	9	11.51	2.619391464
P87294	0.000E0	4.22	3	1.61	2.613796179
Q9HGL2	1.386E7	18.55	7	7.16	2.592451467
P87057	2.145E7	8.83	2	3.49	2.533788421

Appendix Table 1.2: Positive Interactors in the Sec3-GFP Trap (Replicate 2)

Uniprot Accession	Area	Score	Peptides	Score in GFP Control	Fold Increase Over Control
Q10324	2.235E8	118.42	25	0.00	1.184E+16
O13705	3.226E7	29.97	18	0.00	2.997E+15
Q10339	1.084E7	29.63	10	0.00	2.963E+15
Q8NKC2	5.769E7	23.07	8	0.00	2.307E+15
O43032	4.599E6	18.49	6	0.00	1.849E+15
O74956	7.195E6	15.27	5	0.00	1.527E+15
O74853	2.993E6	14.55	5	0.00	1.455E+15
O94362	9.158E6	13.87	4	0.00	1.387E+15
P40236	9.198E6	13.52	6	0.00	1.352E+15
O14233	3.156E6	12.43	3	0.00	1.243E+15
Q9UTK7	2.384E6	11.61	2	0.00	1.161E+15
O59821	3.088E6	10.68	3	0.00	1.068E+15
O74439	2.826E7	10.39	5	0.00	1.039E+15
Q9HDX2	2.381E6	9.67	3	0.00	9.665E+14
O13702	5.997E6	9.65	4	0.00	9.654E+14
Q09189	2.673E6	9.57	3	0.00	9.569E+14
Q10499	3.592E6	9.53	2	0.00	9.531E+14
Q96WW3	8.867E6	8.90	2	0.00	8.895E+14
P40371	3.582E6	8.85	3	0.00	8.851E+14
Q9P5M9	1.050E7	8.47	3	0.00	8.474E+14
O13641	3.764E6	8.43	5	0.00	8.429E+14
P87127	4.128E6	8.42	2	0.00	8.422E+14
Q9UUE4	1.285E6	8.03	1	0.00	8.028E+14
O43001	5.066E6	7.76	4	0.00	7.76E+14
P39750	2.835E6	7.64	2	0.00	7.644E+14
O94669	3.367E6	7.54	5	0.00	7.545E+14
O59712	4.988E6	7.48	4	0.00	7.484E+14
O74551	5.853E6	7.48	3	0.00	7.477E+14
P78929	8.110E6	7.12	2	0.00	7.116E+14
Q9USZ2	6.724E6	7.10	4	0.00	7.095E+14
Q10366	2.940E6	7.09	6	0.00	7.093E+14
Q9US42	2.774E6	6.96	2	0.00	6.957E+14
Q9P7H1	2.522E6	6.89	4	0.00	6.889E+14
O60108	2.683E6	6.68	3	0.00	6.684E+14
O14205	4.204E6	6.55	2	0.00	6.554E+14
O14266	2.448E6	6.52	2	0.00	6.524E+14
O60063	7.942E6	6.43	3	0.00	6.434E+14
Q9Y810	2.275E6	6.06	3	0.00	6.061E+14
O74759	2.218E6	5.88	3	0.00	5.881E+14
O94372	4.240E6	5.77	5	0.00	5.772E+14
O13853	4.754E6	5.74	3	0.00	5.741E+14
Q9P7M8	5.824E6	5.70	2	0.00	5.703E+14
O13903	5.464E6	5.50	2	0.00	5.503E+14
O94443	3.234E6	5.37	1	0.00	5.374E+14
O13910	4.124E6	5.32	2	0.00	5.315E+14
Q9P7X5	2.289E6	5.31	2	0.00	5.307E+14
Q9UTI3	4.679E6	5.09	2	0.00	5.089E+14
O13744	4.632E6	5.09	2	0.00	5.087E+14
Q9Y822	1.832E6	5.05	2	0.00	5.046E+14
Q09849	3.284E6	5.01	3	0.00	5.008E+14
Q10170	8.797E5	5.00	2	0.00	4.995E+14
Q76PC3	5.466E6	4.96	3	0.00	4.96E+14
Q9Y7J2	3.857E6	4.95	2	0.00	4.949E+14
Q9HE00	1.223E7	4.93	2	0.00	4.933E+14
O42973	8.928E5	4.82	1	0.00	4.818E+14
Q09751	4.862E6	4.79	3	0.00	4.794E+14
O94375	2.793E6	4.77	3	0.00	4.769E+14
O42929	3.133E6	4.75	2	0.00	4.748E+14
Q10494	4.102E6	4.70	2	0.00	4.702E+14
Q9C0Y6	3.279E6	4.61	1	0.00	4.61E+14
O74858	1.726E6	4.56	2	0.00	4.563E+14
Q9P791	2.506E6	4.53	2	0.00	4.527E+14
O74215	1.731E6	4.50	2	0.00	4.502E+14
Q9Y7K7	5.294E6	4.42	2	0.00	4.421E+14
P78833	3.544E6	4.24	1	0.00	4.237E+14

Q09897	1.922E7	4.23	3	0.00	4.232E+14
O59683	6.224E6	4.17	4	0.00	4.174E+14
O13636	5.608E6	4.06	1	0.00	4.058E+14
O14279	5.702E6	3.98	1	0.00	3.979E+14
Q9Y7N3	3.315E6	3.93	1	0.00	3.932E+14
Q09844	3.703E6	3.78	3	0.00	3.777E+14
O60153	1.351E6	3.67	1	0.00	3.669E+14
O60112	1.622E6	3.64	1	0.00	3.641E+14
Q09948	3.836E6	3.60	1	0.00	3.6E+14
O14327	1.615E6	3.59	1	0.00	3.591E+14
Q9Y7K8	4.547E6	3.51	2	0.00	3.513E+14
O94721	1.631E6	3.29	1	0.00	3.294E+14
O74308	0.000E0	3.29	1	0.00	3.289E+14
O42851	0.000E0	3.26	1	0.00	3.263E+14
O14195	2.685E6	3.20	1	0.00	3.203E+14
Q09735	4.018E6	3.18	1	0.00	3.178E+14
O13911	7.399E5	3.15	1	0.00	3.145E+14
O13310	4.731E6	3.08	1	0.00	3.077E+14
Q09919	0.000E0	3.05	1	0.00	3.047E+14
O14079	3.502E5	3.03	1	0.00	3.028E+14
Q9USM7	5.872E6	2.98	1	0.00	2.985E+14
Q09842	1.534E6	2.98	1	0.00	2.979E+14
A9ZLL8	5.506E5	2.96	1	0.00	2.955E+14
O14300	3.767E6	2.94	1	0.00	2.937E+14
O14302	1.235E6	2.93	1	0.00	2.929E+14
Q9UTR5	3.103E6	2.91	1	0.00	2.914E+14
O42998	8.811E6	2.91	7	0.00	2.907E+14
O74362	7.321E6	2.88	1	0.00	2.879E+14
Q10275	4.745E6	2.88	1	0.00	2.877E+14
O74898	2.359E6	2.86	1	0.00	2.861E+14
P78831	2.843E6	2.86	1	0.00	2.857E+14
Q02088	1.243E7	2.84	1	0.00	2.841E+14
Q9Y7Z2	4.505E6	2.80	1	0.00	2.801E+14
Q9USJ9	2.606E6	2.71	1	0.00	2.707E+14
O60186	4.591E6	2.69	1	0.00	2.692E+14
Q9UTI8	1.663E7	2.68	2	0.00	2.678E+14
O42877	2.928E6	2.65	1	0.00	2.651E+14
P87242	3.901E6	2.65	2	0.00	2.649E+14
Q9UUA4	5.519E6	2.64	1	0.00	2.644E+14
P10506	1.661E6	2.61	1	0.00	2.607E+14
Q9Y7X9	2.724E6	2.56	1	0.00	2.561E+14
O13950	4.225E6	2.56	1	0.00	2.559E+14
O14368	9.131E6	2.56	2	0.00	2.556E+14
Q9UTN4	8.650E5	2.55	1	0.00	2.549E+14
O74754	6.438E6	2.55	2	0.00	2.547E+14
O13821	5.394E5	2.53	1	0.00	2.533E+14
O94281	9.730E6	2.52	1	0.00	2.52E+14
Q9HDY0	2.185E6	2.51	1	0.00	2.51E+14
Q10304	1.425E6	2.49	1	0.00	2.49E+14
Q76PC7	3.433E6	2.49	1	0.00	2.485E+14
O14076	1.070E6	2.48	1	0.00	2.484E+14
O14158	3.090E6	2.47	2	0.00	2.475E+14
Q09872	5.641E6	2.47	2	0.00	2.469E+14
Q10231	2.726E6	2.47	1	0.00	2.466E+14
O60147	4.446E6	2.47	3	0.00	2.466E+14
Q9P7Q9	2.515E6	2.46	1	0.00	2.463E+14
Q9P370	9.174E6	2.46	1	0.00	2.457E+14
P78953	3.025E6	2.45	2	0.00	2.45E+14
Q9UTL2	1.098E7	2.44	2	0.00	2.44E+14
O94707	1.597E6	2.41	2	0.00	2.406E+14
O59677	2.278E6	2.38	1	0.00	2.376E+14
Q9USZ3	7.314E6	2.35	2	0.00	2.353E+14
Q9C0Z9	2.819E5	2.35	1	0.00	2.348E+14
O74470	1.684E6	2.34	2	0.00	2.337E+14
O60118	0.000E0	2.33	1	0.00	2.327E+14
Q9P6P6	1.425E7	2.32	4	0.00	2.322E+14
O13642	1.189E6	2.32	1	0.00	2.317E+14
O94581	5.153E6	2.32	1	0.00	2.316E+14
O74802	1.174E9	2.30	2	0.00	2.298E+14
O42650	3.446E6	2.30	4	0.00	2.297E+14
O42976	2.166E6	2.30	3	0.00	2.296E+14

Q09933	1.101E6	2.26	1	0.00	2.26E+14
Q9P7C3	1.390E6	2.25	1	0.00	2.251E+14
P48009	4.591E5	2.25	1	0.00	2.249E+14
Q9US55	2.784E6	2.23	1	0.00	2.229E+14
O94563	1.006E7	2.23	1	0.00	2.226E+14
P87170	3.927E6	2.22	1	0.00	2.218E+14
O43089	5.178E6	2.21	1	0.00	2.214E+14
O59737	4.219E6	2.21	1	0.00	2.214E+14
Q1MTQ5	2.274E6	2.21	1	0.00	2.212E+14
Q9HGN6	8.535E5	2.20	1	0.00	2.203E+14
O42653	1.063E6	2.19	1	0.00	2.194E+14
Q9UT34	4.919E5	2.19	2	0.00	2.188E+14
O13829	6.868E6	2.18	1	0.00	2.185E+14
O59747	6.121E6	2.18	1	0.00	2.182E+14
P35669	7.327E5	2.16	1	0.00	2.159E+14
O74460	7.251E6	2.13	1	0.00	2.134E+14
Q9Y820	3.096E6	2.13	2	0.00	2.133E+14
O14295	4.117E6	2.13	2	0.00	2.129E+14
P0CAN8	1.644E6	2.13	1	0.00	2.125E+14
Q9P6N2	3.060E6	2.13	2	0.00	2.125E+14
Q9UR24	5.956E5	2.12	1	0.00	2.122E+14
O94657	7.614E6	2.12	3	0.00	2.12E+14
Q9UTB2	1.270E6	2.12	1	0.00	2.118E+14
O94733	2.133E6	2.11	1	0.00	2.108E+14
P78890	2.134E7	2.11	1	0.00	2.107E+14
Q9USN2	4.006E6	2.08	2	0.00	2.078E+14
Q9UTN3	2.003E6	2.07	1	0.00	2.075E+14
Q10481	3.689E6	2.07	1	0.00	2.071E+14
P87156	7.864E5	2.07	1	0.00	2.071E+14
O94570	3.161E6	2.05	1	0.00	2.055E+14
O94531	1.024E7	2.05	1	0.00	2.053E+14
Q10100	6.059E6	2.03	1	0.00	2.033E+14
Q1MTR0	9.300E5	2.03	1	0.00	2.028E+14
Q9P787	9.417E6	2.03	3	0.00	2.028E+14
P78875	1.744E6	2.03	1	0.00	2.025E+14
O94495	0.000E0	2.01	1	0.00	2.013E+14
Q09920	0.000E0	2.01	1	0.00	2.011E+14
Q9P7H4	9.351E5	2.01	1	0.00	2.005E+14
Q9P7H9	4.963E6	2.00	2	0.00	1.996E+14
Q9P7C9	1.557E6	1.99	2	0.00	1.989E+14
O60150	0.000E0	1.99	1	0.00	1.989E+14
O94412	4.618E6	1.98	1	0.00	1.982E+14
O59742	0.000E0	1.98	1	0.00	1.978E+14
O94399	2.871E6	1.95	1	0.00	1.951E+14
Q9C0U6	2.565E6	1.91	2	0.00	1.91E+14
Q9USN1	4.446E6	1.89	1	0.00	1.891E+14
O74945	3.952E6	1.89	4	0.00	1.89E+14
P50582	2.338E6	1.88	1	0.00	1.882E+14
O42894	2.418E6	1.88	2	0.00	1.88E+14
O74370	1.420E6	1.87	1	0.00	1.875E+14
Q9P7S5	2.485E6	1.87	2	0.00	1.868E+14
Q10245	0.000E0	1.86	1	0.00	1.858E+14
O94505	3.263E6	1.86	1	0.00	1.856E+14
O13701	2.158E6	1.84	2	0.00	1.842E+14
O60067	2.929E6	1.84	1	0.00	1.836E+14
O13882	4.415E6	1.83	1	0.00	1.833E+14
Q9Y7N0	1.687E6	1.82	1	0.00	1.823E+14
O60065	2.164E6	1.79	3	0.00	1.786E+14
O14047	6.780E5	1.79	1	0.00	1.786E+14
P87125	1.097E6	1.78	1	0.00	1.782E+14
O43018	0.000E0	1.78	1	0.00	1.782E+14
Q9US48	2.273E6	1.78	1	0.00	1.779E+14
P05933	0.000E0	1.77	1	0.00	1.769E+14
O14172	1.686E6	1.77	1	0.00	1.767E+14
O14038	2.499E6	1.76	1	0.00	1.755E+14
P30776	0.000E0	1.75	1	0.00	1.749E+14
O74778	3.733E6	1.75	2	0.00	1.746E+14
Q9HFF5	0.000E0	1.74	1	0.00	1.738E+14
P0CT37	3.249E6	1.74	3	0.00	1.737E+14
C6Y4A7	1.075E7	1.73	1	0.00	1.727E+14
Q9USP3	2.345E6	1.72	1	0.00	1.725E+14

O13290	3.026E6	1.72	3	0.00	1.72E+14
Q1K9B6	6.464E5	1.70	1	0.00	1.705E+14
O13871	3.275E6	1.69	2	0.00	1.692E+14
O74889	0.000E0	1.68	1	0.00	1.676E+14
Q9UUM6	4.471E6	1.68	1	0.00	1.675E+14
O42895	2.645E6	1.67	1	0.00	1.672E+14
O74854	1.487E7	1.67	1	0.00	1.671E+14
Q09140	2.150E6	1.66	2	0.00	1.663E+14
Q09793	1.848E6	1.65	1	0.00	1.653E+14
Q10166	0.000E0	1.65	1	0.00	1.645E+14
Q09706	2.330E6	1.64	1	0.00	1.637E+14
O94667	4.123E6	1.63	1	0.00	1.633E+14
P36209	3.502E6	1.63	1	0.00	1.626E+14
O14177	1.589E6	1.62	2	0.00	1.616E+14
O43120	1.068E7	1.62	1	0.00	1.615E+14
O74499	1.744E6	1.60	1	0.00	1.602E+14
O75006	1.621E7	45.48	15	0.00	4.548E+15
O14226	1.616E7	25.46	9	0.00	2.546E+15
O74415	2.166E7	17.08	8	0.00	1.708E+15
O74409	8.478E6	14.32	5	0.00	1.432E+15
O94752	6.986E6	14.26	2	0.00	1.426E+15
Q1MTQ1	4.201E6	9.26	4	0.00	9.259E+14
Q9UQX0	2.209E6	8.91	2	0.00	8.911E+14
O60121	7.501E6	8.46	3	0.00	8.463E+14
O74823	1.998E6	8.31	3	0.00	8.314E+14
Q9UUA2	2.996E6	8.25	2	0.00	8.248E+14
O60096	5.886E6	7.76	4	0.00	7.758E+14
O42854	1.120E6	7.52	2	0.00	7.523E+14
O60072	4.177E6	7.43	5	0.00	7.429E+14
O59702	9.154E6	7.42	3	0.00	7.416E+14
O94488	1.159E7	7.33	5	0.00	7.33E+14
Q10322	5.482E6	6.77	3	0.00	6.775E+14
Q09843	7.344E6	6.56	4	0.00	6.564E+14
Q9HGQ3	2.734E6	5.73	1	0.00	5.729E+14
O14306	1.083E6	5.71	2	0.00	5.706E+14
Q9Y7L6	4.811E6	5.63	2	0.00	5.628E+14
Q9P382	1.849E6	5.32	3	0.00	5.316E+14
O14193	4.024E6	5.18	1	0.00	5.178E+14
O94689	1.815E6	4.66	1	0.00	4.656E+14
O94655	2.426E7	4.63	2	0.00	4.629E+14
P00046	1.148E7	4.55	1	0.00	4.555E+14
Q9C106	1.865E6	4.49	2	0.00	4.494E+14
Q9USH0	3.930E6	4.39	1	0.00	4.389E+14
Q9URZ4	3.946E6	4.35	2	0.00	4.351E+14
O94618	4.511E6	4.29	2	0.00	4.292E+14
O74402	4.709E6	4.09	6	0.00	4.091E+14
O13989	7.207E6	3.83	2	0.00	3.831E+14
Q9UUG2	2.819E6	3.77	2	0.00	3.77E+14
P87232	6.261E6	3.73	3	0.00	3.733E+14
Q10077	8.803E5	3.37	1	0.00	3.375E+14
O74824	1.252E6	3.27	2	0.00	3.269E+14
Q9UUI3	1.084E6	3.16	1	0.00	3.157E+14
Q10143	6.374E5	3.00	1	0.00	3.004E+14
Q12126	3.147E6	2.82	2	0.00	2.823E+14
O13799	2.835E6	2.81	1	0.00	2.814E+14
Q9USQ1	0.000E0	2.73	1	0.00	2.734E+14
O42908	1.324E6	2.63	1	0.00	2.631E+14
O14110	8.447E5	2.55	1	0.00	2.551E+14
O36017	1.234E6	2.49	2	0.00	2.492E+14
Q10437	1.051E7	2.33	2	0.00	2.334E+14
O13953	4.415E6	2.29	3	0.00	2.295E+14
Q10203	6.269E6	2.26	2	0.00	2.257E+14
Q1MTQ7	0.000E0	2.25	1	0.00	2.251E+14
Q9URX7	5.070E6	2.22	3	0.00	2.224E+14
O94534	5.143E6	2.22	3	0.00	2.224E+14
Q10432	3.720E6	2.20	1	0.00	2.204E+14
O13991	2.406E6	2.19	1	0.00	2.19E+14
O59760	2.583E6	2.16	1	0.00	2.158E+14
O13935	5.208E6	2.16	2	0.00	2.158E+14
P28040	2.370E6	2.13	2	0.00	2.13E+14
Q09727	4.950E6	2.12	2	0.00	2.117E+14

Q9P7X0	1.092E7	2.10	2	0.00	2.101E+14
O60111	1.583E7	2.06	2	0.00	2.065E+14
O59824	0.000E0	2.01	1	0.00	2.014E+14
O94264	1.065E6	2.00	1	0.00	2E+14
O14251	8.338E6	2.00	3	0.00	2E+14
O94387	3.977E7	1.95	2	0.00	1.946E+14
P21547	4.845E6	1.93	1	0.00	1.934E+14
O43044	1.962E6	1.89	1	0.00	1.885E+14
Q10310	3.413E6	1.88	1	0.00	1.884E+14
O42919	2.516E6	1.84	2	0.00	1.842E+14
O59722	8.429E7	1.84	2	0.00	1.839E+14
P10505	3.269E6	1.81	3	0.00	1.812E+14
P55306	3.068E6	1.80	1	0.00	1.8E+14
B5BP45	4.834E6	1.77	1	0.00	1.769E+14
Q8WZK2	8.550E5	1.77	1	0.00	1.766E+14
O94447	2.997E6	1.76	2	0.00	1.759E+14
O13993	2.073E6	1.74	2	0.00	1.743E+14
Q6LA55	9.029E7	1.74	2	0.00	1.74E+14
O94680	2.163E6	1.73	1	0.00	1.733E+14
Q09856	1.938E6	1.67	1	0.00	1.675E+14
Q09873	2.430E6	1.65	2	0.00	1.649E+14
Q9P7R8	2.552E6	1.65	1	0.00	1.647E+14
Q9Y7T0	1.549E7	1.63	2	0.00	1.634E+14
Q9C0V7	3.001E8	1.63	1	0.00	1.626E+14
O94598	2.176E8	105.31	26	1.84	57.287654
O74846	1.390E8	110.10	23	2.86	38.504118
O74562	1.984E8	223.70	51	11.58	19.316501
O59672	7.697E6	17.91	8	1.85	9.6749289
O74442	9.046E6	23.12	6	2.67	8.6566638
O94280	2.387E7	14.70	4	2.23	6.5906042
Q10414	9.900E6	12.73	5	2.08	6.1047371
O74764	8.322E6	18.34	6	3.05	6.0220662
Q9HFE6	4.932E6	19.18	7	3.36	5.6991503
Q09176	1.742E7	10.32	3	1.84	5.6205484
O94683	1.167E7	10.25	4	1.96	5.2257843
O14075	9.526E6	10.42	4	2.02	5.1638578
Q9P7C1	9.306E6	10.71	7	2.08	5.151442
O13711	6.198E6	9.89	1	1.93	5.1097326
O43026	6.082E9	654.76	23	129.28	5.0646997
Q9Y7U6	4.319E6	12.17	7	2.42	5.0238441
Q9P6I8	8.635E6	12.65	7	2.52	5.0178611
Q10199	4.409E6	25.95	7	5.18	5.01028
O94590	4.546E6	16.90	4	3.45	4.9029185
P87111	3.086E6	12.81	3	2.63	4.8789911
O94385	4.339E6	12.62	6	2.76	4.5709042
O60173	6.974E6	11.76	4	2.58	4.5590165
Q9P7M5	4.424E7	9.31	2	2.07	4.5041426
O74330	2.856E7	9.88	3	2.20	4.4831233
Q09911	6.269E6	10.75	5	2.40	4.4714436
O94512	4.532E6	12.96	4	2.90	4.4698516
O60064	8.786E6	13.43	5	3.06	4.3825433
O43059	4.554E6	18.85	8	4.31	4.3763039
Q09799	1.156E7	33.97	11	7.79	4.3625232
O94269	9.052E6	16.35	3	3.78	4.3291197
O13648	1.792E7	23.42	9	5.48	4.2769177
P17608	3.531E7	12.03	4	2.84	4.2290318
O13998	1.846E7	30.64	7	7.30	4.1956681
Q9P7P1	9.021E6	7.15	2	1.71	4.1748661
Q09813	3.438E6	8.59	5	2.07	4.157227
O74742	3.623E6	16.62	7	4.03	4.1242148
Q9UUA1	3.662E6	10.18	3	2.49	4.0815638
P25295	6.054E6	13.12	3	3.22	4.0720069
O94414	3.840E6	14.07	3	3.52	3.9941924
Q09868	2.332E7	32.84	7	8.24	3.98586
O94718	3.753E6	7.27	4	1.83	3.9689002
O74978	1.117E7	11.19	5	2.84	3.9426222
Q9US05	8.112E6	11.96	5	3.03	3.9402142
Q12381	4.081E7	27.08	7	6.88	3.9342201
O42901	1.356E7	14.81	4	3.81	3.8894889
Q10478	2.299E6	7.93	2	2.05	3.8658031
O14290	1.892E7	20.67	5	5.35	3.8629952

Q9P3A9	6.719E6	14.62	6	3.82	3.8243233
P04910	1.864E8	29.48	4	7.78	3.7916142
O94616	5.961E7	35.73	10	9.43	3.7912967
O42936	7.853E6	8.29	4	2.20	3.7598916
Q96WW1	4.755E6	12.71	2	3.40	3.7404211
Q9HGM3	9.893E6	28.56	8	7.73	3.6966872
Q9P7V6	5.178E6	9.86	4	2.67	3.6965574
O14206	1.544E7	11.08	7	3.08	3.5929449
O13610	5.129E6	9.79	3	2.74	3.5739471
O59706	4.521E6	7.22	3	2.03	3.5509382
O14099	4.440E6	10.75	4	3.04	3.5355861
O42993	9.733E6	6.83	2	1.94	3.5174332
Q10295	3.801E6	9.13	4	2.61	3.5027737
O14085	5.673E6	9.15	2	2.66	3.4460674
O94311	6.252E6	14.35	2	4.17	3.4437622
O74803	3.402E6	9.74	3	2.84	3.4364303
O94449	1.002E7	8.55	2	2.56	3.340152
Q9Y8G3	8.047E6	11.44	5	3.44	3.3274406
O94288	5.543E6	15.21	6	4.57	3.3254946
Q10452	1.125E7	14.56	5	4.38	3.3225366
Q09729	1.041E7	23.79	5	7.27	3.2708557
O13791	6.084E6	15.09	4	4.67	3.233206
O74191	5.428E7	40.55	7	12.58	3.2222355
O74519	2.900E6	9.77	3	3.04	3.2166714
P36631	1.892E6	7.27	2	2.26	3.2121645
Q09177	9.108E6	17.33	4	5.40	3.2099618
O14179	6.680E6	8.91	2	2.78	3.2052539
Q9Y7R7	6.862E6	6.96	3	2.19	3.1766226
O59725	1.145E7	33.07	10	10.45	3.165059
O74504	1.029E7	10.07	4	3.22	3.1258075
Q9Y7X6	5.428E6	22.27	7	7.21	3.0910961
O94390	5.857E6	11.36	3	3.76	3.0183242
Q9HDT9	5.241E6	23.22	5	7.73	3.0032874
Q09697	1.544E6	5.83	3	1.95	2.993168
Q06975	6.535E7	22.58	5	7.55	2.9900726
Q1MTN8	5.093E6	4.78	1	1.60	2.9833088
O74453	9.328E6	4.81	3	1.61	2.9785808
O14014	4.292E6	5.23	2	1.76	2.9722977
Q92355	5.612E6	6.74	4	2.29	2.9397787
O14341	7.664E6	23.77	4	8.23	2.889396
Q10241	1.397E7	14.56	4	5.06	2.8776358
O14178	1.088E7	18.98	7	6.62	2.8692975
O14139	3.546E6	22.45	8	7.85	2.8593642
Q9P4X3	1.749E7	28.55	10	10.05	2.8399061
O94579	3.040E7	32.84	7	11.65	2.8180867
O59761	9.010E6	10.81	7	3.84	2.8137147
O13874	4.743E6	9.70	5	3.45	2.8078314
Q8TFH3	3.006E7	25.68	7	9.19	2.7953963
O94363	2.588E7	26.60	4	9.53	2.7907505
O74828	1.924E7	13.76	8	4.98	2.7648103
O14176	4.543E6	10.24	4	3.70	2.7640688
P78958	7.400E9	1152.48	31	417.71	2.7590632
O14044	4.943E6	10.50	5	3.83	2.7420179
Q9P7J3	6.291E6	6.12	3	2.26	2.7131631
O42885	3.849E6	12.15	3	4.50	2.7014211
O14324	1.159E7	9.88	2	3.68	2.6840005
P07669	8.653E7	85.45	15	31.87	2.6808012
Q10342	1.359E7	25.03	7	9.39	2.6661791
Q76PD2	1.079E7	19.86	9	7.53	2.6358495
O13867	9.716E6	4.79	4	1.83	2.6112744
P87126	3.077E6	7.23	2	2.77	2.6096128
O60114	4.644E6	22.37	10	8.60	2.6015885
Q09820	1.760E7	55.66	21	21.42	2.5986217
O59701	3.346E6	8.83	4	3.40	2.5941984
O60110	4.086E6	4.17	1	1.62	2.5826312
O14250	9.557E6	19.94	5	7.73	2.5803261
Q10233	8.757E7	8.22	6	3.21	2.5615257
O14019	1.282E7	35.79	7	14.02	2.5524982
O74469	3.952E6	5.91	1	2.32	2.5483458
P87148	3.174E6	10.84	2	4.27	2.5389671
Q10234	1.019E7	16.24	6	6.45	2.5200332

Q9UTB8	3.309E6	7.46	3	2.96	2.5197287
Q09717	2.220E7	16.70	5	6.63	2.5181255
P17610	2.419E7	24.26	8	9.64	2.5168963
Q9C1X1	6.018E6	22.78	9	9.09	2.5057159
Q10137	9.921E6	19.92	6	7.96	2.5025525

Appendix Table 1.3: Positive Interactors in the Sec3-913-GFP Trap (Replicate 1)

Uniprot Accession	Area	Score	Peptides	Score in GFP Control	Fold Increase Over Control
Q8NIL3	1.704E7	16.27	3	0.00	1.627E+13
O74983	1.797E7	13.88	2	0.00	1.388E+13
P08463	1.389E7	9.70	3	0.00	9.699E+12
O60166	2.563E7	9.55	4	0.00	9.546E+12
Q10172	4.915E6	9.23	2	0.00	9.229E+12
O94642	1.224E7	7.77	3	0.00	7.767E+12
O14319	6.139E6	7.23	2	0.00	7.231E+12
O94314	1.005E7	7.13	2	0.00	7.135E+12
P78871	1.179E7	6.60	1	0.00	6.598E+12
O74433	2.669E7	6.50	1	0.00	6.499E+12
Q9HE15	5.730E6	6.36	1	0.00	6.36E+12
O14361	6.579E6	6.33	3	0.00	6.331E+12
Q9URU6	6.724E6	6.13	3	0.00	6.129E+12
Q09746	1.454E6	6.02	2	0.00	6.024E+12
O74414	3.830E6	5.95	1	0.00	5.95E+12
O13838	1.007E7	5.48	2	0.00	5.48E+12
O94522	5.417E6	5.37	1	0.00	5.369E+12
O74731	3.068E6	5.26	1	0.00	5.258E+12
Q9P7C3	8.931E6	5.11	2	0.00	5.114E+12
Q09673	1.215E7	5.07	2	0.00	5.071E+12
Q9Y7J0	2.597E6	5.03	2	0.00	5.028E+12
P78794	2.802E6	4.88	1	0.00	4.885E+12
Q9P7N9	5.144E6	4.87	1	0.00	4.872E+12
Q9URT2	5.890E6	4.78	2	0.00	4.782E+12
Q9UUD0	4.452E7	4.59	2	0.00	4.588E+12
O74865	6.060E6	4.42	2	0.00	4.423E+12
O74969	3.446E7	4.35	1	0.00	4.353E+12
O94632	2.290E6	4.28	1	0.00	4.282E+12
Q10156	5.065E8	4.23	1	0.00	4.227E+12
O74990	5.893E6	4.15	3	0.00	4.145E+12
O74982	1.880E6	4.14	1	0.00	4.14E+12
Q9P375	3.258E7	4.06	1	0.00	4.064E+12
O60121	7.913E6	4.05	2	0.00	4.052E+12
Q9P6P9	2.882E6	3.99	2	0.00	3.991E+12
Q9USZ7	1.277E6	3.97	2	0.00	3.974E+12
Q9US12	1.511E6	3.97	2	0.00	3.974E+12
Q10171	9.896E6	3.92	1	0.00	3.919E+12
Q9HGN6	2.241E8	3.92	1	0.00	3.915E+12
Q10268	1.388E6	3.88	3	0.00	3.879E+12
Q9UUK1	0.000E0	3.87	2	0.00	3.872E+12
O94369	6.217E6	3.78	1	0.00	3.78E+12
Q9UUH0	1.953E8	3.71	2	0.00	3.707E+12
O74906	3.673E6	3.66	1	0.00	3.664E+12
O74794	4.403E6	3.35	1	0.00	3.347E+12
Q9C0Z4	3.195E7	3.08	2	0.00	3.085E+12
P07657	9.392E6	3.08	1	0.00	3.082E+12
Q9P3W1	1.204E6	3.06	1	0.00	3.056E+12
O13950	6.072E6	3.01	2	0.00	3.006E+12
Q10442	5.236E7	2.94	1	0.00	2.936E+12
O74826	5.574E6	2.89	2	0.00	2.888E+12
Q10311	5.214E6	2.88	1	0.00	2.884E+12
Q9UUK0	2.664E6	2.87	1	0.00	2.874E+12
Q09893	2.044E7	2.85	1	0.00	2.852E+12
O42898	2.483E6	2.82	2	0.00	2.822E+12
O94677	4.176E6	2.81	3	0.00	2.81E+12
Q9P6R6	2.107E7	2.80	1	0.00	2.797E+12
O43001	4.504E6	2.77	2	0.00	2.772E+12
Q9UTR5	8.538E6	2.76	2	0.00	2.759E+12
O74866	1.138E7	2.69	2	0.00	2.687E+12
Q9HDZ0	3.798E6	2.68	1	0.00	2.68E+12
Q9UTB0	5.474E6	2.65	1	0.00	2.65E+12
Q9Y7J2	1.021E7	2.65	1	0.00	2.646E+12
Q9P6J6	9.135E6	2.63	1	0.00	2.629E+12
O94626	0.000E0	2.63	1	0.00	2.626E+12

Q9C0W1	6.782E6	2.61	1	0.00	2.606E+12
O74732	9.313E6	2.56	1	0.00	2.562E+12
O94707	4.427E6	2.55	1	0.00	2.551E+12
Q9Y7L0	1.194E7	2.54	1	0.00	2.54E+12
P33277	2.939E6	2.49	1	0.00	2.492E+12
Q10439	4.505E6	2.47	1	0.00	2.474E+12
Q09888	4.157E6	2.44	2	0.00	2.441E+12
O42903	4.035E6	2.42	1	0.00	2.419E+12
Q92353	4.809E7	2.42	2	0.00	2.418E+12
Q9C1X5	7.380E5	2.42	1	0.00	2.417E+12
O14214	5.832E6	2.41	1	0.00	2.415E+12
Q1MTQ5	4.561E6	2.41	1	0.00	2.409E+12
Q9UTQ8	1.465E7	2.36	1	0.00	2.36E+12
O60111	3.954E6	2.35	3	0.00	2.353E+12
O74434	3.384E6	2.33	1	0.00	2.329E+12
Q9Y7K1	7.316E7	2.31	2	0.00	2.309E+12
Q9P7K6	6.214E6	2.29	1	0.00	2.293E+12
Q9P7J0	6.001E6	2.28	1	0.00	2.279E+12
Q9UT28	1.318E7	2.27	2	0.00	2.274E+12
Q10324	4.944E6	2.26	1	0.00	2.257E+12
Q9HGQ2	4.585E6	2.25	1	0.00	2.245E+12
O13771	0.000E0	2.23	1	0.00	2.232E+12
O94680	1.634E7	2.23	2	0.00	2.23E+12
O74463	5.598E6	2.19	1	0.00	2.194E+12
O14360	3.976E6	2.15	1	0.00	2.151E+12
O60095	0.000E0	2.15	1	0.00	2.148E+12
O94257	3.858E6	2.10	1	0.00	2.1E+12
O43018	1.133E7	2.09	2	0.00	2.094E+12
O94290	4.441E5	2.09	1	0.00	2.085E+12
Q09116	1.017E7	2.07	1	0.00	2.067E+12
O59834	0.000E0	2.06	1	0.00	2.065E+12
Q9Y803	6.214E6	2.04	1	0.00	2.04E+12
O94377	3.456E6	2.03	1	0.00	2.033E+12
Q8WZK2	1.823E6	2.02	1	0.00	2.02E+12
Q9USL1	4.139E6	1.99	2	0.00	1.988E+12
O94516	2.608E6	1.96	1	0.00	1.965E+12
O59734	1.305E7	1.95	1	0.00	1.952E+12
Q9HDV3	3.274E6	1.94	2	0.00	1.944E+12
Q9Y7K0	5.605E7	1.91	3	0.00	1.911E+12
Q9UUJ4	9.756E7	1.90	1	0.00	1.9E+12
O94694	7.079E6	1.90	1	0.00	1.896E+12
Q9UT37	7.756E6	1.89	2	0.00	1.886E+12
Q09774	0.000E0	1.87	1	0.00	1.867E+12
O13730	1.438E7	1.86	2	0.00	1.861E+12
O13787	1.455E7	1.85	1	0.00	1.853E+12
Q9URZ4	1.855E7	1.84	2	0.00	1.842E+12
B5BP45	2.181E7	1.84	1	0.00	1.842E+12
O59710	4.432E6	1.83	1	0.00	1.832E+12
Q9UU85	2.442E6	1.83	1	0.00	1.831E+12
Q9P5M9	3.036E7	1.82	1	0.00	1.817E+12
O74876	5.764E6	1.81	1	0.00	1.81E+12
Q10264	2.851E6	1.80	1	0.00	1.8E+12
O14207	0.000E0	1.80	1	0.00	1.799E+12
O14342	0.000E0	1.79	1	0.00	1.787E+12
P87244	5.585E6	1.79	1	0.00	1.786E+12
Q9Y7N0	1.037E7	1.78	2	0.00	1.776E+12
Q01682	1.189E7	1.77	1	0.00	1.772E+12
Q9P7I7	0.000E0	1.76	1	0.00	1.762E+12
O74915	5.656E6	1.76	2	0.00	1.761E+12
O74508	2.545E7	1.76	1	0.00	1.759E+12
P14605	2.055E7	1.75	2	0.00	1.75E+12
Q10302	5.063E6	1.75	1	0.00	1.75E+12
Q09839	0.000E0	1.75	1	0.00	1.749E+12
O60145	1.983E6	1.74	1	0.00	1.743E+12
Q9P6K5	0.000E0	1.74	1	0.00	1.743E+12
O14334	2.826E7	1.74	1	0.00	1.74E+12
Q9HE10	5.013E6	1.74	1	0.00	1.74E+12
Q9UTR0	4.435E6	1.71	1	0.00	1.71E+12
O74772	1.145E6	1.71	1	0.00	1.706E+12
Q9Y7L2	3.598E7	1.71	1	0.00	1.706E+12
Q9Y7T1	4.604E6	1.69	1	0.00	1.692E+12

Q9P7J1	1.740E6	1.69	1	0.00	1.686E+12
Q1MTP1	2.893E8	1.67	2	0.00	1.674E+12
O74737	2.845E7	1.67	2	0.00	1.674E+12
Q9USR2	1.165E8	1.67	2	0.00	1.674E+12
O13895	1.508E6	1.66	1	0.00	1.66E+12
Q12706	4.275E6	1.66	2	0.00	1.659E+12
Q9Y821	9.989E6	1.65	1	0.00	1.648E+12
Q9Y804	2.720E7	1.64	3	0.00	1.645E+12
Q09877	2.446E6	1.64	2	0.00	1.643E+12
Q9C0X7	1.336E8	1.64	1	0.00	1.64E+12
O59826	6.854E5	1.64	1	0.00	1.636E+12
P87152	1.486E7	1.63	3	0.00	1.634E+12
O14188	8.163E6	1.63	3	0.00	1.625E+12
O13959	2.244E7	1.62	1	0.00	1.619E+12
O13945	9.983E6	1.61	1	0.00	1.613E+12
O74542	4.555E6	1.61	1	0.00	1.609E+12
O94688	2.545E7	1.61	1	0.00	1.606E+12
O43066	2.709E7	1.61	2	0.00	1.605E+12
Q9USP3	4.673E7	1.60	1	0.00	1.603E+12
Q09879	0.000E0	1.60	1	0.00	1.603E+12
O13803	4.286E6	1.60	1	0.00	1.603E+12
O14209	3.220E7	11.49	8	0.00	1.149E+13
Q9UT55	1.254E7	8.96	4	0.00	8.96E+12
P48009	2.881E7	5.30	2	0.00	5.303E+12
O94598	6.057E8	5.08	2	0.00	5.084E+12
Q9C0Y5	3.418E7	4.48	2	0.00	4.48E+12
Q9URX2	2.158E7	4.25	1	0.00	4.25E+12
Q9HDZ2	5.256E6	4.01	3	0.00	4.012E+12
O74482	8.879E6	3.84	3	0.00	3.84E+12
P78763	1.339E7	3.77	1	0.00	3.77E+12
O13686	1.410E8	3.61	2	0.00	3.605E+12
O74481	0.000E0	3.47	1	0.00	3.471E+12
O94421	1.999E7	3.40	2	0.00	3.403E+12
O74863	7.969E6	3.40	3	0.00	3.4E+12
Q9P7E0	2.619E7	3.40	1	0.00	3.398E+12
O42975	3.105E8	3.39	2	0.00	3.393E+12
Q9US20	3.975E6	3.02	2	0.00	3.017E+12
P36582	1.230E7	2.97	2	0.00	2.966E+12
O13744	0.000E0	2.92	1	0.00	2.917E+12
Q10331	3.454E6	2.80	3	0.00	2.795E+12
Q9UTA8	2.908E7	2.52	4	0.00	2.522E+12
O60116	3.353E6	2.50	2	0.00	2.504E+12
Q9P7H8	0.000E0	2.50	1	0.00	2.501E+12
Q9P7R3	1.796E7	2.45	1	0.00	2.447E+12
Q8TFF8	3.436E6	2.40	1	0.00	2.401E+12
P79058	1.206E7	2.38	1	0.00	2.379E+12
O74563	3.975E8	2.31	2	0.00	2.313E+12
Q9Y7X8	1.087E7	2.27	1	0.00	2.27E+12
O74456	2.480E7	2.22	1	0.00	2.218E+12
O14132	2.480E7	2.22	1	0.00	2.218E+12
O74797	1.078E7	2.22	1	0.00	2.218E+12
P87234	2.721E7	2.18	1	0.00	2.176E+12
Q9UTC8	2.603E7	2.17	2	0.00	2.172E+12
Q9URY3	9.777E5	2.08	1	0.00	2.08E+12
Q09815	2.665E7	2.04	1	0.00	2.041E+12
O74839	4.274E7	1.96	2	0.00	1.96E+12
Q9HFE8	2.153E7	1.85	5	0.00	1.855E+12
Q1MTQ0	5.037E5	1.79	1	0.00	1.794E+12
O94383	3.281E7	1.77	2	0.00	1.773E+12
Q09829	5.063E6	1.75	1	0.00	1.75E+12
Q9Y7P0	1.526E6	1.75	1	0.00	1.746E+12
Q10062	3.689E7	1.73	2	0.00	1.731E+12
O13863	6.987E6	1.71	1	0.00	1.711E+12
O74421	0.000E0	1.67	1	0.00	1.667E+12
Q09833	2.969E7	1.66	2	0.00	1.662E+12
Q10308	2.138E7	1.66	1	0.00	1.66E+12
O14177	3.014E7	1.66	1	0.00	1.656E+12
O59712	6.801E6	1.64	2	0.00	1.644E+12
O13989	9.458E6	1.64	2	0.00	1.638E+12
O14227	1.548E6	1.63	1	0.00	1.632E+12
Q09798	6.343E6	1.62	2	0.00	1.62E+12

O74359	3.718E7	1.62	3	0.00	1.619E+12
Q09196	1.166E7	1.60	1	0.00	1.603E+12
O94346	6.501E6	23.01	3	2.34	9.8426321
P50519	1.386E7	22.24	3	2.81	7.9165858
Q9USP6	1.632E7	18.30	6	2.45	7.4737097
O13899	1.985E7	13.93	2	1.87	7.4463516
O74478	1.317E7	15.58	6	2.29	6.7926096
Q9HE05	9.818E6	16.94	7	2.53	6.6912032
O00084	1.990E7	11.61	5	1.79	6.4882271
Q09923	6.621E6	17.55	4	2.81	6.252478
Q9UT27	3.044E7	22.96	5	3.92	5.8639356
O94586	2.409E7	14.24	4	2.45	5.8152799
O14099	5.648E6	10.60	4	1.85	5.7458177
Q9UUK7	3.911E7	15.43	5	2.71	5.7026
O74728	8.725E6	9.44	1	1.66	5.6716055
Q9UTH9	1.401E7	11.60	5	2.17	5.3560684
O74856	1.962E7	9.40	5	1.79	5.2376881
Q9HGL4	7.104E6	10.46	4	2.12	4.9407098
Q09751	3.119E7	28.12	6	5.82	4.8290064
Q09818	9.309E6	10.28	3	2.20	4.6840516
O13794	2.072E6	15.66	2	3.51	4.4576896
O94675	6.089E7	10.58	2	2.41	4.394969
O14165	1.737E7	11.29	3	2.63	4.2904258
Q9UTC9	8.037E6	11.30	1	2.66	4.2571926
P78833	9.428E7	51.39	5	12.82	4.0092611
O74382	3.591E7	10.33	3	2.61	3.9555143
Q9US41	2.336E8	118.94	24	30.54	3.8941665
O94548	1.267E7	11.64	2	3.05	3.822495
Q09859	1.523E7	9.63	3	2.54	3.7975259
O13965	9.657E6	10.79	2	2.86	3.7765389
O59800	4.306E6	11.85	2	3.14	3.776327
Q9UTS0	1.299E7	8.71	4	2.32	3.7514869
Q96WV0	1.497E8	58.62	11	15.67	3.7422513
Q10187	1.124E7	16.07	4	4.41	3.6435743
O14096	1.741E7	13.59	7	3.83	3.5514229
O14283	7.161E6	7.49	3	2.12	3.540949
P12000	5.234E6	10.43	1	2.96	3.5308676
Q9UUG8	7.848E6	8.15	2	2.32	3.5169073
Q9UT36	2.061E7	24.31	4	7.01	3.4697812
Q09785	1.311E7	18.37	9	5.36	3.4276449
P40386	7.046E6	11.00	3	3.23	3.4008983
Q9UTH2	4.197E6	9.58	3	2.84	3.370681
O94505	5.095E7	51.42	8	15.46	3.3249719
O94547	1.629E7	22.02	6	6.66	3.3086517
O74867	2.735E7	7.24	3	2.22	3.2608625
O60184	2.164E7	28.69	7	8.86	3.2393995
O94373	2.854E7	19.23	6	6.00	3.2063603
O60125	1.694E7	9.59	3	3.02	3.1769028
P78768	1.564E7	8.12	3	2.58	3.146416
O94497	2.440E7	43.54	11	14.07	3.0942773
Q9USL7	1.058E7	10.80	2	3.50	3.087825
Q9UTI8	7.878E7	14.71	3	4.79	3.0716038
P18869	5.491E8	226.12	21	73.79	3.0642855
Q9P7F7	6.413E6	5.94	2	1.95	3.0458876
Q9C0Y6	1.830E7	9.31	3	3.07	3.0304126
Q10195	2.522E7	7.79	3	2.58	3.0240597
P87113	1.967E7	5.23	3	1.75	2.9977343
O14238	9.467E5	12.46	1	4.17	2.9880604
Q9HE08	1.807E7	8.82	1	2.99	2.9446778
Q9HDW8	1.575E7	6.37	2	2.17	2.9380251
O94721	1.150E7	7.95	2	2.72	2.922535
O14094	1.206E7	11.85	5	4.06	2.9164135
Q9HGP5	3.154E7	37.72	6	12.94	2.9143014
O59739	2.255E7	25.14	4	8.67	2.898981
Q9Y7J3	6.292E6	9.03	3	3.14	2.8774178
O13693	1.303E7	15.20	3	5.33	2.8514093
O94315	8.965E7	15.40	3	5.43	2.8330322
O94286	1.602E7	11.85	4	4.23	2.8003875
P78875	1.035E7	12.97	5	4.66	2.7838171
O74455	4.969E7	48.98	11	17.78	2.7541472
O74504	1.196E7	28.21	4	10.52	2.682004

O94353	2.607E7	9.09	1	3.41	2.661259
O74533	1.603E7	7.48	5	2.82	2.6537133
O14045	9.146E6	6.18	1	2.34	2.6408325
O94650	3.653E7	7.55	2	2.88	2.6196707
Q9UTQ1	2.950E7	26.79	7	10.23	2.61836
Q9USU5	1.309E8	63.20	7	24.19	2.6130233
O74823	5.706E6	6.61	2	2.55	2.594761
Q9P6I7	6.987E7	18.29	5	7.09	2.5786288
O74557	3.623E7	24.42	9	9.51	2.5682211
Q9USJ3	1.665E7	14.09	3	5.52	2.5526512
O13326	1.420E8	73.07	11	28.64	2.5515264
O94246	2.692E7	26.50	7	10.40	2.5478503
P32390	4.924E7	43.85	9	17.21	2.5474812
O13935	8.837E6	14.49	3	5.69	2.5472765
Q03392	2.785E7	33.50	6	13.16	2.5454425
Q9UT02	1.368E7	10.92	4	4.30	2.5373267
O94661	1.407E8	6.22	1	2.46	2.5272742
O42908	2.723E7	39.23	13	15.54	2.5244974
O59868	9.714E7	5.11	4	2.03	2.511316
Q9HGM2	8.930E6	9.65	1	3.85	2.5067545
P87238	1.558E7	19.78	2	7.90	2.5057732

Appendix Table 1.4: Positive Interactors in the Sec3-913-GFP Trap (Replicate 2)

Uniprot Accession	Area	Score	Peptides	Score in GFP Control	Fold Increase Over Control
Q10324	1.529E7	19.27	5	0.00	1.927E+15
P78833	4.153E6	8.10	1	0.00	8.097E+14
Q9HE08	4.031E6	6.61	1	0.00	6.612E+14
Q9UTI8	2.527E7	5.24	2	0.00	5.236E+14
Q09859	1.321E6	3.50	1	0.00	3.504E+14
O74382	2.439E6	3.38	1	0.00	3.378E+14
O13863	1.603E6	2.76	1	0.00	2.762E+14
O13744	2.066E6	2.54	1	0.00	2.544E+14
O60166	0.000E0	2.22	1	0.00	2.225E+14
Q9UTA8	1.641E7	2.03	2	0.00	2.028E+14
O13693	6.469E6	1.86	1	0.00	1.857E+14
O13895	1.706E6	1.63	1	0.00	1.631E+14
O74545	3.478E6	11.38	1	0.00	1.138E+15
Q10481	4.187E6	10.65	2	0.00	1.065E+15
O94362	3.748E6	10.18	5	0.00	1.018E+15
P28758	8.686E6	8.77	2	0.00	8.774E+14
Q10494	1.841E6	7.39	2	0.00	7.393E+14
O94617	3.120E6	6.81	1	0.00	6.805E+14
Q09842	1.399E6	5.93	1	0.00	5.931E+14
O59771	2.414E6	5.24	1	0.00	5.237E+14
Q96WW3	1.459E6	4.62	2	0.00	4.62E+14
Q02088	6.623E6	4.61	1	0.00	4.609E+14
O13636	3.488E6	4.35	1	0.00	4.35E+14
P33075	6.387E6	4.26	2	0.00	4.255E+14
Q9US43	4.604E6	4.20	2	0.00	4.201E+14
P78929	5.713E6	4.16	2	0.00	4.161E+14
Q9UTI3	1.520E6	4.10	1	0.00	4.102E+14
O14295	2.122E6	3.99	2	0.00	3.991E+14
O14280	8.730E6	3.93	1	0.00	3.927E+14
Q9Y7K7	2.073E6	3.78	1	0.00	3.777E+14
O60108	1.383E6	3.72	2	0.00	3.722E+14
O13808	1.543E6	3.67	1	0.00	3.671E+14
O74898	1.586E6	3.16	1	0.00	3.158E+14
O42650	1.006E6	2.82	1	0.00	2.823E+14
P78790	1.536E6	2.75	1	0.00	2.749E+14
O59747	1.714E6	2.71	1	0.00	2.709E+14
Q9Y810	2.550E6	2.61	1	0.00	2.608E+14
Q9UUA4	1.139E6	2.49	1	0.00	2.486E+14
O94563	5.995E6	2.47	1	0.00	2.468E+14
O74439	1.694E6	2.39	1	0.00	2.393E+14
O13986	2.882E7	2.32	1	0.00	2.325E+14
Q09695	1.010E6	2.31	1	0.00	2.31E+14
O43032	5.250E5	2.24	2	0.00	2.235E+14
Q92366	7.235E6	2.22	1	0.00	2.218E+14
P87170	0.000E0	2.21	1	0.00	2.207E+14
Q9P6P6	5.477E6	2.20	1	0.00	2.199E+14
Q9P7M8	2.138E6	2.19	1	0.00	2.19E+14
P79060	1.707E6	2.12	1	0.00	2.122E+14
O94386	2.938E7	2.09	1	0.00	2.091E+14
O60091	0.000E0	2.05	1	0.00	2.052E+14
Q10170	7.891E5	2.04	1	0.00	2.037E+14
Q9UUL4	0.000E0	2.01	1	0.00	2.01E+14
Q9Y705	2.132E6	2.01	1	0.00	2.008E+14
Q9US48	1.856E6	1.98	1	0.00	1.982E+14
Q9US46	1.117E8	1.93	1	0.00	1.932E+14
O94657	2.851E6	1.93	1	0.00	1.925E+14
Q10100	5.105E6	1.92	1	0.00	1.922E+14
P32372	0.000E0	1.88	1	0.00	1.881E+14
Q10165	0.000E0	1.85	1	0.00	1.851E+14
P87295	5.051E6	1.80	1	0.00	1.804E+14
Q09908	0.000E0	1.80	1	0.00	1.803E+14
Q76PC3	1.926E6	1.79	1	0.00	1.786E+14
P0CAN8	7.837E5	1.73	1	0.00	1.729E+14
O59674	0.000E0	1.71	1	0.00	1.715E+14

O94613	1.066E6	1.71	1	0.00	1.706E+14
Q9USN0	2.102E8	1.68	1	0.00	1.677E+14
O74854	8.905E6	1.66	1	0.00	1.662E+14
Q9P787	3.812E7	1.64	2	0.00	1.638E+14
O13890	4.641E5	1.63	1	0.00	1.631E+14
Q9USH0	2.590E6	9.77	2	0.00	9.774E+14
Q09843	2.464E6	8.90	3	0.00	8.899E+14
O59702	4.035E6	6.51	2	0.00	6.515E+14
O60121	2.294E6	5.80	3	0.00	5.805E+14
O94752	3.245E6	4.53	1	0.00	4.534E+14
O14306	1.292E6	4.13	1	0.00	4.129E+14
O74409	1.926E6	2.91	1	0.00	2.907E+14
Q9UUB1	2.896E6	2.90	1	0.00	2.895E+14
Q9UQX0	1.562E6	2.72	1	0.00	2.724E+14
Q10203	3.353E6	2.45	1	0.00	2.453E+14
O60111	6.365E7	2.29	1	0.00	2.292E+14
Q9UUD0	6.966E6	2.25	2	0.00	2.249E+14
Q1MTQ7	2.799E6	2.07	1	0.00	2.072E+14
O74690	2.624E7	2.02	1	0.00	2.021E+14
O42919	2.241E7	1.93	1	0.00	1.934E+14
O13991	8.015E5	1.86	1	0.00	1.857E+14
Q9P5N0	0.000E0	1.62	1	0.00	1.622E+14
O60064	9.758E6	30.57	9	3.06	9.9793706
P79009	3.948E7	20.68	5	2.43	8.5196704
O94280	1.055E7	14.18	6	2.23	6.3596493
O42993	7.983E6	11.21	2	1.94	5.7669189
O60173	3.447E6	12.94	5	2.58	5.0140488
O13998	8.452E6	32.60	5	7.30	4.4641916
O94504	2.947E7	35.30	7	8.05	4.3851418
Q9Y7R7	2.700E6	9.56	1	2.19	4.3603469
O43062	3.131E6	9.24	1	2.17	4.264921
O74442	7.300E6	10.88	5	2.67	4.0711978
O14301	2.478E6	7.34	3	1.96	3.744101
Q9P7A1	2.482E6	6.82	2	1.89	3.609834
Q9UTB8	5.549E6	10.39	2	2.96	3.5093498
O74825	1.199E6	9.54	2	2.73	3.4936827
O13711	1.334E6	6.30	1	1.93	3.2546278
Q9P804	1.125E7	31.54	6	10.68	2.9540474
Q10340	8.485E5	5.58	2	1.89	2.9456756
P17608	1.600E7	8.37	2	2.84	2.9418551
Q10066	1.565E7	29.74	5	10.24	2.9051494
O13640	5.313E6	8.44	1	2.96	2.8538276
O74820	5.985E6	10.71	1	3.86	2.7757719
Q9C0Y5	1.898E7	6.12	2	2.22	2.7622547
O59681	5.184E6	22.01	4	8.13	2.7061113
P87238	7.445E5	12.52	2	4.67	2.6796794
O13928	7.525E6	17.47	4	6.57	2.6585741
O43026	3.944E9	337.55	23	129.28	2.6109994
Q09176	1.031E7	4.79	3	1.84	2.6094177
O14290	5.657E6	13.87	3	5.35	2.592702
O59739	4.187E6	16.55	2	6.42	2.5794447
Q92367	2.626E6	4.24	2	1.69	2.5048023